‘Alles ist relativ.’

A. Einstein

Members of the Examination Committee:

Prof. dr. ir. Christian V. Stevens (Promoter)
Department of Sustainable Organic Chemistry and Technology
Faculty of Bioscience Engineering
Ghent University

Prof. dr. ir. Frank Devlieghere (Chairman)
Department of Food Safety and Food Quality
Faculty of Bioscience Engineering
Ghent University

Prof. dr. ir. Filip Tack (Secretary)
Laboratory of Analytical Chemistry and Applied Ecochemistry
Faculty of Bioscience Engineering
Ghent University

Prof. dr. Koen Binnemans
Departement Chemistry
Faculty of Science
KU Leuven

Prof. dr. ir. Mathias D'hooghe
Department of Sustainable Organic Chemistry and Technology
Faculty of Bioscience Engineering
Ghent University

Prof. dr. Johan Van der Eycken
Department of Organic Chemistry
Faculty of Science
Ghent University

Dr. ir. Yves Génisson
Laboratoire de Synthèse et Physicochimie de Molécules d'Intérêt
Université Paul Sabatier (Toulouse)

Promoter: Prof. dr. ir. C. Stevens
Research Group SynBioC
Department of Sustainable Organic Chemistry and Technology
Faculty of Bioscience Engineering, Ghent University

Dean: Prof. dr. ir. G. Van Huylenbroeck

Rector: Prof. Dr. Anne De Paepe

UNIVERSITEIT GENT

ir. Cedric Maton

Design and Properties of Novel Peralkylated Imidazolium Ionic Liquids

Thesis submitted in fulfillment of the requirements
for the degree of Doctor (PhD) in Applied Biological Sciences: Chemistry

Dutch translation of the title:

Ontwikkeling en synthese van nieuwe geperalkyleerde imidazolium ionische vloeistoffen.

ISBN number:

978-90-5989-657-4

Cover photo:

Imidazolium room temperature ionic liquids
X-ray image (Dr. N. Brooks)

Ghent, October 2013

The author:

ir. Cedric Maton

The promoter:

Prof dr. ir. C. V. Stevens

PREFACE

Na vier jaar onderzoek is dit werk het resultaat van wat gelukt en minder goed is gelukt. Voor het tot stand komen van dit werk, zijn er een aantal mensen die specifiek moeten bedankt worden. Vooreerst wil ik de professoren van de jury bedanken, voor het vele lees- en verbeterwerk. De medewerkers van het “Mapil”-project ben ik dankbaar, prof. Binnemans en prof. Fransaer, voor het mogelijk maken van de samenwerking en de conferenties en natuurlijk de medewerkers die bijgedragen hebben tot dit werk. Hiervoor wil ik zeker de Leuvense medewerkers Dr. Neil Brooks, Dr. Stijn Schaltin, Sil Wellens, Evert Vanecht en Gana niet vergeten. Daarnaast droegen ook Dr. Ewa Liwarska-Bizukojc (Łódź), prof. Kristof Van Hecke e cara Klicia bij tot het welslagen van dit onderzoek. Deze (internationale) samenwerking heeft aan dit lab-curiosum zeker een meerwaarde gegeven en draagt er ook toe bij dat de vergaarde kennis opgeslagen is in ons collectieve “ROM”-geheugen.

Naast het welslagen van het project moest natuurlijk nog de synthese op poten gezet worden, en hiervoor is zeker het vertrouwen, de hulp en medewerking van prof. Stevens niet te onderschatten. De vele ideeën, de bijsturing waar nodig, de hulp bij de officiële zaken en zeker de gemoedelijke sfeer zitten verweven in deze thesis en zal ik niet snel vergeten. Daarnaast verdient Nils zeker een pluim voor het omgaan met zijn bikkelharde onderwerp en dito thesisstudent, en zeker ook voor het ineensteken van het labo op het vierde en de samenwerking naar manuscripten en ideeën toe. Naast hem was het aangenaam werken op het bureau, en de collega’s (An, Fien, Karel, Thomas, Gert, Tamara, Sara, Frederik, Karen) op het zesde hebben daar zeker toe bijgedragen.

Tijdens het synthese werk was het ook aangenaam vertoeven in het labo, en zeker de tijd op het vierde heeft me met plezier in actie doen schieten. Daarna vond ik evenveel plezier op het vijfde, zeker omdat ik daar de meest plezante thesistudenten mocht begeleiden. Jan en Carla, bedankt voor de wel zeer fijne samenwerking en het eindeloze maar plezante discussiëren over de muziek op de radio. Daarnaast ben ik alle studenten en doctorandi as well as the people from abroad, in het lab dankbaar. Jullie zijn niet op te noemen maar wel allemaal fantastisch op je eigen manier en ik wens je allemaal je mooiste dromen toe. Zeker niet te vergeten zijn Pieter, Ans, Els, Andy en Dries. Niettegenstaande jullie arbeid op de achtergrond, zijn jullie onmisbaar en fantastisch om mee samen te werken.

Niet in het minste te bedanken zijn ook de mensen die het mogelijk maakten me te ontspannen na het werk, mijn ouders, broer en zus en vrienden. Ook al waren wetenschappelijke discussies soms niet aan de orde, toch was het goedkeuren om bezig te zijn met wat ik graag deed, genoeg. Bedankt daarvoor alleen al, maar zeker ook om mijn zeer uitgebreide studieperiode de meest aangename te maken die een mens zich kan inbeelden.

TABLE OF CONTENTS

LIST OF ABBREVIATIONS

AF: Acetophenone
Amim: 1-allyl-3-methylimidazolium
BA: Benzaldehyde
Beti: bis(pentafluoroethyl)sulfonylimide
CIL: Carbonate Ionic Liquid
COD: Chemical Oxygen Demand
CSR: Chiral shift reagent
CSRN: Copper-gauze Supported Raney Nickel catalyst cartridge (CatCart®)
DFT: Density Functional Theory
DMC: Dimethyl carbonate
DOC: Dissolved Organic Carbon
DO: Dissolved Oxygen concentration
e.e.: Enantiomeric Excess
EB: Ethylbenzene
FAP: tris(pentafluoroethyl)trifluorophosphate
GC-FID: Gas Chromatography – Flame Ionisation Detection
IL: Ionic Liquid
IR: Infrared spectroscopy
(HP)LC-UV: (High Pressure) Liquid Chromatography – Ultraviolet detection
LC-MS: Liquid Chromatography – Mass Spectrometry
MAPIL: Material Processing in Ionic Liquids
(R)mim: (R-)methylimidazolium
MR: Microreactor
MW: Microwave irradiation
NMR: Nuclear Magnetic Resonance Spectroscopy
OUR: Oxygen Uptake Rate
PEA: 1-Phenylethanol
R.T.: Room Temperature
RTIL: Room Temperature Ionic Liquid
TGA: Thermogravimetric Analysis
TNRN: Thales Nano Commercial Raney Nickel catalyst cartridge (CatCart®)
ToF: Time-of-flight
VSS: Volatile Suspended Solids
WWTP: Waste Water Treatment Plant

I) INTRODUCTION AND GOALS

The research performed in this PhD thesis is conducted within the framework of the MAPIL project (acronym for “Materials Processing in Ionic Liquids”). This project is a collaboration of different partners from both the industry and the academic world. The industrial partners steer the project by bringing in the technical demands. The academic partners apply their divergent expertise in the different fields of material chemistry, such as physical chemistry, organic synthesis and electrochemistry.

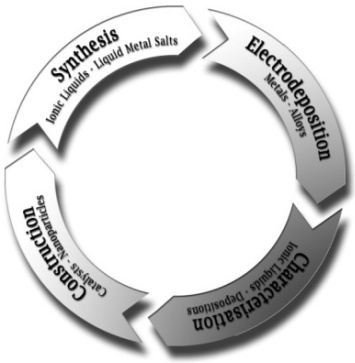

Figure 1: Visual summary of the different work packages and the interaction in the MAPIL project.

The project is divided in different work packages, of which the research part is represented in Figure 1 as a continuous wheel. This represents the interaction of the different disciplines. These disciplines are amongst others the organic synthesis of novel ionic liquids and liquid metal salts with the investigation of their properties and the electroplating of different metals, alloys, catalysts and nanoparticles by electrodeposition in ionic liquids as well as the characterisation of the newly constructed materials.

The partners conducting the organic synthesis investigate routes towards large-scale and accessible novel and cheap ionic liquids and deep-eutectic solvents and will evaluate their properties as well as their applicability in e.g. electrochemistry, solvation of macromolecules, CO_2 binding and organic synthesis. The inorganic section includes the synthesis of liquid metal salts, electroplating in ionic liquids of different metals (e.g. germanium, aluminium, platinum, tungsten, molybdenum) and alloys (e.g. brass, zinc-nickel alloy) and design and synthesis of novel catalysts. The interplay between the different research activities and the partners of the MAPIL project and the accessibility of the know-how and expertise in divergent disciplines will result in the added value of the performed research. This synergistic interaction will become apparent throughout the following chapters.

Ionic liquids were discovered in 1914 as $[EtNH_3][NO_3]$, this compound was found to melt at 12 °C.[1] Nowadays, an increasing amount of compounds are being investigated and reviewed. Ionic liquids are in fact *molten salts*, since they are completely composed of ions. The oppositely charged ions are interacting with ionic bonds. These are too strong for the products to completely volatise and often lead to a solid salt.

Nonetheless, slightly coordinating ions can be designed, which inductively or mesomerically delocalise the charge over multiple atoms. For cations, often heteroatomic alkylated species are applied (e.g. imidazolium, pyridinium, phosphonium or ammonium, ...), while for anions different species have emerged in the past (e.g. chloroaluminate, $[AlCl_4]^-$) and in recent years (e.g. bistriflimide, $[NTf_2]^-$). As the low symmetry and the low coordinating properties of these ions hinder them to form a crystal easily, the salts obtain a large liquid range. In some papers, the arbitrary 100 °C is regarded as the melting point limit under which a compound is called an ionic liquid.[2] But as this number is only arbitrary, it is more sensible to declare compounds *room temperature ionic liquids* (RTILs) if they are liquid at ambient temperature. Where possible, the viscosity of the obtained liquids should be low, which facilitates their manipulation.

As ionic liquids are completely composed of ions, they are often investigated as electrolytes (e.g. in dye sensitised solar cell electrolytes, in lithium-ion batteries and electrolytes for metal deposition).[3] Due to their high thermal stability and fluidity, they have also been studied as heat transfer fluids (HTF)[4] or as revolutionary solvents for (bio)catalysis[5] and lignocellulosic biomass.[6] The possibility for modification also allows their investigation as stationary phases in chromatographic analysis.[7]

The goal of this specific research part is situated in the organic synthesis part of the project, more specifically in the design of novel imidazolium ionic liquids with a broad scope of applicability. While several influences on the stabilities will be studied, the properties should stay within a workable range. The method to achieve the improvement of the properties is to make use of accessible imidazolium ionic liquids, which are easily modified during their synthesis. Thus, a major goal will be to design fully substituted imidazolium ionic liquids and to investigate their stability. Nonetheless, the substances need to maintain their applicability and their liquid character. These key properties of the newly designed compounds will also be studied.

The designed solvents should fit within the concept of *green chemistry*. This implies a sustainable synthesis of a sustainable product, with a thorough understanding of the end-of-life treatment and environmental fate. All of these properties will be addresses as broadly as possible in the experimental section.

First of all, the focus will be on the improvement of the sustainability of the synthesis methodology, i.e. on thorough investigation of the synthetic chemistry (i.e. mechanisms, reagent choice) to improve yields and hence the carbon economy. Optimising the synthesis chemistry and post-processing does not only decrease the environmental impact but, as the overall costs decrease, optimisation is also economical beneficial and will allow efficient scale-up.

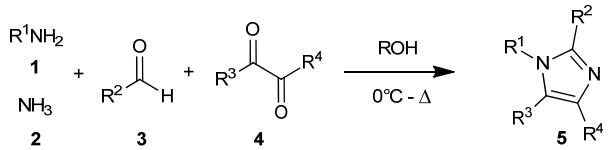

Scheme 1: Debus-Radziszewski imidazole synthesis.

The imidazole scaffolds will be synthesised via the Debus-Radziszewski imidazole synthesis reaction. This multicomponent reaction is a condensation reaction between an α-dicarbonyl compound, an aldehyde, an ammonia source and a primary amine to functionalise one of the nitrogens at once (Scheme 1).[8] The mechanism is believed to involve the condensation between an amine, ammonium and the dicarbonyl compound. After this, ring closure and aromatisation occurs by the aldehyde. Most common side products are the oxazole, formed by expulsion of the amine, the 1*H*-imidazole and when glyoxal is used as dicarbonyl compound, also coupled 2,2'-diimidazoles can occur.[8-9]

To decrease side product formation, the influence of the sequence of product addition, as well as the influence of the expelled water will be investigated. The investigation and fine-tuning of reaction conditions will be further aided by the application of continuous flow technology (Scheme 2), as was already performed in our research group.[10] Different systems available at the department of Sustainable Organic Chemistry and Technology (Ghent University) will be evaluated for their applicability on the imidazole synthesis. The systems have divergent specifications: e.g. channel diameter, reactor length and specific temperature and pressure range. These continuous flow syntheses will allow a large-scale synthesis with a minimum of side products formed due to the inherent precise monitoring of the reaction conditions. Furthermore, post-processing of the reaction mixture will be evaluated on e.g. the recycling of solvents and unreacted reagents, type and amount of solvents and reagents used during work-up and post reaction purification methods, maintaining a high level of purity of the compounds.

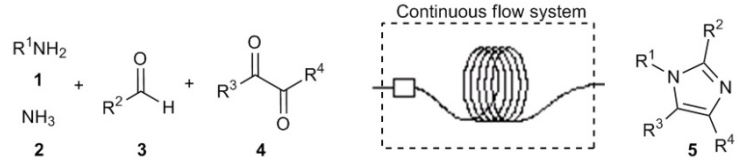

Scheme 2: Schematic representation of Debus-Radziszewski reaction in a continuous flow set-up.

In the synthesis of ionic liquids, the use of continuous flow processes is in line with the search for greener methodology. Due to the microscopic channels, mass and heat transfer are improved and if the conversion increases, the need for purification is reduced. The continuous flow technology has already been used for the synthesis of ionic liquid precursors[11] and the quaternisation thereof[12] (see further section III.1.4).

Whenever possible, linear synthesis routes will be redesigned into convergent synthesis routes. While intensive modification of highly functionalised scaffold molecules is avoided, highly modified pieces will be brought together in the final steps. The synthesis routes towards ionic liquids are particularly susceptible to this strategy as the last two steps include a metathesis step and a quaternisation in which a highly modified alkyl chain R^3 and anion $[A]^-$ can be combined with the imidazole scaffold (Scheme 3).

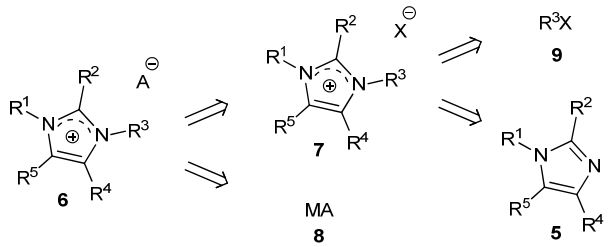

Scheme 3: General retrosynthetic scheme of the convergent imidazolium ionic liquid synthesis, involving metathesis with a specialised anion and quaternisation with possible functionalised compounds.

Novel methods will be evaluated in the metathesis of the anions, circumventing the generation of equimolar amounts of metal salts and in particular the application of toxic silver salts, which also induces a quantitative disposal. Apart from synthesis optimisation, the overall efficiency of the metathesis procedures will be evaluated, as residual starting material (e.g. neutral alkylimidazole, halides, water)[13] can have an important influence on the IL's properties. Since, in general, the purity of the finally synthesised ionic liquids will be mainly dependent on this step, close examination of possible contaminants is necessary in this step. The application of dimethyl carbonate (DMC) in the quaternisation of imidazoles, as patented by BASF in 2001 will here be assessed.[14] In this method, theoretically, a methylated imidazolium cation and a methyl carbonate anion are formed. Upon addition of the Brønsted acid of the desired anion, the methyl carbonate anion decomposes into volatile CO_2 and MeOH which can be removed by evaporation (Scheme 4).

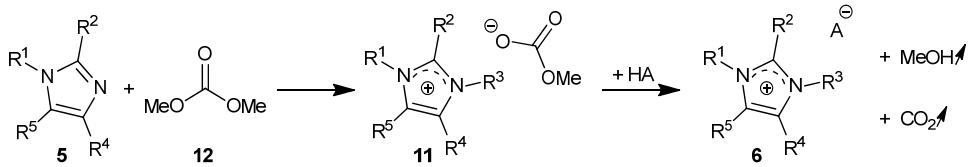

Scheme 4: Synthesis of methyl carbonate ionic liquid 11 from the neutral alkylimidazole 5 and DMC and subsequent metathesis with formation of volatile MeOH and CO_2.

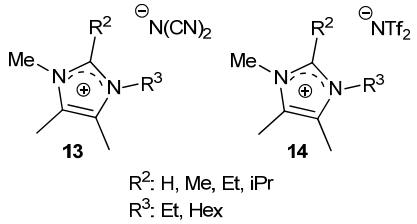

Figure 2: First library of dicyanamide and bis(trifluoromethylsulfonyl)imide peralkylated imidazolium salts.

At first, completely substituted (peralkylated) imidazole scaffolds will be prepared by means of the optimised Debus-Radziszewski reaction procedure. Upon quaternisation, completely substituted imidazolium cations will be obtained (Figure 2). The introduction of alkyl chains will substitute the most reactive hydrogen atoms on the aromatic ring and inductively neutralise the positive charge of the cation. However, the increased Van der Waals interactions will bring about higher melting points. Therefore, also longer *N*-alkyl chains, known for decreasing the melting point of ILs, will be introduced; in the positions C4 and C5 on the ring, initially only methyl groups will be evaluated. Formaldehyde based imidazolium salts, bearing a proton as R^2, will complete the series. The melting points and/or viscosities of series of the obtained analogues with different anions (Figure 2) will be analysed by respectively Differential Scanning Calorimetry (DSC) and by means of a viscometer equipped with a spindle for small samples. These analyses will be performed at the department of Chemistry of KU Leuven.

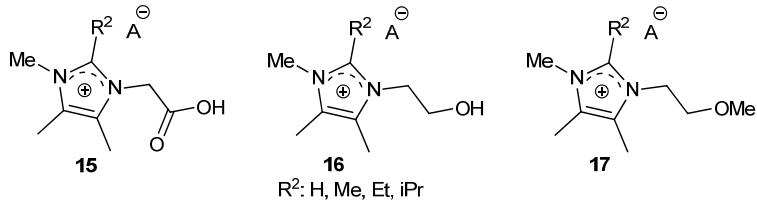

Figure 3: Introduction of functionalities in the cationic core and subsequent derivatisation.

Building on the knowledge obtained from the first series of analogues, different functionalities such as esters, ethers, alcohols and unsaturated moieties can be introduced, to obtain functionalised ionic liquids, again with varying properties (Figure 3). The precursors of these ionic liquids, bearing a handle in the molecule, can be further derivatised to combine different functionalities. At this point, the introduction of renewable compounds can allow the introduction of these functionalities at once. This also allows the exploitation of chiral pool molecules, such as amino acids, and hence the introduction of chiral moieties in ionic liquids (Scheme 5).

The designed ionic liquids should have an intrinsic improved sustainability. Although ILs are generally called *green solvents* for having almost no vapour pressure, a high flash point and autoignition temperature and being recyclable,[15] the true *greenness* of the IL lies mainly in its

application range, which is defined by the recyclability, the stability and the power to replace more polluting or less persistent predecessors, hence being the *safer chemical*.

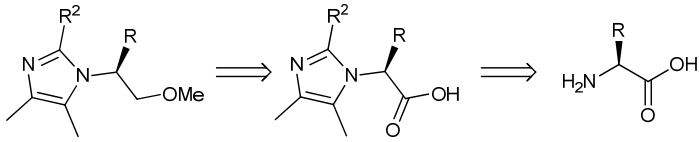

Scheme 5: Retrosynthetic scheme of chiral, amino acid derived imidazoles.

The aim of the synthesis research in the project is application driven, i.e. ionic liquids with adequate stability are required. This stability of ionic liquids is defined in several ways. First, the thermal stability is the resistance to decomposition at elevated temperatures. Second, the application of ionic liquids as electrolytes requires ionic liquids with a high electrochemical stability (e.g. the azepanium salts[16]). This is the resistance to receive or donate electrons from or to electrodes, and is has been described in the literature.[17] Finally, a high chemical stability of the ionic liquids (e.g. by introducing an isopropyl substituent[18]) allows them to be used as recyclable solvents in organic synthesis. To achieve information on the stabilities, the thermogravimetric analysis (TGA) and electrochemical window (ECW) measurements are performed by the collaborators at the department of Metallurgy and Material Engineering (MTM) of KU Leuven. The application in organic synthesis will be evaluated at our department (Sustainable Organic Chemistry and Technology, Ghent University).

The influence of ionic liquids properties contributing to (electro)chemical stabilities are reviewed by colleague Nils De Vos (paper due to be published in Angewandte Chemie). The thermal stability properties will be broadly discussed in the literature overview (see section II). Although these papers describe the limitations of the applicability, the structure-stability relationships can only be investigated by the design of series of analogues. Aided by the design of functionalised ionic liquids, the influence of these specific functionalities may be investigated.

Finally, apart from clean synthesis (efficient synthesis and use of renewable building blocks), and inherently increased sustainability (increased lifetime, recyclability and substitution or reduction of (hazardous) chemicals), a '*green chemica*l' should be "designed for degradation". Therefore, post-application fate of the ionic liquids will be evaluated by means of biodegradability testing of a selected library of imidazolium ionic liquids.

The thus obtained library of analogues will be interesting for understanding the structural influence on the divergent properties discussed above. Moreover, this knowledge will finally allow to rationally select the right modifications in order to design solvents with the requested properties.[19]

II) LITERATURE REVIEW:

THERMAL STABILITY OF IONIC LIQUIDS

1. Introduction

Ionic liquids (ILs) have a very large liquid range (e.g. [C_4mim][NTf_2]: -89 to 450 °C as compared to EtOH: -114 to 78 °C).[20] This range is restricted by their glass forming (T_g) or melting temperature (T_m), which are both mostly below ambient temperature, leading to room temperature ionic liquids (RTILs), and often even below 0 °C. Because of their non-boiling character, the upper temperature limit is given by their thermal degradation point. Although the non-volatile and non-flammable character of ILs is outpaced,[15, 21] the very low vapour pressure of ILs implies a very low volatility and flammability, which in turn gives them their 'green' character as well as engineering advantages. Due to these properties, together with their low corrosivity and high chemical resistance, a myriad of high temperature applications for ionic liquids have been proposed already, e.g. solvents for organic reactions at high temperature,[22] solvents for cellulose,[6, 13a, 23] thermal energy storage (TES)[24] and heat-transfer fluids (HTF),[25] high-temperature lubricants,[26] propellants,[27] curing of ionogels[28] and in analytical apparatus, such as matrices in matrix-assisted desorption/ionisation time-of-flight mass spectrometry (MALDI-ToF)[29] or as stationary phase in gas chromatography.[30] In order to determine the thermal behaviour and the temperatures which allow for a correct and safe application, it is important to study the behaviour of ionic liquids at elevated temperatures and to understand the degradation mechanisms.

These studies can give valuable information on maximum operating temperature, the speed of decomposition and the decomposition products.[31] However, there is an important contribution of the methodology on the obtained results, e.g. the variation in heating rate already shows different thermal decomposition pathways and kinetics.[27a] Therefore, the chosen methods should be in line with the engineered heat exposure in the target application, as well as with the possible contact with gas-flow or the open atmosphere. For long-term high temperature applications, a maximum weight loss at a given minimum temperature can be given, although a single parametric temperature value can give valuable comparative information. The question that is rising therefore is how thermal stability is defined and how it should be evaluated.[32] In this literature review the thermal stabilities, degradation mechanism and analysis methodologies known up to date will be presented, hereby focussing on pure conventional non-protic ionic liquids, i.e. ion pairs comprised of one cation and one anion, neither immobilised or polymerised.

2. Measurement of thermal stability

2.1. Short-term thermal stability

Ionic liquids are often claimed as thermally stable because of their very high decomposition temperature. Many thermal stability measurements are done by thermogravimetric analysis (TGA), more specifically ramped temperature analysis (also called step-tangent or dynamic analysis) with most common heating rates: 10 °C min^{-1} and 20 °C min^{-1}.[25a, 33] This type of experiment is also referred to as short-term stability.[20]

Table 1: Short-term thermal stabilities (T_{onset}, °C) of ammonium and imidazolium based IL with divergent substitution patterns.[1]

Ammonium ionic liquids		[secC_4mim][BF_4]	362[34]
[$N_{1,1,18,18}$][Br]	225[33a]	[C_5mim][Cl]	262[34]
[N_{2222}][Cl]	264[35]	[C_5mim][BF_4]	408[34]
[N_{2222}][BF_4]	383[35]	[secC_5mim][Cl]	273[34]
[N_{2222}][PF_6]	388[35]	[secC_5mim][BF_4]	366[34]
[N_{2222}][NTf_2]	439[35]	[eC_3mim][Cl][c]	284[34]
[N_{2222}][Beti][a]	470[35]	[eC_3mim][BF_4][c]	363[34]
[N_{2222}][Me][b]	411[35]	[C_6mim][Cl]	128[20], 253[33b]
[N_{4444}][NTf_2]	403[35]	[C_6mim][BF_4]	348[20]
[N_{4444}][Beti][a]	423[35]	[C_6mim][PF_6]	390[33b], 439[20]
[N_{4444}][Me][b]	403[35]	[C_6mim][NTf_2]	428[36]
[N_{6222}][$N(CN)_2$]	230[37]	[C_8mim][Cl]	243[33b]
[C_2C_1pyrrol][$N(CN)_2$]	250[37]	[C_8mim][PF_6]	376[33b], 416[20]
Imidazolium ionic liquids		[C_8mim][NTf_2]	425[36]
[C_2mim][Cl]	285[35]	[C_{12}mim][Cl]	239[33a]
[C_2mim][Br]	311[35]	[C_{16}mim][Cl]	230[33a]
[C_2mim][I]	303[35]	[Amim][Cl][d]	249[23]

[1] The nomenclature of ILs is not generalised up to date, although the nomenclature applied here follows a general consensus. The ion-pair is given between brackets, [Cat][An]. Hereby, the cations are either denoted with a heteroatom symbol followed by digits denoting the alkyl chain length (commas are used to avoid ambiguity), or denoted with an abbreviation for the core i.e. imidazolium (im), pyridinium (pyr), pyrrolidinium (pyrrol), or piperidinium (pip). The latter are preceded by the substituents, i.e. C_n: alkyl chain with length n; or m_n: methyl groups with number n, the first one being placed on the *N*-atom. The (in)organic anions are denoted with their chemical formula or with an abbreviation for the more complex organic anions, i.e. Me (methide, $[C(CN)_3]^-$), Beti (bis(pentafluoroethylsulfonyl)imide), FAP (tris(pentafluoroethyl)trifluorophosphate).

$[C_2mim][CF_3CO_2]$	150[38]	$[Amim][BF_4]$[d]	400[39]
$[C_2mim][MeSO_4]$	390[40]	[Bnmim][Cl]	278[34]
$[C_2mim][EtSO_4]$	408[40]	[mBnmim][Cl][e]	248[34]
$[C_2mim][TfO]$	440[38]	$[Bnmim][BF_4]$	384[34]
$[C_2mim][N(CN)_2]$	275[41]	$[mBnmim][BF_4]$[e]	228[34]
$[C_2mim][MeSO_3]$	293[42]	*C2/4/5 substituted imidazolium salts*	
$[C_2mim][CF_3SO_3]$	348[42]	$[C_2m_2im][Br]$	322[35]
$[C_2mim][BF_4]$	450[35], 445[25a]	$[C_2m_2im][Cl]$	287[35]
$[C_2mim][PF_6]$	375[35]	$[C_2m_2im][PF_6]$	500[35]
$[C_2mim][AsF_6]$	416[35]	$[C_2m_2im][NTf_2]$	456[35]
$[C_2mim][NTf_2]$	419[42], 439[36], 410[33a] 440[38], 455[35]	$[C_2m_2im][Beti]$[a]	420[35]
$[C_2mim][C(CN)_3]$	450[35]	$[C_3m_2im][Cl]$	260[33a], 286[35]
$[C_2mim][Beti]$[a]	462[35]	$[C_3m_2im][BF_4]$	390[33a]
$[C_3mim][Cl]$	282[35], 269[34]	$[C_3m_2im][PF_6]$	399[35]
$[C_3mim][BF_4]$	393[34]	$[C_3m_2im][NTf_2]$	457[25a], 462[35], 462[43]
$[C_3mim][PF_6]$	335[35]	$[C_4m_2im][Cl]$	257[33a]
$[C_3mim][NTf_2]$	452[35]	$[C_4m_2im][BF_4]$	380[43], 405[33a]
$[isoC_3mim][Cl]$	277[34]	$[C_4m_2im][PF_6]$	373[43], 425[33a]
$[isoC_3mim][I]$	296[35]	$[isoC_4m_2im][BF_4]$	350[33a]
$[isoC_3mim][BF_4]$	370[34]	$[isoC_4m_2im][PF_6]$	382[33a]
$[isoC_3mim][PF_6]$	332[35]	$[C_{10}m_2im][BF_4]$	400[33a]
$[isoC_3mim][NTf_2]$	432[35]	$[C_{10}m_2im][PF_6]$	420[33a]
$[C_4mim][Cl]$	125[20], 264[43], 234[33a] 254[33b], 268[34]	$[C_{16}m_2im][Cl]$	239[33a]
$[C_4mim][Br]$	273[43]	$[C_{16}m_2im][BF_4]$	400[33a]
$[C_4mim][I]$	265[33b]	$[C_{16}m_2im][PF_6]$	400[33a]
$[C_4mim][MeSO_4]$	395[40]	$[C_{16}m_2im][Br]$	253[33a]
$[C_4mim][EtSO_4]$	387[40]	$[C_{20}m_2im][Br]$	259[33a]
$[C_4mim][N(CN)_2]$	300[43]	$[C_{20}m_2im][BF_4]$	390[33a]
$[C_4mim][TfO]$	392[43]	$[m_5im][I]$	303[35]
$[C_4mim][BF_4]$	360[44], 361[43], 403[33b] 424[25a], 380[34]	$[m_5im][PF_6]$	401[35]
$[C_4mim][PF_6]$	349[33b]	$[m_5im][NTf_2]$	470[35]
$[C_4mim][NTf_2]$	409[42], 427[36], 439[33b] 450[20]	$[Am_2im][BF_4]$[d]	332[33a]
$[C_4mim][Me]$[b]	413[43]	[2-phenylethyl-$m_2$im][PF_6]	386[33a]
$[secC_4mim][Cl]$	278[34]	[2-phenylethyl-$m_2$im][Br]	275[33a]

All TGA experiments were performed under N_2 atmosphere and at a heating rate of 10 °C min^{-1}, unless indicated. In references ([20, 39]) an argon atmosphere was used, in references ([34-35]) the heating rate was 20 °C min^{-1}. The pan material was platinum for references ([20, 33b]), aluminium for references ([25a, 35-36, 43]), the others were unspecified. [a] [Beti]: bis(pentafluoroethylsulfonyl)imide; [b] [Me]: tris(trifluoromethylsulfonyl)methide; [c] [eC_3mim]: *N*-(1-ethylpropyl)-*N'*-methylimidazolium; [d] [Amim] = *N*-allyl-3(*N'*)-methylimidazolium; [e] [mBnmim]: *N*-(1-methylbenzyl)-*N'*-methylimidazolium.

The short-term stability experiments (Figure 4) give rise to a point of thermal degradation, which is at times termed T_{decomp}, but in order to avoid ambiguity, we will further use T_{onset} to depict the short-term stability. T_{onset} is in fact a value calculated by the thermal analysis software, which is the translation of the intercept of two linear functions: the baseline of zero weight loss and the tangent of weight vs. temperature upon decomposition.[20, 43]

The actual degradation already starts at a lower temperature (T_{start}) than the T_{onset}.[45] Recent work of Del Sesto *et al.* proves that conventional ionic liquids such as [C_4mim][NTf_2] and [C_4mpyrrol][NTf_2] already start degrading at temperatures of about 150 °C.[46] Hence, the maximum operating temperature is considerably lower (e.g. [C_2mim][BF_4] has a T_{onset} of 455 °C but decomposes at 1.37 wt.% h^{-1} at 200 °C).[25a] It should be stressed that T_{onset} gives an overestimation of the thermal stability (sometimes T_{onset} > 400 °C), since the actual critical temperature is passed through quickly.[32b] Typically, the ramped temperature method is also characterised by a temperature of maximum degradation (T_{peak}) in between 10 to 100 °C higher than T_{onset}.[33a] Also reported is T_{dec} or $T_{10\%}$, which reflects the temperature at which a weight loss of 10% is observed, and other research groups have also applied this technique.[47] Although this is a true physical property compared to the calculated T_{onset}, the experiments are still performed at a heating rate of 10 °C min^{-1} and hence give an overestimation of the true thermal stability.

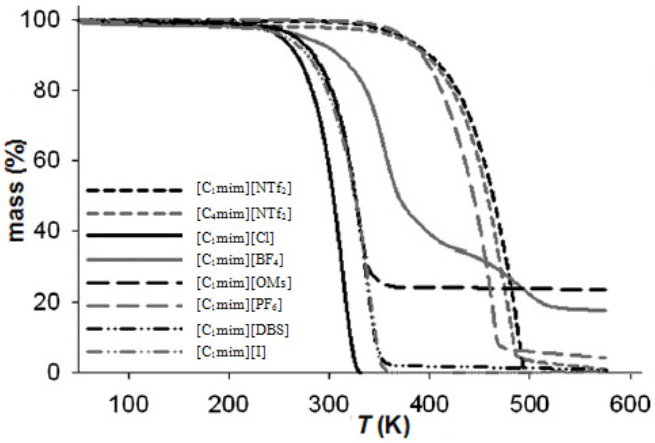

Figure 4: Ramped temperature TGA (20 °C min^{-1}, Pt pans) of imidazolium salts with different anions (DBS: paradodecylbenzenesulfonate).[25d]

While the ramped temperature TGA method offers a fairly good reproducibility if well-defined,[48] and although T_{onset} correlates well with e.g. the flash point[15a, 21b] and the activation energy of thermal decomposition,[13a] this parameter is not very significant due to lack of parameter knowledge.[49] Because of the high heating rate, decomposition and evaporation do

not reach equilibrium and the temperature profile in the sample is hard to be figured out. The temperature profile is dependent on several factors, such as the viscosity and heat transfer, heating rate, exo- and endothermic decomposition reactions, instrumentation and sample geometry and mass. Increasing the mass of the sample from 13 to 30 mg was shown to give an overestimation of the T_{onset} of 50 °C at a heating rate of 10 °C min^{-1}. Hence, it is advisable to always report the sample mass and to compare results of samples with similar mass when analysing a series of ionic liquids.[49]

2.2. Contribution of evaporation

Partial evaporation of ionic liquids can also contribute to mass loss, although volatilisation of ILs is not related to their decomposition.[32b, 50] Hereby, imidazolium ionic liquids with $[NTf_2]^-$ counter ions are considered relatively volatile as compared to their $[MeSO_3]^-$ and $[CF_3SO_3]^-$ analogues, although having vapour pressures substantially lower than hexadecane and anthracene (e.g. $P_{vap,500K}$ for $[C_2mim][NTf_2]$: 0.10 Pa, $[C_2mim][MeSO_3]$: 0.014 Pa, $[C_2mim][CF_3SO_3]$: 0.013 Pa).[42, 51] In particular for the 'volatile' ILs, evaporation has to be taken into account when the IL is in permanent contact with an inert gas which flows over or through the sample. Whether there is any contribution of evaporation is analysed by performing isothermal TGA experiments with different inert gasses (H_2 and N_2), the observed mass loss should be different for the different inert gasses.[42] Therefore, the flow rate and type of the purge gas is to be reported. The higher the heating rate, the bigger part of the ramped temperature experiment in which the evaporation dominates over decomposition and the lower the temperature in isothermal experiments, the higher the contribution of evaporation.[32b, 52] For a correct and complete thermal mass loss calculation, ΔH_{vap} and P_{vap} should be taken into account.[32b, 52] Although there is a lot of research being performed on the thermodynamic properties of ionic liquids,[53] this is beyond the scope of this section.

2.3. Short-term stability derived parameters

Next to the discussed weight change curves (m vs. t), other ramped temperature measurements can give additional information on the thermal behaviour. Thus, the derivative function (dm/dt vs. t) shows the behaviour at a given temperature,[54] and is used as control mechanism in High Resolution Modulated Thermogravimetric Analysis (HRMTGA).[32a] In this technique, the heating rate is variable beneath a nominal value (e.g. 2 °C min^{-1}) as a function of the mass loss rate. This way, T_{onset} is reduced and closer to the actual start of the degradation, hence closer to long-term stability parametric temperatures. Calorimetric information (exothermic vs. endothermic decomposition) can be accessed by monitoring the difference of jacket and sample temperature (ΔT vs. t)[13a] or by synchronous scanning differential thermal analysis (SDTA, see par. 2.3, p11).[35] Apart from temperature, pressure

and colour change can be quantitatively measured as well.[13a] Given the dependence of the thermal degradation on the heating rate, rapid heating (> 5 °C s^{-1}) implies different degradation mechanisms. Superfast heating of ionic liquids has already been applied by laser ablation or confined rapid heating, providing information on degradation patters upon e.g. combustion or application in mass spectrometry.[27a, 50a] [55]

2.4. Long-term thermal stability

To overcome the limitations posed by the ramped temperature TGA method and to obtain more profound information of the stability at higher temperatures, it is necessary to perform 'long-term' isothermal (static) TGA measurements for prolonged times (e.g. 2, 15 or 20 h).[20, 25c, 49, 56] These thermal analyses will give rise to rates of decomposition at a given temperature instead of critical or onset temperatures. Isothermal analyses show that in 10 hours over 10 weight% can be lost at temperatures lower than T_{onset} (Figure 5). The information obtained in these experiments is further elaborated in section 6.

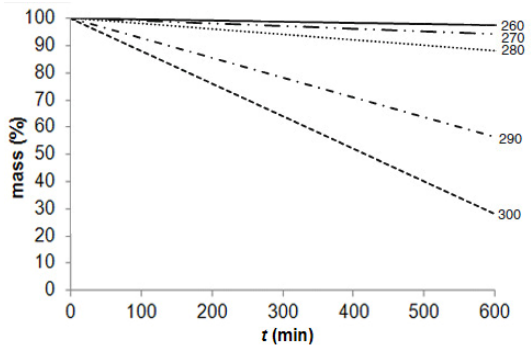

Figure 5: Isothermal gravimetrical analyses of [C_4mim][Br] at temperatures of T_{onset} ± 20 °C, N_2-atmosphere.[48b]

For uniform reporting and interpretation of long-term thermal stability, the right criterion is to be applied, and different ways have been proposed. First, the weight loss for a given time and temperature (depending on the application) can be given, (e.g. *dm*([Amim][Cl], 100 °C, 15 days) = 1.9%).[23] Second, a maximum weight loss can be suggested a priori, leading on the one hand (e.g. 1%) to the maximum time (life-time) the IL can be held at a given temperature (e.g. $t_{1\%}$(200 °C, [C_4mim][PF_6]) = 2.0 days),[25d] or on the other hand (e.g. 10%), to the maximum temperature at which no more than this weight loss occurs for a given time (e.g. $T_{10\%,10h}$([C_4mim][$N(CN)_2$]) = 110 °C).[57]

3. Influence of salt structure on thermal stability

3.1. Type of cationic core

Thermal stability is often claimed as merely dependent on the anion of the ionic liquid, but this is only the case when arrays of analogous cations are studied. Although analogues with different anions do have very divergent properties, it is clear that there is a great difference in reactivity between cation types. Thus, it is shown that pyrrolidinium ionic liquids are more temperature resistant than their imidazolium, pyridinium and non-cyclic tetraalkylammonium counterparts, in that order.[35, 41, 45, 58] In the series of saturated cyclic ammonium salts, the stability was found to decrease in the order pyrrolidinium > piperidinium ≈ morpholinium.[47d, 59] In the following paragraphs nitrogen containing ionic liquids will be elaborated first, after which also ILs with phosphorous and sulphur containing cations will be discussed.

3.2. Nitrogen-based ionic liquids

3.2.1) Influence of N-substituents

In general, the alkyl chain length of the cation has a significant influence on the thermal stability of ionic liquids. Increasing the alkyl chain length decreases the thermal stability, this is observed for imidazolium ionic liquids with basic $[Cl]^-$,[33b] and weakly coordinating $[BF_4]^-$, $[PF_6]^-$,[49, 60] or $[NTf_2]^-$ anions.[33b, 36] This same decrease of stability was observed in a series of diaryl dialkylammonium chlorides. The stability decreased by variaying the aromatic moiety. Furthermore, it was clear that the diaryl diethylammonium chloride derivatives started degrading at substantially lower temperatures that their diaryl dimethylammonium analogues. Upon increment of the number of carbon atoms between the central nitrogen and the aryl substituent, a decrease in thermal stability was also apparent.[61] The same trend is observable in *N*-alkyl-*N*-methylpiperidinium bis(trifluoromethylsulfonyl)imide salts ($[C_n mpip][NTf_2]$) in both short and long-term experiments. The reduction of thermal stability upon increased alkyl chain length, is believed to be due to the increased stability of both carbenium ion and carbon radicals when the alkyl chain length increases.[62]

In an isothermal experiment without inert atmosphere, Kosmulski *et al.* also observed a decreased thermal stability for imidazolium $[PF_6]^-$ and $[TfO]^-$ salts with increasing the alkyl chain length.[49] An opposite trend was found by Zhang *et al.* in an isothermal experiment at 285 °C under argon atmosphere. At 285 °C, $[C_6mim][PF_6]$ is not stable, although $[C_8mim][PF_6]$ shows no decomposition. Conversely, at 333 °C, the weight loss rate is again much higher for the salt bearing the longest alkyl chains.[20]

Branching of the alkyl substituents on imidazolium salts also influences thermal stability, although dependent on the anion. Thus, Erdmenger *et al.* found that the branched imidazolium $[Cl]^-$ salts are more stable, while the branched imidazolium $[BF_4]^-$ salts are less stable than their linear counterparts (Table 1). This observation is explained by the differences in degradation mechanisms (*vide infra*).[34] The same decrease in stability is found for isopropyl substituted imidazolium salts ($[isoC_3mim][PF_6]$ and $[isoC_3mim][NTf_2]$) and also for isobutyl substituted imidazolium salts ($[isoC_4mim][BF_4]$ and $[isoC_4mim][PF_6]$).[33a, 35] When the nitrogen is substituted with benzyl, an increase in thermal stability of the $[Cl]^-$ salt was found, while on the other hand, the benzylated $[BF_4]^-$ salt was not as stable as the linear analogues, suggesting the predominance of an S_N1 degradation mechanism in ionic liquids with non-coordinating anions. The *N*-(1-methylbenzyl)-*N'*-methylimidazolium cation however, showed lower stabilities than the linear analogues when combined with either $[Cl]^-$ or $[BF_4]^-$. This indicates that here, the enhanced stabilisation of the benzylic cation by the methyl group provokes an S_N1 mechanism in the case of the $[Cl]^-$ salt too.[34] Because of the promising stabilities of *N*-benzyl substituted imidazolium ionic liquids combined with more basic anions, 1-benzyl-3-methylimidazolium triflate [Bzmim][TfO] (**21**) and 1-(4-methoxyphenyl)-3-methylimidazolium triflate [MPmim][TfO] (**22**) (Figure 6) were used as a liquid phase stable up to 260 °C in GLC (gas-liquid chromatography) by Anderson and co-workers.[30a]

Imidazolium ionic liquids containing unsaturated side chains possess generally lower thermal stability than their fully saturated analogues. Increasing distance between alkene and nitrogen in imidazolium ionic liquids leads to increased thermal stability, while alkyne functionalities imply decreased stability (propargyl vs. allyl), attributed to the rigidity of the group.[32a]

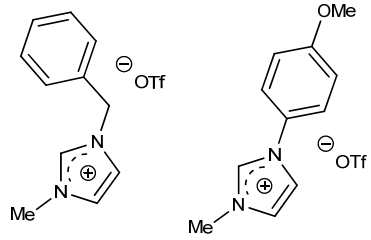

21 **22**

Figure 6: Examples of imidazolium cations with improved thermal stabilities: [Bzmim][TfO] and [MPmim][TfO].[30a]

The thermal stabilities of ether containing ammonium $[NTf_2]$ salts, i.e. the diethyl-bis-(2-methoxyethyl)ammonium $[N_{22(1O2)(1O2)}]^+$, ethyl-tris-(2-methoxyethyl)ammonium $[N_{2(1O2)(1O2)(1O2)}]$, methyl-tris-(2-methoxyethyl)ammonium $[N_{1(1O2)(1O2)(1O2)}]^+$ and tetrakis-(2-methoxyethyl)ammonium $[N_{(1O2)(1O2)(1O2)(1O2)}]^+$ salts, were characterised by T_{onset} values in the range 280-370 °C, indicating that these polyalkoxyalkylammonium salts are less stable than their hydrocarbon analogues.[63] Reduction of thermal stability is also observed upon introduction of alkoxylated side chains in pyrrolidinium, piperidinium and imidazolium

cations.[64] In general, a small decreasing effect is found for an increasing number of alkoxy groups on the thermal stability.[65] Not only alkoxylated side chains have an adverse effect on the thermal stability, also cyclic ammonium ionic liquids with ether functionalities incorporated in the *N*-heterocyclic core have decreased T_{onset} values compared to their cyclic alkyl analogues, i.e. morpholinium and, more significantly, oxazolidinium salts are less temperature resistant than their respective analogous piperidinium and pyrrolidinium salts.[63b, 66] The influence of the distance between the ether functionality and the nitrogen atom is apparent. Thus, methoxymethyl groups are much more susceptible to thermal degradation (up to 100 °C decrease) than analogues containing methoxyethyl side chains. Also, much lower resistant to thermal degradation than their hydrocarbon analogues are the symmetrical methoxyalkyl substituted imidazolium salts (alkyl: C_3 to C_{12}), with a decreased stability for the shorter alkylchains.[67] The thermal instability of alkoxymethyl substituents is attributed to the increased acidity of the protons on the OCH_2N carbon. Although the instability could clearly be attributed to these alkoxy substituents for the $[BF_4]^-$ and $[NTf_2]^-$ salts, while this was not observed for the (perfluoroalkyl)trifluoroborate ($[R_FBF_3]^-$) anion. This observation demonstrates the *virtual* independency of thermal stability on the cation structure when combined with low-stability anions, as is demonstrated in Figure 7.[63b]

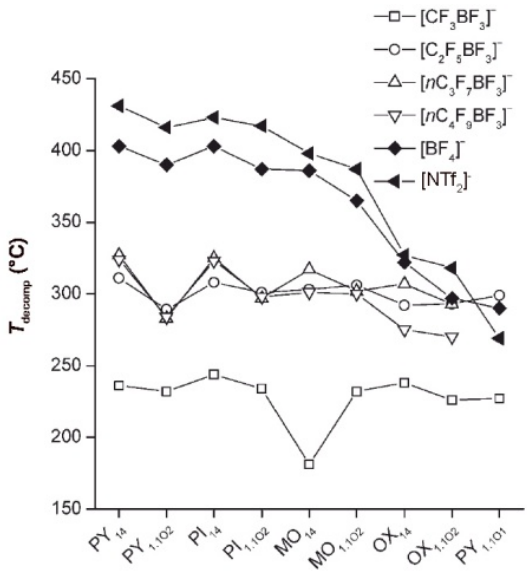

Figure 7: T_{onset} of different cyclic quaternary ammonium cations combined with (in)organic fluorinated anions. Cations: pyrrolidinium (PY), piperidinium (PI), morpholinium (MO), oxazolinium (OX); alkyl groups: 1: methyl, 4: butyl, 1O2: methoxyethyl, 1O1: methoxymethyl.[63b]

3.2.2) Influence of C-substituents

Generally, substitution of imidazolium ring protons by methyl groups leads to only a small increase in thermal stability.[25c, 25d, 35] Although methyl substitution at the imidazolium C2

clearly renders more stable ionic liquids, increased alkylation of this position does not lead to an increased thermal stability.[33a, 35, 43, 45, 68] This might be explained by the acidity of the C2 proton (pK_a: ±25),[69] which can be deprotonated by sufficiently basic anions.[35] However, methyl substitution in the 2-position was found to raise the thermal stability of ionic liquids containing not only halide, but also perfluorinated inorganic and perfluorinated organic anions. Only for the $[Beti]^-$ anion, which has the highest T_{onset} in the latter experiments, an anomaly is observed (see Table 1).[33a, 35] The difference in T_{onset} between $[C_4mim][Cl]$ and $[C_4m_2im][Cl]$ is as large as 23 °C.[33a] The influence of the substitution pattern of pyridinium $[Br]^-$ and $[NTf_2]^-$ salts was investigated by Crosthwaite *et al*. The thermal degradation behaviour of a series *N*-hexylpyridinium $[C_6pyr]$, *N*-hexyl-3-methylpyridinium $[C_6mpyr]^+$ and 3,5-dimethyl-*N*-hexylpyridinium $[C_6m_2pyr]^+$ was compared. In the case of the $[Br]^-$ salt, no obvious difference is seen, but for the $[NTf_2]^-$ salts, an increase of degree of substitution clearly leads to an increase of the thermal degradation resistance. Upon ethyl substitution in the 2-position, the adverse effect is observed. Moreover, it was found that the introduction of a substituted amino group (dimethylamino and piperidino group) in the 4-position leads to the stabilisation of the positive charge and hence to an increased thermal stability.[45]

3.3. Dicationic ionic liquids

This novel class of ionic liquids has found application in various field such as stationary phases in GC and GLC chromatography,[30a-c] high temperature lubricants,[26] and as solvents.[22c] For example, a Claisen rearrangement at 250 °C was successfully performed in the dicationic 1,9-bis-(3-methyl-1-imidazolyl)nonane ionic liquid ($[C_9(mim)_2][NTf_2]$).[22a] The thermal stabilities of dicationic ionic liquids are higher than those of their monocationic building blocks.[47b, 70] The *germinal dicationic* (with two identical cations) imidazolium and pyridinium ionic liquids $[C_9(mim)_2][NTf_2]$ and $[C_9(mpyr)_2][NTf_2]$ have an increased thermal stability, with a T_{onset} of about 150 °C above the decomposition temperature of $[C_4mim][NTf_2]$.[70] The same increase in stability is found for unsymmetrical dicationic ionic liquids, which comprise two different cations.[71] The observed higher thermal stability of dicationic ionic liquids is attributed to the greater charge and intermolecular interactions, their higher molecular weight, higher density, smaller free volume and higher shear viscosity.[30c] The reversibility of the degradation reactions allows the recombination of the fragments which do not move away due to this 'cage effect'.[47b]

The type of linker between the two cations also has an important influence on the thermal stability, changing the linker from 1,4-dimethylene-2,3,5,6-tetrafluorobenzene to 1,4-dimethylenebenzene and further to a polyether chain in imidazolium dicationic ionic liquids increases the thermal stability.[26a] Imidazolium based dicationic ionic liquids connected with PEG-linkers have also been synthesised, they show similar thermal resistance as do

dicationic ionic liquids with hydrocarbon linkers.[30c] Apart from nitrogen-based dicationic, also phosphonium dicationic ionic liquids show improved thermal performance over their monocationic analogues.[30b]

3.4. Phosphonium ionic liquids

Tetraalkyl phosphonium dicyanamide salts are thermally more stable than their corresponding tetraalkylammonium salts. In a series of phosphonium dicyanamide salts, the decomposition temperature at which 10% weight loss occurs ($T_{10\%}$, Table 2) is about 100 °C higher than for the analogous ammonium salts.[47a] However, the long-chain phosphonium chloride salts $[P_{888n}][Cl]$ (n = 2-14) have a T_{onset} from 295 to 330 °C, which is relatively low compared to pyridinium or imidazolium based salts.[72] This was confirmed by the decrease of T_{onset} with about 54 °C for $[P_{66614}][NTf_2]$, as compared to $[C_2mim][NTf_2]$.[32a]

Table 2: Temperatures of 10% weight loss ($T_{10\%}$, 10 °C min^{-1}) of polyalkoxy phosphonium and their analogous ammonium ionic liquids.[47a]

IL[a]	$T_{10\%}$ (°C)
$[P_{2225}][N(CN)_2]$	393
$[P_{2228}][N(CN)_2]$	394
$[P_{222(101)}][N(CN)_2]$	278
$[P_{222(201)}][N(CN)_2]$	244
$[P_{4441}][N(CN)_2]$	387
$[P_{4448}][N(CN)_2]$	389
$[N_{2225}][N(CN)_2]$	270
$[N_{2228}][N(CN)_2]$	271
$[N_{222(101)}][N(CN)_2]$	154
$[N_{4441}][N(CN)_2]$	260

[a] (1O1): methoxymethyl, (2O1): methoxyethyl.

The unsaturated allyltributylphosphonium salt $[P_{444(Al)}][NTf_2]$ was found to have a higher temperature stability than its corresponding saturated analogue $[P_{4443}][NTf_2]$.[73] The same increase in thermal stability upon introduction of unsaturated moieties was found for the analogous (4-pentenyl)triethylphosphonium ($[P_{222(Pe)}][NTf_2]$) and benzyltriethylphosphonium ($[P_{222(Bz)}][NTf_2]$) salts.[73-74] It is presumed that the interaction of the empty d-orbitals of the phosphonium cation with the counter anion is assisted by the π-electron systems provided by the unsaturated carbons, resulting in an additional increase of the bond strength.[73]

3.5. Sulfonium ionic liquids

Both cyclic and linear tertiary sulfonium ionic liquids are found to be less thermally stable than imidazolium and quaternary ammonium salts.[75] In ramped temperature experiments, a very narrow temperature range in which decomposition takes place was found for different trialkylsulfonium dicyanamide salts; all ionic liquids start degrading between 176 and 183 °C, indicating a very small contribution of the cation structure. In a long-term thermal stability test, trimethylsulfonium dicyanamide lost about 5% of its weight after 12 h at 100 °C. The weight loss is attributed to the thermolytic formation of volatile dimethylsulfide and non-volatile methyl dicyanamide.[76] Thermal degradation of alkyldimethylsulfonium $[PF_6]^-$ and $[NTf_2]^-$ salts was investigated by Yang *et al.*, while Fang and co-workers also investigated alkyldiethylsulfonium and alkylethylmethylsulfonium $[NTf_2]^-$ salts. All these ILs start decomposing at temperatures of about 270-315 °C, although the hexyldimethylsulfonium salt, $[S_{116}][PF_6]$, is stable up to 390 °C.[77] For trialkylsulfonium $[NTf_2]^-$ salts, a reduction in thermal stability is observed when functional groups (cyano, ether and ester groups) are introduced.[65a]

3.6. Type of anion

The thermal stability of analogous salts with different anions correlates well with the anion hydrophobicity, since this is a measure for the hydrogen bonding capacity and hence often the nucleophilicity.[33b] In general, the thermal stability of common anions can be condensed to the following relative order: $[PF_6]^-$ > [Beti]$^-$ > $[NTf_2]^-$ > $[BF_4]^-$ > $[Me]^-$ ~ $[AsF_6]^-$ > $[I]^-$, $[Br]^-$, $[Cl]^-$.[33, 35, 78] In $[P_{66614}]^+$ salts, the thermal stability decreases consistently in the order $[NTf_2]^-$ > $[FAP]^-$, $[N(CN)_2]^-$ > $[Cl]^-$ > $[MeSO_4]^-$.[32a] It is clear that halides significantly reduce thermal stability since they possess both a relative big nucleophilic and basic character. The observed results are in line with the corresponding nucleophilicity order in ionic liquids. Lancaster *et al.* found that I^- is more nucleophilic than Cl^-, which is a little more nucleophilic than Br^- (I^- >>Cl^- > Br^- >F^-). This might indicate an S_N2 character of the thermal degradation of halide salts.[79] Basicity of anions should also be considered, in order not to exclude the possibilities of elimination. As basicity decreases in the order F^- > Cl^- > Br^- > I^-, the chloride salts will show greater vulnerability to elimination as well. In general $[Br]^-$ salts are about 10 to 30 °C more stable than their $[Cl]^-$ counterparts, however $[I]^-$ salts have about the same stability as the $[Br]^-$ salts.[33a, 35] The non-coordinative anions exert a higher thermal stability, the (perfluoroalkylsulfonyl)imides and $[PF_6]^-$ showing the best stabilities.

The cyclic ammonium analogues combined with the $[R_FBF_3]^-$ anion (R_F = C_4F_9, C_3F_7, C_2F_5) were all found to have thermal decomposition temperatures (T_{onset}) of about 280 to 330 °C, independent on the cation (Figure 7). The $[CF_3BF_3]^-$ salt was found to decrease T_{onset} with an

additional 50 °C, due to a decomposition reaction in which a difluorocarbene is formed ($[CF_3BF_3]^- \rightarrow [BF_4]^- + CF_2$).[80]

The influence of alkylsulfate anions in piperidinium, pyrrolidinium and morpholinium salts on thermal stabilities were investigated by Wu *et al.*[47d] The thermal decomposition pattern of these salts reveals that the first stage thermal decomposition (fast decomposition from 100 to ca. 20 wt.%) of these ILs, represented by T_{onset}, is related to the structure of the anions; the thermal stability of anions at T_{onset} being methylsulfate > ethylsulfate. The second stage thermal decomposition at higher temperatures (370 - 700 °C) of these ILs is more related to the structure of the cations. The imidazolium salts with different alkylsulfates investigated by Holbrey *et al.* showed no distinct differences in T_{onset}, although the weight loss percentage observed in the range 50-400 °C was substantially bigger for the ethylsulfate derivatives than for the methylsulfates.[40]

The decrease in nucleophilicity by fluorinating the anion is directly translated into thermal stability, thus, upon fluorination of the $[OMs]^-$ anion, more stable $[TfO]^-$ imidazolium salts are obtained.[25d] Replacing the $[NMs_2]^-$ anion by the fluorinated $[NTf_2]^-$ anion in ammonium, imidazolium and phosphonium salts, also increased the T_{onset} with over 100 °C.[81] Between different fluorinated anions, thermal stability decreases also with increasing nucleophilicity, thus Bonhôte *et al*. noticed the superior stabilities of $[TfO]^-$ and $[NTf_2]^-$ salts over to the $[CF_3COO]^-$ anion (see Table 1).[38]

Han *et al.* noticed a decrease of the thermal stability, independent on the cation species, when passing from $[NTf_2]^-$ to the $[N(SO_2F)_2]^-$ (bis(fluorosulfonyl)imide) anion.[65a] Sulfonium IL comprising the latter anion were still found more thermally stable than their $[N(CN)_2]^-$ analogues.[65a] Since salts with the asymmetric $[(FSO_2)N(SO_2C_2F_5)]^-$ anion also show reduced thermal stability with respect to $[NTf_2]^-$ salts, the reduced thermal stability is explained by the greater lability of FSO_2-functions towards pyrolysis.[82]

4. Influence of environment and impurities

Although (fast) ramped temperature analyses do not always show clear differences between oxygen and nitrogen purged experiments and the low solubility of O_2 in ILs is proposed to lead to only little influence of the applied atmosphere,[23, 35] a dependence of the atmosphere on the decomposition behaviour can be demonstrated.[33a, 62] For both the tetraalkylammonium halide salt $[N_{1,1,18,18}][Br]$[33a] and the cyclic ammonium salts $[C_n mpip][NTf_2]$ (n = 3-8),[62] a lower T_{onset} was observed in the presence of air. In the latter case, both ramped temperature and isothermal experiments showed degradation temperatures of about 50 °C lower in the presence of air compared to those in an inert atmosphere.[83] The presence of air seems to

decrease the T_{onset} significantly for imidazolium $[PF_6]^-$ and $[BF_4]^-$ salts, however, this decrease was not found for the same cation type with halide anions. This suggests a lower activation energy for the non-oxidative decomposition than for the oxidative degradation of halide containing imidazolium ionic liquids, and a fairly higher activation barrier for non-oxidative decomposition in the ILs with inorganic perfluorinated anion types. In the same way, thermal decomposition temperatures of imidazolium salts comprising the organic perfluorinated anion $[NTf_2]^-$ are also influenced by the atmosphere, albeit to a lesser extent.[33a]

In general, the presence of water alters ionic liquid properties significantly, and drying of the ionic liquids will improve the thermal stability. In contrast to $[C_4mim][NTf_2]$, which is less stable in the presence of water, a higher thermal stability of $[C_4mim][PF_6]$ and $[C_4mim][Cl]$ is found in the presence of water.[13a, 33b] Although no volatile compounds are formed by reaction of ILs with water,[21b] water in particular can alter heat transfer properties and consequently influence ramped temperature TGA measurements. Hence, the presence of water can explain for the anomalies found in some publications[49] and in particular hygroscopic IL such as nitrates should be thoroughly dried before investigation,[27a, 84] although water-equilibrated IL can be analysed, dependent on the application conditions.[48b] Investigation of water equilibrated ionic liquids (up to 31 wt.% H_2O in $[C_2mim][BF_4]$) shows that water does not affect the decomposition on isothermal gravimetric analysis, although it was presumed that water in combination with the anion would lead to the formation of HF. A clear weight loss is observed at about 100 °C, which is attributed to the evaporation of the present water. The resulting salt acts as if it is in its pure form.

Analogously to the presence of water, the addition of 10 mol% Cl does not affect the isothermal gravimetric behaviour.[25a] The independency of the isothermal decomposition rate on addition of chloride is in line with the observation where at first a fast weight decrease is observed, attributed to and seen as a measure of impurities, followed by a constant weight decrease, specific for the ionic liquids.[49] In a ramped temperature experiment, the addition of small amounts of $[C_4C_1mim][Cl]$ to $[C_4C_1mim][BF_4]$ leads to an equimolar loss of $[C_4C_1mim]$.[56a] Other residual starting material might also decrease thermal stability, e.g. basic imidazole can subtract C2 protons in imidazolium IL, leading to carbenes which can undergo further degradation reactions. Apart from ionic liquid synthesis, also recycling of IL contributes to contamination, thus, recycled $[C_2mim][Ac]$, used for spinning of cellulose, shows a significant lower thermal stability.[13a]

The influence of inorganic impurities on the thermal stability was investigated by Kosmulski *et al*. A significant raise in isothermal weight loss is observed upon addition of amorphous silica, and also upon addition of TiO_2 and Al_2O_3, albeit to a lesser extent, indicating the possible catalytic activity of oxides.[49] Therefore, careful selection and reporting of pan material

(crucible in which the sample is placed during a TGA experiment) is paramount (most commonly used are aluminium, alumina and platinum). Thermal decomposition is generally lower on aluminium than on alumina pans, but this is nonetheless dependent on the salt structure. Thus, in contrast to the imidazolium salts with organic (perfluorinated) anions, which are not or only little more stable on aluminium pans, a faster decomposition of the $[Br]^-$ salts is observed in aluminium pans.[31] The T_{onset} values of imidazolium $[PF_6]^-$ salts are in between 51 and 106 °C higher on alumina pans. Moreover, for these $[PF_6]^-$ salts, an exothermic decomposition occurs on aluminium pans, while this is an endothermic reaction on the alumina pans.[35] This difference is less pronounced for imidazolium $[TfO]^-$ salts, which give only slightly lower degradation temperatures on aluminium. For these salts, no significant difference was found between alumina pans and homemade silver pans.[49]

Bridges *et al.* have constructed $[C_4C_1mim][NTf_2]$ based Nanoparticle-Enhanced Ionic Liquids (NEILs) as heat-transfer fluids by deliberate addition of Al_2O_3 and carbon black to the IL and studied their thermal stability by long-term isothermal heating. The obtained data suggests that no significant weight-loss occurs below 300 °C and that the impurities in the ionic liquid cause only a small increase in the isothermal decomposition rates.[25c]

5. Mechanisms of decomposition

The exact mechanism of thermal ionic liquid degradation is not straightforward since multiple parameters must be taken into account. Thus, the decomposition mechanisms are subject to multiple simultaneous initiation reactions (i.e. homolytic cleavage and proton transfer), autocatalytic effects and finally, competing reaction pathways with different reaction rates dependent on temperature and heating rate.[27a]

5.1. Analytical and computational methods

Apart from short and long-term (calorimetric) TGA and superfast heating experiments (*vide supra*), other techniques have been applied in the publications cited. These specialised techniques can contribute to the exact unravelling of the thermal degradation pathways, mainly by identification of the degradation products. Thus, investigation of thermal stabilities has already been performed by coating the ionic liquid in fused silica capillaries which are heated and monitored by FID or mass spectrometry (MS),[30c, 30d, 70] as well as by pyrolysis-GC,[60, 85] headspace GC/MS,[13a] pyrolysis-MS,[31] TGA-MS,[4, 23, 52, 55] and thermal desorption mass spectroscopy (TDMS).[33a] Although TGA-MS is a very powerful method, it should be noted that the absence of molecular ions does not necessarily exclude vaporisation, since the transfer of TGA to MS and pressure differences herein involved hinder the detection.[52] Recently, also a highly sensitive potentiometric titration method has been applied to

investigate long-term thermal stability behaviour of ionic liquids at elevated temperatures.[86] Chowdhury *et al*. have applied a 'confined rapid thermolysis', i.e. an analysis of degradation products formed by heating the sample to above 400 °C within 5s. The (very small) sample is hereby confined between two heaters which allow a very high heating rate. In combination with FTIR and ToF-MS, the formed degradation products can be monitored on-the-fly.[27a] All these methods are preferentially aided by mathematical (*in silico*) predictions and modelling, which in turn can be verified by the experimental results.[23, 32b, 55, 87]

5.2. Anion degradation

Ngo *et al.* observed the heat transfer for a series of ionic liquids in a SDTA experiment. Herein it is clear that in general, ionic liquids have an endothermic degradation mechanism, probably by loss of an alkyl chain. In contrast to imidazolium ionic liquids containing inorganic anions (e.g. $[PF_6]$),[60] thermal degradation of those with perfluorinated organic anions such as $[NTf_2]^-$ and $[Beti]^-$ generally occurs exothermic.[35] The observed exothermic behaviour is due to the presence of sulfonyl groups, as evolution of SO_2 is predicted by DFT calculations (Scheme 6).[87] An exception however, is the *N*-isopropyl substituted imidazolium salt $[isoC_3mim][NTf_2]$, which has an endothermic degradation since the alkyl chain is cleaved off first. Also for tetraalkylammonium salts comprising these fluorinated organic anions a lower degradation temperature and an endothermic reaction is observed, indicating a similar mechanism, in which the decomposition of the cation is more readily established. Furthermore, the endothermic degrading salts change thermodynamic behaviour (i.e. from endothermic to exothermic degradation) halfway the weight loss process in the presence of oxygen.[35] For dicyanamide salts, Kroon *et al*. predicted by means of DFT calculations that the decomposition reaction differs from the expected formation of *N*,*N*,*N*-dicyanomethylamine (Scheme 7) and is therefore referred to as a reverse Menshutkin-like decomposition reaction.[87]

As in imidazolium type ionic liquids increased thermal stability is observed for increasing ring substitution (from $[C_4mim]^+$ over $[C_4m_2im]^+$ to $[m_5im]^+$ salts),[35] it is suggested that the removal of (acidic) protons decreases the thermal degradation. A proposed decomposition mechanism therefore involves proton abstraction to produce both volatile anion-derived acids and imidazolium-derived carbenes.[33b] Thus, during thermal decomposition of $[C_2mim][Ac]$, acetic acid was observed by headspace GS/MS analysis.[13a] However, the inverse relation between substitution and stability was found in DFT-calculations by Kroon *et al.*, who attributed the lower thermal stability of 2*H*-imidazolium ionic liquids to the acidity in the presence of traces of water.[87]

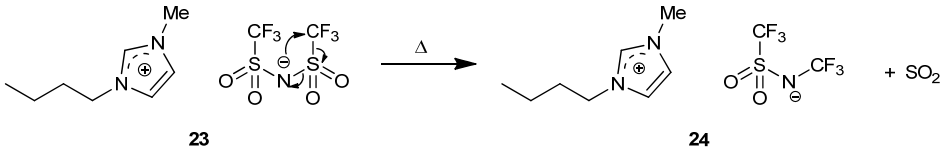

23 **24**

Scheme 6: Exothermic thermal decomposition of the bis(trifluoromethylsulfonyl)imide anion.[87]

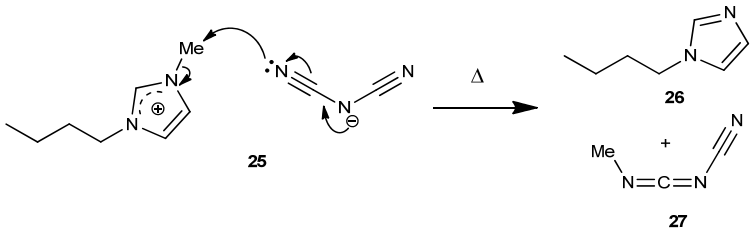

25 **26** **27**

Scheme 7: Thermal decomposition of $[C_4mim][N(CN)_2]$ via a reverse Menshutkin-like reaction.[87]

The thermal degradation of imidazolium $[BF_4]^-$ salts was predicted by *ab initio* calculations to form alkylimidazoles, alkylfluorides and BF_3 and in the presence of water, an alcohol and HF might be formed.[87] Since the formation of HF upon pyrolysis of both $[BF_4]^-$ and $[PF_6]^-$ salts is experimentally confirmed, an alkaline trap should be used when performing thermolytic analysis on these types of ionic liquids.[85]

Baranyai *et al.* did some interesting work on the speciation of degradation products of imidazolium IL by pyrolysis mass spectrometry.[31] Three ILs were examined: $[C_2mim][NTf_2]$, $[C_2mim][NMs_2]$ and $[C_2mim][Br]$. Upon pyrolysis of $[C_2mim][NMs_2]$ and $[C_2mim][Br]$, the neutral 1-alkylimidazoles were almost exclusively detected as cation degradation products, predominantly 1-ethylimidazole but also 1-methylimidazole, indicating the higher vulnerability of the methyl substituent. The anions were found to be alkylated for the $[NMs_2]^-$ and $[Br]^-$ salt, although alkylated $[NTf_2]^-$ species were not detected, neither were any of their corresponding (super)acids. In addition to these decomposition species, also dimethylsulfone was detected upon pyrolysis of $[C_2mim][NMs_2]$, originating from the methylated anion.

Upon thermal degradation of the commercial ILs $[P_{66614}][CH_3(CH_2)_8CO_2]$ and $[P_{66614}][NTf_2]$ in ambient atmosphere, mainly organophosphorous compounds with different number (dependent on the oxidation state) and length of hydrocarbon substituents are found, next to H_3PO_4, presumably originating from the reaction of P_2O_5 and water. Among the degradation products of the phosphonium bis(trifluoromethylsulfonyl)imide salt, also SO_2, SO_2CF_3, CF_2CF_2 and HF were found.[4] Investigation of $[C_2mim][NTf_2]$ degradation shows that CF_3, F and NH_2 as anion fragments are responsible for the subsequent cation decomposition.[52]

5.3. Reverse Menshutkin reaction

In imidazolium salts, a major thermal degradation component is the neutral 1-alkylimidazole.[88],[23, 27a, 31] The reverse Menshutkin reaction, which is the dealkylation process furnishing neutral species, is possible at temperatures as low as 100 °C, which is below commonly applied temperatures in TGA experiments.[89] On the other hand, no imidazole ring degradation occurs up to 600 °C (no formation of HCN).[27a, 85, 90] Hence, the main degradation mechanisms in the temperature range of thermogravimetrical experiments will include loss of an alkyl chain. Thus, the formation of alkylhalides has already been demonstrated in ammonium[60] and imidazolium halide salts.[85] The stability of ILs in general might therefore be described by the kinetics of both reverse Menshutkin and Menshutkin reactions, the nucleophilicity of both anion and neutral 1-alkylimidazole or other corresponding building block, the kinetics of evaporation and the boiling points of the degradation products (Scheme 8). Hence, a lower thermal stability can be expected for ionic liquids derived from smaller neutral building blocks (such as alkylamines).

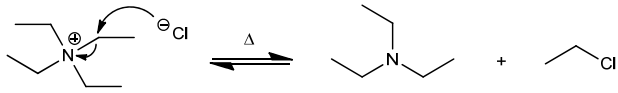

28 29 30

Scheme 8: Reverse Menshutkin reaction for $[N_{2222}][Cl]$.

The degradation of [Amim][Cl] and $[C_4mim][Cl]$ proceeds via two channels: reverse Menshutkin reaction on both the *N*-substituents. Given the higher thermodynamic stability of allylchloride and BuCl vs. MeCl, the decomposition pathway at lower temperatures is proposed to be the formation of methylimidazole and AllylCl or BuCl, respectively. Increasing temperature should lead to the cleavage of the methyl group. The formed AllylIm, BuIm and BuCl are susceptive to further decomposition, the latter two are even never directly detected by MS.[23]

In the rapid thermolysis experiment of $[C_2mim][Cl]$ by Chowdhury *et al*., also the formation of both (MeCl + EtIm) and (EtCl + MeIm) was observed, although it was clear that the pathway involving substitution of the methyl group was dominant. More important, the FTIR spectra never indicated the formation of HCl (a strong IR absorber), which means no direct proton transfer occurs to the anion,[27a] although the reaction of alkylchlorides with water can induce HCl formation.[13a] No difference is found in degradation pattern between $[Cl]^-$ and $[Br]^-$ imidazolium salts.[85] Since MeCl is stable against degradation in these MS-experiments, CH_3^+ peaks are observed in the MS-spectra. The IL $[C_2mim][NO_3]$ pyrolyses to form $MeONO_2$ or $EtONO_2$, however, while also more EtIm than MeIm mass peaks are observed, here the amount of CH_3^+ peaks is relatively small, indicating the involvement of the nitrate counter ion

in both dealkylation and secondary reactions. Nitric acid (HNO_3), formed by abstraction of ring protons by the anion was not found, although MeOH was found as a degradation product, indicating that a methoxide is formed as a secondary degradation product of $MeONO_2$, which in turn deprotonates the imidazolium C2, C4 and C5 positions and can couple to form the detected methoxyethylimidazole.[27a]

In contrast to the higher thermodynamic stability of degradation products formed by loss of the longest alkyl chain, nucleophilic attack will preferentially occur on the methyl substituent, this is a result of the higher steric hindrance of the longer alkyl chain. Moreover, by increasing the alkyl chain length, this preference will increase.[27a, 31, 85] Hence, thermal degradation is kinetically driven. The calculated charge pattern of imidazolium salts by Natural Atomic Orbital (NAO) analysis shows partial positive charges on the carbons adjacent to the nitrogen, which confirms the proposed thermal degradation mechanism via nucleophilic attack. Moreover, the higher partial positive charge on the methyl group gives an additional explanation to the higher vulnerability of the *N*-methyl substituent.[91] This vulnerability is also reflected by the lower thermal stability of different dimethylimidazolium salts as compared to $[C_2mim]^+$ salts.[25d]

5.4. S_N1 vs. S_N2

To distinguish between the S_N1 and S_N2 mechanisms in the reverse Menshutkin reaction, some key research was done by Chan *et al*. They investigated the rate at which different substituents are cleaved off in dialkylimidazolium halide salts and found the relative rates to decrease in the order: allyl (2.8) > methyl (1.0) > benzyl (0.56) > ethyl (0.14) > propyl (0.095) > butyl (0.04). Furthermore, an even lower rate of cleavage for the isopropyl group and no cleavage at all for the conjugated vinyl and phenyl groups was found. However, due to the low volatility and high reactivity of benzyl halides, the actual rate was considered higher than suggested by the data. Given the higher rates of cleavage of the allyl and benzyl groups, an S_N1 mechanism could here be proposed, although this would implicate the isopropyl to cleave readily as well, which is not the case. Neither was a rearrangement from propyl derivatives into the more stable isopropyl derivatives evident in any case. This would certainly be the case if the propyl group was to be cleaved via an S_N1 process. As a conclusion, S_N1 mechanism might be possible for the allyl and benzyl substituted salts, in the other cases steric factors are more important and S_N2 kinetics are dominant.[88]

The degradation of halide imidazolium ionic liquids in particular is proposed to proceed via an S_N2 mechanism, since the observed degradation rate follows the nucleophilicity order of the halides.[33a] To distinguish between S_N1 and S_N2 as the underlying mechanisms, the effect of changing the anion was investigated, since pyrolysis via an S_N2 mechanism should depend on the nucleophilicity and size of the anion. In the case of $[C_2mim]^+$ salts, the ratio of 1-

methylimidazole to 1-ethylimidazole formed increases, as expected, with decreasing anion size (from I^- over Br^- to Cl^-). Smaller anions show a lower preference for Me to Et. 1-Allyl-3-methylimidazole $[Amim]^+$ salts were investigated since here no alkene elimination is possible and due to the high volatility of allylhalides, requaternisation can be excluded. Mainly 1-methylimidazole is found, with an increasing amount of 1-allylimidazole when decreasing the size of the halide anion. This controversial result is explained by the possibility for both S_N1 and S_N2' at the least hindered side of the allyl group. However, a pure S_N1 mechanism would only allow 1-methylimidazole to be formed. The same is valid for 1-benzyl-3-methylimidazolium $[Bnmim]^+$ salts, but here also 1-benzylimidazole is formed. A bigger proportion benzylimidazole should be formed with decreasing anion size, which is verified in the experiments. Since the benzylhalides exert a low volatility and high reactivity, the amount of 1-methylimidazole was lower than expected. As a conclusion, substituents forming stable carbenium ions do not exclusively cleave via S_N1 mechanism and in general, the anion plays an important role in degradation mechanisms.[88]

While the chloride anion of imidazolium chloride ionic liquids can contribute to an S_N2 reverse Menshutkin reaction, this mechanism is hindered by branching of the alkyl chains. Therefore, halide salts with branched substituents are more thermally stable. The degradation of salts with the non-nucleophilic $[BF_4]^-$ anion on the other hand, is proposed to proceed via an S_N1 mechanism to give the neutral 1-alkylimidazole and a substituted alkyl carbenium ion. Therefore, the branched imidazolium tetrafluoroborate salts are less stable than their linear analogues.[34] The same trend was found for isopropyl substituted imidazolium $[PF_6]^-$ and $[NTf_2]^-$ salts and also for isobutyl substituted imidazolium $[BF_4]^-$ and $[PF_6]^-$ salts (see Table 1).[33a, 35]

In $[C_4C_1pyrrol][BF_4]$, an S_N2 mechanism is calculated to be dominant,[87] while in imidazolium ionic liquids comprising non-coordinative anions, the possibility of both S_N1 and S_N2 mechanisms is experimentally confirmed. Thus in the thermal decomposition of $[C_2mim][NTf_2]$, the ratio of S_N2 vs. S_N1 was estimated to be 93 to 7%, but more important, the ratio of elimination vs. substitution was estimated to be 77% vs. 23%, revealing the importance of elimination for ILs comprising non-coordinative anions.[52]

5.5. Thermal rearrangement reactions and alkene formation

Upon pyrolysis of $[C_4mim][Br]$, 1-butene is found, while in $[C_4mim][BF_4]$ also ethylene, propylene, (*E*)-2-butene and (*Z*)-2-butene are found.[85] Thermolysis of ionic liquids containing less coordinating anions hence occurs rather at the longer alkyl chain side, in contrast with the halide anions which preferentially react at the methyl side. The increase in alkene formation by thermal cleavage is a result of the low nucleophilic character of the anion. In addition to

butenes, the thermal rearrangement reactions of $[C_4mim][BF_4]$ also lead secondarily to ethane and propylene as well as 2-fluoropropane and 1-fluorobutane. The formation of shorter alkenes indicates the possibility of cleavage of the C-C bond in addition to the C-N bond. The decomposition of $[PF_6]^-$ salts shows a similar pattern as for the $[BF_4]^-$ salts. However, pyrolysis of the latter does not lead to organic compounds containing boron, while thermal decomposition of $[PF_6]^-$ salts lead to the formation of PF_3 and phosphorous containing organic compounds, although the substances could not be identified. Another key difference is the formation of neutral 1-alkylimidazoles with cleaved C-C bonds, e.g. ethylimidazole in the case of $[C_4mim][PF_6]$, apart from alkenes. Pyrolysis of $[C_4mim][TfO]$ does not lead to any C-C bond fragmentation or halide addition products, this can be attributed to the strong C-F bond. Here, fragmentation of the anion into SO_2 and CF_3H is observed as well as butenes.[85]

When $[C_2mim][NTf_2]$ is subjected to thermal analysis, next to neutral 1-alkylimidazoles, 1*H*-2-ethylimidazole and 1*H*-2-methylimidazole are detected (Scheme 9).[31] The formation of the latter compounds is presumed to originate from thermal rearrangement reactions. These rearrangement reactions could be of the sigmatropic type, since free-radical pathways are experimentally excluded.[90] A similar rearrangement was also detected upon laser ablation of $[C_nmim][Cl]$ (n=4,6).[50a]

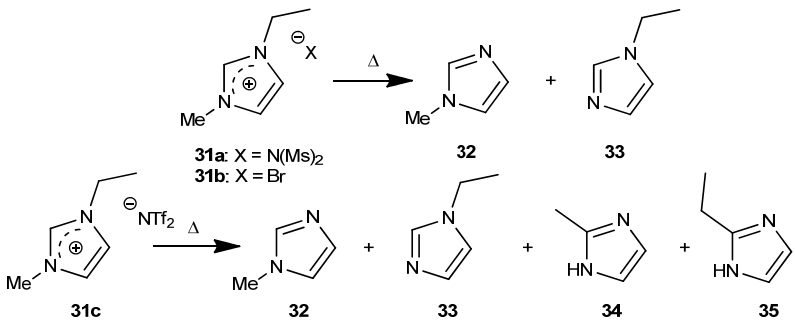

Scheme 9: Formation of neutral 1-alkylimidazoles in ionic liquids containing coordinating anions (up), and formation of neutral 1-alkylimidazoles and rearrangement products (below).[31]

When increasing the length of the alkyl chain R in a series of $[NR_4][BF_4]$ salts, a decrease of thermal stability was observed in the order Bu ≈ Me > Et > Pr. This is in accordance with the calculated activation energies for the dealkylation reaction (Scheme 10), which decreases upon elongation of the alkyl chain. However, an anomaly was found for the tetrabutylammonium tetrafluoroborate $[N_{4444}][BF_4]$, which has an activation energy as large as for the methyl derivative. This increased activation energy was attributed to the formation of an aziridine ring by intramolecular rearrangement during the first-stage decomposition and loss of hexane, preceded by the elimination of one alkyl chain (Scheme 11). This cyclisation of

the triethylamine was proposed to occur via the quaternairy ammonium product but was not mechanistically explicated further.[60, 92]

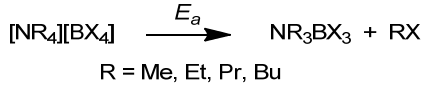

Scheme 10: Reverse Menshutkin-like reaction as depicted for tetraalkylammonium haloborates.[60]

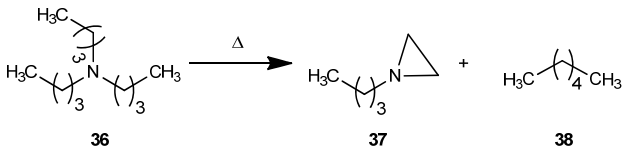

Scheme 11: Second stage intramolecular formation of aziridines in $[N_{4444}]^+$ salts.[60]

6. Kinetics of thermal degradation

The thermal decomposition is a process under kinetic control and the understanding of this process allows for time-saving modelling and prediction of the thermogravimetric properties. To investigate thermal degradation kinetics, generally, isothermal TGA measurements are applied. At a given temperature, the weight loss is linear and the rate increases as the temperature increases (see the mass vs. *t* plot in Figure 5), this suggests complete removal of volatile products and no alteration in reaction pattern over time (dm/dt = C). The overall mass loss is the sum of evaporation and degradation and, for a constant temperature, both terms are constant (dm_{vap}/dt = C'; dm_{deg}/dt = C").[52] However, at higher temperatures the linear regime is abandoned after a certain amount of time.[23, 56b] The rate is regarded as of pseudo-zeroth order (first order-derived with constant reagent concentration), since the volatile degradation products are removed from the sample. The zero-order rate constant *k* is the slope in the mass vs. *t* plot. Equation 1 shows the relation between *k* and conversion α, which is in turn derived from the initial weight (W_i) and weight at time *t* (W_t).[31, 48b, 49, 56b] The degradation rate (not evaporation) corresponds to the Arrhenius law (equation 3), and is pressure independent.[42]

Wooster *et al*. propose to calculate $t_{0.99}$ (time at which 1% mass loss occurs) from Equation 1 after obtaining *k* for different temperatures. These $t_{0.99,T}$ can be plotted against the temperature *T* and the resulting curve can be fitted by an exponential equation from which $t_{0.99}$ for every temperature can be derived.[48c]

$$\frac{d\alpha}{dt} = k \Leftrightarrow \alpha = kt + C \qquad \text{(Equation 1)}$$

$$\alpha = \frac{(W_i - W_t)}{W_i} \qquad \text{(Equation 2)}$$

$$k = A.e^{\left(\frac{-Ea}{R.T}\right)}$$ (Equation 3)

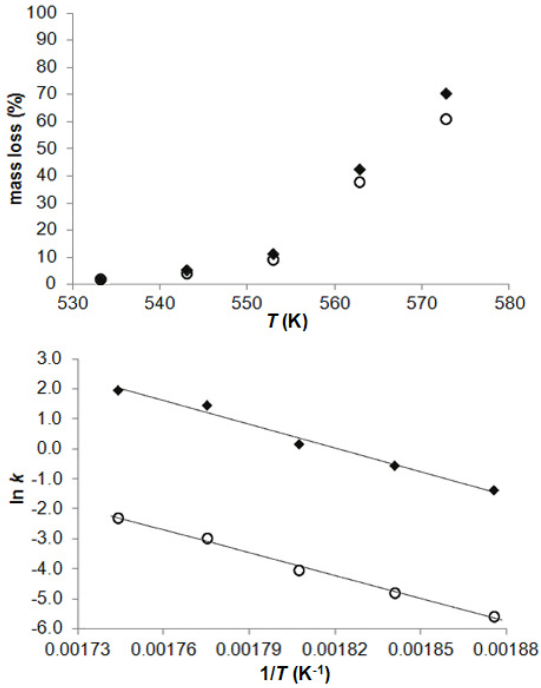

Figure 8: Mass loss after 10 h vs. temperature in isothermal experiments (top) and Arrhenius plot (bottom) for [C_4mim][Br] (♦) and [C_8mim][Br] (○).[48b]

The activation energy E_a and the pre-exponential parameter A can be derived from the Arrhenius plot (natural log of the rate k vs. $1/T$, Figure 8). Since (i) the mass loss rate for a given temperature does not change over time and (ii) the contribution of evaporation is assumed to be small, an overall E_a and A can be determined comprising both evaporation and degradation. The knowledge of these parameters allows the prediction of the 'life-time' (time in function of weight loss) of ILs at different temperatures, within the boundaries of validity of the TGA-experiment.[23, 25d] However, as can be seen in Table 3, inter-experimental variability leads to diverse parameters.

These parameters can also be derived from non-isothermal (ramped temperature) TGA measurements by pre-defined methods, which can be found in the specialised literature.[25d, 57, 93] One way is to derive them from the plot where, for a given conversion in the experiment, the inverse of the temperature at which this conversion is reached, is plotted in function of the log of the heating rate of the experiment (Figure 9). The kinetic parameters are then derived via algorithms provided by the ASTM.[94]

Table 3: Kinetic parameters derived from isothermal TGA experiments (valid from 150-200 °C).

IL	E_a (kJ mol^{-1})	A (min^{-1})

$[C_4mim][Cl]$[56b]	121	3.8×10^{10}
$[C_6mim][Cl]$[56b]	117	1.0×10^{10}
$[C_4mim][Br]$[48b]	212.50	2.43×10^{18}
$[C_8mim][Br]$[48b]	219.69	8.46×10^{20}
[Amim][Cl][23]	125	3.0×10^{13}
$[C_4mim][Cl]$[23]	129	2.8×10^{13}

On the other hand, given only evaporation occurs at lower temperatures, thermodynamic vaporisation parameters can a priori be derived from the low temperature isothermal experiments (for $[C_2mim][NTf_2]$: T < 350 °C)[52] followed by numerical solving of the derivative equation proposed by Seeberger *et al*. with the non-isothermal TGA data (mass vs. time for an array of different heating rates) giving E_a and A. The former mathematical model shows to be consistent with experimental values for both isothermal and ramped temperature thermogravimetrical analyses.[32b]

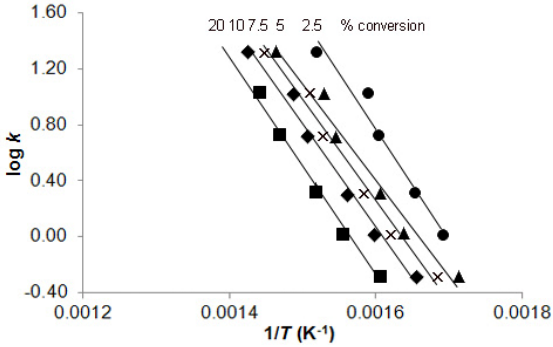

Figure 9: Families of mass conversion plotted in function of the heating rate for $[C_4mim][PF_6]$.[25d]

Hao *et al.* have modelled the degradation patterns of $[C_4mim][Cl]$ and [Amim][Cl] via DFT calculations, hereby calculating the energies of the transition states of the reverse Menshutkin reaction, which correspond well to the experimental values (from 120 to 134 kJ mol^{-1}). However, the latter should be regarded to as relative values, since during calculations, the ILs are simplified to single molecules in an ideal gas model at zero degrees.[23]

7. Conclusions

The properties of different ionic liquid families were elaborated, giving overall orders of thermal stability. Hereby, attention should be paid to the 'masking' effect that less stable counter-ions can have on the ion under investigation.

Different tools for analysis and prediction of the thermal stability are discussed. Although T_{onset} gives an overestimation of the actual degradation temperature, ramped temperature analysis is valuable if interpreted as such and given with detailed information on apparatus and conditions (heating rate, sample weight, apparatus and pan type and gas flow rate). Hereby, the effect of the presence of oxygen is inferior to the effect of the flow rate of inert gas (accounting for evaporation) and the heating rate. Mathematical models (based on ramped temperature TGA measurements) allow for a rapid complete identification of thermal stability properties where otherwise time consuming isothermal TGA analyses are necessary. However, attention should be given to the validity-boundaries of these tools in order not to extrapolate data.

For investigation of the degradation mechanisms, several powerful analysis methods are known up to date. These unambiguously reveal the cleavage of the N-C bond as main degradation process. Ionic liquids with basic anions will predominantly decompose via a S_N2 pathway. The ILs comprising non-coordinative anions also show elimination and sometimes rearrangements. The possible formation of inorganic acids should be considered when water is present. The latter analysis methods allow for verification of molecular modelling. Combined these methods allow synthetic chemists to design solvents which meet the stability requirements.

The high dependency of the results on the experimental factors is detrimental for comparison of data from different sources. Therefore, an overview of these factors and an extensive rationale for predicting the relative stability is given in this section. The future research towards thermal stability of ionic liquids for engineering applications should analyse the IL with thought for evaporation or at given temperatures for which evaporation kinetics are known.

III) RESULTS AND DISCUSSION

1. Peralkylated imidazolium ionic liquids

1.1. Synthesis of imidazoles

Peralkylated imidazoles were synthesised via a modified Debus-Radziszewski[2] reaction.[8, 95] This condensation reaction of a 1,2-diketo compound, ammonia, an amine and an aldehyde forms tetrasubstituted imidazoles and water. Earlier research showed that the imidazole synthesis is very effective at 120 °C, and that application of an excess of amine (**1**) does not lead to higher yields.[10] Since the starting materials are volatile, pressure vials were used in order to keep these volatile components in the reaction mixture. This also allows for the use of methanol as a solvent. Methanol can easily be removed via rotary evaporation and also takes up some of the reaction water, hence it is the most appropriate solvent. The substituents on the C2 and N1 positions are built in directly via the corresponding aldehydes and amines, eliminating the need for bases and haloalkanes for the *N*-alkylation or for the nucleophilic substitution at the C2 positions, which normally suffers from a low yield.[96]

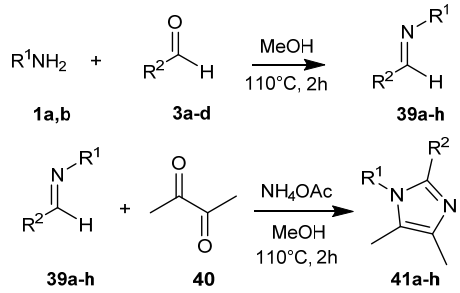

Compound	R^1	R^2	Yield (%)
41a	Et	H	42
41b	Et	Me	38
41c	Et	Et	36
41d	Et	iPr	41
41e	Hex	H	40
41f	Hex	Me	38
41g	Hex	Et	32
41h	Hex	iPr	38

Scheme 12: One-pot modified Debus-Radziszewski reaction procedure with intermediate imine formation.

Previous research at both our research group and beyond, showed that the addition of acetic acid increases the selectivity towards the *N*-alkylated imidazole, although then *N*-alkyl

[2] In 1858, Heinrich Debus reported on the condensation of glyoxal with ammonia and formaldehyde to form imidazoles. Bronisław Leonard Radziszewski modified this reaction in 1882 to a four component reaction in which *N*-alkylated imidazoles were formed.

acetamides were formed.[10, 97] Therefore, a new set-up circumventing the use of AcOH was elaborated. The condensation was performed as a two-step multicomponent reaction, which allows the selective synthesis of *N*-alkylated imidazoles. In a first step, the intermediate imine was generated, which was then reacted with the ammonia source and the 1,2-diketone in a second step (Scheme 12). After reaction, the conversion of starting material was in between 32 and 42% and the product was extracted from the reaction mixture with a 0.5 M HCl solution. The aqueous phase was made alkaline and extracted. After removal of the solvent by rotary evaporation, the resulting oil was purified by distillation under reduced pressure.

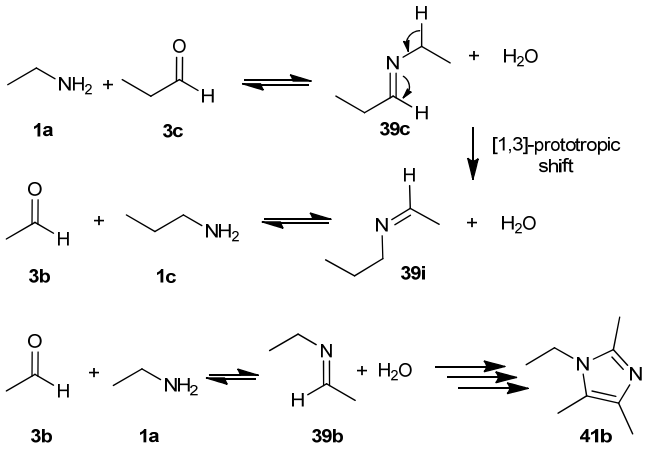

Scheme 13: [1,3]-prototropic shift of ethylpropylideneamine (39c) and subsequent formation of 1-ethyl-2,4,5-trimethylimidazole (41b) in alkaline media.

This reaction sequence yielded pure *N*-alkylated imidazoles as expected, although in the synthesis of hexyl derivatives, a small amount (up to 12 mol% of the extracted mixture) of 1*H*-imidazoles was obtained. In order to remove the 1*H*-imidazoles from the reaction mixture, it was sufficient to extract the alkaline aqueous phase with hexanes, since the 1*H*-imidazoles are not soluble in this solvent. There is, however, an exception to the selectivity: after reaction with propionaldehyde to form 1,2-diethyl-4,5-dimethylimidazole (**41c**), 38 mol% of 1-ethyl-2,4,5-trimethylimidazole (**41b**) was found in the extracted mixture. This is assumed to be caused by a [1,3]-prototropic shift during the imine formation, as depicted in Scheme 13.

During the synthesis of the *N*-hexyl derivative 2-ethyl-1-hexyl-4,5-dimethylimidazole (**41g**), the same formation of the 2-methyl analogue (**41f**) was observed, but this formation of a side product was never observed with other aldehydes. To circumvent this problem, an alternative approach was followed, in which the 1,2-diketone (**40**) and the amine (**1**) were mixed in the first step. In this way, no 1-alkyl-2,4,5-trimethylimidazole (**41b** or **41f**) was formed.

1.2. Continuous flow synthesis of the *N*-hexyl imidazoles

Batch experiments led to the selective synthesis of *N*-alkylated imidazoles via a priori imine formation. Synthesis of these imidazoles in continuous flow (of which the upscaling is reffered to as numbering-up) allows for production at an industrial rate. Earlier research at the department of Sustainable Organic Chemistry and Technology, using a *Cytos CPC college system* showed that imidazoles were synthesised optimally at 120 °C in a continuous flow reactor with a residence time of 118 min and using solutions of the starting materials at a 0.5 M concentration.[10] Although in this former set-up, the amine and the aldehyde were not mixed before being pumped into the reactor, here the goal was to synthesise the imine in batch, and subsequently react it with NH_4OAc and the 1,2-diketone in the continuous flow reactor (Figure 10). The reactor had an internal volume of 48 mL and was equipped with two pumps (with pumping speeds v_1 and v_2) for both the influent solutions.

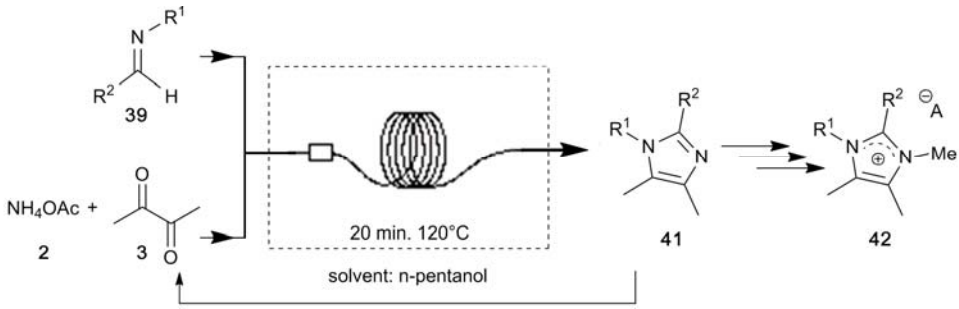

Figure 10: Scheme of the microreactor setup mixing unit and residence time unit within the dashed square.

Continuous flow synthesis of *N*-hexylimidazoles was performed in n-pentanol, allowing the reaction to be carried out at a temperature of 120 °C, which exchludes the need to pressurise the system. In a first attempt, the solubility limit of starting materials was examined and 1.0 M was found to be the maximum concentration for dissolution of NH_4OAc in n-pentanol. However, at this concentration, a substantial amount of 1*H*-imidazole was formed. Therefore, a lower concentration was applied. At a concentration of 0.5 M of NH_4OAc, no 1*H*-imidazole was found, and this concentration was used during further experiments. In a second step, the flow rate and hence residence time were optimised.

The yield and throughput of 1-hexyl-4,5-dimethylimidazole (**41e**) and 1-hexyl-2,4,5-trimethylimidazole (**41f**) for pump speeds from 0.5 to 2.0 mL min^{-1} (= v_1 = v_2), in intervals of 0.25 mL min^{-1}, were determined by GC-FID analysis. The response factor used was calculated from the total obtained yield after distillation, i.e. in Figure 11, the maximum obtainable yield and throughput after purification are given as a function of the residence time (t_{res}). The best yields of extracted product (36 %) were those obtained with a flow rate of 2 ×

0.5 mL min^{-1}, i.e. a t_{res} of 48 min. Additional prolongation of the residence time would not increase the yield significantly (Figure 11). To obtain a sufficient throughput combined with an acceptable yield, a t_{res} of 20 min was chosen. For the analogous 2-ethyl-1-hexyl-4,5-dimethylimidazole (**41g**) and 1-hexyl-2-isopropyl-4,5-dimethylimidazole (**41h**), the same conditions were applied and no analytic experiments in function of t_{res} were performed. Although, to avoid the earlier observed prototropic shift during continuous synthesis of 2-ethyl-1-hexyl-4,5-dimethylimidazole, n-pentanol solutions of preformed 3-ethylimino-butan-2-one and NH_4OAc with propionaldehyde were used.

After collection of the reaction mixture at a rate of ca. 4 grams per hour, the water formed in the reaction and the solvent were distilled off, yielding a dark liquid which could be extracted and distilled in the same way as in the batch procedure. The distilled solvent was successfully recycled and used for subsequent microreactor experiments. The n-pentanol was hereby not dried, demonstrating the negligible influence of water in the modified Debus-Radziszewski reaction procedure. During final distillation of 1-hexyl-2-isopropyl-4,5-dimethylimidazole (**41h**) a small fraction of another compound was obtained, but this compound could not be identified.

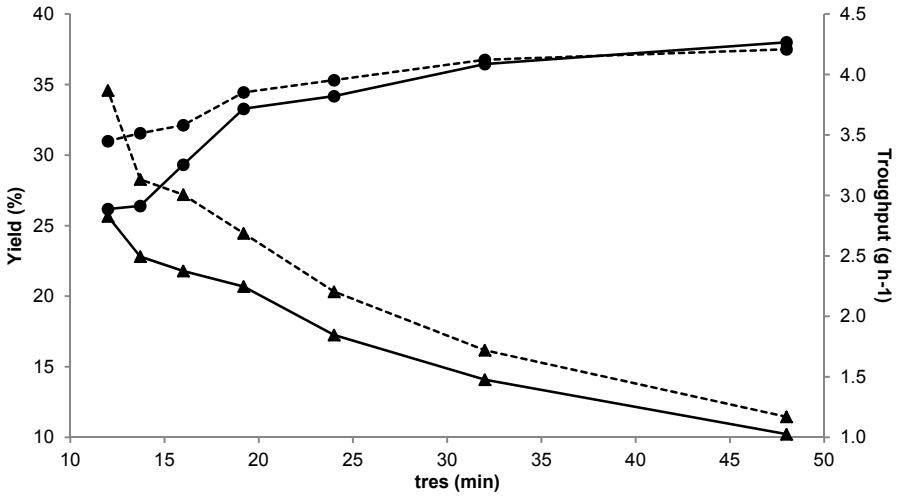

Figure 11: Yield after purification (%) (●) and throughput (g h^{-1}) (▲) of 1-hexyl-4,5-dimethylimidazole (41e) (solid) and 1-hexyl-2,4,5-trimethylimidazole (41f) (dashed) in the CPC College system microreactor.

The synthesis of the *N*-ethylimidazole derivatives was not feasible however, the gaseous $EtNH_2$ would volatilise and form gas bubbles in the microreactor channels. This expansion reduces the residence time of the liquid phase and also severely disturbs the heat and mass transfer. The application of aqueous $EtNH_2$ could have been applied, however, the batch reactions performed with $EtNH_2$ (aq.) suffered from lower yields, due to an increased side product formation.

The plot (●) in Figure 11 is the inverse of the yield (and throughput) vs. the applied pump speed (= v_1 + v_2), but gives a more comprehensible overview. Moreover, this plot translates the conversion of the reaction over time. Hence, apart from a controllable system, in which temperature, reaction time and concentration can be precisely adjusted to exclude the 1*H*-formation, the microreactor allows for a superficial study of the reaction kinetics, by plotting the effluent composition vs. the residence time.

1.3. Thorough purification of imidazoles

Certain imidazoles gave clear liquids after distillation (e.g. 1-ethyl-4,5-dimethylimidazole and 1-hexyl-4,5-dimethylimidazole), while other give intensive yellow liquids, which darkened even upon storage at -18 °C in the absence of air and light, although being pure by NMR analysis. The colouration was intensive upon quaternisation, and this could eventually lead to black salts. The colouration was also found in commercially available ionic liquids and was attributed to very low-level (parts per billion) compounds with very high extinction coefficients.[98] Therefore, different post-quaternisation decolouration methods were already reported in literature. Thus, good decolouration was achieved by means of activated charcoal[99] combined with silica gel[98] or alumina,[100] while reversed phase packing was used for ionic liquids with hydrogen bonding anions.[101] Unfortunately, none of these post-quaternisation purification methods were found effective for the compounds synthesised in this research.

Synthesis of the 1*H*-2-isopropyl-4,5-dimethylimidazole (*vide infra*) gave a clear precipitate in a coloured reaction mixture. This indicates that side reactions of the amines and carbonyl compounds induce the colouration of the imidazoles. Upon quaternisation, it is likely that temporary local higher temperatures induce the colouration.[99] Although some of the here synthesised peralkylated ionic liquids (e.g. the iodide salts, *vide infra*) could be recrystallised, the room temperature ionic liquids could not be purified in this way. Moreover, the acetone applied as recrystallisation solvent was earlier reported to also lead to colourisation.[100] Therefore, it was chosen to apply an intensive purification on the imidazoles.

1.3.1) Reduction and distillation

During reduction of the amino acid derived compound **88b** (Scheme 30, p67), it was found that the black colour disappeared, hence, ionic liquids giving colouration problems were treated with 20 weight% $NaBH_4$ in methanol and again distilled after reaction. This yields transparent liquids (*yield 80%*). The treatment of the black oil, obtained after extraction of the imidazoles from the reaction mixture, with $NaBH_4$ or $LiAlH_4$, did not lead to a reduced

coloration of the distilled imidazoles. Hence, this laborious and resource demanding method was only applied when necessary.

1.3.2) Transformation into the imidazolium hydrochloride salt

Some of the imidazoles could be transformed into their hydrochloride salts by bubbling an excess of freshly prepared dry HCl gas through an imidazole solution in CH_2Cl_2. Initially, it was proposed that this could not be applied to all imidazoles, e.g. 1-allyl-2-isopropyl-4,5-dimethylimidazole (**59a**, Scheme 20) turned black very fast upon addition of hydrochloride, probably due to reaction of HCl with the double bound, although 1-allyl-2*H*-4,5-dimethylimidazole (**41i**), also comprising a double bond, could be obtained as its hydrochloride salt.

After complete neutralisation of the free imidazole base, the salt solution could be evaporated and recrystallised in acetone. This furnished very pure crystals, harvested after long storage at -18 °C. Alternatively, an excess of Et_2O could be poured into the solution, after which the salts precipitated as a powder. Not only was the later method the fastest, it also gave higher yields, e.g. 1-ethyl-2,4,5-trimethylimidazole hydrochloride salt (**43b**): 93%. Direct precipitation by bubbling HCl gas through an ethereal solution was not successful. Attempts to obtain a solid fraction by acidifying the black liquor obtained after extraction of the crude imidazole mixture were also unfruitful, hence, distillation prior to precipitation is necessary. The purified imidazole was finally obtained by extraction from an alkaline aqueous solution with EtOAc. An aliquot of ice water was added to compensate for the heat generated during the neutralisation of the hydrochloride salt.

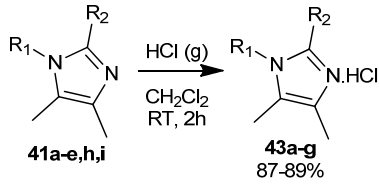

41a-e,h,i **43a-g** 87-89%

Scheme 14: Formation of imidazolium hydrochloride salts by bubbling dry HCl through a dichloromethane solution of the imidazoles. Identification of the compounds is given in Table 4.

These salts were found by coincidence after extraction of one specific batch of the hydrophobic 1-hexyl-2-isopropyl-4,5-dimethylimidazolium hydrochloride salt (**43f**), which unexpectedly led to the formation of a solid. After several unsuccessful quaternisation attempts, intensive NMR study of the unreactive compound led to the observation of small downfield shifts. This indicated that the 1-hexyl-2-isopropyl-4,5-dimethylimidazolium hydrochloride salt (**43f**) is quite hydrophobic and migrates from the acidic aqueous phase to the CH_2Cl_2 phase. This particular problem was circumvented by substituting the extraction

solvent by the less polar EtOAc. Because these compounds are not considered as ionic liquids but rather as salts, their melting points are given in this section. As apparent from Table 4, the melting points of the HCl salts are higher than the analogous *N*-methyl iodide salts (*vide infra*). Nonetheless, the same trend is found in melting points upon alternating the C2 substituent.

Table 4: Melting points (T_m) in °C of the imidazolium HCl salts and *N*-methylimidazolium iodide salts.

HCl salt	Imidazole	R^1	R^2	T_m HCl salt (°C)	T_m iodide salt (°C)
43a	**41a**	Et	H	210	136
43b	**41b**	Et	Me	172	134
43c	**41c**	Et	Et	123	n/a[a]
43d	**41d**	Et	iPr	131	121
43e	**41e**	Hex	H	130	52
43f	**41h**	Hex	iPr	120	35
43g	**41i**	Allyl	H	137	n/a[b]

[a] No solidification observed; [b] Compound is not synthesised.

1.4. Synthesis of ionic liquids

Continuous flow processes find many applications in ionic liquid synthesis (quaternisation), as this allows reduction of solvent[102] and quaternisation agent usage, improved parameter control, as well as a safer process for scaling up. Thus, the solvent-free syntheses of 1-ethyl-3-methylimidazolium ethylsulfate ($[C_2mim][EtSO_4]$),[103] 1-ethyl-3-methylimidazolium trifluoromethylsulfonate ($[C_2mim][TfO]$)[104] and 1-butyl-3-methylimidazolium bromide ($[C_4mim][Br]$)[102] have already been successfully established in a continuous flow process. The precise heat and mass transfer control and consequent elimination of thermal runaway can also reduce the colouration associated with the temporary local high temperatures discussed in the previous section.

The quaternisation of peralkylated imidazoles in continuous flow was not investigated due to the small scale synthesis, the toxicity of the reagents and the absence of an innovation. The batch-wise synthesis is elaborated in the next section, while alternative ways to form ionic liquids, circumventing halide salt formation and the thus implied metathesis methods are described in section III.4.

1.4.1) Quaternisation of imidazoles

To avoid the presence of starting materials in the end product, iodomethane (MeI) was used for quaternisation of the imidazoles. The use of the reactive MeI allows for a quantitative alkylation reaction and a complete removal of the alkylating reagent, due to the low boiling point in comparison with other alkylating agents, e.g. dimethylsulfate and bromoalkanes. The corresponding ionic liquids were thus obtained by adding MeI dropwise to a solution of the desired imidazole in dry acetonitrile.

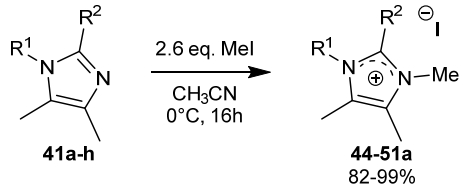

Scheme 15: Methylation of the imidazole core (41a-h) with methyl iodide to form the iodide ionic liquids (44-51a). Identification of the compounds is given in Table 5.

This exothermic reaction was conducted at 0 °C, to avoid evaporation of MeI. The reaction was monitored by ^{1}H NMR and after completion (overnight), the solvent and excess MeI were removed *in vacuo*. *N*-ethyl substituted imidazolium iodide salts were slightly coloured solids. These solids could be recrystallised in dry acetone which allowed to obtain transparent crystals. *N*-hexyl substituted imidazolium iodide salts were obtained as transparent yellow oils. These oils were dissolved in CH_3CN and washed with hexanes to completely remove any traces of the imidazole precursor. The latter ionic liquids were never thoroughly dried to avoid thermally induced degradation reactions caused by the nucleophilic iodide anion. Melting points of the solid iodide salts are reported in Table 5.

The colouration upon methylation was most pronounced in the case of the 2-ethyl derivatives, which turned black after a few hours. The liquid iodide salts were also susceptible to colouration upon storage at ambient temperature, even when shielded from light. Therefore, storage at -18 °C under a nitrogen atmosphere is advised, but immediate use in the metathesis reaction is preferred. After metathesis, colouration does no longer occur, hence the colouration is induced by the oxidative properties of iodide. The solid salts could be recrystallised and stored under ambient conditions.

1.4.2) Metathesis of imidazolium iodide ionic liquids

The silver dicyanamide, used during metathesis, was synthesised by dissolving $NaN(CN)_2$ in demineralised water to which a small excess of $AgNO_3$ was added (Scheme 16). Immediately after addition of the $AgNO_3$, a white solid precipitated. The mixture was stirred vigorously for

multiple hours at 50 °C to ensure complete cation exchange. The precipitate was filtered off, rinsed with demineralised water and dried under reduced pressure.

The iodide ionic liquids were transformed into the corresponding dicyanamide and bis(trifluoromethylsulfonyl)imide salts according to metathesis reactions described in literature (Scheme 17).[41, 105] Efficient mixing was ensured by mild heating. Upon metathesis with $AgN(CN)_2$ of the *N*-hexyl derivatives in demineralised water, precipitation of yellow AgI in an oily matrix was observed, therefore, a 2:1 mixture of demineralised water and CH_3CN was used to ensure efficient mixing. Excess $AgN(CN)_2$ and AgI were filtered off and the solvent was removed *in vacuo*, after which the remainder of contaminants was precipitated in CH_2Cl_2 at -18 °C. The metathesis reaction with $LiNTf_2$ was performed with only a 3 wt.% excess, hereby avoiding the presence of residual $LiNTf_2$, which influences the electrochemistry of the ionic liquids.[100] Excess $LiNTf_2$ and LiI were washed out with demineralised water. Upon residual halide control by addition of $AgNO_3$ to an aqueous solution of the $[N(CN)_2]^-$ salts and to the washing water of the $[NTf_2]^-$ salts, no precipitation was visible.[19]

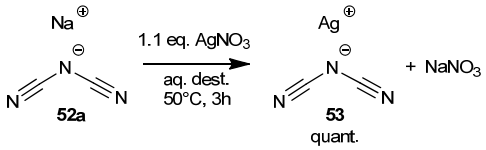

Scheme 16: Metathesis of sodium dicyanamide with silver nitrate to form silver dicyanamide.

After metathesis, the ionic liquids were thoroughly dried before further experiments were conducted. Drying proceeded for 4 to 8 hours at a pressure of 0.5 mbar and at temperatures of 80 and 120 °C for the $[N(CN)_2]^-$ and $[NTf_2]^-$ salts, respectively. The water content of the samples was analysed by a coulometric Karl Fischer titration, the $[N(CN)_2]^-$ salts all contained less than 500 ppm of H_2O, while $[NTf_2]^-$ salts all had water contents lower than 200 ppm (Table 6).

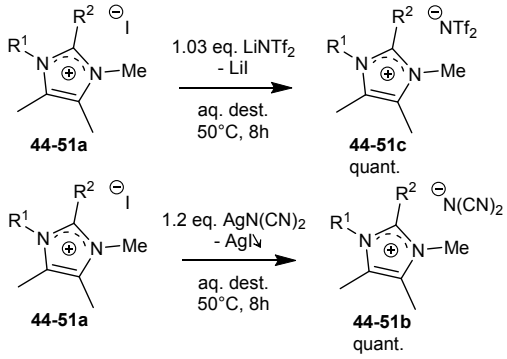

Scheme 17. Aqueous metathesis of iodide salts (44-51a) into the corresponding bis(trifluoromethylsulfonyl)imide (44-51b) and dicyanamide ionic liquids (44-51c). Identification of the compounds is given in Table 5.

1.5. Melting point and viscosity of the ionic liquids

Alkylation on C2 prevents the formation of a hydrogen bond. Normally, this hydrogen bond reduces both melting point and viscosity in three ways: (i) the charge transfer established by this bond decreases the Coulomb forces,[106] (ii) the hydrogen bond can hinder a good stacking of the molecules by distortion of the crystal lattice[47c] and (iii) the C2 proton is an interaction site which allows the free movement of the anion through the plane of symmetry of the cation, resulting in an increased entropy.[91] Therefore, alkylation at the C2 position is expected to increase the melting points, as was shown earlier by several research groups.[38, 91] For the same reasons, the substitution of the C4 and C5 protons, which can form weak hydrogen bonds,[41] by methyl groups, might be expected to further increase the melting points.

Most of the *N*-ethylimidazolium salts were solid at room temperature, however, all the *N*-hexylimidazolium salts remained liquid at room temperature (Table 5). In general, the observed melting points are higher than the reported values for the corresponding non-peralkylated salts ([C_2mim][NTf_2] -3 °C, [C_2mim][$N(CN)_2$]: 21 °C).[38, 41] It is suggested that increased Van der Waals attraction forces and the suppression of hydrogen bonding are the main causes for this increase in melting points.

However, as represented in Table 5, melting points do not increase upon methylation at the C2 position as expected. Contrarily, T_m seems to be inversely related to the degree of substitution at C2. Only for [$C_2Ci_3m_3$im][NTf_2] (**47b**), a higher melting point is observed than for [$C_2C_2m_3$im][NTf_2] (**46b**). Therefore, the possibility of entropy reduction by hindered isopropyl rotation in the [$C_2Ci_3m_3$im]$^+$ cation was investigated. From NMR spectral data and semi-empirical calculations (RM1 model, Hyperchem 8.0), which attributes a rotational energy barrier of 80 kJ mol^{-1}, it is assumed that there is free rotation. As a conclusion, the increased melting point of [$C_2C_{i3}m_3$im][NTf_2] compared to [$C_2C_2m_3$im][NTf_2] cannot be attributed to a decrease in entropy when going from ethyl to isopropyl C2 substitution.

All *N*-ethyl derivatives solidify very rapidly upon cooling but do not crystallise, except for the iodide salts. This behaviour was already previously reported for the [C_2C_1mim][NTf_2] ionic liquid.[38] On the other hand, the *N*-hexyl derivatives do not show any phase transition after keeping the samples at -60 °C for several hours. Since the *N*-hexyl salts are expected to have melting points of about 60-70 °C lower than their iodide precursors (as is the case for the *N*-ethyl derivatives), this observation suggests that these ionic liquids undercool very well.

Table 5: Melting points (T_m) of the synthesised peralkylated ionic liquids.

	IL[a]	R^1	R^2	A^-	T_m (°C)
44a	$[C_2m_3im][I]$	Et	H	I^-	136
45a	$[C_2C_1m_3im][I]$	Et	Me	I^-	134
46a	$[C_2C_2m_3im][I]$	Et	Et	I^-	n.s.[b]
47a	$[C_2C_{i3}m_3im][I]$	Et	iPr	I^-	121
44b	$[C_2m_3im][NTf_2]$	Et	H	NTf_2^-	58
45b	$[C_2C_1m_3im][NTf_2]$	Et	Me	NTf_2^-	59
46b	$[C_2C_2m_3im][NTf_2]$	Et	Et	NTf_2^-	32
47b	$[C_2C_{i3}m_3im][NTf_2]$	Et	iPr	NTf_2^-	42
44c	$[C_2m_3im][N(CN)_2]$	Et	H	$N(CN)_2^-$	87
45c	$[C_2C_1m_3im][N(CN)_2]$	Et	Me	$N(CN)_2^-$	42
46c	$[C_2C_2m_3im][N(CN)_2]$	Et	Et	$N(CN)_2^-$	n.s.[b]
47c	$[C_2C_{i3}m_3im][N(CN)_2]$	Et	iPr	$N(CN)_2^-$	25
48a	$[C_6m_3im][I]$	Hex	H	I^-	52
49a	$[C_6C_1m_3im]I]$	Hex	Me	I^-	n.s.[b]
50a	$[C_6C_2m_3im][I]$	Hex	Et	I^-	40
51a	$[C_6C_{i3}m_3im][I]$	Hex	iPr	I^-	35
48b	$[C_6m_3im][NTf_2]$	Hex	H	NTf_2^-	n.s.[c]
49b	$[C_6C_1m_3im][NTf_2]$	Hex	Me	NTf_2^-	n.s.[c]
50b	$[C_6C_2m_3im][NTf_2]$	Hex	Et	NTf_2^-	n.s.[c]
51b	$[C_6C_{i3}m_3im][NTf_2]$	Hex	iPr	NTf_2^-	n.s.[c]
48c	$[C_6m_3im][N(CN)_2]$	Hex	H	$N(CN)_2^-$	n.s.[c]
49c	$[C_6C_1m_3im][N(CN)_2]$	Hex	Me	$N(CN)_2^-$	n.s.[c]
50c	$[C_6C_2m_3im][N(CN)_2]$	Hex	Et	$N(CN)_2^-$	n.s.[c]
51c	$[C_6C_{i3}m_3im][N(CN)_2]$	Hex	iPr	$N(CN)_2^-$	n.s.[c]

[a] The 1*N*-alkyl substituents are identified by 'C_2' or 'C_6' (referring to the number of carbon atoms in the alkyl chain); The C2 alkyl substituents – if present – methyl, ethyl and isopropyl are identified with 'C_1', 'C_2', or 'C_{i3}' respectively. The 3*N*-, 4- and 5-methyl substituents are combined to 'm_3', while imidazolium is referred to with 'im'; numbering of the R-groups is depicted in Scheme 15; [b] No solidification at room temperature; [c] No solidification at -60 °C.

As can be seen in Table 6, the viscosity of $[C_6m_3im][NTf_2]$ (**48b**) ionic liquid is about the same as that of the regular $[C_6mim][NTf_2]$ (71 mPa·s, 25 °C).[107] Furthermore, methyl substitution at the 2-position increases the viscosity by 51 mPa·s, which is within the same range as the viscosity increase of $[C_2C_1mim][NTf_2]$ measured by Noack *et al.*[47c] This increase was already reported by Hunt *et al.* to be more pronounced for the larger and more diffuse anions.[91] On the

other hand, the viscosities of the dicyanamide salts are substantially larger than those of the non-4,5-alkylated imidazolium ionic liquids (e.g.: $[C_2mim][N(CN)_2]$: 21 mPa·s (20 °C),[41] $[C_6mim][N(CN)_2]$: 47 mPa·s (25 °C)[108]). Only small variations in viscosities of the dicyanamide salts are observed. In general, an increment of the viscosities can be measured when the degree of substitution increases.

Table 6: Viscosities of $[C_6R^2m_3im][NTf_2]$ and $[N(CN)_2]^-$ salts (in mPa·s at 25 °C), Karl Fisher water content (in ppm) between brackets.

Compound	Cation	$[NTf_2]$ (**b**)	$[N(CN)_2]$ (**c**)
48	$[C_6m_3im]$	84 (87)	242 (305)
49	$[C_6C_1m_3im]$	135 (83)	250 (325)
50	$[C_6C_2m_3im]$	113 (79)	305 (/)
51	$[C_6C_{i3}m_3im]$	382 (97)	265 (420)

In previous research, $[N(CN)_2]^-$ salts were found to have lower viscosities than their $[NTf_2]^-$ analogues,[37] however, in this research, this was found to be true only for the 2-isopropylimidazolium salts ($[C_6Ci_3m_3im]^+$). Since molar densities of $[N(CN)_2]^-$ are higher than those of $[NTf_2]^-$ salts,[109] the cations in the $[N(CN)_2]^-$ salts are presumed to be more densely packed and thus the Van der Waals contribution to the melting points and viscosities might be larger.

1.6. Chemical stability

Begtrup reported earlier on the methylation of the C2 position with MeI after deprotonation of imidazolium salts with NaH. Upon addition of multiple equivalents NaH, the introduced methyl group could be deprotonated and alkylated until the 2-isopropylimidazolium was formed. The latter compound showed no tendency to further alkylation.[110] The base stability of the thus obtained 2-isopropyl substituted imidazolium ionic liquid $[C_4C_{i3}mim][NTf_2]$ was investigated and the compound was suggested to withstand Grignard reagents. Experiments with an organolithium compound gave only a very modest yield of addition product, therefore it was proposed that the ionic liquid imidazolium ring was lithiated. Handy suggested the stability against Grignard reagents to be due to preferable perpendicular position of the isopropyl proton to the ring π-orbitals, which does not allow a stabilisation of the lone electron pair. However, we have found the isopropyl group to be able to rotate and moreover, upon deprotonating, the isopropyl secondary carbon atom changes hybridisation state. Therefore, we attribute the base stability to the increase of pK_a.[111]

The base stability of the ionic liquids was first investigated by means of deuterium exchange in neutral and alkaline media, as demonstrated in Table 7. All IL were soluble in the 7:3 CD_3OD/D_2O mixture. After one week, still no deuterium exchange was observable for the $[C_6m_3im][NTf_2]$ (**48b**) ionic liquid (entry 1). After a very fast complete deuterium exchange in 0.1 M KOH on C2 (entry 2), which was also reported earlier,[96] no further reaction took place in the timespan of one week. In a 0.1 M KOH solution, no deuteration of any of the $[C_6C_{i3}m_3im][NTf_2]$ (**51b**) protons was observed (entry 3).

Table 7: Conditions and results of base stability experiments.

Entry	IL	Reaction conditions	Results
1	**48b**	7:3 CD_3OD/D_2O[a]	1h, 1d, 7d: 0 atom% D[b]
2	**48b**	7:3 CD_3OD/D_2O 0.1 M KOH[a]	1h: 97 atom% D[b] 1d: 98 atom% D[b] 7d: 99 atom% D[b]
3	**51b**	7:3 CD_3OD/D_2O 0.1 M KOH[a]	12h: 0 atom% D[c]
4	**51c**	1 M NaOH in H_2O, 24h, Δ	53 % IL[d]
5	**51b**	1 M NaOH in H_2O, 24h, Δ	97 % IL[d]
6	**51b**	2 M BuLi	Formation of **55**[e]
7	**51b**	2 M BuLi, -10 °C, D_2O[f]	30 min, 1h: 0 atom% D[c]

[a] 0.1 M of ionic liquid concentration, experiments conducted at r.t.; [b] H/D exchange on C2 monitored by ^{1}H NMR; [c] No deuterium exchange observable by NMR; [d] Percentage of IL recuperated; [e] See Scheme 18. [f] D_2O was added after the indicated amount of time.

The stability against Hofmann elimination of both hydrophilic $[C_6C_{i3}m_3im][N(CN)_2]$ (**51c**) and hydrophobic $[C_6C_{i3}m_3im][NTf_2]$ (**51b**) was tested by refluxing the ionic liquids in a strong basic aqueous solutions (entries 4 and 5). After 24h, the reaction mixtures were extracted multiple times with CH_2Cl_2. In both cases, the extracted fraction was pure IL, however in the former case, only 53 % was recuperated. Additional extraction of the organic phase could attribute this loss to solvation of the hydrophilic IL in the aqueous phase, furthermore, no other products than IL were found in the aqueous phase by HPLC-MS.

In a last instance, the stability of the IL (**51b**) in the presence of organolithium reagents was investigated in a model lithiation reaction as depicted in Scheme 18 (entry 6). After one hour, the reaction was quenched with H_2O and the presence of the product diphenylmethanol (**55**) was demonstrated by GC-FID. The reaction mixture was slightly coloured after reaction. Since it was not excluded that the base was scavenged by the bromobenzene prior to attack on the ionic liquid in the reaction mixture, the result of addition of 2 M BuLi (in hexanes) to IL was evaluated by quenching this mixture with D_2O (entry 7). Although the mixture turned completely black, no deuteration of the ionic liquid was observed.

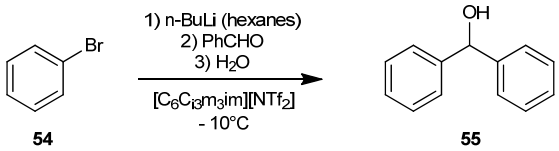

Scheme 18: Model lithiation reaction in ionic liquid 51b.

1.7. Thermogravimetrical analysis

Although dynamic thermogravimetrical analysis does not give a clear view on the long-term stability of ionic liquids at elevated temperatures, it does provide valuable information on the influence of variation of the salt composition on the thermal stability. The onset temperature for thermal decomposition T_{onset}, i.e. the calculated intercept of the line where no weight loss occurs and the tangent upon weight loss, is given in Figure 12 and Table 8. For most of the salts, a lower thermal stability for the *N*-hexyl substituted analogues is observed, although literature states that the alkyl chain length should not affect the thermal degradation temperature.[33b] A significant reduction of T_{onset} for the 2*H*-imidazolium salts (**44c**, **48c**, Table 8) is apparent, this is in agreement with different experimental results.[15a, 33a, 41, 43, 58b]

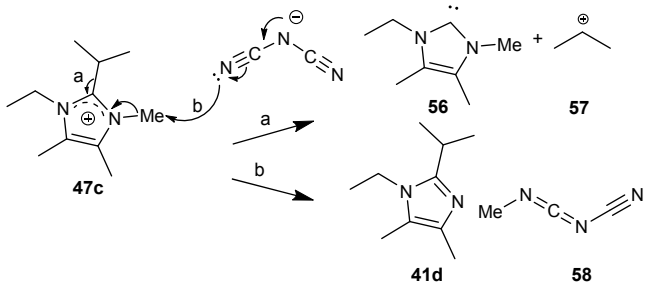

Scheme 19: Carbene formation via an E1 mechanism (a) and reverse Menshutkin-like reaction for the imidazolium dicyanamide salts as proposed by Kroon *et al.* (b).[87]

Two decomposition mechanisms are proposed: on the one hand an E1-type elimination (Scheme 19, a), forming a volatile carbene and an isopropyl cation at high temperatures,[33b] and on the other hand the reverse Menshutkin-like reaction (Scheme 19, b).[87] Although the reported ionic liquids have only weakly coordinating anions, Hofmann elimination cannot be excluded.

The decomposition of the bis(trifluoromethylsulfonyl)imide salts is assumed to proceed via the exothermal decomposition of the anion, releasing SO_2.[87] At a heating rate of 10 °C min^{-1}, all the $[NTf_2]^-$ salts were found to be stable up to 400 °C, which was set as the upper limit of measurement.

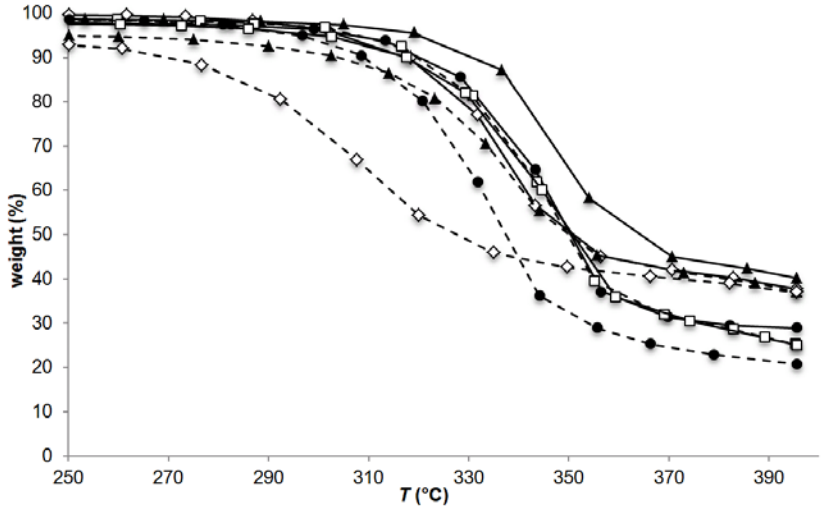

Figure 12: Thermogravimetrical analysis of 1-ethyl-3,4,5-trimethylimidazolium dicyanamide (44-47c) (solid) and 1-hexyl-3,4,5-trimethylimidazolium dicyanamide (48-51c) (dashed) salts with different substitution on C2: H (◊), Me (▲), Et (□) and iPr (●).

Table 8: Onset temperature (T_{onset}) for thermal decomposition for dicyanamide ionic liquids (10 °C min^{-1}, Ar).

	IL	T_{onset} (°C)
44c	$[C_2m_3im][N(CN)_2]$	312
45c	$[C_2C_1m_3im][N(CN)_2]$	329
46c	$[C_2C_2m_3im][N(CN)_2]$	322
47c	$[C_2C_{i3}m_3im][N(CN)_2]$	324
48c	$[C_6m_3im][N(CN)_2]$	273
49c	$[C_6C_1m_3im][N(CN)_2]$	310
50c	$[C_6C_2m_3im][N(CN)_2]$	322
51c	$[C_6C_{i3}m_3im][N(CN)_2]$	309

1.8. Electrochemical analysis

Cyclic voltammograms (CVs) of a series of completely substituted imidazolium salts were recorded at 90 °C to investigate the influence of the substituents on the electrochemical stability. The tested salts were the 2-alkyl-1-hexyl-3,4,5-trimethylimidazolium bis(trifluoromethylsulfonyl)imide derivatives, since the bis(trifluoromethylsulfonyl)imide salts have the lowest viscosity and the hexyl-substituted imidazolium salts have a higher cathodic stability. The increased stability is due to the inductive donating character, which lowers the

electron affinity (EA) of the cation,[112] but also to the steric hindrance of the hexyl chain, hindering the positive charge to approach the vicinity of the cathode (Figure 13).[62, 113]

Table 9: Cathodic limit (V_{cat}), anodic limit (V_{an}) potential and electrochemical windows ΔV (in V vs. Fc^+/Fc). Cut-off current density j = 0.3 A dm^{-2}, at 90 °C with CV, Pt working electrode.

R^2	H (**48b**)	Me (**49b**)	Et (**50b**)	iPr (**51b**)
V_{cat}	-2.20	-2.47	-2.50	-2.70
V_{an}	1.53	1.53	1.58	1.48
$\Delta V = V_{cath} - V_{an}$	3.73	4.00	4.08	4.18

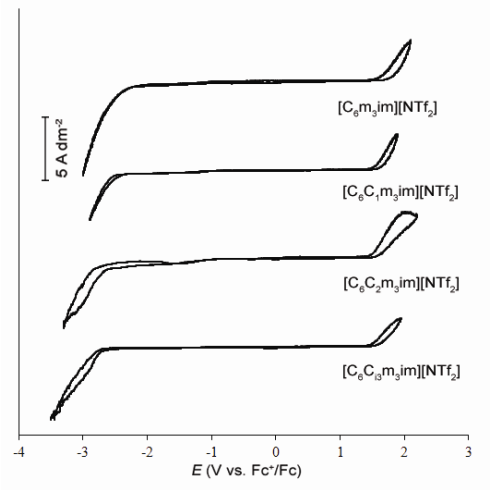

Figure 13. Cyclic voltammograms of $[C_6R^2m_3im][NTf_2]$, (R^2: H, Me, Et, iPr); Pt working electrode at 90 °C.

Cathodic and anodic decomposition potentials as well as the electrochemical window are given in Table 9. These are the potentials with an observed current density of 3 mA cm^{-2}, the current density at which all baseline noise could be neglected. Although $[NTf_2]^-$ anions can influence the cathodic decomposition behaviour,[114] and imidazolium cations can be oxidised at positive potentials,[115] a clear qualitative effect on the electrochemical window by the substituents was observed. The stability against cathodic reduction of the cation increases by changing the alkyl substituent in the order (H < Me < Et < iPr), and at positive potentials no significant influence was apparent. Thus, as for the *N*-hexyl substitution, the increased substitution on the C2 position is also believed to increase the cathodic stability by increment of both steric bulk and electron density in the aromatic system.

1.9. Conclusions

Tetrasubstituted imidazoles are readily synthesised via a one-pot reaction. Formation of 1*H*-imidazole is thereby avoided. It is also possible to synthesise the *N*-hexylimidazoles using continuous flow technology, which can provide the imidazoles on an industrial scale. The imidazole core is easily methylated with methyl iodide to obtain imidazolium iodides, and subsequent metathesis reactions give dicyanamide and bis(trifluoromethylsulfonyl)imide ionic liquids in almost quantitative yields.

The *N*-ethyl substituted imidazolium iodide salts are solid, which allows for an easy purification, while the *N*-hexylimidazolium iodide analogues are liquid at room temperature. Although these imidazolium ionic liquids are fully substituted, the dicyanamide and bis(trifluoromethylsulfonyl)imide salts all remain liquid below 100 °C and several are liquid at room temperature. The *N*-hexyl substituted derivatives undercool easily, and thus possess a wide liquid range. Unlike literature values, melting points are found to decrease upon methylation at the C2 position. However, viscosities increase upon increasing the alkyl groups, which is in agreement with previous research.

Thermal stability is clearly increased upon alkylation of the C2 position, however a distinct effect was not observed when changing the alkyl substituent from methyl to isopropyl. On the other hand, the best electrochemical performance was observed for the isopropyl substituted derivative. This stabilising effect was attributed to both steric hindrance and inductive neutralisation of the positive charge. Compared to conventional imidazolium ionic liquids, these fully substituted ionic liquids are resistant against strong alkaline conditions.

2. Peralkylated alkoxy- and alkenylimidazolium ionic liquids

In the previous chapter, it was demonstrated that completely substituted imidazolium salts (in particular 2-isopropylimidazolium salts) possess improved thermal and (electro)chemical stability, while the melting points do not increase dramatically.[68, 111] Due to the increased substitution of these peralkylated imidazolium ionic liquids, melting points (T_m) of *N*-ethyl substituted analogues are above room temperature, while longer *N*-alkyl chains (C_6) decrease T_m, however increase viscosity.[68] In order to decrease melting points and viscosities of short chained, completely substituted imidazolium salts, the incorporation of different functional groups is evaluated.

2.1. Synthesis of imidazoles

The previously optimised (i.e. sequential) Debus-Radziszewski reaction procedure (Scheme 20) allowed the synthesis of 1*N*-allyl-2-isopropyl-4,5-dimethylimidazole (**59a**), 1*N*-(2-hydroxyethyl)-2-isopropyl-4,5-dimethylimidazole (**59b**) and 2-isopropyl-1*N*-(2-methoxyethyl)-4,5-dimethylimidazole (**59c**). The yield of the imidazole synthesis reaction was always in the same order of magnitude. However, the selectivity of the substituted imidazole over 1*H*-2-isopropyl-4,5-dimethylimidazole (**60**) differs.

The selectivity was related to the properties of the amine used (Table 10). Upon addition of NH_4OAc, a competing transamination on the intermediate imine (**39**) can occur. Imines with more electron donating substitution led to a higher selectivity. This is likely due to (i) higher stability of the intermediate imine towards transamination and (ii) faster reaction to form the imidazole. Hence, the addition in portions of NH_4OAc and diketone decreases the formation of the side product. Although a steric factor will contribute, which is apparent from the two first entries in Table 10, it is the electron withdrawing nature of the hydroxyl group which reduces selectivity.

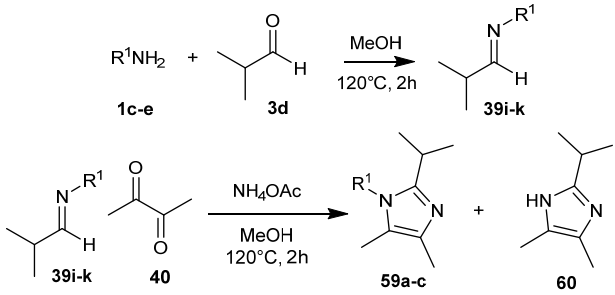

Scheme 20: The previously optimised Debus-Radziszewski reaction procedure, with formation of products 59a-c and the side product 1*H*-imidazole 60. Identification of the compounds is given in Table 10.

Table 10: Yield of 1*N*-alkyl-2-isopropyl-4,5-dimethylimidazole after distillation and selectivity in the modified Debus-Radziszewski reaction procedure with different amines.

Imidazole	Amine	Yield (%) (**4**)	Selectivity (%) (**4**/**4**+**5**)[c]
41d	Ethylamine	42	100
41h	Hexylamine	40	88
59a	Allylamine	63	88
59b	Hydroxyethylamine	/	75
59b	Hydroxyethylamine[a]	38[b]	95
59c	Methoxyethylamine	53	86

[a] Addition in portions; [b] crude yield; [c] measured by ^{1}H NMR.

If present in large quantities, the formed 1*H*-analogue could be precipitated from the crude mixture in acetonitrile, yielding the pure side product. During vacuum distillation, the remainder of the side product crystallises in the still, since it is not distillable in the workable range due to its hydrogen-bonding properties. Analogously, the hydroxyethyl derivative (**59b**) could not be distilled, and was therefore applied as such in the further functionalisation with both dimethylsulfate and iodomethane as methylating agents and allyl bromide (Scheme 21). While the methylating agents gave rise to formation of *N*-alkylated products, the allyl bromide was found to be very selective towards *O*-alkylation. This selectivity occurs most probably since the oxygen anion is a hard nucleophile compared to the nitrogen atom. The allyloxyethyl derivative was successfully distilled to obtain a clear yellow oil. The distilled imidazoles were obtained as clear liquids or as slightly yellowish liquids in which the colour sometimes spontaneously intensifies over a few days, only **59c** was a solid.

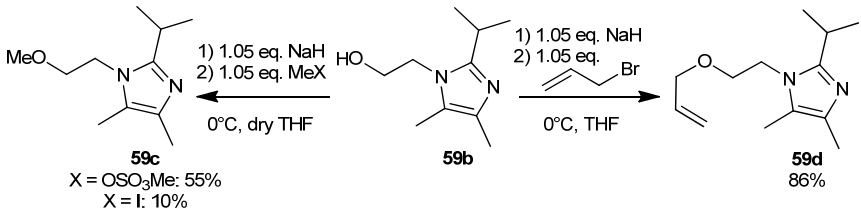

Scheme 21: Alkylation of the crude 2-imidazolylethanol (59b) with allyl bromide, dimethylsulfate and methyl iodide. Conversions are determined in the reaction mixture by ^{1}H NMR and in reference to the amount of 59b present in the crude starting material.

2.2. Synthesis of ionic liquids

The least symmetric ionic liquids, containing an *N*-methyl substituent (**61**-**63**), were synthesised by methylating the tetraalkylimidazole (**59a**,**c,d**) with methyl iodide (MeI) or methyl methanesulfonate (MeOMs) (Scheme 22). The methylation with MeI proceeded smoothly at 0 °C overnight, while reaction with MeOMs needed to be refluxed for over 24

hours. The latter reaction could be accelerated by microwave heating for 30 min at 80 °C. The low volatility of MeOMs allowed the use of a smaller excess of methylating reagent. An overview of the applied nomenclature and alkylation agents used are given in Table 11.

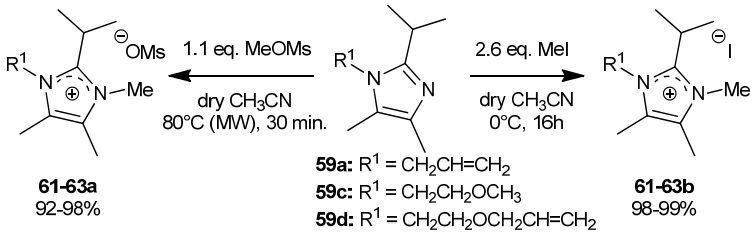

Scheme 22: Methylation of the tetraalkylimidazoles. Identification of the compounds is given in Table 11.

Quaternisation with allyl bromide or allyl methanesulfonate always required high temperatures and/or long reaction times. Reactions in conventional flask proceeded very slowly. After 32 h at 50 °C only 16% of **41d** was converted with allyl methanesulfonate, after 16 h at 60 °C only 46%, while at 80 °C after 24 and 38 hours, still only 77 and 95% were converted. Fortunately, here too, microwave irradiation could be applied to very efficiently accelerate the synthesis (Scheme 23). In all allylation reactions, formation of a side product was observed: small quadruplets of the (NCH_2) were visible in the ^1H NMR spectrum (in $CDCl_3$) upfield (4.2 ppm) of the (NCH_2) of the desired end product (4.3 ppm), accounting for 11-28 mol%. Prolonged heating of the mixture at high vacuum and washing an aqueous solution with Et_2O or EtOAc removed the starting materials, however, the side product was then still present and is therefore most likely a salt.

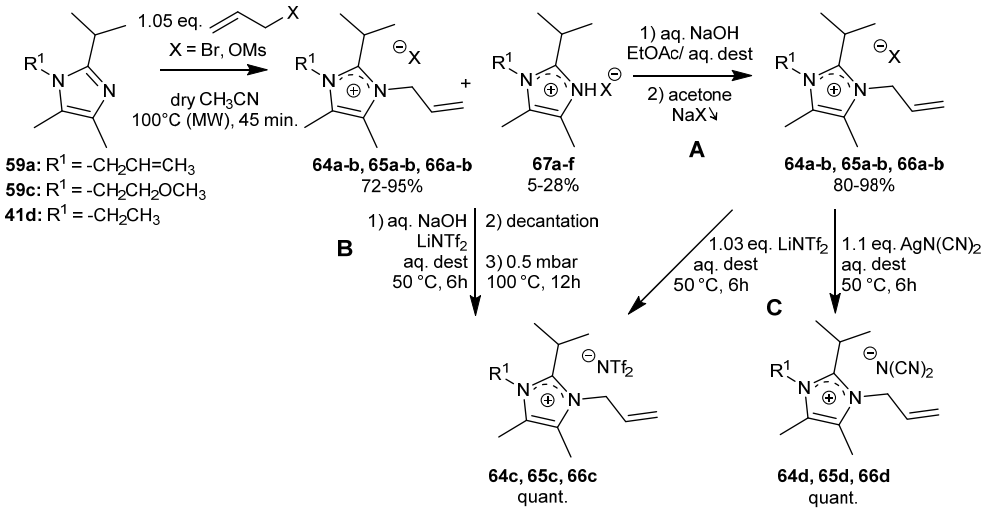

Scheme 23: Synthesis of allyl functionalised imidazolium salts by quaternisation and metathesis. X = OMs (64a-66a), X = Br (64b-66b). Identification of the compounds is given in Table 11.

The formation of HOMs or HBr by the action of water was proposed, leading to inert protonated imidazoles (**67**, Scheme 23), although the presence of AllOH could not be proven by LC-MS or GC. The use of intensively dried CH_3CN (percolated over alumina and stored over 3Å Molecular Sieves) did not decrease the formation of side products, while the use of dichloromethane led to formation of multiple side products. Hence, the reaction mixture was neutralised with a stoichiometric amount of NaOH in demineralised water and the formed free imidazole base was extracted with EtOAc from the aqueous mixture. When the water was removed by rotary evaporation or lyophilisation, crystals of NaOMs or NaBr were formed in the ionic liquid. Dissolution of the mixture in hot acetone gave a fine suspension, which could be filtered after cooling (pathway A, Scheme 23); complete removal of NaOMs was confirmed by ^{1}H NMR, although residual traces of NaOH could not be excluded. A fine suspension of NaBr was removed by precipitation from an aliquot of CH_2Cl_2 and subsequent filtration. Direct metathesis into the hydrophobic $[NTf_2]^-$ salt allowed the use of a small excess of NaOH solution (pathway B). In this case, residual sodium salts were discarded with the aqueous phase and the residual neutral imidazole was removed by distillation. The pentaalkylimidazolium derivatives were obtained quantitatively after metathesis. To obtain the $[NTf_2]^-$ and $[N(CN)_2]^-$ salts of both *N*-methylated and *N*-allyl analogues, standard metathesis reactions could successfully be applied on the extracted mesylate or bromide salt (pathway C, Scheme 23). The metathesis involved the use of a small excess of $LiNTf_2$ or $AgN(CN)_2$. In the synthesis of compounds **64c**, **65c** and **66c**, pathway B was applied. Given the precipitation of NaOMs in the ionic liquids and acetone and the ability to monitor residual NaOMs or HOMs species via ^{1}H NMR, all $[NTf_2]^-$ and $[N(CN)_2]^-$ salts could be obtained via halide and silver-free ionic liquid synthesis by adding $LiNTf_2$ or $NaN(CN)_2$, respectively, to an aqueous solution of the methanesulfonate salts (Scheme 24). The $[NTf_2]^-$ salt was obtained by decanting and washing the organic layer, while the $[N(CN)_2]^-$ salt was obtained by evaporation of the aqueous solution and precipitation of the sodium salts in an acetone or CH_2Cl_2 solution. Nonetheless, in the synthesis of the $[NTf_2]^-$ salts, the commercially available allyl bromide was used. To obtain the *N*-allylimidazolium $[N(CN)_2]^-$ salts (**61d**-**63d**), the methanesulfonate pathway was chosen, as NaOMs was more easily removed than NaBr, which led to a finer suspension.

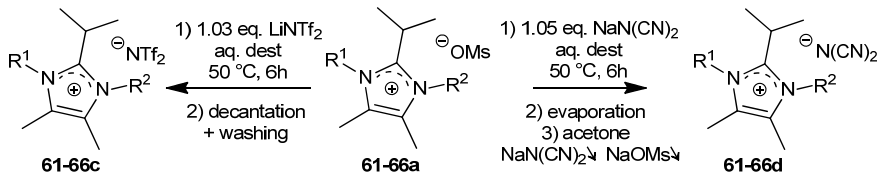

Scheme 24: Metathesis of methanesulfonate $[OMs]^-$ salts into $[NTf_2]^-$ and $[N(CN)_2]^-$ ionic liquids. Identification of the compounds is given in Table 11.

Table 11: Overview of synthesised ionic liquids, quaternisation agent (RX) and physical state at room temperature.

	Ionic Liquid[a]	R^{1}[b]	R^{2}[b]	RX	Physical state
61a	$[C_AC_1C_{i3}m_2im][OMs]$	allyl	methyl	MeOMs	liquid
61b	$[C_AC_1C_{i3}m_2im][I]$	allyl	methyl	MeI	liquid
61c	$[C_AC_1C_{i3}m_2im][NTf_2]$	allyl	methyl	MeI	liquid
61d	$[C_AC_1C_{i3}m_2im][N(CN)_2]$	allyl	methyl	MeOMs	liquid
62a	$[C_{2O1}C_1C_{i3}m_2im][OMs]$	methoxyethyl	methyl	MeOMs	cryst.
62b	$[C_{2O1}C_1C_{i3}m_2im][I]$	methoxyethyl	methyl	MeI	cryst.
62c	$[C_{2O1}C_1C_{i3}m_2im][NTf_2]$	methoxyethyl	methyl	MeI	cryst.
62d	$[C_{2O1}C_1C_{i3}m_2im][N(CN)_2]$	methoxyethyl	methyl	MeOMs	cryst.
63a	$[C_{2OA}C_1C_{i3}m_2im][OMs]$	allyloxyethyl	methyl	MeOMs	liquid
63b	$[C_{2OA}C_1C_{i3}m_2im][I]$	allyloxyethyl	methyl	MeI	liquid
63c	$[C_{2OA}C_1C_{i3}m_2im][NTf_2]$	allyloxyethyl	methyl	MeI	liquid
63d	$[C_{2OA}C_1C_{i3}m_2im][N(CN)_2]$	allyloxyethyl	methyl	MeOMs	liquid
64a	$[C_AC_2C_{i3}m_2im][OMs]$	allyl	ethyl	AllOMs	liquid[c]
64b	$[C_AC_2C_{i3}m_2im][Br]$	allyl	ethyl	AllBr	solid
64c	$[C_AC_2C_{i3}m_2im][NTf_2]$	allyl	ethyl	AllBr	cryst.
64d	$[C_AC_2C_{i3}m_2im][N(CN)_2]$	allyl	ethyl	AllBr	solid
65a	$[C_AC_AC_{i3}m_2im][OMs]$	allyl	allyl	AllOMs	liquid[c]
65b	$[C_AC_AC_{i3}m_2im][Br]$	allyl	allyl	AllBr	liquid[c]
65c	$[C_AC_AC_{i3}m_2im][NTf_2]$	allyl	allyl	AllBr	cryst.
65d	$[C_AC_AC_{i3}m_2im][N(CN)_2]$	allyl	allyl	AllBr	cryst.
66a	$[C_{2O1}C_AC_{i3}m_2im][OMs]$	allyl	methoxyethyl	AllOMs	glass
66b	$[C_{2O1}C_AC_{i3}m_2im][Br]$	allyl	methoxyethyl	AllBr	liquid
66c	$[C_{2O1}C_AC_{i3}m_2im][N(CN)_2]$	allyl	methoxyethyl	AllBr	liquid
66d	$[C_{2O1}C_AC_{i3}m_2im][NTf_2]$	allyl	methoxyethyl	AllBr	liquid

[a] C_{i3}: 2-isopropyl; for convenience, the *N*-methyl group is referred to as C_1; [b] R^1 and R^2 are the substituents as depicted in Scheme 24; [c] very viscous liquid: very slow crystallisation: not completely crystallised after several weeks.

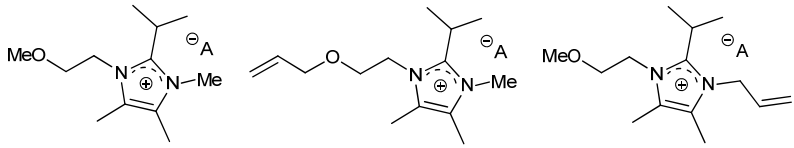

62a-d 63a-d 66a-d

Figure 14: Ether containing imidazolium ionic liquids.
Anions (A^-): a: $[OMs]^-$; 62b,63b: $[I]^-$; 66b: $[Br]^-$; c: $[N(CN)_2]^-$; d: $[NTf_2]^-$.

2.3. Melting points and viscosities

By several research groups, alkene functionalities were shown to reduce viscosity, this was proposed to be due to an increased planarity which allows a molecular 'flow' with little resistance.[39] Schneider *et al.* found 1-allyl-3-methylimidazolium bromide ($[C_AC_1im][Br]$) to be crystalline, although readily undercooled.[116] The symmetrically allyl functionalised 1,3-diallylimidazolium bromide and bis(trifluoromethylsulfonyl)imide ($[C_AC_Aim][Br]$ and $[C_AC_Aim][NTf_2]$) are not solid, therefore the allyl group seems to increase the undercooling properties, presumably by increasing the possible hydrogen bond donor sites.[117]

The substitution of alkyl groups by iso-electronic alkyl ether chains (Figure 14) induces repulsion between neighbouring oxygen atoms, leading to significant ion pairing and to intermolecular hydrogen bonding interactions between imidazolium hydrogens and alkoxy oxygen lone pairs. This combined effect leads in general to higher melting points (T_m) and glass transition temperatures (T_g) than the alkyl analogues.[38, 118] However, the oxygen lone pairs are believed to reduce the electrostatic interaction between anion and cation. Thus, reduction of T_m and viscosity reduction is nonetheless observed upon substitution of alkyl chains by alkyl ether chains in imidazolium,[64] ammonium[65a] as well as in phosphonium ionic liquids.[47a] Moreover, as sometimes no difference is observed at all,[119] this trend is not unambiguously applicable to all ionic liquid analogues and should be investigated for every analogue separately.

As can be seen in Table 11, the more symmetric compounds with non-coordinating anions (**64**, **65**) are (crystalline) solids. When combined with more basic anions ($[Br]^-$, $[OMs]^-$), very viscous liquids were obtained. Although some of them formed crystals at room temperature, isolation from the mother liquor could not be achieved. Their readily crystallisable $[NTf_2]^-$ and $[N(CN)_2]^-$ salts indicate that (i) the high symmetry induces rapid crystallisation (ii) the hydrogen bonding capacities of $[Br]^-$ and $[OMs]^-$ hinder crystallisation. This suggests an extra possible hydrogen bonding site provided by the allyl group (apart from isopropyl and NCH_3 protons). This extra hydrogen bonding site increases entropy,[91, 120] and the interaction with the coordinating anions is also visible by the chemical shift in the ^1H NMR spectra (in $CDCl_3$). In our studies, we did never observe solidification of the $[C_AC_1C_{i3}im]^+$ analogues. The incorporation of methoxyethyl side chains (C_{2O1}) in the cation leads to more readily

crystallising salts, although room temperature ionic liquids (RTILs) were obtained when combined with $[NTf_2]^-$ or $[N(CN)_2]^-$ (see Table 12). When combined with an allyl substitution, again solidification is hindered. Only the $[C_{2O1}C_AC_{i3}m_2im][OMs]$ salt was found to solidify (as a glass). Hence, the main factor in the solidification of the salts is the methoxy group.

Solidification could be forced for **64b** and **65d** by rapidly undercooling the samples with liquid nitrogen and recrystallising the thus formed white flakes in acetone. In a single case (**65a**), the salt could be precipitated by adding ether dropwise to an acetone solution of the crude mixture. For other derivatives rapid cooling did not lead to crystallised products. Holding the samples for prolonged times at different elevated temperatures to reduce viscosities and hence promote crystal formation did not produce crystals in any case.

Table 12: Melting points (in °C) of alkoxy and alkenyl derivatised imidazolium ILs, $[R^1R^2C_{i3}m_2im][A]$.

	R^1	R^2	[OMs] (**a**)	[I]/[Br][a] (**b**)	$[NTf_2]$ (**c**)	$[N(CN)_2]$ (**d**)
62	C_{2O1}	C_1	132	123	22	20
64	C_A	C_2	[c]	109	58	28
65	C_A	C_A	41	[c]	63	60
66	C_{2O1}	C_A	70[b]	[c]	[c]	[c]

[a] For compound 62, the halide salt is the $[I]^-$ salt, otherwise the $[Br]^-$ salt; [b] Glass transition temperature; [c] Compound is liquid.

Table 13: Viscosities of $[R^1R^2C_{i3}m_2im][A]$ (in mPa s at 23 °C), water content (in ppm) between brackets.

	R^1	R^2	$[NTf_2]$ (**c**)	$[N(CN)_2]$ (**d**)
61	C_A	C_1	721 (320)	2520 (4860)
62	C_{2O1}	C_1	131 (250)	380 (330)
63	C_{2OA}	C_1	286 (140)	306 (310)
64	C_A	C_2	[a]	2350 (1370)
66	C_{2O1}	C_a	860 (290)	1075 (560)

[a] Compound 64c is solid.

Viscosities of the liquid salts are given in Table 13. Halide and methanesulfonate salts are omitted because of their very high viscosities. The salts of analogues **62** and **64** (except **64c**) were found to be liquid at the analysis temperature and therefore also analysed. Derivatives containing an alkoxy side chain have a reduced viscosity compared to the ones containing alkenyl side chains, which were very viscous. Of the derivatives combining both functionalities (**63**, **66**), the salts with the $[C_{20A}C_1C_1im]^+$ cation (**63**), bearing both functionalities in one substituent and substituted with *N*-methyl, have the lowest viscosity.

2.4. Crystallographic analysis

The high melting points induced by the alkylation pattern of some of the ionic liquids described here mean that it is possible to study them in the solid state. One of the most powerful techniques is single crystal X-ray diffraction, which gives absolute atomic positions and arrangements of molecules as well as accurate intermolecular distances. This analysis was performed at the department of Chemistry at KU Leuven. From a comparison of the intermolecular distances in the different compounds, the relation between intermolecular interactions and melting points can be probed. Single crystals could be grown and analysed with X-ray diffraction in the case of the following six compounds: **62a**, **62b**, **62c**, **64c**, **65c** and **65d**. Within this set, three have the same cation (**62a**, **62b** and **62c**), three have the same anion (**62c**, **64c** and **65c**) and a further set of two (**65c** and **65d**) also have the same cation. The last compound **65d**, containing a $[N(CN)_2]^-$ anion is valuable as crystallographic information on dicyanamide ionic liquids is scarce.

In all bis(trifluoromethylsulfonyl)imide containing salts, the anions are distorted at 100 K, consistent to earlier observations,[119b, 121] and in trans-conformation, indicating the low hydrogen-bonding ability between cation and the $[NTf_2]^-$ anion.[122]

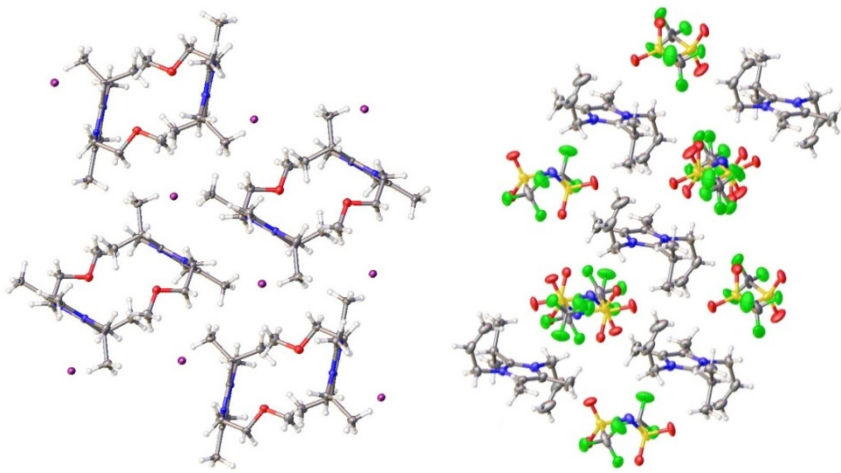

Figure 15: Formation of bilayers with intercalated anions in $[C_{2O1}C_{i3}m_3im][I]$ (62b) (left) and alternated ion pairing in $[C_AC_AC_{i3}m_2im][NTf_2]$ (65c) (right).

In the non-peralkylated $[C_{2O1}C_1im][Br]$, increased ion paring in the solid state was observed by repulsion of neighbouring oxygens. In this salt, cations form layers governed by π-π stacking, and different conformations of the pendant alkoxy chains with respect to the imidazolium ring within the different moieties in the unit cell were found.[118] Controversially, in $[C_{2O1}C_1C_{i3}m_2im][I]$ (**62b**) no such multiple conformers exist, presumably by steric hindrance of

the alkyl chains or by elimination of hydrogen-bonding acceptor sites for intermolecular hydrogen-bonding. Cationic bilayers are formed with the alkoxy groups pointed inwards, and the anions intercalated between the bilayers (Figure 15, left). Hereby, the interaction of the oxygen lone pairs with the anions negative charge is minimised while compromising the inter-oxygen distance. The cations are not perfectly stacked on top of each other, therefore the layers are slightly tilted.

In $[C_{2O1}C_1C_{i3}m_3im][OMs]$ (**62a**) no cationic bilayer is found, i.e. anion and cation are alternated. Since a decrease in repulsion between the $[OMs]^-$ anion and methoxyl group compared to the iodide salt is unlikely to be significant, the driving force for forming the alternating layers is believed to be the anion size and increased hydrogen-bonding. The cationic bilayer is also absent in the $[NTf_2]^-$ salts of other cations, e.g. in **65c** (Figure 15, right) and the destruction of the cationic bilayer when anion size is increased, is earlier observed in $[C_{2O1}mim][PF_6]$ as well.[119b]

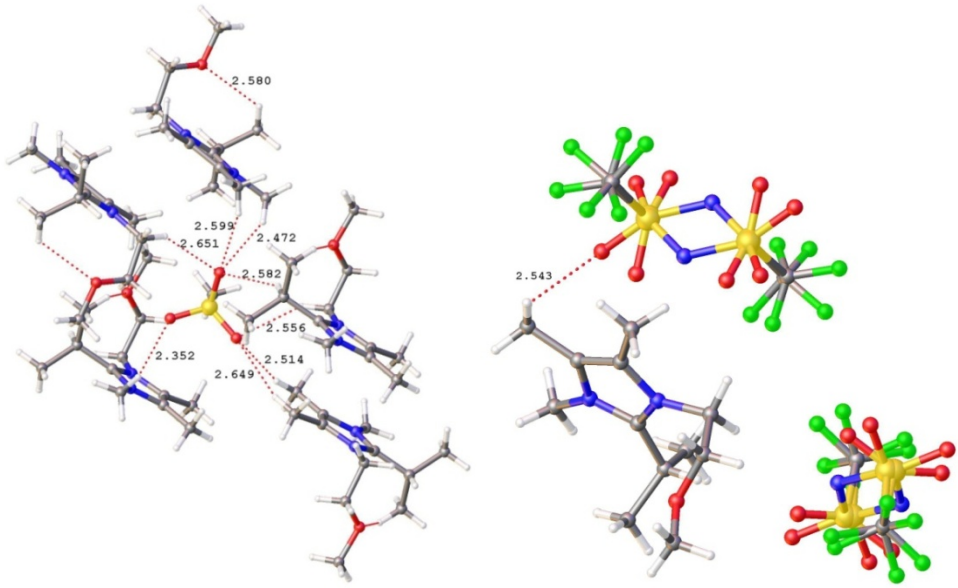

Figure 16: Presentation of the crystal structure of $[C_{2O1}C_1C_{i3}m_2im][OMs]$ (62a) (left) with intra- and intermolecular C–H···O bonds and $[C_{2O1}C_1C_{i3}m_2im][NTf_2]$ (62c) (right) with intermolecular C–H···O bonds.

The structures of **62a**, **62b** and **62c** all contain a $[C_{201}C_1C_{i3}m_2im]^+$ cation and in each structure the C_{2O1} group lies perpendicularly to the imidazolium ring as was also earlier observed in $[C_{201}C_1C_1im][Br]$, $[C_{201}C_1C_1im][PF_6]$[119b] and $[C_{201}C_1im][I]$.[118] Moreover, this was found by DFT calculations to be the most stable conformation of the C_{2O1} group with respect to the imidazolium ring by Fei *et al.*[118] There is an intramolecular C–H···O hydrogen bond formed

between the methoxy group and one of the hydrogen atoms of the methyl on the isopropyl group of **62a** (Figure 16, left) and **62b**, but not in **62c** (Figure 16, right).

A strong difference in interaction can be found upon anion variation between the different compounds **62a**, **62b** and **62c**. In **62a**, eight interactions via C–H···O from the cation to the anion can be found, while in **62b**, six C–H···I interactions are found, and finally, **62c** contains only 0.5 C–H···O cation-anion interactions, i.e. with only one of the two crystallographically distinct anions (Figure 16, right). A clear relationship can be found between the number of intra- and intermolecular interactions and the melting point, i.e. **62a** (nine interactions) has a melting point of 132 °C, **62b** (seven interactions) has a melting point of 123 °C and **7c** (0.5 interactions) and has a melting point of 22 °C.

In the series of $[NTf_2]^-$ containing ionic liquids **62c**, **64c** and **65c**, all containing low melting points, a low number of intermolecular interactions was found in all of the crystal structures. In compound **62c**, the melting point is near room temperature (22 °C), compound **65c** has the highest number of interactions (i.e. 1 and 3 interactions with the two crystallographically distinct anions) and the highest melting point (63 °C), while **64c** has as much intermolecular interactions as **62c** but only a slightly lower melting point (58 °C) than **65c**.

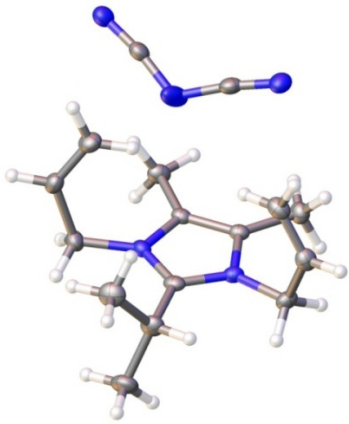

Figure 17: ORTEP diagram of $[C_AC_AC_{i3}m_2im][N(CN)_2]$ showing the two allyl groups on the same side of the imidazolium plane and the $[N(CN)_2]$ anion. Displacement ellipsoids are drawn at the 50% probability level.

The ionic liquids $[C_AC_AC_{i3}m_2im][NTf_2]$ (**65c**) and $[C_AC_AC_{i3}m_2im][N(CN)_2]$ (**65d**) contain the same cation but the cation has a different conformation in the two structures. In **65c**, the two allyl groups are located on opposing sides of the imidazolium ring (Figure 15, right), whereas in **65d**, they are on the same side of the ring (Figure 17). The structure of **65d** contains three intermolecular C–H···N interactions between the cation and the $[N(CN)_2]^-$ anion, so comparable to those in **65c**, but **65d** has the lower melting point (47 °C compared to 63 °C).

2.5. Electrochemical analysis

In previous research in our group,[68] it was shown that completely substituted imidazoles possess wider electrochemical windows (ECWs) than their non-substituted analogues. Hence, the effect of the functionalities on the electrochemical window can be investigated without interference of the imidazolium ring hydrogen atoms, which are all substituted. Moreover, the influence of the functionalities, altering the rheologic or complexing behaviour of the substances, on the electrochemical performance can be investigated. On the one hand, alkenes induce generally a minute stability increase at the cathode, while substantially at the anode.[39, 123] On the other hand the effect of alkoxyl groups on the electrochemical windows was earlier found to be very small or absent.[119a, 124] The anodic (V_{an}) and cathodic limit potentials (V_{cat}) and electrochemical windows (ΔV) of compounds **61-66c** are given in Table 14, with a cut-off current density value of 0.25 A dm^{-2}, which is the value at which all baseline noise can be ignored.

Table 14: Cathodic limit (V_{cat}), anodic limit (V_{an}) potential and electrochemical windows ΔV (in V vs. Fc^+/Fc). Cut-off current density j = 0.25 A dm^{-2}, at 90 °C with CV, Pt working electrode.

Ionic Liquid		V_{cat}	V_{an}	ΔV
61c	$[C_AC_1C_{i3}m_2im][NTf_2]$	-2.58	1.61	4.19
62c	$[C_{2O1}C_1C_{i3}m_2im][NTf_2]$	-2.24	1.47	3.71
63c	$[C_{2OA}C_1C_{i3}m_2im][NTf_2]$	-2.26	1.21	3.47
64c	$[C_AC_2C_{i3}m_2im][NTf_2]$	-2.44	1.68	4.12
65c	$[C_AC_AC_{i3}m_2im][NTf_2]$	-2.3	1.82	4.12
66c	$[C_{2O1}C_AC_{i3}m_2im][NTf_2]$	-2.33	1.49	3.82

In the compounds analysed, the introduction of the ether function decreases both the anodic and cathodic stability, while the decrease of the latter is more pronounced (Figure 18). This reduction of the cathodic stability seen for ether functionalised cations was earlier attributed to a certain complexation of the oxygen electron lone pairs to the positive charge, distributing the charge and hence rendering the parent cation more stable but the ether function less stable towards reduction, reducing the overall cathodic stability.[80]

On the anodic side, it appears that allyl groups can increase the oxidative stability (V_{an}(**61c**) < V_{an}(**65c**) and V_{an}(**62c**) < V_{an}(**66c**); Table 14). Hence, there is a clear influence of the unsaturated side chains on the oxidative stability. Given the high vulnerability of unsaturated bonds towards oxidation compared to saturated side chains, this observation was attributed by Min *et al*. to the formation of a passivation layer on the electrode formed by oxidation of the unsaturated bonds.[39] However, introduction of allyl groups shifts the overall electrochemical window to the anodic side, which can be attributed to electron withdrawal from the ring.

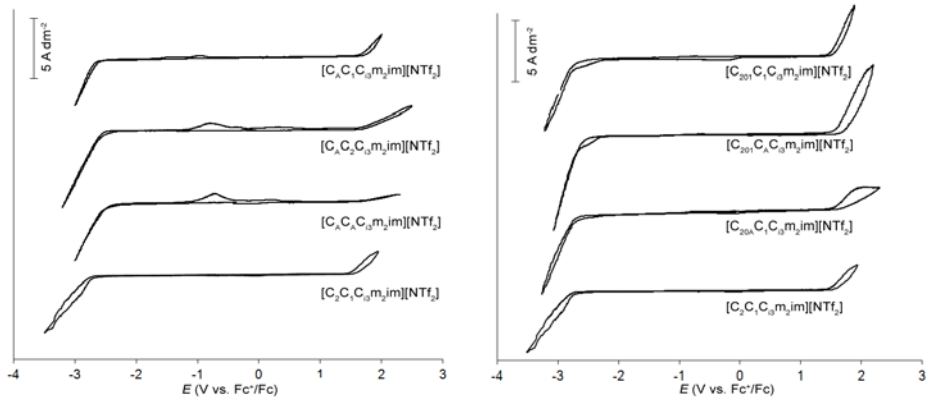

Figure 18: ECWs of alkenyl (left) and alkoxy (right) functionalised peralkylated ionic liquids, X-axis: potential *E* vs. Fc^+/Fc, Y-axis: current density *j*, at 90 °C with LSV, Pt working electrode.

2.6. Application in synthetic reactions

Apart from the rheological implications, the oxygen with its lone-pair electrons is not seldom introduced in ionic liquids to enhance metal complexation and transport properties, e.g. for Li[125] and Mg.[124, 126] The latter was introduced by means of commercial MeMgBr in THF solutions in e.g. 1-allyl-3-(2-methoxyethyl)-2-methylimidazolium bis(trifluoromethylsulfonyl)-imide ($[C_{2O1}C_AC_1im][NTf_2]$) by Kakibe *et al.*[124] This particular ionic liquid possesses improved conductivity and is sufficiently stable to withstand the Grignard reagents.

Given the omnipotence of organometallic compounds with regard to C-C bond formation, the application of Grignard reactions in ionic liquids has already attracted specific attention. Thus, phosphonium salts are up to date very successful, the hydrophobic tetraoctylphosphonium bis(trifluoromethylsulfonyl)imide allows addition reactions with commercial THF solutions of PhMgBr. The stability is attributed to the shielding of the most acidic protons by the long alkyl chains. Unfortunately, the lipophilic character of the cation hampers the extraction of the products.[127] In analogous salts substituted with an alkyl ether moiety an accelerating effect of the addition reaction is observed. Although reaction with pure PhMgBr (i.e. after evaporation of the THF) was successful, generation of the Grignard reagent in this ether containing ionic liquid could not be achieved.[128] Commercial solutions of Grignard reagents have also been applied in 2-alkylimidazolinium and imidazolium salts.[18, 111] The synthesis of the Grignard reagent was obtained by Chan *et al.* in *N*-butylpyridinium tetrafluoroborate $[C_4py][BF_4]$.[129]

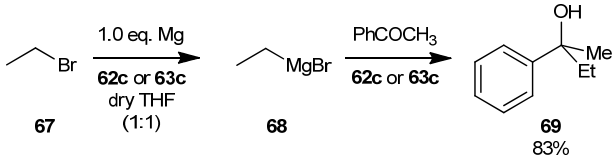

Scheme 25: Application of ionic liquids 62c and 63c in the Grignard addition reaction of ethylmagnesiumbromide and acetophenone.

Grignard addition reactions in ionic liquids are in general performed using the hydrophobic $[BF_4]^-$, $[PF_6]^-$ or $[NTf_2]^-$ salts, which allows an aqueous reaction work-up.[18, 126-127] On the other hand, the organomagnesium compounds were found to be stabilised by the anion of the tetraalkyl phosphonium decanoate salt.[130] Therefore, next to the alkoxy derivatised $[NTf_2]^-$ salts $[C_{201}C_1C_{i3}m_2im][NTf_2]$ (**62c**) and $[C_{20A}C_1C_{i3}m_2im][NTf_2]$ (**63c**), also their $[OMs]^-$ analogues (**62a** and **63a**) were proposed for evaluation.

First, the synthesis of EtMgBr via the Grignard reaction of EtBr with magnesium was evaluated. Neither in **62c** nor in **63c** the reaction succeeded even after prolonged heating at 120 °C. Therefore, small amounts of dry THF were added step by step. The reaction proceeded smoothly when a 1:1 mixture of IL to THF was reached (Scheme 25). When the reaction was complete, the solvent was removed *in vacuo* and acetophenone was added dropwise to the mixture at 0 °C. After completion of the addition reaction, the ionic liquid was washed with water and the products were extracted with Et_2O. The addition products were analysed by GC-FID and acetophenone was found to be converted in 72 to 83% yield. The remainder of the organomagnesium compound might have reacted with residual water in the ionic liquids. Since **62a** and **63a** are insoluble in THF, these ionic liquids were not further evaluated.

2.7. Conclusions

The previous reported modified Radziszewski reaction can successfully be applied in the synthesis of alkenyl and alkoxy substituted imidazoles, although side product formation is found to be dependent on the nature of the amine. The imidazoles can be transformed in their corresponding ionic liquids via the earlier described method or aided by microwave irradiation. In quaternisation reactions with allyl bromide and allyl methanesulfonate, a side product needs to be extracted from the resulting ionic liquids. The obtained (after metathesis) salts show high crystallinity when incorporating an alkoxy moiety due to the constraint conformation, but show improved undercooling properties when an allyl substituent is introduced, unless the salt possesses high symmetry. Compared to alkyl functionalised IL, the electrochemical window of the alkenyl substituted imidazolium salts shifts towards more positive potentials, while derivatives with alkoxy substitution have a decreased electrochemical window. In general a high chemical stability could be observed for these ionic liquids.

3. Chiral peralkylated imidazolium ionic liquids

3.1. Introduction

In the previous chapter it was shown that 1-methoxyethyl-2-isopropyl-3,4,5-trimethylimidazolium ionic liquids have moderate viscosities, while their melting points are around room temperature. Alkenyl substitution decreased the melting points, at the expense of the viscosity. Increased (asymmetric) branching of the *N*-alkoxyl chains might decrease the symmetry and hinder the packing efficiency of the ion pairs. In this way, the crystal forming properties of alkoxy functionalities might also be suppressed. Next to the rheological implications, the introduction of short chained chiral moieties also allows the exploitation of chiral pool molecules, i.e. naturally occurring, enantiopure building blocks, which are preferentially cheap and can be obtained via fermentation or enzymatic synthesis, i.e. via renewable synthesis.

The stability of the previously described ionic liquids (e.g. **62c** and **63c**) towards Grignard reagents invites for the design of an enantiopure recyclable ionic liquid which is stable enough to withstand bases with no degradation nor racemisation. This type of chiral imidazolium ionic liquids could find its application as recyclable (co)-solvents in asymmetric addition reactions. An ionic liquid able to perform this task, should have a low viscosity and a high chemical stability.

The field of chiral ionic liquids is wide and still growing. Some of these compounds have found application e.g. in chiral C-C bond formation via Michael addition,[131] or as chiral shift reagents (CSRs) for the determination of enantiomeric purity by NMR.[132] A very brief outline of the currently known imidazolium ionic liquids based on the chiral pool is given in the next paragraphs, although for a complete overview of this very extensive field, review literature on the topic should be consulted.[133]

Next to the introduction of chiral aminoalcohols in the imidazole synthesis reaction,[134] the introduction of amino acids in ionic liquids has already been extensively studied. They have been applied in their native forms as both the cationic and anionic part of ionic liquids. Also single transformations as well as dual transformations have been applied to achieve ionic liquids. The divergent synthesis routes towards amino acid based ionic liquids was extensively reviewed by Plaquevent *et al.*[133b]

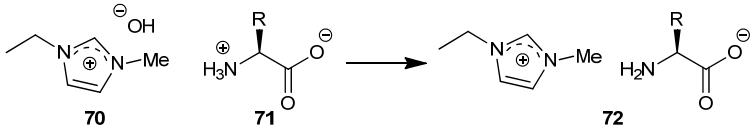

Scheme 26: Synthesis of amino acid containing ionic liquids by neutralisation of [C_2mim][OH], leading to an extended library of ionic liquids.[135]

The application of amino acids in their zwitterionic form was studied by the group of Ohno.[135] They have synthesised a library of 20 ionic liquids with different amino acids as anion, combined with the $[C_2mim]^+$ cation, since this cation proved to always form room temperature ionic liquids (Scheme 26). The improved solubility of the amino acids in molecular solvents by their transformation into ionic liquids opens up possibilities for many new applications.

Amongst the many other derivatised amino acid based imidazolium ionic liquids, the group of Luis has reported several ionic liquids based on amino acid derived imidazoles, i.e. amino acid based imidazolylesters, -amides and -alcohols.[132b, 136] Alternatively, amino acids have been applied in the synthesis of imidazolinium ionic liquids.[132d, 137]

Lactate derived quaternisation agents were already applied by Jodry and Mikami to obtain a chiral ester containing ionic liquid (**73,** Figure 19). However, the ester function is not chemically stable, as it has an acidic proton in the α-position.[132e] The compound **73** was synthesised by substitution of the lactate derived trifluoromethanesulfonate ester, however, a complete racemisation was observed when the synthesis was performed at 0 °C. Bao *et al.* reported on the transformation of ethyl L-lactate into a quaternisation agent by benzylation of the secondary alcohol, subsequent reduction of the ester and tosylation of the primary alcohol, resulting in the ionic liquid **74** .[131c] Analogously, chiral dicationic imidazolium salts were prepared with a tartrate-derived quaternisation agent,[131c] while imidazolium ionic liquids comprising the lactate or tartrate anion have also been reported.[138]

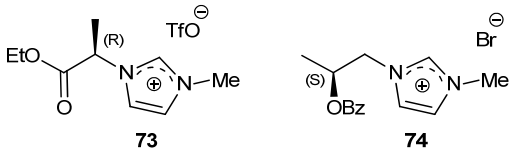

Figure 19: L-lactate derived imidazolium salts applied as chiral shift reagent (left)[132e] and in asymmetric Baylis-Hillman reactions (right).[131c]

Another important group of chiral pool molecules are the terpenes, e.g. camphor, borneol, menthol and pinene. These compounds are predominantly obtained via extraction or semi-synthetic production. Their sulfate and sulfonate acids were already reported as chiral ionic

liquid anions.[132c, 139] Nevertheless, they have also been modified in order to obtain terpene-derived cations. To that end, chloromethyl mentylethers have shown to be directly applicable as quaternisation agents, leading to menthoxymethyl derived imidazoles (**75**, Figure 20), while several terpenols can also be coupled to the imidazolium core by means of chloroacetyl chloride, with formation of ester functionalised chiral imidazolium cations (**76**) Note that the chemical stability of these two compounds is doubtable.

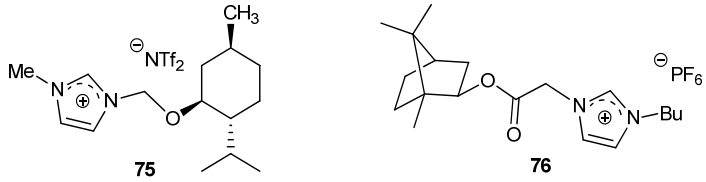

Figure 20: Menthoxymethyl substituted (left)[140] and borneol derived (right)[141] chiral imidazolium ionic liquids.

Alternatively, the use of an α-pinene derived oxazolinium ionic liquid (Figure 21) has been evaluated in the 1,4-addition of diethylzinc to cyclohexenone.[131a] The addition of 35 mol% of this particulate IL to the neat reaction mixture could induce an e.e. of 76%. Here, the effect of the IL was attributed to a complexation with the copper catalyst.

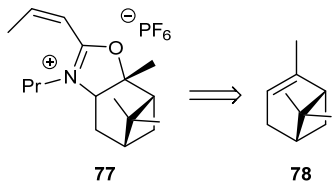

Figure 21: An α-pinene derived oxazolinium ionic liquid applied in Michael addition reactions.[131a]

Based on the knowledge from the previous chapters, the goal in this part of the research was to design enantiopure ionic liquids with high stability. If the asymmetric centre is situated in the cation, both hydrophobic and hydrophilic ionic liquids can be obtained. To assure high stability, low viscosity and metal transport properties, the amino acid carboxylates were transformed into the alkoxy-substituted derivatives. The introduction of chiral pool based moieties in the cation of imidazolium ionic liquids by either a priori synthesis of a chiral imidazole or application of a chiral quarterisation agent was studied. The routes towards different chiral imidazolium ionic liquids were evaluated on their synthesis, i.e. reproducibility (robustness), yields and enantioselectivity.

3.2. Synthesis of amino acid derived ionic liquids

The use of amino acids in ionic liquids has several advantages. (i) The presence of the amino group can be exploited in the previously optimised Debus-Radziszewski reaction procedure, via the intermediate imine, which is then converted into the imidazole by addition of ammonium acetate and diacetyl. Moreover, the optimisation of the continuous flow process might allow large scale production of amino acid based imidazoles.

(ii) The thus obtained imidazole derivatives possess a carboxylate function, which is an easily modifiable handle to introduce a myriad of functionalities. However, the focus here will be on the conversion to the ether derivatives via the ester (Scheme 27). This implies that also the commercially available amino acid esters can be used.

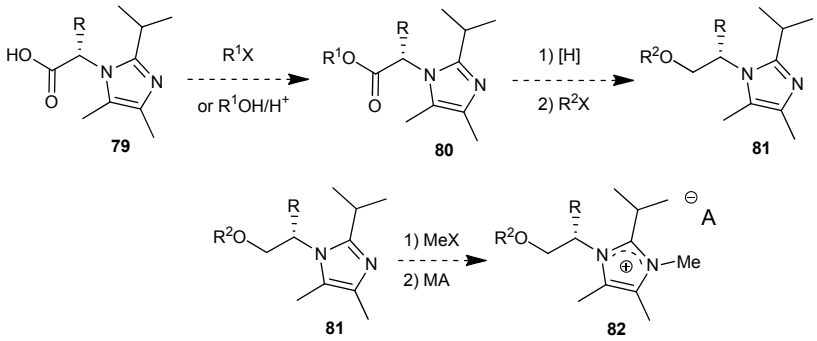

Scheme 27: Transformation of the amino acid derived imidazoles into the ester and the ether derivatives and subsequent conversion of the alkoxy-substituted imidazoles in chiral ionic liquids.

(iii) The building blocks are naturally occurring compounds, making their use environmentally safe and they are most often industrially prepared via enantioselective renewable processes.[142]

The amino acids of interest here, besides glycine (Gly), are alanine (Ala), serine (Ser) and threonine (Thr) (Figure 22). The simplest of chiral amino acids, alanine, introduces a methyl group on the position adjacent to the imidazole. Serine provides a second alcohol function to be converted into an ether function, in order to create an increased concentration of ether functions in the liquid, although a prochiral imidazole is created when R^1 and R^2 are the same. The optical rotation will then be dependent on R^1 and R^2. This can be circumvented by the introduction of threonine, introducing two chiral centres.

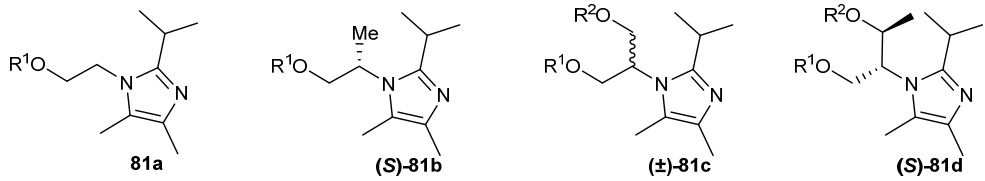

Figure 22: Different envisioned amino acid based 1-alkoxy-2-isopropyl-4,5-dimethylimidazoles, derived from (fltr.) Gly, Ala, Ser and Thr.

3.2.1) Via amino acid zwitterions

Bao *et al*. reported on the synthesis of amino acid based imidazoles via slow addition of the ammonia source and diketone to a hot methanol solution of the amino acid and aldehyde.[136a] This strategy was evaluated with D/L-alanine **(*rac*)-83** and after reaction, a solid was obtained upon evaporation of the volatiles. The intermediate sodium salt **(*rac*)-84** could not be purified by aqueous extraction (amino acid cannot be separated), or by distillation as it is non-volatile. Therefore, a second step was needed in which the sodium salt **(*rac*)-84** is converted into its ester.

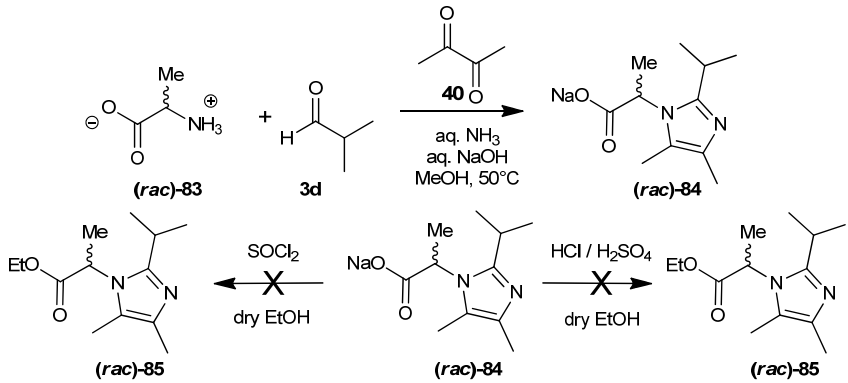

Scheme 28: Modified Debus-Radziszewski reaction with zwitterionic amino acid and ammonium hydroxide, and subsequent esterification using $SOCl_2$, HCl or H_2SO_4.

Addition of H_2SO_4 or dry HCl to an ethanolic mixture did not lead to the formation of the ethyl derivative. The presence of the imidazole zwitterion and neutralisation of the inorganic acids might have hindered the esterification here although HCl was added sufficiently long in order to neutralise the complete solution. Nonetheless, application of $SOCl_2$ in ethanol was also unsuccessful (Scheme 28). In one case, upon H_2SO_4 catalysed esterification, only 1% of the ethyl ester could be purified via column chromatography. The ^{1}H NMR spectrum of the obtained (*S*)-*O*-ethyl-2-(2-isopropyl-4,5-dimethylimidazolyl)propionate (**(*rac*)-85**) showed the presence of two diasterotopic hydrogens on the OCH_2 group (10.7 Hz difference between the two OCH_2 quadruplet signals, while a ^2J-coupling is not observed).

3.2.2) Via amino acid esters

The direct application of glycine and alanine methyl ester HCl salts (**86a** and **86b**, respectively) in the previously optimised (i.e. sequential) Debus-Radziszewski reaction procedure gave very poor yields. The end product could not be purified from the extract. It was anticipated to be due to the presence of the HCl, making the amino group less nucleophilic. Therefore, an alternative setup was used in which the imine was synthesised in CH_2Cl_2, in the presence of Et_3N (Scheme 29). Subsequently, the imine was applied in the second step of the modified Debus-Radziszewski reaction. In both cases, the presence of the resulting product **88** could be demonstrated by GC-FID, but no product could be isolated.

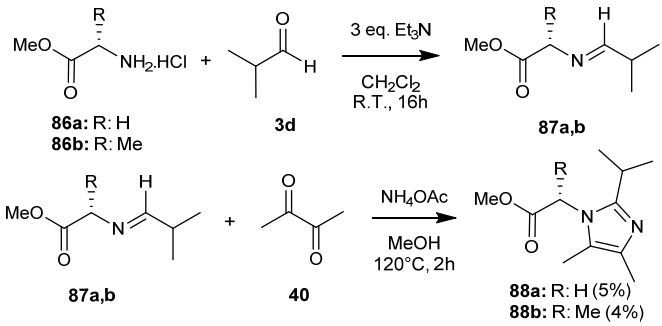

Scheme 29: Synthesis of amino acid derived imidazolyl esters via intermediate imine formation in CH_2Cl_2.

Since the yield and selectivity via the modified Debus-Radziszewski reaction were not satisfying, the synthesis in strong alkaline medium was evaluated. Addition of one equivalent of NaOH to deprotonate the hydrochloride salt in the first step and addition in several portions in the second step, led to the best results obtained (Scheme 30).

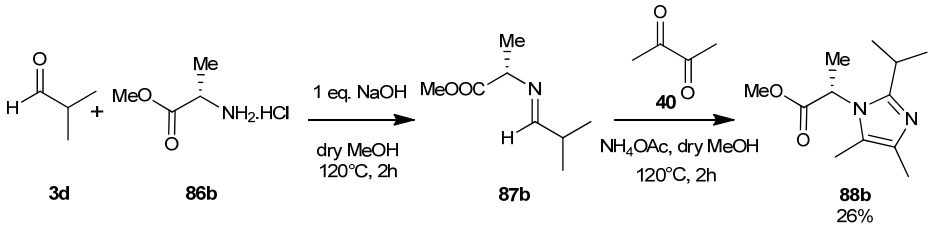

Scheme 30: Modified Debus-Radziszewski reaction procedure, using one equivalent of NaOH to deprotonate the hydrochloride salt. In the second step, the diketone and NH_4OAc were added in 4 portions over time.

The imidazolyl ester **88b** was present and could be purified via acid-base extraction. NMR analysis of the evaporated extract, showed the presence of the ester **88b** (in 26% yield), while also a substantial amount of the 1*H*-2-isopropyl-4,5-dimethylimidazole (**60**) was formed (16%). Hence, the selectivity towards the *N*-substituted imidazole was 61%, which is lower than with any other amine noted in Table 10. The combination of a sterically hindered centre and the

electron-withdrawing effect on the amino function are detrimental to the selectivity and hence also to the yield. Crystallisation of **60** in acetone or preferably CH_3CN was successful, but the last crop could not easily be removed. Distillation could be applied to finally purify the ester, however leading to a substantial mass loss. This demonstrated the low thermal stability of imidazoles with an ester group.

The remainder of the side products was removed by filtration over a column packed with neutral alumina. The very low yields of compounds **88b** and **88c** (Table 10) were attributed to the steric hindrance and therefore, serine and threonine based imidazole synthesis was not further examined. Preliminary experiments to obtain an amino alcohol from the commercially available amino acid esters (reducing the electron withdrawal effect) failed due to the high aqueous solubility of the different compounds.

Table 15: Yield of 1*N*-alkyl-2-isopropyl-4,5-dimethylimidazole obtained after distillation and selectivity in the modified Debus-Radziszewski reaction with different amines.

Imidazole	Amine	Yield (%) (**4**)	Selectivity (%) (**4**/**4**+**5**)[b]
41d	Ethylamine	42	100
41h	Hexylamine	40	88
59a	Allylamine	63	88
59b	Hydroxyethylamine	/	75
59c	Methoxyethylamine	53	86
88b	*O*-Me-Alanine·HCl[a]	26[b]	61
88c	*O*-Me-Serine·HCl[a]	18[b]	64

[a] Amino acid methyl ester hydrochloride salt, synthesis as in Scheme 30; [b] measured by ^{1}H NMR.

Since the imidazolyl ester **88b** degraded during distillation, and the majority of the 1*H*-imidazole **60** could be removed via crystallisation, the crude mixture of **88b** was used in subsequent reduction step (Scheme 31). The reduction with sodium borohydride proceeded smoothly and allowed the isolation of the imidazolyl alcohol (**89**) in moderate to good yields. Subsequently, methylation of the alcohol to the ether functionalised imidazoles (**59c**, **90**) was achieved by slow addition of Me_2SO_4 to the sodium alkoxide.

The product was obtained by alkaline aqueous washing to remove the *N*-alkylated side product and unreacted alcohol. Only a small increase of the maximum yield at 0 °C (52%) was found by reducing the temperature to -78 °C (58%) . Application of potassium hydride in combination with 18-6 crown-ether at -78 °C to obtain a more reactive alkoxide did not improve the yield. Since (i) the intermediate alcohol **89** is not distillable and (ii) the majority of

88 was found to be destructed upon distillation, the reaction was carried out with the crude imidazolyl alcohol and the alkoxyimidazole (**59c**, **90**) was distilled.

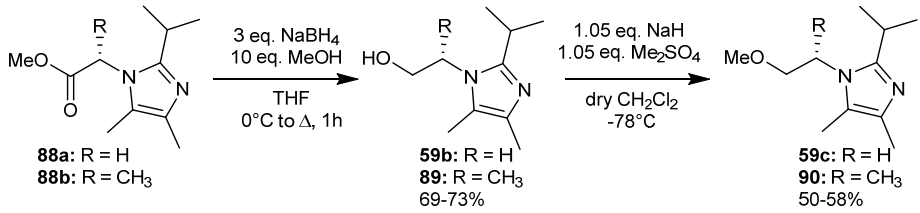

Scheme 31: Optimised conditions for the transformation of imidazolyl ester 88 into the ethers 59c and 90.

The reduction of the black imidazolyl ester led to a colourless product. Therefore, the strong colouration of imidazoles and their liquid salts might result from oxidised species which can be removed by reduction. This was further used for the purification of other imidazoles, see section III.1.3.1. The use of degassed solvents to avoid oxidation was not feasible, as the reaction vessels were opened multiple times during reaction for the addition of reagents. Here too, the small fraction of coloured species, distilled with the product, induces colouration upon methylation with MeI.

The ^{13}C and ^{1}H NMR spectra (in $CDCl_3$) of the imidazoles **88b** and **90** showed the presence of two different diasterotopic methyl groups on the isopropyl substituent. The two resulting doublet signals in ^{1}H NMR were separated by 3.3 Hz and 11.6 Hz in **88b** and **90,** respectively. NMR analysis at higher temperature, and comparison with 1,2-diisopropyl-4,5-dimethylimidazole, showed that the shifts were not resulting from a hindered rotation.

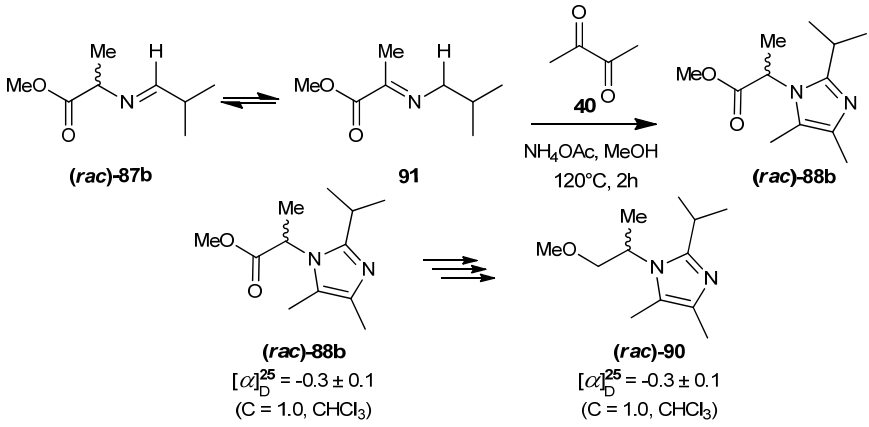

Scheme 32: Formation of the stabilised α-imino-ester 91 under alkaline conditions, leading to racemisation. The optical rotations of the ester 88b and ether 90 show the complete racemisation.

The enantiomeric purity of imidazoles **88b** and **90** was assessed by optical rotation and NMR spectroscopy with the chiral shift reagent (*R*)-1-anthracen-9-yl-2,2,2-trifluoroethanol, also known as Pirkle's alcohol (**102**, Figure 24, p75). The two isopropyl doublets were found to be split by an equimolar amount of Pirkle's alcohol by ca. 12 Hz and 35 Hz in **88b** and **90**, respectively. As depicted in Scheme 32, racemisation occurs already in the first step of the modified Debus-Radziszewski reaction.

The racemic mixture of 2-isopropyl-3-methoxyprop-2-yl-4,5-dimethylimidazole was used in the ionic liquid synthesis as shown in Scheme 33. The ionic liquids were obtained quantitatively as pale yellow oils.

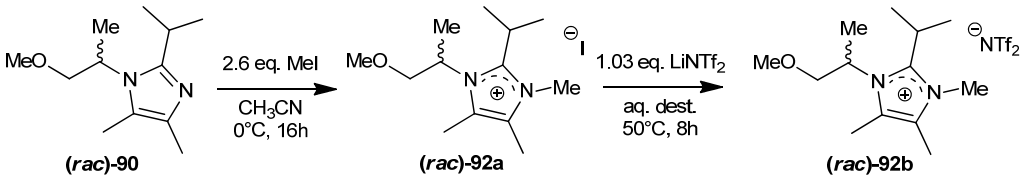

(*rac*)-90 (*rac*)-92a (*rac*)-92b

Scheme 33: Synthesis of the racemic 2-isopropyl-3-methoxyprop-2-yl-4,5-dimethylimidazolium iodide and bis(trifluoromethylsulfonyl)imide ionic liquids via the standard procedures.

3.3. Synthesis of ionic liquids using a chiral quaternisation agent

In order to overcome the low yield and post processing of the chiral imidazoles, a chiral moiety was introduced in the quaternisation step. The thus resulting convergent synthesis would allow for an increase of the overall yields and also for the fast synthesis of a divergent library of analogues. The lactate derived chiral moiety was provided with an ether functionality and a leaving group by subsequent methylation, reduction and mesylation (Scheme 34).

3.3.1) Synthesis of the quaternisation agent

The methylation step of ethyl lactate was successfully performed with MeI and NaH,[143] this method allowed to perform the reaction at low temperatures. The pure NaH was added to a mixture of ethyl L-lactate and methyl iodide. Hereby, all base (NaH and formed alkoxide) was immediately reacted, preventing racemisation or self-condensation of the alkoxide. The one-pot reaction of methylation and reduction was found to be impossible as violent gas formation occurred upon addition of the reducing agent (both $LiAlH_4$ as $NaBH_4$) in the presence of iodide salts. Therefore, the work-up included partial evaporation of THF and aqueous extraction of the salts from an Et_2O solution.

The majority of the Et_2O was evaporated at low temperatures, in order to dissolve the (*S*)-ethyl-2-methoxy-propionate (**(*S*)-94**) in dry THF for reduction of the ester (Scheme 34). The moderate yields of **(*S*)-95** were initially attributed to the high volatility during the intensive evaporation of THF. However, the persistent efforts to evaporate at very low temperatures and to get reproducible yields, suggest degradation (e.g. by alkene formation) or a high water solubility of the product. Evaluation of the reagent amounts might improve the yields further.

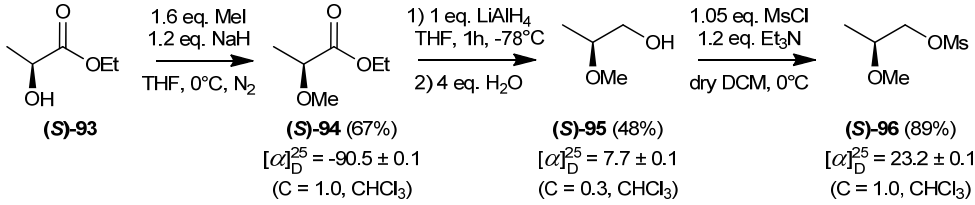

Scheme 34: Synthesis of (*S*)-2-methoxypropyl methanesulfonate.

The methylated ester was reduced to the alcohol by very slow addition of $LiAlH_4$ at low temperatures to prevent thermal runaway. After addition of a minimal amount of water, filtration and evaporation, the alcohol **(*S*)-95** was obtained. As the reduction of the ester proceeded so efficiently, also the less reactive $NaBH_4$ was evaluated, however the obtained yields (23-30%) were even lower due to the acidic aqueous work-up. The obtained alcohol **(*S*)-95** could be transformed into **(*S*)-96** via a standard procedure using methanesulfonyl chloride. The end product (*S*)-2-methoxypropyl methanesulfonate (**(*S*)-96**) was obtained as a clear liquid after short-path vacuum distillation.

In both the first and the last step (Scheme 34), the base was added dropwise to a mixture of the reagents in order to avoid a too high alkalinity which could, especially in a mixture of ethyl L-lactate (**(*S*)-93**) and ethyl 2-methoxypropionate (**(*S*)-94**) lead to partial racemisation.

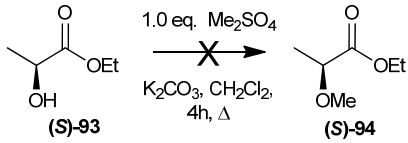

Scheme 35: Evaluation of dimethyl sulfate (DMS) in the methylation of ethyl L-lactate.

Alternatively, dimethyl sulfate (DMS) in combination with potassium carbonate was evaluated as methylating agent (Scheme 35). Although racemisation might occur due to the high amount of base needed, the conditions were evaluated as they allow easy work-up, i.e. filtration of the side products ($KMeSO_4$, $KHCO_3$ and K_2CO_3) vs. evaporation, extraction, drying and evaporation when using MeI. Moreover, if this method was to be found to racemise the

products, the procedure would still be useful in the racemic synthesis (see Scheme 39). Maximum one equivalent of DMS was used since an excess present in the second step would consume the reducing agent and removal of the toxic compound would require evaporation at high temperature after reaction (T_b(DMS): 188 °C). Unfortunately, the methylation reaction did not proceed smoothly, and after twenty four hours a complex mixture was obtained.

3.3.2) Application in quaternisation reaction

As previously observed for other methanesulfonate esters, high temperatures were required to obtain the quaternised product **98a** (Scheme 36). The reaction was only completed after 90 min (45 min for **97a**) under microwave irradiation at 100 °C and the product needed to be evaporated at high temperatures for prolonged times to remove the excess of the starting materials. In the case of **97a**, a pale yellow oil was obtained. The 2*H*-imidazoles and their imidazolium salts were always only slightly coloured, indicating the absence of contaminants with high extinction coefficients in these compounds.

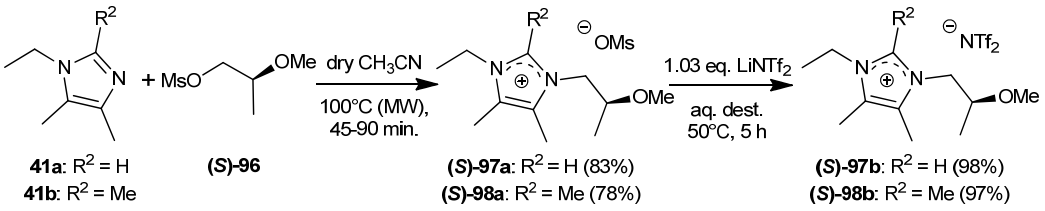

Scheme 36: Quaternisation with the (*S*)-2-methoxypropyl methanesulfonate and subsequent metathesis.

After quaternisation by microwave irradiation, here too a side product (20 mol% in **98a**) was observed in the ^{1}H NMR spectra. Analogously to the MsOH formation during alkenyl substituted imidazolium salt synthesis (section III.2.2), the product signals were found slightly upfield, indicating a protonated imidazolium salt. Since elimination of the (S)-2-methoxypropyl methanesulfonate was not expected to readily occur, it was clear that here too, water was involved in a concurrent nucleophilic attack.

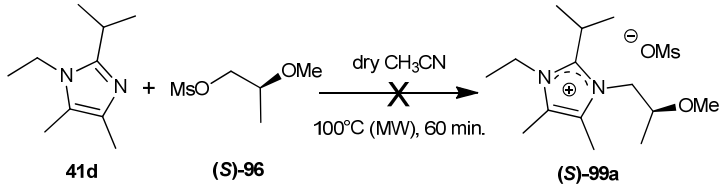

Scheme 37: Failed microwave mediated quaternisation of 1-ethyl-2-isopropyl-4,5-dimethylimidazole with the (*S*)-2-methoxypropyl methanesulfonate.

The isopropyl derivative did not lead to any reaction under stringent conditions (Scheme 37). The maximum conversion obtained was 12% after one hour of microwave irradiation at 100

°C, although most often just starting materials were found. Irradiation during 2h at this temperature or at 100 °C did not improve the conversion. Therefore, another method was applied, in which the 1*H*-2-isopropyl-4,5-dimethylimidazole was reacted with the (*S*)-2-methoxypropyl methanesulfonate (Scheme 38).

The synthesis of 1*H*-2-isopropyl-4,5-dimethylimidazole (**60**), was achieved by performing the Debus-Radziszewski reaction in one step and adding two equivalents of NH_4OAc. Very rapidly, the product was formed as a fine suspension in the reaction solvent. After acid-base extraction, 89% of the 1*H*-imidazole could be isolated. Deprotonation of this imidazole and application in the reaction with (*S*)-2-methoxypropyl methanesulfonate, yielded the (S)-2-isopropyl-1-(2-methoxypropyl)-4,5-dimethylimidazole (**(*S*)-100**) in 61%. The main side product formed was the double alkylated imidazolium cation. The pure compound **(*S*)-100** could be obtained as a colourless liquid via short-path vacuum distillation.

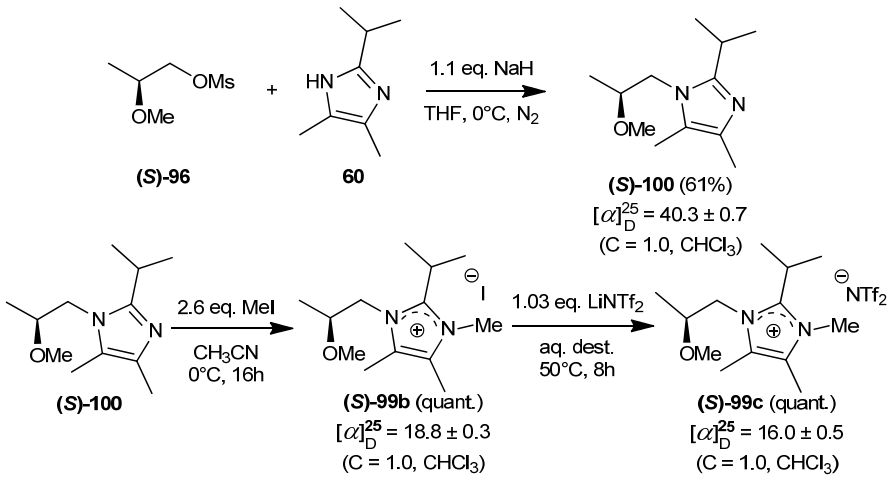

Scheme 38: Synthesis of (*S*)-2-isopropyl-1-(2-methoxypropyl)-4,5-dimethylimidazole ((*S*)-100) and subsequent application of this imidazole in the standard ionic liquid synthesis and metathesis.

The obtained chiral imidazole could be successfully applied in the ionic liquid synthesis with methyl iodide and subsequent metathesis with lithium bis(trifluoromethylsulfonyl)imide to obtain quantitatively the chiral imidazolium ionic liquids **(*S*)-99b** and **(*S*)-99c** respectively.

3.3.3) Enantiomeric purity assessment

During the synthesis of the intermediates and the ionic liquids, several times bases and high temperatures were applied, which might have led to product racemisation. Analysis of the enantiomeric purity of the ionic liquids thus formed, was in first instance performed via optical rotation. The obtained optical rotations ($[\alpha]_D^{25}$, Table 16) indicate that no complete racemisation

occurs during the synthesis, under the applied alkaline conditions and high temperatures. This is a good indicator that these type of compounds have potency to withstand demanding reaction conditions, i.e. high temperatures and alkalinity.

From the obtained values, it is clear that changing the anion from $[I]^-$ or $[OMs]^-$ to $[NTf_2]^-$ decreases the specific optical rotation $[\alpha]_D^{25}$. This is at least partially the result of the decreased concentration of chiral centres present, as the molecular weight increases upon metathesis with the $[NTf_2]^-$ anion (see Table 16).

Table 16: Summary of the specific optical rotations (°) of the (*S*)-2-methoxypropyl substituted imidazole and imidazolium ionic liquids, combined with the concentration in $CHCl_3$ at which this value was measured and the molecular weight.

Compound	$[\alpha]_D^{25}$	C ($\times 10^{-2}$ g mL^{-1})	MW (g mol^{-1})
97a	20.3 ± 0.5	0.4	324.2
97b	14.9 ± 0.7	0.4	477.44
98a	16.1 ± 0.5	0.4	338.23
98b	12.3 ± 0.2	0.4	491.47
100	40.3 ± 0.5	0.3	210.32
99b	18.8 ± 0.3	0.4	352.25
99c	16.0 ± 0.5	0.4	505.50

The achiral ethyl 2-hydroxy-propionate was obtained via hydrogenation of ethyl pyruvate over a Raney Nickel catalyst in continuous flow (see section V.1). The hexane solution containing 87% alcohol was partially evaporated before methylation with MeI via the optimised procedure. After methylation, the crude mixture was used in the consecutive reduction and mesylation steps, after which the pure racemic methane sulfonate **(*rac*)-96** was obtained by distillation (Scheme 39).

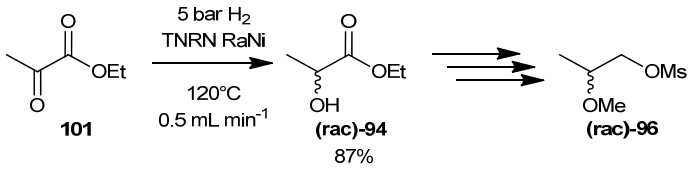

Scheme 39: Synthesis of racemic 2-methoxypropyl methanesulfonate.

The racemic 2-isopropylimidazole and 2*H*- and 2-methylimidazolium salts (Figure 23) were obtained via the corresponding procedures and were all found to be synthesised in good yield and purity, as confirmed by mass-spectrometry and NMR spectroscopy. The different imidazolium salts and chiral imidazole derived from the achiral compound were analysed by

optical rotation. The obtained results and the comparison with the chiral derivatives showed that racemic mixtures of compounds **(*rac*)-97a**, **(*rac*)-98a** and **(*rac*)-100** were obtained by functionalisation with the racemic pyruvate derived methanesulfonate ester **(*rac*)-96**.

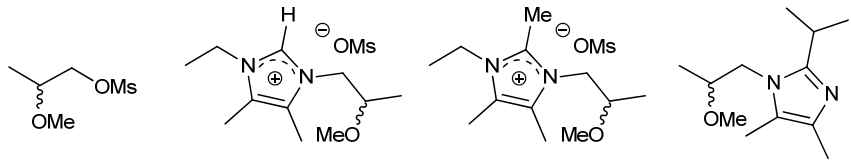

(*rac*)-96	**(*rac*)-97a**	**(*rac*)-98a**	**(*rac*)-100**
$[\alpha]_D^{25}$ = -0.2 ± 0.8	$[\alpha]_D^{25}$ = -0.3 ± 0.4	$[\alpha]_D^{25}$ = -0.7 ± 1.2	$[\alpha]_D^{25}$ = 0.4 ± 1.3
(C = 1.0, $CHCl_3$)	(C = 1.0, $CHCl_3$)	(C = 1.0, $CHCl_3$)	(C = 1.0, $CHCl_3$)

Figure 23: Different racemic 2-methoxypropyl substituted compounds used for enantiomeric purity assessments.

To determine the enantiomeric purity and detect the presence of the (*R*)-enantiomer in the different compounds, NMR spectroscopy was applied.[144] Therefore, chiral shift reagents (CSRs, Figure 24) were added to both the (*S*)-2-methoxypropyl substituted compounds and the obtained racemic mixtures. The most common non-derivatising CSR, Pirkle's alcohol (1-anthracen-9-yl-2,2,2-trifluoroethanol, **102**), possesses an acidic proton and was therefore expected to interact with the neutral imidazoles. However, in contrast to the amino acid derived imidazoles, no signal shifts were observed upon addition the of Pirkle's alcohol to the basic imidazole (**(*S*)-100**), and no splitting of signals in the racemic mixture (**(*rac*)-100**).

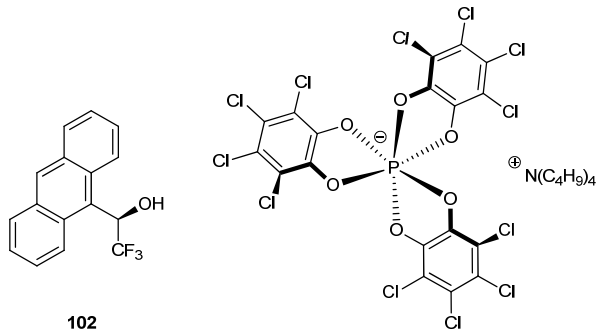

102 **103**

Figure 24: Non-derivatising chiral shift reagents Prikle's alcohol (left) and the Δ-Trisphat anion (right).

A second CSR which was evaluated, is the tetrabutylammonium salt of the Δ-Trisphat anion (Tris(tetrachlorobenzenediolato)phosphate, **103**).[145] In this anion, no hydrogens are present, although the butyl chains of the cation gave a small overlap with the product signals. Unfortunately, when combined in equimolar amount with the salt **(*rac*)-98a**, also no signal splitting was observed

A final method which was evaluated to determine the enantiomeric purity was chiral HPLC. In this method the product is passed over a column with chiral packing with an isocratic eluent mixture. This method is, in contrast to the standard HPLC method a normal phase method, using apolar solvent mixtures, preferably hexanes. Unfortunately, none of the ionic liquids dissolve in hexanes and therefore EtOH was added. None of the obtained chromatograms of the chiral imidazole, the three chiral imidazolium salts and all of their racemic mixtures (the methanesulfonate ester cannot be monitored by UV-detection and was hence not investigated) were valuable in order to calculate the enantiomeric purity, i.e. no chiral resolution was observed. This might be attributed to the presence of too large amounts of EtOH in the injection sample. Analysis of the enantiomeric purity could nevertheless demonstrate if racemisation occurs during synthesis, storage or application.

3.4. Conclusions

The amino acid based pathway has the lowest carbon economy in the first step, i.e. the imidazole synthesis. Unfortunately, the first step was also found to completely racemise the product. The lactate based pathway has only modest losses in the final steps, but requires a low yielding synthesis of the quaternisation agent. The introduction of the chiral centre via the quaternisation agent allows to apply this convergent synthesis to a library of organic bases. Due to the non-reactivity of the lactate derived quaternisation agent towards the 2-isopropyl substituted imidazole, this convergent synthesis was abandoned. Nonetheless, the chiral imidazole **(*S*)-100** could be synthesised and applied in ionic liquid synthesis via standard synthesis procedures. This indicates that the chiral imidazole can be quaternised via divergent methods, e.g. using allyl bromide, methyl iodide or dimethyl carbonate. This allows for the introduction of a myriad of anions. The 2-methoxypropyl substituted imidazolium salts were found to be non-racemic, it is to say that at least scalemic mixtures were obtained. Unfortunately the enantiomeric purity could not be proven via standard methods such as NMR or HPLC. None of the ionic liquids synthesised showed any solidification.

4. Alternative ionic liquid preparation

The general synthesis of ionic liquids consists of a quaternisation followed by metathesis. As quaternisation proceeds most efficiently with alkyl halides, methods were initially introduced to substitute the insufficiently stable and strongly coordinating halide anions for less basic and more stable anions, leading to ionic liquids with improved stability and rheology.[13b]

There is a great interest in novel and greener preparation methods leading to more pure ionic liquids, since the previously mentioned general methodology poses different concerns. First of all, the exchange of anions via transition metal salts[37] or via an anion exchange resin[146] generates equimolar amounts of (polluting) metal halides or hydrogen halide acid respectively. Second, quaternisation with alkyl halides induces halide contamination of the ionic liquid end product. It is known that minute amounts of halides can poison expensive catalysts and alter the physical properties.[13b, 147]

Finally, the use of silver salts, of interest in the preparation of water soluble ionic liquids and most commonly applied in the synthesis of dicyanamide ionic liquids,[37, 148] is expensive and leads to silver contamination of waste streams. The step preceding the actual metathesis, involves $AgNO_3$ precipitation with $NaN(CN)_2$ in water (*vide supra*, Scheme 16) and involves formation of substantial amounts of contaminated aqueous and solid waste. Moreover, silver halides only precipitate slowly from aqueous solutions, the metathesis is therefore sometimes carried out in organic solvents.[149] Nonetheless, silver halides are slightly soluble in these solvents and in ionic liquids as well, leading to silver contamination of the end product in this case too.[150]

MacFarlane *et al.* have analysed the iodide contamination in ionic liquids prepared with $AgN(CN)_2$ by means of mass spectrometry and found a concentration < 0.5 wt.% $[I]^-$ (being the detection limit).[37] As this does not exclude the presence of residual silver metals, an alternative method was recently reported.[151] This method comprises the melting of $[C_2mim][Cl]$ with the sodium or lithium salts of the desired anion (i.e. $LiNTf_2$, $NaBF_4$, $NaN(CN)_2$, NaSCN), dissolution of the resulting melt in CH_2Cl_2 or THF and filtration led to the pure ionic liquids, as no residual chlorine was observed by high resolution mass spectroscopy. The use of the 'phenolate platform' to synthesise hydrophilic ionic liquids was recently described by Lethesh *et al*.[152] Hereby, the *tert*-butylphenolate salt of the cation of choice is mixed with the Brønsted acid of choice in an aqeuous medium, after which the *tert*-butylphenol migrates to the hydrophopic layer.

To overcome the problem of halide contamination, the direct synthesis using methylating agents which provide the desired anion immediately as 'by-product' has been applied by several research groups. Although this method is free from waste-generation, it is not feasible for the weakly coordinating $[NTf_2]^-$ and $[N(CN)_2]^-$ anions, as their methylated derivatives do not exist. The strongly methylating (carcinogenic) character of e.g. methyltrifluoromethanesulfonate (MeOTf) limits the industrial use, although microreactor technology can here introduce a safe process alternative (*vide supra*).[104] Nonetheless, amongst others, imidazolium trifluoroacetates, trifluoromethanesulfonates, methyl- and ethylsulfates and alkylnitrates have already been successfully synthesised via this direct alkylation.[38, 40, 153] Recently, an anion exchange method was reported in which bromide anions are exchanged with methylsulfate by addition of dimethylsulfate and evaporation of the volatile methyl bromide.[154]

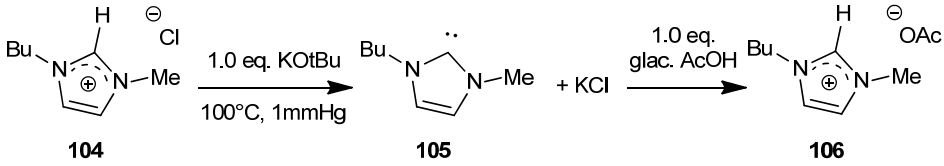

104 **105** **106**

Scheme 40: Halide free ionic liquid synthesis procedure patented by Earle and Seddon.[155]

Seddon *et al.* filed a patent in which, after quaternisation of *N*-alkylimidazoles with ethyl trifluoroacetate or butyl methanesulfonate, the anions were exchanged by evaporation of their corresponding acids upon addition of HPF_6 or HBF_4.[156] An alternative method applying Brønsted acids, was filed in another patent by the same group. Here, the imidazolylidene carbene was prepared and isolated under reduced pressure in a Kugelrohr apparatus, which was then reacted with the acid to afford the 2*H*-imidazolium salt (Scheme 40).[155] Brønsted acids have also been applied to exchange anions in carbonate ionic liquids (*vide infra*).

In the following sections alternative metathesis procedures will be proposed and evaluated in order to tackle the before mentioned problems of ionic liquid purity, waste generation and toxicity. The focus will be on the reduction of the amount and the toxicity of reagents and by-products, the reduction of energy demands but also of solvents, especially water, which are contaminated after use. Finally, these novel methods should allow the synthesis of very pure ionic liquids.

One of the most promising quaternisation agents is dimethyl carbonate (DMC),[157] which is a greener alternative to both quaternisation and metathesis. However, not many groups have applied this technique, probably due to the absence of an autoclave or high pressure reaction vessels in the laboratory environment. In the next section first the synthesis and quaternisation of methanesulfonate ionic liquids will be elaborated.

4.1. Synthesis and metathesis of methanesulfonate salts

Although the use of methyl methanesulfonate (MeOMs) will not be accepted in large-scale industrial processes since it is a carcinogenic and toxic compound, several researchers have reported methane sulfonate ([OMs]$^-$) based ionic liquids.[158] In this research, the rheology of methanesulfonate ionic liquids as well as their applicability as a handle for anion metathesis are evaluated. The interest in this method is a priori based on the observation of the NaOMs precipitation (see section III.2.2) and practically, for circumventing silver dicyanamide based synthesis, which did not always straightforwardly lead to compounds of high purity. The latter silver salt mediated metathesis is based on the fact that silver halides are less soluble than $AgN(CN)_2$, which is synthesised from $NaN(CN)_2$ (Scheme 16). Hence, the direct application of $NaN(CN)_2$ reduces the ionic liquid synthesis with one step.

The synthesis of the methanesulfonate salts does not proceed smoothly in the normal synthesis setup, i.e. acetonitrile at 0 °C. Applying higher temperatures, in solvents such as acetonitrile or toluene, did not ameliorate the conversion (see section III.2.2). The more stringent conditions achieved in the microwave reactor did allow efficient conversion, although no (very) high temperatures were required. The results verify the efficient heating in a pressurised vial with accurate temperature control, since there is no special effect originating from microwave irradiation.[159]

Table 17: Applied reaction conditions during methanesulfonate ionic liquid synthesis with imidazoles 41a-d.

IL	R	eq. MeOMs	*T* (°C)	*t* (min)
44d	H	1.1	100	30
45d	Me	1.0	80	40
46d	Et	1.1	80	30
47d	iPr	1.1	80	60

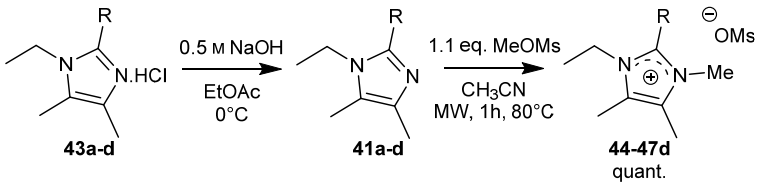

43a-d **41a-d** **44-47d** quant.

Scheme 41: Neutralisation of the recrystallised imidazolium hydrogen chloride and subsequent quaternisation with methyl methanesulfonate to obtain methanesulfonate salts of high purity (R = H, Me, Et, iPr).

Table 17 shows the applied conditions for the methylation of 2-alkyl-1*N*-ethyl-4,5-dimethylimidazoles (**41a-d**) with methyl methanesulfonate. The methylation reaction of

compounds **41a-c** was studied on a 1 gram scale, which was added to 4 mL of dry CH_3CN in a small microwave vial (6 mL). The heating (reaction temperature and time) was minimised in order to decrease the colouration of the ionic liquids as much as possible. It was found that 80 °C was sufficient to reach complete conversion, although then 40 minutes were required. After 30 minutes, small amounts of starting imidazole were still present, although these could efficiently be removed, together with the excess of MeOMs, by washing an aqueous solution multiple times with ethyl acetate (EtOAc). More lipophilic cations (*N*-hexyl or *N*-allyloxyethyl substituted imidazoles) can induce losses in this step, although this did not pose a problem for any of the *N*-ethylimidazolium salts. The 1-ethyl-2*H*-3,4,5-trimethylimidazolium methanesulfonate ionic liquid (**44d**) was the only solid compound. The other analogues could not be crystallised from acetone or an acetone-Et_2O mixture, addition of a too high amount of Et_2O always led to the separation of a liquid layer.

The large scale synthesis was evaluated by methylating 7 grams of the 2-isopropyl substituted imidazole (**41d**) with 1.1 eq. MeOMs. Hereto was added only 10 mL of CH_3CN as then the volume upper limit of the large microwave vial was reached. To ensure complete reaction, the mixture was heated and stirred for 1 hour in the microwave reactor. During large scale production of 1-ethyl-2*H*-3,4,5-trimethylimidazolium methanesulfonate (**44d**), the exothermic reaction initiates immediately upon addition of the methyl methanesulfonate, producing a substantial amount of heat, causing the solvent to boil. This leads to mass loss, but more important to the exposure to toxic MeOMs. Hence, the vial must be sufficiently cooled and manipulated carefully. As this rapid heating was not found for the other imidazole derivatives, this indicates the faster reaction of the less sterically hindered 1-ethyl-2*H*-4,5-dimethylimidazole. Overall, the optimised conditions for the quaternisation of imidazoles with methanesulfonate are as given in Scheme 41 (for the 1 gram synthesis, 40 minutes is sufficient), followed by washing an aqueous solution with ethyl acetate.

Table 18: Conditions used during metathesis of methanesulfonate ionic liquids with $NaN(CN)_2$ of the samples provided for sodium analysis (*vide infra*).

IL	R	eq. $NaN(CN)_2$	*t* (h)	Solvent
44d	H	1.2	4	CH_2Cl_2
45d	Me	1.2	20	$CHCl_3$
46d	Et	1.5	20	$CHCl_3$
47d	iPr	1.2	40	$CHCl_3$

In Table 18, the different conditions applied in the metathesis of the methanesulfonate ionic liquids into the dicyanamide ionic liquids are given. The methanesulfonate salts were dissolved in demineralised water and 1.05 to 1.5 equivalents of $Na(CN)_2$ were added. The

mixtures were heated to 50 °C and stirred overnight to ensure complete exchange of the ions (Scheme 42). After reaction, the water was removed by rotary evaporation, and acetone was added. The dissolution of the wet ionic liquid in acetone allows precipitation of the main part of NaOMs and excess $NaN(CN)_2$. After filtration, the solvent and residual water were removed by rotary evaporation and the ionic liquid was dissolved in dichloromethane or chloroform and stored at -18 °C for at least 4 hours. This allowed the precipitation of the remainder of the sodium salts. This last step was repeated until no further precipitation was observed. Subsequently, the resulting ionic liquid was obtained after evaporation of the solvents and the contamination could be evaluated.

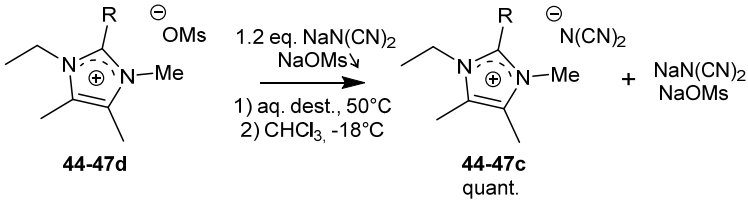

Scheme 42: Metathesis of imidazolium methanesulfonate ionic liquids into the dicyanamide ionic liquid with the by-products formed.

Thus, remaining NaOMs or imidazolium $[OMs]^-$ salt could be monitored by ^1H and ^{13}C NMR. Here it was found that addition of 1.05 eq. $NaN(CN)_2$ did not lead to complete conversion, while no residual methanesulfonate anion was observed when applying a larger excess (1.2 eq.) $NaN(CN)_2$. The residual $NaN(CN)_2$ cannot be monitored by NMR and therefore ICP-MS sodium analyses were applied on the ionic liquid samples.

Approximately two grams of the freshly prepared imidazolium dicyanamide ionic liquids **44-47c** were provided to *Desmet Ballestra* (Zaventem) for sodium analysis. The different samples were prepared via the optimised quaternisation procedure, but with different conditions for the metathesis reaction with $NaN(CN)_2$ as given in Table 18. In Table 19 the expected and experimental sodium content is given. The complete mineral composition analysis table is given in experimental section (Table 31). The large excess of $NaN(CN)_2$ used during the synthesis of **46c** was expected to pollute the end product, moreover the chloroform solutions were turbid although no precipitate could be filtered off. The analyses show that a hundred-fold higher sodium content is present in **46c** than in the compounds **45c** and **47c** where the sodium content is negligible. Since no sodium methanesulfonate was observed in **46c** by NMR, the sodium content is attributed to a high amount of residual sodium dicyanamide present (3 mol%). During metathesis of the solid methanesulfonate salt **44d**, the mixture was heated for only 4 hours and dichloromethane was used instead of chloroform during the final precipitation steps. Since the resulting dicyanamide is also a solid, the visual evaluation of the

metathesis reaction is hindered, and prediction on the sodium content was not made (Table 19). The experimental sodium content here show a result intermediate to those of **46c** and **45c**, hence not negligible. Therefore, it is proposed to increase metathesis times to 20 hours and to use chloroform to precipitate the residual $NaN(CN)_2$. An excess of chloroform should be used to hinder precipitation of the solid imidazolium salt in the case of **44d**.

Table 19: Expected sodium contamination and analytical ICP-MS results (in ppm and mol% vs. the IL) of the synthesised dicyanamide salts.

IL	R	Physical state	Expected content	sample mass (g)	mass Na (ppm)	mol% Na (%)
44c	H	Solid	/	1.0027	160	0.27
45c	Me	Liquid	Low	0.449	18	0.03
46c	Et	Liquid	High	0.5188	1803	3.25
47c	iPr	Liquid	Low	0.9992	8.7	0.02

4.2. Quaternisation and metathesis using dimethyl carbonate

The interest in the synthesis of ionic liquids by the quaternisation of organic bases with dimethyl carbonate (DMC) initiated some 20 years ago by the work of Albert and Mori.[160]

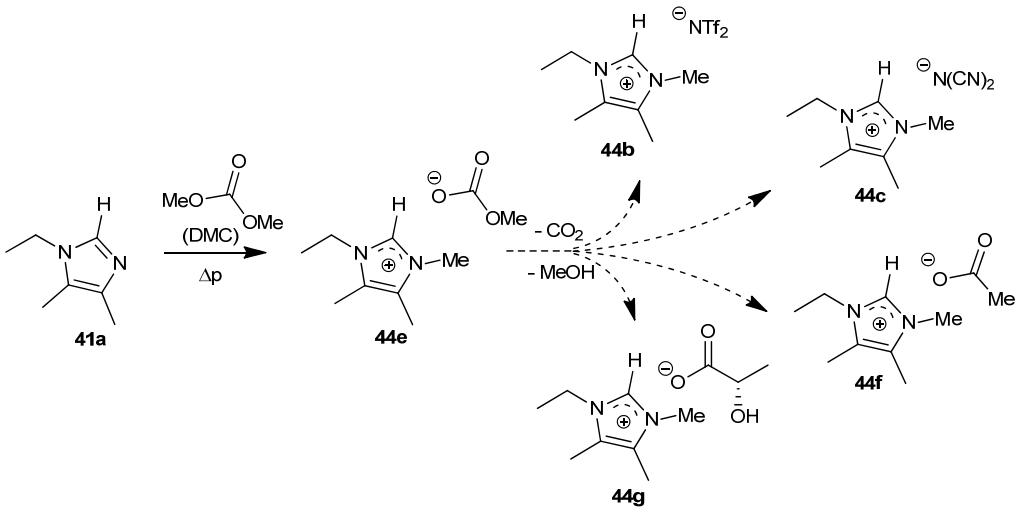

Scheme 43: Synthesis of intermediate imidazolium methyl carbonate salt and metathesis towards a library of imidazolium ionic liquids by means of Brønsted acids.

First, this methylating agent is environmently friendly because of both its synthesis and its biodegradability.[157] That is to say, since the 1980s, DMC is synthesised from CO and MeOH over a Cu(I) catalyst, a method developped by Enichem, Italy.[161] Second, quaternisation of neutral building blocks with DMC leads to methyl carbonate ionic liquids (carbonate ionic liquids, CILs).

These carbonate ionic liquids can easily be methatisised with the Brønsted acid of the anion of choice, hereby, the methyl carbonate anion decomposes into MeOH and CO_2. Alternatively, the carbonates can be precipitated by addition of calcium salts. In this way, a library of analogues can be synthesised very efficiently starting from different Brønsted acids (Scheme 43). The hydrogen carbonate ionic liquids are currently commercialy available as a novel tool called CBILS© (Carbonate Based Ionic Liquid Synthesis) from Proionic GmbH (Austria).

In the reaction of a nucleophile with dimethyl carbonate (DMC), both alkylation ($S_{N,Al}$) and acylation ($S_{N,Ac}$) can occur, depending on the temperature (Scheme 44). At reflux (T_b of DMC: 90 °C), only the reversible $S_{N,Ac}$ occurs, while alkylation requires temperatures higher than 120 °C, preferably above 160 °C. Therefore, the alkylation reaction is mostly performed in an autoclave or a sealed vial, where the autogenous pressure keeps the DMC in the liquid phase.[157]

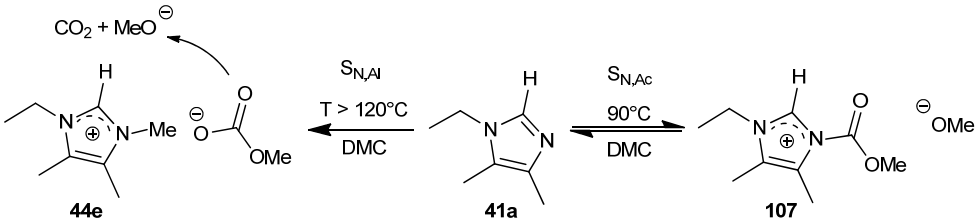

Scheme 44: Predicted temperature dependent outcome of the reaction of imidazoles with DMC.[157]

An alternative to the sealed reactor is application of the microwave reactor, which is resistant to high pressures and allows precise temperature control. The application of microwave irradiation in the methylation reaction of different organic bases (e.g. acyclic and cyclic amines, imidazoles) with DMC was intensively studied by Holbrey *et al*.[162] They found an important increase of the reaction rate by increasing the base to DMC ratio from 1:1 to 1:2 and increasing the temperature from 130 to 140 °C, while further increment of both parameters only led to small increases of the reaction rate.

In the first sections, the influence of different conditions on the conversion of different imidazoles with dimethyl carbonate will be discussed. The optimisation of temperature, reagent stoichiometry and reaction times will be elaborated. In a subsequent section, the analysis of the reaction mixtures by NMR will be discussed as well as the observations of some remarkable side reactions. Finally, the application of the carbonate ionic liquids (CILs) in metathesis reactions will be discussed.

4.2.1) Reaction optimisation

a) Quaternisation of 2-isopropylimidazoles

Reacting 1-ethyl-2-isopropyl-4,5-dimethylimidazole (**41d**) with DMC at 140 °C under microwave irradiation for 12h led to a conversion of 60% (entry 1, Table 20). Application of microwave irradiation at 170 °C always led to evaporation of the volatiles, not allowing any reaction. Therefore, in the further experiments given in Table 20 and 21, thick wall pressure vials were used, which were submerged in an oil bath at 170 °C. However, the temperature resistance of the screw caps is limited to 180 °C and exceding this temperature leads to rupture and explosion of the pressure vials.

Table 20: Conditions of quaternisation of 1-ethyl-2-isopropyl-4,5-dimethylimidazole (41d) with DMC and conversion as determined by ^{1}H NMR (entries 10-13 are discussed in section III.4.2.4).

Entry	Catalyst	Solvent	Conversion (%)	DMC (eq.)	*T* (°C)	*t* (h)
1		neat	60	2	140 (MW)	12h
2		neat	crude	2	170	24h
3	0.20 eq. $BF_3{\cdot}OEt_2$	neat	76	2	170	5h
4		1 eq. MeOH	81	3	170	27h
5		1 eq. MeOH	100	6	170	24h
6	0.20 eq. $BF_3{\cdot}OEt_2$	0.5 eq. MeOH	100	3	170	24h
7	0.04 eq. $BF_3{\cdot}OEt_2$	0.5 eq. MeOH	100	3	170	24h
8	0.20 eq. $BF_3{\cdot}OEt_2$	1.5 eq MeOH	100	3	170	8h
9	50 w% K10	1.5 eq MeOH	100	3	170	24h
10	50 w% K10	1.5 eq MeOH	65	3	170	3h
11	50 w% K10	1.5 eq MeOH	75	3	170	6h
12	50 w% K10	1.5 eq MeOH	15	3	150	3h
13	50 w% K10	1.5 eq MeOH	22	3	150	6h

Performing the quaternisation reaction of 1-ethyl-2-isopropyl-4,5-dimethylimidazole (**41d**) in a sealed pressure vial at 170 °C (entry 2), led to the complete conversion of the starting material, although a very complex mixture was obtained. To increase the contact of DMC and the imidazole in the liquid phase, the addition of solvents was evaluated. The addition of CH_3CN and MeOH increased the conversion, however multiple products were still formed. Drying of the solvent over 3Å molecular sieves did not have a significant effect on the outcome of the reaction. Addition of 1 eq. MeOH and 3 eq. DMC led to 81% conversion after 24h (entry 4), although a pure product could be obtained after washing an acetonitrile solution of the reaction mixture with Et_2O.

To reduce the formation of side products, increase the conversion and speed up the reaction (in order to reduce temperature and colouration), the effect of a catalytic amount of Lewis acid was evaluated by addition of 4 to 20 mol% of $BF_3{\cdot}OEt_2$ to a neat solution of imidazole and two eq. DMC. After 16h of reaction with 10 mol% $BF_3{\cdot}OEt_2$ and after 5h with 20 mol% (entry 3), 76% conversion was obtained. Combination of a small amount of solvent (0.5 weight eq. MeOH), an increased amount of DMC and only 4 mol% of catalyst, led to complete conversion after 24h, without the formation of side products (entry 7). Application of 20 mol% $BF_3{\cdot}OEt_2$ and 1.5 weight eq. of MeOH allowed complete conversion after 8h (entry 8).

The halogenated character of $BF_3{\cdot}OEt_2$ does not fit in the Green Chemistry concept. Moreover, the catalyst formed side products, which could not be completely removed from the resulting reaction mixture as shown by ^{19}F NMR. Therefore, alternative catalysts were required. Clay minerals are known to have Lewis acidic activity,[163] and they are solid. This means that they allow removal by filtration and recycling in contrast to $BF_3{\cdot}OEt_2$. Thus, K10 (an iron (Fe) doped Montmorillonite clay mineral) was introduced in the reaction mixture by 10, 20, 50 weight equivalents. Without activation (drying) of the catalyst, the reaction was completed after 24 hours and showed reduced side product formation (entry 9). Hence, compared to $BF_3{\cdot}OEt_2$, the demanded reaction times were longer and the catalyst loading was higher. The K10-clay could be successfully recovered by filtration, after which it was dried and recycled, and proved equally reactive as in the first runs.

b) Quaternisation of 2-methylimidazoles

The methylation reaction with dimethyl carbonate of 1-ethyl-2,4,5-trimethylimidazole (**41b**) proceeded as slow as with the 2-isopropyl derivatives. Here too, 24 hours of reaction were required for complete conversion under the conditions as optimised for the 2-isopropyl derivatives. Remarkably, signals of the 2-Me group are often not visible or reduced in ^1H NMR and diffuse in ^{13}C NMR spectra (in $CDCl_3$). Clearly, this is a result of deuterium exchange with the protonated imidazole (see section III.4.2.2).

c) Quaternisation of 2H-imidazoles

2*H*-Imidazole **41a** was found to be completely converted to different products (**111**, **114**, Figure 27, p88) without any catalysis upon heating in a thick wall pressure vial. Entries 1-3 in Table 21 show the influence of temperature and reaction time. First, 140 °C is the lower temperature limit of the reaction, and 170 °C is needed to react DMC with imidazoles sufficiently fast (imidazoles are the least reactive amongst the neutral organic bases).[162] Second, upon comparison with 2-alkylimidazoles, the necessary reaction times are quite short, i.e. one to four hours were sufficient (entries 4-7). As also observed during quaternisation of 2-alkylated imidazoles with DMC, addition of K10 catalyst supressed the formation of side products here, product **114**. Since compound **114** was later found not to be

an unwanted side product, the addition of solvent and K10 catalyst are not beneficial for the outcome during the methylation of 1-ethyl-4,5-dimethylimidazole (entries 8-12, Table 21).

Table 21: Conditions of quaternisation of 1-ethyl-2*H*-4,5-dimethylimidazole (41a) with DMC and amounts of starting imidazole and products 111 and 114, analysed by ^{1}H NMR.

Entry	K10 (w%)	MeOH (eq.)	DMC (eq.)	*T* (°C)	*t* (h)	**41a**	**111**	**114**
1	0.1	0	6	140	2	100	0	0
2	0	0.5	3	145	4	60	32	7.6
3	0	0.5	3	175	2.3	0	87	13
4	0	0.5	3	170	1	64	36	0
5	0.5	0.5	3	170	5	8	84	8
6	0.5	0.5	3	170	6	0	88	12
7	0	0.5	3	175	4	0	92	8
8	0.5	0	6	175	2.75	0	85	15
9	0.2	0	6	175	4	0	88	12
10	0.1	0	6	175	1	0	82	18
11	0	0	6	175	2	0	70	30
12	0	0	6	170	2	0	50	50

4.2.2) Structure of the CILs

a) Structure of the 2-alkylimidazolium carbonate ionic liquids.

Quaternisation of 1-ethyl-2-isopropyl-4,5-dimethylimidazole (**41d**) performed without a catalyst and with the addition of 1 eq. MeOH and 6 eq. DMC showed complete conversion (entry 5,

Table 20). After evaporation at 100 °C at 0.5 mbar, clean NMR spectra were obtained, although neither ^{13}C nor ^{1}H NMR revealed the methyl carbonate (**47e**) or methoxide (**47g**) anion (Figure 25). Therefore reaction mixtures were not as thoroughly evaporated in further experiments. In this way, clean spectra of the imidazolium cation were obtained with additional peaks at 3.49 (MeOH) and 3.47 ppm ($[CH_3CO_3]^-$) in ^{1}H NMR (the cumulative integrations not accounting for 3 protons). In the ^{13}C NMR spectrum of the freshly filtrated and evaporated reaction mixture, MeOH, $[CH_3O]^-$ and $[CH_3CO_3]^-$ were observed. The signals found near 59, 52 and 157 ppm (Figure 26, spectrum A) are respectively attributed to the $[MeO]^-$ and the $[CH_3COO]^-$ anion.

Upon addition of water and subsequent evaporation, the $[MeO]^-$ and $[CH_3CO_3]^-$ signals at 59, 52 and 157 ppm disappeared (Figure 26, spectrum B), due to the shifting of the equilibrium to the hydrogen carbonate IL (**47f**) or the hydroxide IL (**47h**), since MeOH has the lower boiling

point. This indicates that interconversion of hydrogen carbonate to methyl carbonate anions and vice versa is possible by reaction of the anion with the solvent. In spectrum B, only a signal at 160 ppm is observed apart from the imidazolium signals, attributed to hydrogen carbonate anion (**47f**). By means of this spectrum the presence of compound **47h** cannot be excluded.

The $[MeCO_3]^-$ salts (**47e**) were not found to be stable without the presence of methanol for all cations investigated, and upon evaporation, mixtures of methyl carbonate (**47e**) and hydrogen carbonate (**47f**) were formed, to be eventually completely transformed to the hydrogen carbonate salt over time. The transformation of the anions is elaborated in the next section. The ^{1}H NMR analysis of the 2-alkylimidazolium $[HCO_3]^-$ salts in $CDCl_3$ or CD_3CN did never reveal the $[HCO_3]^-$ proton, nor was the 2-methylgroup visible. This was due to H/D exchange with the solvent (see next section).

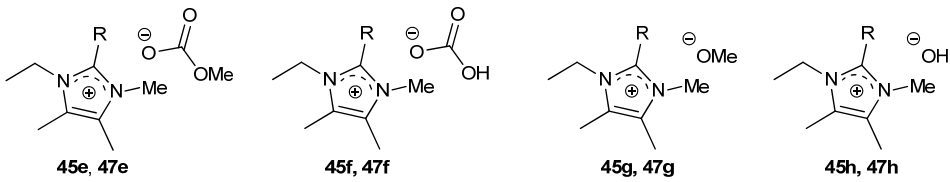

Figure 25: Proposed analogues of ionic liquids with different anions formed during methylation reaction with DMC (R= Me (45), iPr (47)).

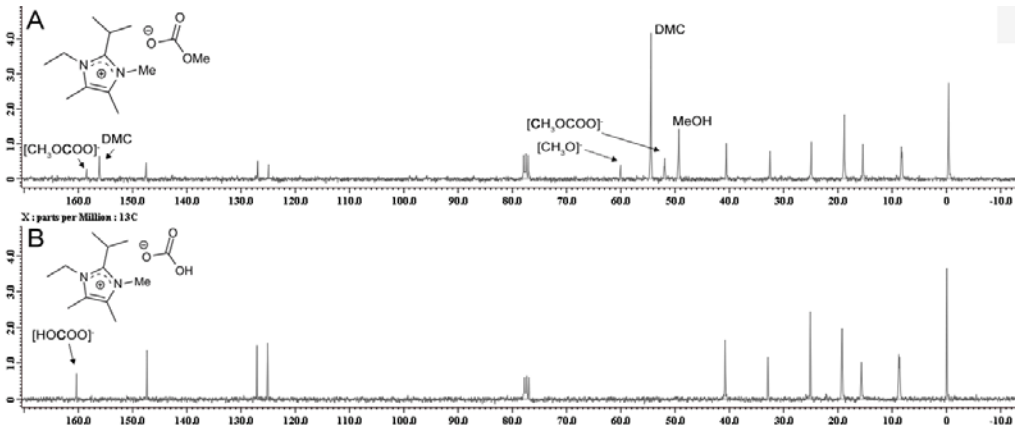

Figure 26: ^{13}C NMR spectra ($CDCl_3$) of 1-ethyl-2-isopropyl-3,4,5-trimethylimidazolium salt, as the reaction mixture, containing different anions (47e, 47g) and MeOH (A), and the $[HCO_3]^-$ salt, 47f (B).

b) Structure of the 2H-imidazolium carbonate ionic liquids

Upon quaternisation of imidazoles containing hydrogen on the C2 position, the acidity of this C2 proton increases. Given the formation of salts with alkaline carbonate anions and the release of substantial amounts of CO_2, the combination with these 2*H*-imidazoles was expected to involve carbene formation and other characteristic behaviour. The group of

Holbrey and Rogers was the first to completely describe the formation of the zwitterionic carboxylate **110b** during reaction of 1-methylimidazole with DMC in high yields.[164] The formation is attributed to an $S_{N,Al}$ mechanism and deprotonation by the $[MeCO_3]^-$ anion (Scheme 45). Later, they reported on the conversion of these carboxylates into hydrogen carbonates as ionic liquid precursors (CBILS©).[165] Alternatively, hydrogen carbonate salts can be prepared by oxidation of formate salts over a Pd catalyst, as patented in 2006 by BASF.[166]

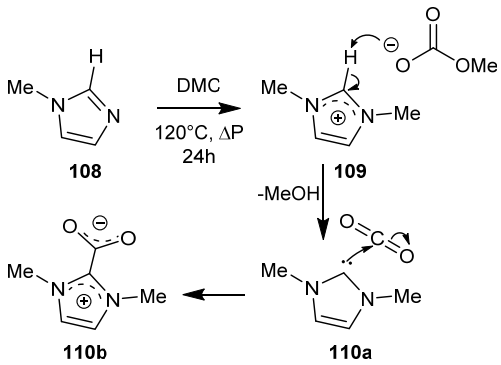

Scheme 45: Formation of the zwitterionic carboxylate 110b by reaction of 1-methylimidazole with dimethyl carbonate. The formed product precipitates from the acetonitrile reaction solution and is obtained in high yields.[164]

In the ^{1}H NMR spectra (in $CDCl_3$) of the reaction mixtures of 1-ethyl-2*H*-4,5-dimethylimidazole (**41a**) with DMC, multiple quadruplets, triplets and singlets (accounting for NCH_2, CH_3 and NCH_3 respectively) were observed in a small ppm range. This suggests that a series of analogues is formed via both $S_{N,Ac}$ and $S_{N,Al}$ mechanisms. The proposed possible analogues are illustrated in Figure 27. Amongst them (the starting material is not observed) are two analogues forming the major fraction (later assigned to **111** and **114,** see Table 21), and two other compounds accounting for a smaller quantity (0.1-0.2 eq.). In the ^{1}H NMR spectra, the major products **111** and **114** are identified by a singlet (NCH_3) at 3.90 and 3.96 ppm, resp. and a quadruplet (NCH_2) for **111** at 4.1 ppm and for compound **114** more downfield at 4.2 ppm. The deshielding observed for analogue **114** indicated an extra electron withdrawal by a carbonyl group (e.g. compounds **112, 113** and **114** in Figure 27). A complex mixture of singlet signals between 3.4 and 3.7 ppm hinders the assignment of methyl signals (corresponding with the $[OMe]^-$ or $[MeCO_3]^-$ anions, cations **111**-**113**, or the zwitterion **114**.

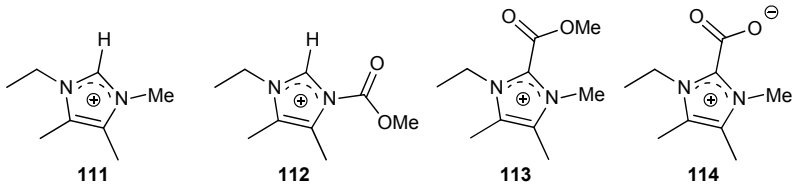

Figure 27: Proposed analogues of imidazolium cations formed during quaternisation of 1-ethyl-2*H*-4,5-dimethylimidazole (41a) with DMC.

Aromatic ^{1}H NMR signals (indicating a C2 proton) were only found for the entries containing starting imidazole (at 7.30 ppm) (entries 1 and 2, Table 21) and for the anion exchanged salts (after addition of a Brønsted acid). These singlets were not found in the mixtures containing no starting materials (entries 2, 3 and 5), although all tetraalkyl-2*H*-imidazolium ionic liquids, methylated via standard procedures (e.g. with alkyl halogenides or methanesulfonate esters), have specific aromatic singlets with accurate integration. Since spectra of freshly prepared or concentrated $CDCl_3$ solutions of CILs did contain an aromatic signal (integrating for less than one proton), the absence of the aromatic singlets is attributed to H/D exchange of the C2 proton with the deuterated solvent, promoted by the basicity of the anions (Scheme 46).

Hence, in the presence of carbonates, the $CDCl_3$ (pK_a: ±15)[167] can be deprotonated and immediately receives a deuterium/proton back (pK_{a1}(H_2CO_3): ±6, pK_{a2}(H_2CO_3): ±10).[165c] The loss of the aromatic singlet in the ^{1}H NMR spectra by hydrogen-deuterium (H/D) exchange is very fast and does not need any heating. Hence, the exchange is promoted by the carbonate anions and the excess of deuterated solvent. Upon abstraction of the deuterium by the carbonate, the latter can donate this deuterium atom (for $MeCO_3D$) or either a proton or deuterium (for HCO_3D) to any basic site (originating from the solvent or the cation) in the mixture. The analogous reaction happens at the exchangeable proton sites at the imidazolium cation (Scheme 46). This means that after a short time, all $[HCO_3]^-$ anions are deuterated, and are hence not visible in the ^{1}H NMR spectrum (Scheme 46). The loss of this singlet is experimentally confirmed in $CDCl_3$ (pK_a: ±15)[167], but also in CD_3CN (pK_a: ±31),[69] although they have been reported in literature at 9.6 ppm in DMSO-d_6 (pK_a: ±35).[69, 165c]

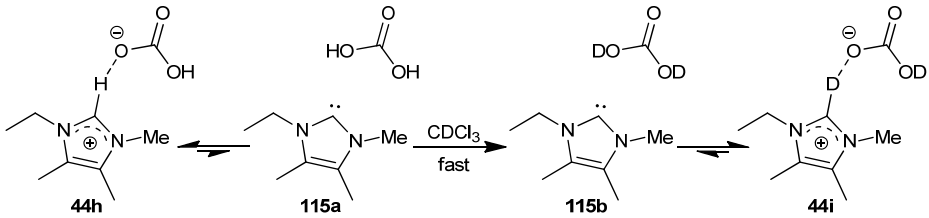

44h **115a** **115b** **44i**

Scheme 46: Equilibrium of the carbonate ionic liquid with the carbene and fast H/D-exchange in $CDCl_3$. Note that deuteration of the carbonate molecule occurs via the anion.

In several trials, a solid fraction of the residue obtained after solvent evaporation was found to be insoluble in acetone, hexanes, diethylether, but proved to be soluble in chlorinated solvents and protic solvents, as well as in hot acetonitrile. Therefore, this solid fraction was recrystallised in an acetonitrile:acetone (3:1) mixture, or washed with an acetonitrile:acetone (1:1) mixture. The resulting crystals were obtained in 7 to 21% yield in the first crop. After solvent evaporation of the mother liquor, subsequent and important crops of crystals form over time, yielding successive crops (up to 4 times, total yield 40-50%).

^{1}H NMR analysis of the crystals allowed the elucidation of the reaction mixture spectra and the assignment of the signals. In $CDCl_3$, two compounds were present, i.e. the hydrogen carbonate salt **44h** (with cation **111**) and the carboxylate **114**. The ratio of the compounds was always ca. 3:1, respectively. No change is noticeable over time (72h), but upon mild heating of the $CDCl_3$ solution (60 °C, 2h), the amount of **114** decreases, to eventually disappear (*vide infra*). In ^{13}C NMR, the major compound **44h** has peaks in the range of other 2*H*-imidazolium salts (Spectrum B, Figure 29), but distinctive here are an intense signal at 160 ppm (accounting for $[HCO_3]^-$) and the broad peak for C2 at 136 ppm, which correlates with a proton singlet at 9.64 ppm. The smaller signals in Spectrum B belonging to the carboxylate **114** are the peak of C2 at 141 ppm and a relatively large carboxylate peak at 156 ppm. The composition of the solid is verified by the complete transformation in the pure ionic liquid upon addition of a Brønsted acid, regenerating the imidazolium 2*H* signal.

The group of Rogers have earlier observed the presence of two components (the carboxylate and methyl carbonate salt) in DMSO-d_6 NMR spectra of $[C_4mim][MeCO_3]$, and attributed this to the presence of these two compounds in the reaction mixture.[162] Therefore, the here obtained solid fraction was first believed to be either the 3:1 mixture of the hydrogen carbonate salt (**44h**) and carboxylate (**114**) or alternatively, the pure hydrated carboxylate ($[C_2m_3im\text{-}COO].H_2O$), which decomposes into the hydrogen carbonate salt (**44h**) upon dissolution in $CDCl_3$. Nonetheless, single crystal X-ray diffraction data (analyses performed at the department of Inorganic and Physical Chemistry, University of Ghent) showed that the obtained crystals were the pure 1-ethyl-3,4,5-trimethylimidazolium hydrogen carbonate salt ($[C_2m_3im][HCO_3]$, **44h**), in which the anion pairs are stabilised by *H*-bonding towards each other and the cations by π-stacking (Figure 28). The crystals do not contain the crystal water reported by the group of Rogers.[165c, 168]

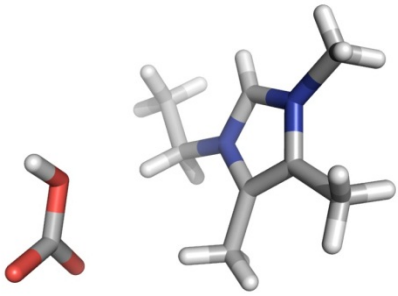

Figure 28: Single crystal X-ray diffraction image of the $[C_2m_3im][HCO_3]$ salt 44h.

Given the formation of the pure **44h** ($[C_2m_3im][HCO_3]$) salt as a crystalline solid, the carboxylate zwitterion **114** observed in the ^{1}H NMR spectra of these crystals in $CDCl_3$ is

formed in situ by thermodynamic stabilisation and water expulsion (Scheme 47). Since no carboxylate is formed in D_2O and only a very small amount in CD_3OD, the carbonate salts **44e** ($[C_2m_3im][CH_3CO_3]$) and **44h** are better stabilised in these solvents. Moreover, the amount of expelled water upon dissolution of the **44h** in $CDCl_3$ could hinder the complete carboxylate formation via a dynamic equilibrium (Scheme 47). The recurring 3:1 ratio of hydrogen carbonate **44h** vs. carboxylate **114** observed in $CDCl_3$ might be an indication of the stabilisation of the expelled water by three hydrogen carbonate molecules.

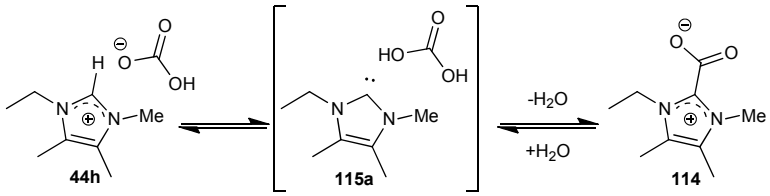

Scheme 47: Acid-base equilibrium between hydrogen carbonate imidazolium salt (44h) and the unstable carbene (115a) which is trapped as the corresponding carboxylate (114).

An equilibrated formation of the carboxylate (**114**) from the dissolved methyl carbonate salt (**44e**) formed during the reaction, and the subsequent transformation into the hydrogen carbonate crystals (**44h**), explain the successive low yielding crops of crystalline $[C_2m_3im][HCO_3]$. The solid product **44h** is removed from the equilibrium and its formation is dependent on the reaction with air moisture or water present in the reaction or recrystallisation solvents (Scheme 48).

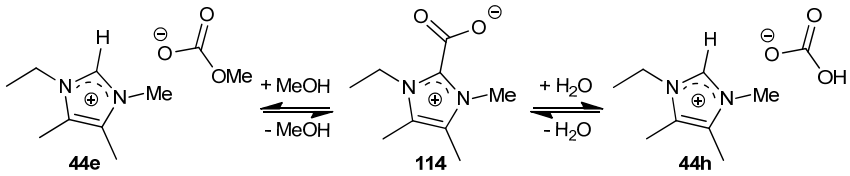

Scheme 48: Equilibrium of the imidazolylidene carboxylate (114) with the methyl carbonate salt (44e) and the hydrogen carbonate salt (44h).

This proposed conversion was experimentally confirmed. Upon dissolution of the powder or crystals in MeOH and subsequent evaporation, a liquid is obtained, in which only the methyl carbonate salt **44e** was observed by ^{13}C NMR (Spectrum A, Figure 29). Upon consecutive dissolution of the mixture in water and evaporation, the hydrogen carbonate was once again obtained, shifting the carbonate C=O ^{13}C-signal again back from 159 ppm ($[MeCO_3]^-$) to 160 ppm ($[HCO_3]^-$). This proves the possibility of the interconversion as shown in Scheme 48.[165c] The reactivity of the carboxylate with regard to protic, nucleophilic solvents, demonstrates the influence of solvent choice and presence of water on the product outcome.

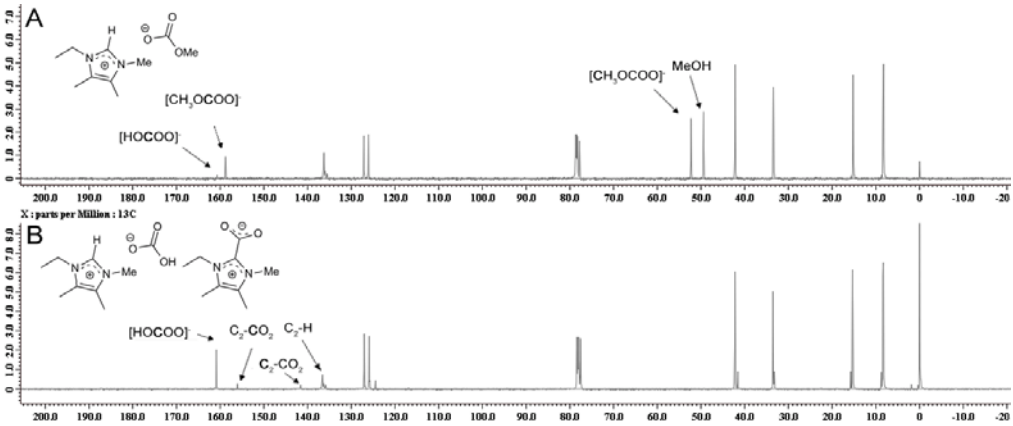

Figure 29: ^{13}C NMR spectra ($CDCl_3$) of the formation of the methyl carbonate (44e) in the presence of MeOH (Spectrum A) and 1-ethyl-2*H*-3,4,5-trimethylimidazolium hydrogen carbonate (44h) in equilibrium with the carboxylate (114) (Spectrum B).

The efficient interconversion also shows that, upon mild evaporation, the carbonate anions do not decompose and an equimolar amount of CO_2 remains present independent of the carboxylate formation. Although this conversion reaction of the anions can be accelerated via the carboxylate **114**, as shown in Scheme 48, the carboxylate is not necessary as interconversion of anions was observed in the $[C_2C_{i3}m_3im]^+$ salts too (from **47e** to **47f**).

c) Carboxylate formation and synthesis

Since almost no CO_2 is lost upon dissolution of the crystalline $[C_2m_3im][HCO_3]$ and most of the carbonate anions can be regenerated from the carboxylate, it seems that the imidazolylidene carbene immediately forms a carboxylate. As the chances of dissolved CO_2 and a free carbene colliding are very slim, the decomposition of H_2CO_3 might be promoted by the nucleophilic carbene,[169] to form the carboxylate at once (i.e. negligible lifetime of the intermediate **115a** in Scheme 47). This can be supported by the calculated energies of formation for carboxylates from carbenes and CO_2, which show no activation energy barrier at all.[170]

As seen in Scheme 48, the carboxylate **114** is rapidly transformed into the hydrogen carbonate salt **44h** by addition of protic solvents and the reverse reaction is only likely upon evaporation. The lower ratios of **44h** to **114** sometimes obtained in the reaction mixtures (Table 21) are attributed to the high reaction temperature which favours the anion decomposition ($\Delta S > 0$), leading to formation of CO_2 and an increase of the solution alkalinity. Note that this is a reversible anion decomposition, as the CO_2 cannot be lost in the pressurised vials and is stored as the carboxylate. Furthermore, increased temperatures (175 vs. 170 °C) led to higher ratios of **44h** to **114**.

Although the carboxylate is thermodynamically favoured over the hydrogen carbonate[165c] and even more stable when the *N*-substituents are not bulky and allow for a planar *p*-orbital overlap,[170] it was not possible to isolate the carboxylate. This was attributed to the formation of the solid hydrogen carbonate salt **44h**.

Except for very bulky imidazolylidene derived carboxylates, only the *N*,*N*'-dimethylimidazolium carbonate is solid and sufficiently stable to precipitate from solution (Scheme 45). In general, imidazolylidene carbenes have a very high affinity for CO_2 and therefore, 2*H*-imidazolium ionic liquids combined with basic anions (e.g. [C_4mim][OAc]) are excellent for the chemisorption of carbon dioxide.[171] The zwitterionic carboxylates themselves are also of particular interest, as they have already been applied in the synthesis of hydrogen carbonate ILs (which are commercially available as CBILS©),[165c] or directly in IL syntheses,[168] as easy to handle pre-catalysts[172] and as CO_2 transfer reagents in carboxylation reactions.[173]

4.2.3) Basicity of the CILs and [Cl]⁻ formation

As mentioned in the previous section, upon mild heating and/or extensive evaporation of the $CDCl_3$ solution the intensity of the carboxylate (156 ppm) and the $[HCO_3]^-$ signals (160 ppm) are reduced in the ^{13}C NMR spectrum. In both cases the carboxylate and carbonate signals eventually disappear completely, indicating the loss of CO_2. After evaporation of the $CDCl_3$ mixture, a solid is obtained. This solid could be recrystallised, although the molecular structure was not clear. It is to say that the formation of $[OMe]^-$ or $[OH]^-$ salts, due to loss of CO_2 (Scheme 49), is unlikely. First, the 2*H*-imidazolium hydroxides are unstable (non-existing)[174] and second, alkoxide anions are unlikely to be formed in the presence of the imidazolylidene carbene.[170] Moreover, the $[OH]^-$ and $[OMe]^-$ anions are not experimentally observed in combination with the 2*H*-imidazolium cation, although [C_4mim][OMe] was reported by Seddon and Earle, with the ^{13}C NMR signal (of a neat sample) for the anion at 42.3 ppm (in $CDCl_3$).[155]

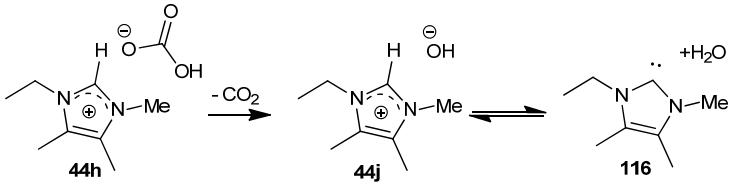

Scheme 49: Decomposition of the hydrogen carbonate salt upon heating to form the hydroxide salt and the imidazolylidene carbene.

The solids obtained are analysed by single crystal X-ray diffraction and are found to be the [C_2m_3im][Cl] salt (Figure 30). This remarkable result is explained by the alkaline action of the salts on chloroform residues originating from NMR sampling or recrystallisation (Scheme 50).

Upon abstraction of the proton of $CHCl_3$,[3] one chloride is expelled to form dichlorocarbene (reaction 1), which forms consecutively the unstable dichloromethanol and formylchloride (reactions 2 and 3). The latter decomposes rapidly into carbon monoxide (CO) and a chloride anion. Overall, 3 $[OH]^-$ anions are converted to 3 $[Cl]^-$ anions, with formation of water and CO (reaction 5).

In contrast to the H/D exchange, the formation of the $[Cl]^-$ salt is not readily established, i.e. ^{13}C NMR spectra of carbonate salts can be recorded in $CDCl_3$. On the contrary, it requires evaporation and heating. The proton transfer required during carboxylate formation and H/D exchange in $CDCl_3$ prove that both the imidazolium cation and $CDCl_3$ can be deprotonated. It is believed that upon heating and evaporation of the solution, decomposition of the dihydrogen carbonate (H_2CO_3) leads to the increase of the concentrations of CCl_3^- (pK_a: ±15)[167] and/or the more basic imidazolylidene carbene (pK_a: ±25 (DMSO); pK_a: ±36 (CH_3CN))[69, 175]. The loss of the dihydrogen carbonate as a proton source, allows the chloroform to decompose to the dichlorocarbene. On the contrary, in the presence of neutral carbonates, the CCl_3^- anion is immediately protonated ($pK_{a1}(H_2CO_3)$: ±6, $pK_{a2}(H_2CO_3)$: ±10)[165c], hindering the complete decomposition. Scheme 50 shows that exact one molecule of H_2O is needed to establish the decomposition of one $CDCl_3$ molecule (and transformation of three anions), therefore, after evaporation and decomposition of the carbonate anion, contact with air might provide sufficient water to establish the complete anion transformation.

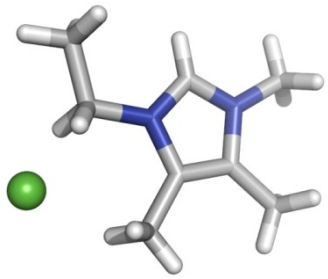

Figure 30: Single crystal X-ray diffraction image of the $[C_2m_3im][Cl]$ (44k) salt.

[3] Note that the proton abstracted from chloroform mentioned throughout this section can also be a deuterium ion. Analogously, chloroform mentioned can be deuterochloroform, and the single crystal X-ray diffraction analyses do not distinguish between deuterium or hydrogen.

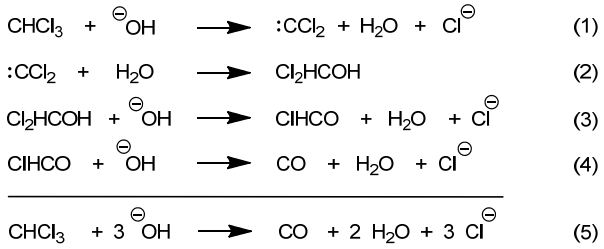

Scheme 50: Degradation reactions of chloroform in alkaline medium.[176]

The 2-isopropylimidazolium and 2-methylimidazolium chloride salts cannot be retrieved in the same way. To control whether the carbonate anions can possibly deprotonate chloroform to create chloride anions and carbon monoxide (see Scheme 50), the 2-alkylimidazolium derivatives were boiled in $CHCl_3$. However, no formation of the chloride salt occurrs, i.e. the carbonate peak does not disappear. Although for the $[C_2C_1m_3im]^+$ salt, some decomposition of the cation is observed, the $[HCO_3]^-$ signal remains visible on ^{13}C NMR. It seems that the imidazolylidene carbene is necessary to accomplish degradation of chloroform. Hence, during the heating process, the carbonate decomposition is aided by the carboxylate formation, eventually leading to the basic carbene, prior to chloroform decomposition. Alternatively, after evaporation of the volatiles, the basic carbene is left, deprotonates freshly added chloroform and stabilises the newly formed chloride anion.

The chloride and carbonate salts can be clearly distinguished by their large difference in melting points and by infrared absorption spectra. The chloride salt $[C_2m_3im][Cl]$ (T_m: 250 °C) has characteristic absorption peaks at 2953 and 1937 cm^{-1}, while the hydrogen carbonate salt $[C_2m_3im][HCO_3]$ (T_m: 149 °C) has a broad absorption peak at 1617 cm^{-1}. Furthermore, once the $[Cl]^-$ salt (**44k**) is formed, the aromatic singlet can be emerged in the ^1H NMR spectrum after shaking the $CDCl_3$ solution with a drop of water (Scheme 46), this is not the case for the $[HCO_3]^-$ salt.

4.2.4) N-Protonated imidazoles

In entries 10 to 13 (Table 20, p84), in which the reaction was preliminary stopped after three or six hours, 15% to 75% of the end product was found, while no starting material was observed in the ^1H NMR spectrum (in $CDCl_3$). In the spectrum, peaks analogous to the free imidazole were shifted slightly upfield, although here an *N*-methyl peak was missing. This spectrum is typical for protonated imidazoles (**117**), which are proposed to be formed by neutralisation of $MeCO_3H$, originating from DMC and water (Scheme 51). The amount of protonated imidazole found, indicates the amount of $MeCO_3H$ present in the reaction mixture. This in turn indicates the minimum amount of water, present in the solvent or dimethylcarbonate, needed to react with DMC (up to 0.85 eq. H_2O vs. 1-ethyl-2-isopropyl-4,5-

dimethylimidazole (**41d**) in entry 12 in Table 21). Formation of $MeCO_3H$ during work-up could be excluded since the protonated imidazoles were not always found in experiments where unreacted imidazole was still present (e.g. entries 1, 2 and 4). This indicates that (i), elevated temperatures are needed for the substitution reaction of DMC by water, (ii) a significant amount of DMC is consumed by water present in the mixture and (iii) protonated imidazoles can react further by the presence of the basic anions in the reaction mixture.[177]

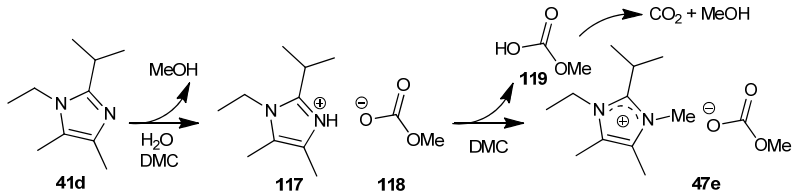

Scheme 51: Formation of hydrogen methyl carbonate (118) by reaction of water with DMC. The methyl carbonate anion deprotonates the hydrogen imidazolium cation (117) and liberates CO_2 and a free imidazole, which can be methylated to form the *N*-methylimidazolium methyl carbonate salt (47e).

The proposed hypothesis was verified by reacting 1-ethyl-2,4,5-trimethylimidazolium hydrochloride salt (**43b**) with dimethyl carbonate (Scheme 52). Protonated imidazolium salts cannot be quaternised with MeI, although by using DMC as methylating agent, the salts can be successfully quaternised. Here, this is probably due to catalytic amounts of water present, forming monomethyl carbonate. This means that monomethyl carbonate is sufficiently weak as a base to liberate the imidazole, allowing the latter to react with freshly formed MeCl or dimethyl carbonate. The monomethyl carbonate is formed by an anion exchange between **43b** and **45e**, therefire, only a trace of water is needed. The reaction to form **45i** proceeded very clean, quantitatively and was completed in three hours, giving a white powder. This illustrated that any 1*H*-imidazolium salt, containing the desired anion in stoichiometric amounts, can be methylated by reaction with DMC to form the *N*-methylimidazolium salt with the desired anion.

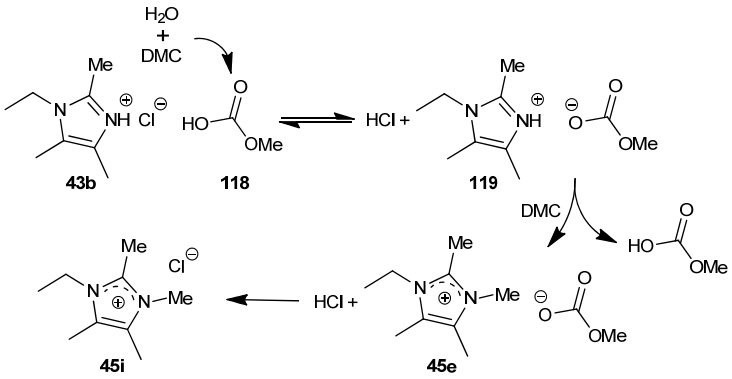

Scheme 52: Quaternisation and *in situ* metathesis of 43b via neutralisation by the methyl carbonate anion. The latter needs only to be present in catalytic amounts, as it is regenerated from compound 45e.

As mentioned in the imidazole purification section, the hydrochloride salts of peralkylated imidazoles are often solid and can be recrystallised, making this method very interesting towards the synthesis of the chloride salts, which was also experimentally confirmed for the chloride salt **44k** (using equal amounts of solvent, catalyst, dimethyl carbonate and the same temperature as for the methylation reaction of 1-alkylimidazoles).

4.2.5) Carbon dioxide formation

Upon opening of the sealed pressure vial, in every experiment for every imidazole analogue, a substantial amount of CO_2 evolved. The sealed vials were always pressurised and had to be opened carefully. Only at -78 °C, the evolution of gas from the liquid phase can be supressed.

Given the multiple side products obtained upon quaternisation of the 2*H*-imidazole derivatives with DMC (*vide supra*) and the large amount of CO_2 formed, methylation was initially assumed to proceed at least partially with the involvement of compound **120** (Scheme 53). However, trials at lower temperatures (140 °C) to selectively promote $S_{N,Ac}$, did not allow to observe any reaction with the compounds **41b,d** at all.

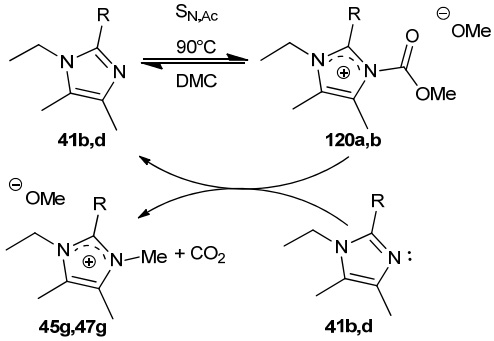

Scheme 53: Proposed CO_2 formation via $S_{N,Al}$ and $S_{N,Ac}$ of imidazoles with DMC (R = Me, iPr).

In preliminar work on dimethyl carbonate alkylation, Tundo stated that the alkylation reaction ($S_{N,Al}$) is irreverisble as the formed methyl carbonate anion decomposes to CO_2 and $[MeO]^-$.[178] Later, Holbrey *et al*. proposed that the anion only decomposes upon protonation.[164] This can be confirmed by the present work, i.e. carbonate anions do not degrade during the reaction or over time. Since during the described experiments, water is found to play an important role, the most plausible explanation for the CO_2 formation, is the reaction of water with DMC, to form H_2CO_3, which decomposes to water and CO_2.

4.2.6) Metathesis of the CILs

After crystallisation and filtration of the 1-ethyl-2*H*-3,4,5-trimethylimidazolium hydrogen carbonate ($[C_2m_3im][HCO_3]$) salt, it could be applied successfully in metathesis reactions with Brønsted acids, such as acetic acid, lactic acid or aqueous $HNTf_2$ (80%). Hereby, CO_2 gas

evolved and the temperature of the mixtures slightly increased. To assure complete reaction, the products were stirred in distilled water and heated to 50 °C overnight.

Dicyanamide salts could not be obtained via the corresponding Brønsted acid, nonetheless, the ammonium salt (**52b**) could be applied in the metathesis reaction. Ammonium dicyanamide can be synthesised by percolating a $NaN(CN)_2$ solution through an acidic ion exchange resin (high sodium affinity), which is neutralised with an ammonium solution prior to the exchange reaction (Scheme 54).[179] After evaporation of the collected aqueous solution, $NH_4N(CN)_2$ is obtained as a white powder in good purity (as analysed by elemental analysis). This process is possible on a large scale, although stoichiometric amounts of ion exchange resin are needed and the recyclability of the resin was not investigated.

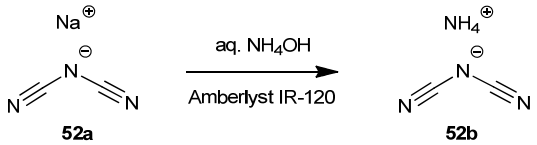

52a **52b**

Scheme 54: Metathesis with ammonia to form ammonium dicyanamide ($NH_4N(CN)_2$) via an ion exchange resin.

The most straightforward metathesis reaction is with aqueous $HNTf_2$. The use of $HNTf_2$, which is cheaper with regard to its lithium salt, is more environmentally benign since no carcinogenic quaternisation agents are used and no stoichiometric amounts of lithium salts are formed as a by-product. Here, a small excess of the bis(trifluorosulfonylmethyl)imide acid leads to rapid and complete conversion, while the remainder of the acid can be evaporated.

Upon application of the more hygroscopic acetic or lactic acid, problems regarding the stoichiometry of the metathesis reaction arise. Namely, even after extensive evaporation, the anion signals in ^{1}H NMR integrations are too large (accounting for ca. 1.2 eq.), probably due to strong intermolecular (H-bonding) interactions. The excess of acid originated by faulty mass calculation of the Brønsted acid and/or the carbonate salts, comprising a mixture of anions, which are not always visible by NMR. Although the removal of the carbonate anion can be monitored by ^{13}C NMR, detection of minute excesses of acid cannot be achieved by standard spectrometric and spectroscopic methods such as NMR, IR, LC, GC or MS. Only Elemental Analysis (EA) can prove that the compound is pure, on condition that the compound is solid, which was not the case for the acetate or lactate salts.

Alternatively, the stoichiometry can be improved by addition of solid ammonium or calcium salts, or by the direct quaternisation of recrystallised protonated imidazolium salts, such as imidazolium hydrochloride salts (*vide supra*). The latter method uses protonated imidazolium salts which exist of equimolar amounts of imidazole and the desired Brønsted acid, given these compounds are solid and can be recrystallised.

4.3. Conclusions

Completely substituted imidazoles can successfully be methylated using dimethyl carbonate. Although K10 Montmorillonite is found to be an excellent catalyst, which allows complete conversion without formation of side products, the high temperatures applied still lead to very intense colouration. In the case of the 2*H*-imidazolium salts, the product is solid and can be recrystallised to obtain a colourless compound. In the case of the liquid 2-alkylimidazolium salts, the product can be washed with Et_2O in CH_3CN or with EtOAc in demineralised water.

The carbonate anions are stable and do not decompose under ambient conditions, unless a carboxylate can be formed. This carboxylate is formed from a carbene, which reacts immediately with the mutually formed H_2CO_3. The carbene derived from $[C_2m_3im][HCO_3]$ has a very high affinity for CO_2 and the resulting carboxylate is thermodynamically favoured, although unstable in contact with air or nucleophilic and protic solvents. The presence of this compound in the reaction mixture was confirmed by ^1H NMR analysis in CD_3OD, while the amount is strongly dependent on the solvent. The formation of the carboxylate is more pronounced in chloroform and might be the crucial step in chloroform decomposition to form the chloride anion.

The carbonate salts are reactive species, which will transform when dissolved in different solvents or left open at ambient air. Thus, $[imidazolium][MeCO_3]$ forms the (sometimes crystalline) $[imidazolium][HCO_3]$ when in contact with air moisture. The conversion of the $[MeCO_3]^-$ to the $[HCO_3]^-$ anion is observed in water, while in the presence of methanol, the methyl carbonate anion is stable.

The methanesulfonate ionic liquids were found to be easily prepared via microwave irradiation. Except for the 2*H*-imidazolium salt, the methanesulfonate ionic liquids were all room temperature ionic liquids. After metathesis with sodium dicyanamide, the by-product sodium methanesulfonate and the excess sodium dicyanamide could be precipitated and removed via filtration. The ICP-MS analysis of the obtained ionic liquids showed that this procedure allowed a complete removal of sodium salts from the ionic liquids.

To conclude, a comparison between the silver, the methanesulfonate and dimethyl carbonate mediated ionic liquid synthesis methods is given in Table 22. Here, it is shown that both toxicity and resource usage are considerably reduced by applying imidazolium methanesulfonate salts in ionic liquids. One drawback is that chloroform is used to completely precipitate NaOMs, although in the silver mediated metathesis of iodide ionic liquids, also dichloromethane is applied to precipitate remainders of AgI. ICP-MS analyses of synthesis experiments where other solvents are used to precipitate NaOMs, might allow to circumvent

this problem, although a hydrophobic solvent allowing ionic liquid dissolution is the solvent of choice.

In the dimethyl carbonate based metathesis, no halogenated solvents are required, although here the main drawbacks are the high temperature, long reaction times and colouration of liquid samples (solids can be recrystallised). Dimethyl carbonate, which is the methylating agent, is also used as a solvent and is not disposed in the atmosphere due to its relatively high boiling point (T_b DMC: 90 °C). For the preparation of dicyanamide ionic liquids, a two-step metathesis is needed, since ammonium dicyanamide ($NH_4N(CN)_2$) is prepared prior to the ionic liquid metathesis (just as $AgN(CN)_2$ is prepared from $NaN(CN)_2$ prior to metathesis).

Table 22: Comparative study between the silver based, methanesulfonate and dimethyl carbonate based quaternisation and metathesis methods of a 10 gram sample.

	Method	[Cation][I] + $AgN(CN)_2$	[Cation][OMs] + $NaN(CN)_2$	[Cation][CH_3CO_3] + $NH_4N(CN)_2$
Quaternisation	Solvent	100 mL CH_3CN	10 mL CH_3CN	2 mL MeOH[a]
	Conditions	0 °C, 12h	80 °C (9W), 1h	170 °C, 24h
	Methylating agent	2.6 eq. MeI	1.1 eq. MeOMs	3 eq. DMC
	Removal of excess methylating agent	evaporation	extractionl	evaporation
Metathesis	Reaction steps	2 reaction steps	1 reaction step	2 reaction steps
	By-product	AgI (insoluble)	NaOMs (hydrophilic)	MeOH, CO_2

[a] **Large scale experiments were not conducted, therefore the solvent volume given is calculated.**

5. Biodegradability of ionic liquids

5.1. Introduction

Apart from clean synthesis and an inherently green application, a *greener* chemical should be *designed for degradation*.[180] This implies (i) rational design of products to enhance the environmental decomposition and (ii) complete understanding of the end-of-life fate of ionic liquids as part of their properties before the introduction in new technologies. The study on the biodegradability of ionic liquids is increasing and was initiated by the group of Gathergood and Scammells.[181] It is known that biodegradability of ionic liquids is in general very low, although ester functionalities can increase the biodegradability (Figure 31). The amount of (eco)toxicological reports on ILs increased by e.g. the research of Stolte[182] and here it appears that the toxicity exceeds that of conventional molecular solvents (IC_{50} ten-folds lower than for dichloromethane), aggravating with increasing *N*-alkyl chain length. The influence of the *N*-alkyl chain length is apparent on both toxicity and biodegradability and they both increase spectacularly for n=4, to increase gradually on going to n=8.[183]

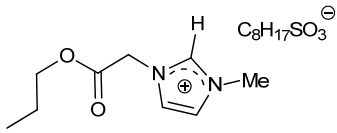

121

Figure 31: *N*-propyloxycarbonylmethyl-substituted imidazolium octylsulfonate (121) as the first *readily biodegradable* ionic liquid.[184]

Aquatic toxicity of chemical compounds is related to the biodegradability, not only for its environmental fate, but also for potential removal in wastewater treatment plants (WWTP). Thus, a decreased growth of microorganisms upon addition of ionic liquids to activated sludge systems is already observed, indicating a cytotoxic effect of the compounds.[183a, 185] Unfortunately, the (aquatic) toxicity of the peralkylated ILs was not assessed.

The newly synthesised completely substituted imidazolium ionic liquids are evaluated on their environmental impact, in collaboration with Dr. Ewa Liwarska-Bizukojc. Dr. Liwarska-Bizukojc, collaborator at the Institute of Fermentation Technology and Microbiology at the Łódź University of Technology, has gained expertise on the biodegradability of imidazolium ionic liquids and the study of their influence on activated sludge systems.[186]

The behaviour of the peralkylated ionic liquids in activated sludge systems is evaluated in two ways. First, the *ready* and *inherent biodegradability* of the ionic liquids is evaluated based on standard methods of the Organisation for Economic Cooperation and Development (OECD),

the Closed Bottle Test (OECD 301D)[187] and the Zahn-Wellens/EMPA test (OECD 302B), respectively.[188] Second, the oxygen uptake rate (OUR) is evaluated.

In the Closed Bottle Test, 5 mg L^{-1} of the ionic liquid is added as the only carbon source to a mineral nutrient solution containing a small inoculum of a mixed culture. In this test, the inoculum is the final clean water effluent of a municipal wastewater treatment plant in Zgierz, Poland. The biodegradation is then monitored every 7 days by the dissolved oxygen concentration (DO) via a modified Winkler titration. This allows the calculation of the ratio of oxygen consumption (corrected with a blank for the pure inoculum) to the total calculated chemical oxygen demand (COD). The biodegradability of organic chemicals is described as *readily biodegradable* if the oxygen consumption exceeds 60% of the COD in 28 days and within a time-span of 10 days after the lag-phase. Due to high dilution in this test, exceeding toxicity threshold limits of the compounds on the microorganisms is prevented. A drawback of this test is the possible perturbation of the oxygen consumption by nitrification.

Compounds that are not *readily biodegradable* are evaluated on the *inherent biodegradability*, which implies a decrease of at least 20% of dissolved organic carbon (DOC) after 28 days and a gradual decrease in time. The tetra- and penta-alkylimidazolium salts are evaluated using the Zahn-Wellens/EMPA test. Here, the chemical compound is brought in an aerated and agitated solution at 50 mg L^{-1} containing a relatively large amount of carefully prepared activated sludge (ca. 490 mg VSS L^{-1})[4], collected from the aeration chamber of the Zgierz wastewater treatment plant. The biodegradation is monitored by the DOC level, which is analysed with an IL550 TOC-TN analyser (Hach Lange). In this test too, a negative result does not exclude the biodegradation of the compound in a diluted solution containing other carbon sources. Both tests are run in parallel with a reference compound, sodium dodecylsulfate (SDS), in order to monitor the activated sludge activity and to calculate the net oxygen consumption realised by the tested compound.

The oxygen uptake rate and Monod kinetics of the biodegradation of the peralkylated ionic liquids is studied in a batch bioreactor. The tests are performed by introducing a synthetic waste water containing 300 mg of peptone, 100 mg of sodium acetate, 50 mg of potassium monophosphate, 50 mg of sodium bicarbonate, 50 mg of ammonium dihydrogen phosphate, 5 mg of magnesium sulphate and 5 mg of sodium chloride per litre in the bioreactor. To this synthetic waste water is added biomass, taken from the laboratory activated sludge system, which is adapted to this synthetic wastewater, to a concentration of 2.2 mg of DOC mg VSS^{-1}

[4] VSS: Volatile Suspended Solids: the volatile amount by incineration of Total Suspended Solids (TSS, dry mass of non-dissolved solids in the activated sludge).

as well as allylthioureum to inhibit nitrification.[189] Typical IL runs are performed by addition of 50 mg L^{-1} of ionic liquid to the synthetic waste water. Apart from these tests, two types of control tests are made, a type I control is the same as the typical IL tests but without the addition of ionic liquid, while type II of the control runs are performed with the ionic liquid as the sole carbon source, removing peptone and sodium acetate from the composition of the synthetic wastewater. During the experiments, DO and OUR are monitored online via an optical dissolved oxygen probe (ProODO™, YSI Environmental) combined with analytical software. The measured DO and OUR allow the calculation of Monod kinetics, i.e. the maximum specific growth rate μ_{max} and the saturation constant K_S.[190]

5.2. Experimental results

In a first assessment, four different tetra and penta-alkylated imidazolium iodide salts are tested on their biodegradability. The structures, given in Figure 32, demonstrate that the analogues have different C2 substitution or an increased *N*-alkyl chain when combined with a C2 proton.

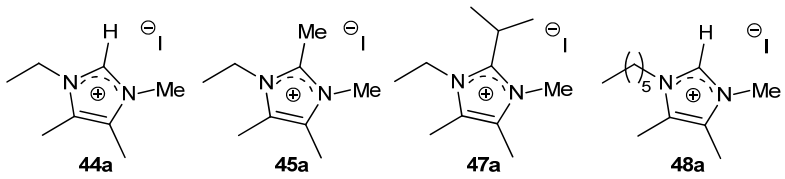

Figure 32: List of *N*-alkylimidazolium ionic liquid analogues used in the biodegradation tests.

In the Closed Bottle Test, the *ready biodegradability* is evaluated on small concentrations with minimal inoculum. The measurements of the DO with a 7-day interval, allow to calculate the degree of biodegradation. As demonstrated in Table 23, no ionic liquid biodegradation is observed in the first 14 days, while the reference compound sodium dodecyl sulfate is biodegraded for about 80%. After four weeks, the degree of biodegradation is the highest (9.1%) for the analogue bearing the *N*-hexyl chain (**48a**) and the lowest (2.1%) for the 2-methyl compound **45a**. Therefore, none of the compounds can be classified as *readily biodegradable*.

Table 23: Mean degree of biodegradation with standard deviation (%) during the Closed Bottle Test at 7-day intervals.

t (d)	**44a**	**45a**	**47a**	**48a**	SDS
7	0	0	0	0	75.4±3.58
14	0	0	0	0	79.5±2.14
21	1.70±0.51	0	1.42±0.46	1.13±0.22	81.0±1.75
28	**6.23±2.4**	**2.11±1.4**	**6.64±1.34**	**9.07±0.95**	**86.8±2.47**

In the agitated and aerated Zahn-Weller/EMPA test, the decrease in DOC is only 1.8 to 2.7% for the ionic liquids while the reference compound SDS shows a DOC decrease of 99.9% after 28 days. Here too, the highest loss is found for the *N*-hexyl substituted compound **48a**. Isocratic UPLC analyses show no decrease in IL concentration for the compounds **44a**, **45a** and **47a**, while the concentration of compound **48a** decreases by 33%. This test also allows the evaluation of adsorption by analyses of a sample after three hours of aeration. A fast decrease (not gradually in time) in concentration indicates adsorption processes taking place. Only *N*-hexyl analogue **48a** (3.5%) and the reference compound SDS (35.1%) show adsorption.

During the oxygen uptake rate (OUR) tests, the oxygen concentration and uptake rate is monitored for activated sludge systems containing one of the four ionic liquids. The control tests of type I and sample runs containing compounds **44a**, **45a** and **47a** show μ_{max} and K_S levels in the same range of municipal waste water, while for compound **48a**, the μ_{max} slightly exceeds this range and the K_S value is about the threefold of the values obtained in the other runs (including the blank run), although still within the range of normal municipal waste water. This indicates that first, the presence of ionic liquids do not hinder the growth of the activated sludge system and second, a low biodegradation of compound **48a** is obtained, increasing the available carbon substrate and hence also the growth rate. In the type II OUR tests, the oxygen uptake rate never exceeds 1 mg O_2 l^{-1} h^{-1}, which indicates that the ILs are not accessible as the sole carbon source. This was observed earlier in the non-peralkylated IL [C_4mim][Br] as well.[184]

Table 24: Mean values of maximum specific growth rate (μ_{max}) and saturation constant (K_S) with standard deviation in the type I OUR test.

	44a	**45a**	**47a**	**48a**	SDS
μ_{max} (h^{-1})	0.115±0.030	0.157±0.083	0.114±0.021	0.553±0.143	0.105±0.017
K_s (mg O_2 l^{-1})	10.09±1.43	9.93±0.71	12.08±1.26	30.23±8.83	10.77±1.28

In conclusion, an increased biodegradability is obtained for the 2*H*-imidazolium salts (**44a** and **48a**) and *N*-hexyl substituted imidazolium salts (**48a**). Among the lower biodegrading compounds **45a** and **47a**, the 2-isopropyl substituted compound (**47a**) shows the highest degradation in the Closed Bottle Test. Two phenomena are therefore proposed: (i) substitution with longer alkyl chains on the nitrogen and on the cation core in general, increase the lipohilicity and hence increase adsorption and biodegradation, (ii) the presence of a C2 proton increases the biological affinity for the compounds.

The overall results clearly indicate that ionic liquids are very poorly biodegradable and environmentally persistent, although not toxic to the activated sludge system. Ionic liquid contamination of water streams should be avoided and post-processing of contaminated aqueous waste streams is necessary in order to avoid the compounds to break through the WWTP system.

5.3. Future analysis

The cooperation between the departments of Sustainable Organic Chemistry and Technology of Ghent University and the Institute of Fermentation Technology and Microbiology of Łódź University of Technology, is launched in 2012 and will encompass future work on selected analogues to investigate the role of structure and properties on the environmental fate of ionic liquids. A list of ten new compounds is therefore already mutually composed.

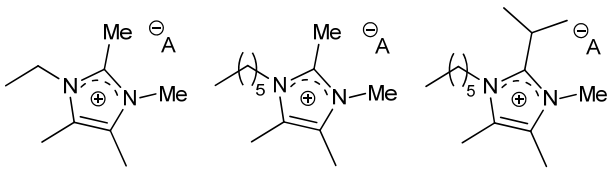

Figure 33: List of *N*-ethyl and *N*-hexyl substituted imidazolium ionic liquid analogues to be tested on biodegradability.

Figure 33 shows the iodide and bis(trifluoromethylsulfonyl)imide salts of *N*-ethyl and *N*-hexyl peralkylated imidazolium cations which will be studied to compare *N*-ethyl with *N*-hexyl salts. Most probably, the increasing biodegradability by increased hydrophobicity (observed between compounds **44a** and **48a**, Figure 32) will be confirmed in this way. More interesting, this allows the investigation of the contribution of the C2- and *N*-substituents by a comparison of the pairs (**44a**, **48a**), (**45a**, **49a**) and (**47a**, **51a**). If for every pair an equivalent biodegradability increase is observed when substituting the *N*-ethyl analogue for the *N*-hexyl analogue, then the increased biodegradability might be attributed mainly to the *N*-substituent

alone. However, when the increase is more pronounced for the 2*H*-imidazolium pair (**44a**, **48a**), then the overall hydrophobicity is the major factor, as the change in overall hydrophobicity is the largest for the pair (**44a**, **48a**). Finally, it is not excluded that actually the biggest difference in biodegradability is found in the 2-alkylimidazolium pairs, which would indicate a dominating effect of the C2 proton, allowing biological adsorption.

Second, in this future part also the bis(trifluoromethylsulfonyl)imide analogues (**45b**, **49b** and **51b**) will be investigated. Here, the influence of the potential toxic anion and the low water solubility will be assessed. Nonetheless, the influence of the anion on the aquatic toxicity has been found to be absent,[183a, 185] except for octylsulfate anions, which increases biodegradability for both imidazolium ([C_4mim]) and ester-functionalised imidazolium salts (**121**, Figure 31), in the Closed Bottle Test to 25 and 49%, respectively.[183b] Therefore, possible ion exchange should be taken into consideration, i.e. biological adsorption of the imidazolium cation and dissolution of the bis(trifluoromethylsulfonyl)imide anion. An additional quantification of the dissolved $[NTf_2]^-$ anion might be of added value here.

Finally, the contribution of *N*-alkoxy substituents to the environmental fate of the ILs will be evaluated (Figure 34). The ether functionalities introduce an extra interaction and reaction site, and might induce biodegradation via the alcohol and oxidation of the latter. Furthermore, the alkoxy side chain and an alkyl chain are isoelectronic, however, ether functionalities decrease the K_{OW} of imidazolium ILs (decrease of hydrophobicity).[191] By incorporation of an allyl functionality on the oxygen, both reactivity and lipophilicity are increased remarkably, therefore compounds **63b** and **63c** are expected to have an increased biodegradability.

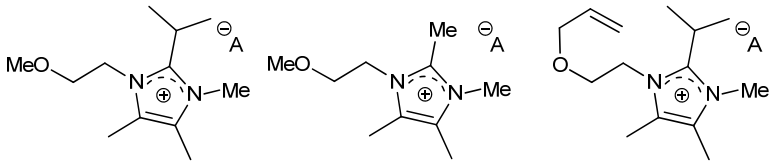

62b: A = I
62c: A = NTf_2

122a: A = **I**
122b: A = NTf_2

63b: A = I
63c: A = NTf_2

Figure 34: List of *N*-alkoxy substituted imidazolium ionic liquid analogues to be tested on biodegradability.

6. Imidazolium liquid metal salts

At the department of Chemistry of KU Leuven, research is on-going on the synthesis of *Ionic Liquid Metal salts*. This type of compounds is developed from metal ions ligated with neutral bases. The increment of cation size with these neutral ligands decreases the Coulombic forces. Aided by weakly coordinating anions, metal salts with melting points in the workable range are obtained. Thus, liquid metal salts are developed which possess the qualities of ionic liquids (low volatility, high conductivity) and have a very high metal concentration. These compounds possess very high current densities and hence are extremely useful in electrochemical metal deposition.

In this way, already liquid copper salts are obtained. These salts are ligated by acetonitrile and have a chemical formula which is $[Cu(CH_3CN)_4][NTf_2]$.[192] Also silver liquid metal salts have been synthesised and investigated, here the metal cation is combined with neutral, monodentate bulky amines such as *tert*-butylamine and piperidine or the bidentate ethylenediamine.[193]

The achieved procedures for the incorporation of different functionalities allows the evaluation of these moieties in the liquid metal salt synthesis. An array of earlier synthesised imidazoles is completed by 1-allyl-2*H*-4,5-dimethylimidazole (**41i**) and 2*H*-1-(2-methoxethyl)-4,5-dimethylimidazole (**41j**) (Figure 35). Thus, a series of 3 imidazoles bearing different substituents on the C2 position and a series of 4 imidazoles with varying *N*-substituents can be used for comparative investigation.

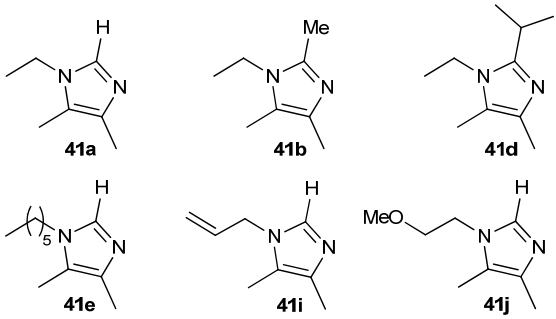

Figure 35: Imidazole analogues probed for liquid metal salt synthesis.

The newly designed 2*H*-1-methoxyethyl-4,5-dimethylimidazole (**41j**) is achieved in moderate yields (42%), analogous to the earlier obtained imidazoles. After work-up of the 1-allyl-2*H*-imidazole synthesis, a second compound is observed. The desired *N*-allylimidazole could not be isolated by fractional distillation. ^{1}H NMR spectra showed that this second compound also includes an allyl group (accounting for 17% in ^{1}H NMR) and was therefore proposed to be the

product of a rearrangement (Scheme 55), induced by the high temperatures and alkaline conditions. Analogous thermal rearrangement reactions in *N*-allylimidazoles were observed by Begg *et al.* (Scheme 56).[90] In this case, the concerted mechanism via a [3,3] sigmatropic rearrangement and a subsequent [1,5]-*H* sigmatropic shift was experimentally confirmed. An exact mechanism (free radical, sigmatropic) could not be designated by the authors. In this case, the alkaline conditions might have led to the formation of **123**. This anion might be involved in a [2,3] sigmatropic rearrangement. Although the upfield shifts in both ^{1}H and ^{13}C NMR (in $CDCl_3$) and the absence of a corresponding aromatic proton signal strongly suggest the formation of the isomer **125**, the LC-MS spectrum of the mixture did not confirm the presence of this compound.

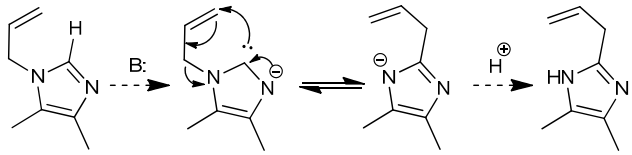

41i **123** **124** **125**

Scheme 55: Proposed side product formation via base induced rearrangement mechanism.

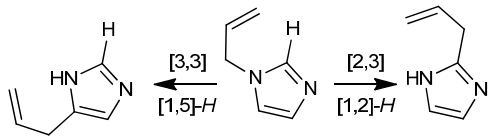

127 **126** **128**

Scheme 56: Formation of 4-allylimidazole (127) by consecutive thermal [3,3] and [1,5]-*H* sigmatropic rearrangement reactions and 2-allylimidazole (128).[90]

Fortunately, the desired *N*-allyl compound **41i** could be isolated via recrystallisation of the imidazolium hydrochloride salt in 29% yield. However, the side product could not be isolated from the mother liquor, and is therefore believed to be degraded due to the acidic conditions. Synthesis of the 1*N*-(2-allyloxyethyl)-2*H*-4,5-dimethylimidazole (**41l**), in a similar way as for the 1*N*-(2-allyloxyethyl)-2-isopropyl-4,5-dimethylimidazole (**59d**), was unsuccessful (Scheme 57). Since the alcohol (**41k**) could not be isolated in a pure form, the crude mixture was further used. The combination of impure alcohol and reaction of the base with the C2 proton is believed to lead to side products formation and yield decrease.

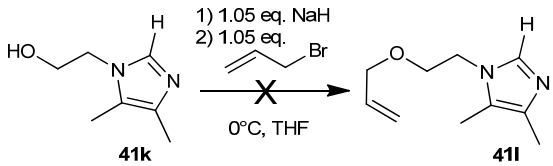

41k **41l**

Scheme 57: Transformation of the imidazolyl-ethanol (41k) into the (2-allyloxyethyl)-4,5-dimethylimidazole (41l).

Table 25:Composition and melting points of liquid metal salts.

Liquid metal salt	Imidazole	R^1	R^2	T_m (°C)
$[Ag(C_2m_3im)_2][NTf_2]$	C_2m_3im (**41a**)	Ethyl	H	81
$[Ag(C_2C_1m_3im)_2][NTf_2]$	$C_2C_1m_3im$ (**41b**)	Ethyl	Me	94
$[Ag(C_2C_{i3}m_3im)_2][NTf_2]$	$C_2C_{i3}m_3im$ (**41d**)	Ethyl	iPr	76
$[Ag(C_6m_3im)_2][NTf_2]$	C_6m_3im (**41e**)	Hexyl	H	[a]
$[Ag(C_Am_3im)_2][NTf_2]$	C_Am_3im (**41i**)	Allyl	H	[a]
$[Ag(C_{2O1}m_3im)_2][NTf_2]$	$C_{2O1}m_3im$ (**41j**)	Methoxyethyl	H	51

[a] Compounds are liquid at room temperature.

The synthesised silver liquid metal salts are composed of a monovalent silver ion and the provided imidazoles and they have the general formula $[Ag(imidazole)_2][NTf_2]$. Four of the designed metal salts are solid at room temperature (Table 25), and the trend in their melting points is completely analogous to the trends observed in the melting points of the ionic liquids based on the respective imidazoles (see Table 5 and Table 12). The melting point of the *N*-methoxyethyl substituted derivative, being relatively low, confirms that the introduction of the methoxyethyl moiety induces crystallinity without increasing the melting point exceptionally.

Holding the liquid samples at -60 °C for a prolonged period did not lead to any crystal formation. This demonstrates the increased undercooling properties of hexyl and allyl substituted imidazolium salts. The formation of salts with melting points above room temperature allowed crystallisation and single crystal X-ray diffraction analysis. Although the asymmetric unit only consist of half of the anion and cation, a complete picture is given in Figure 36.

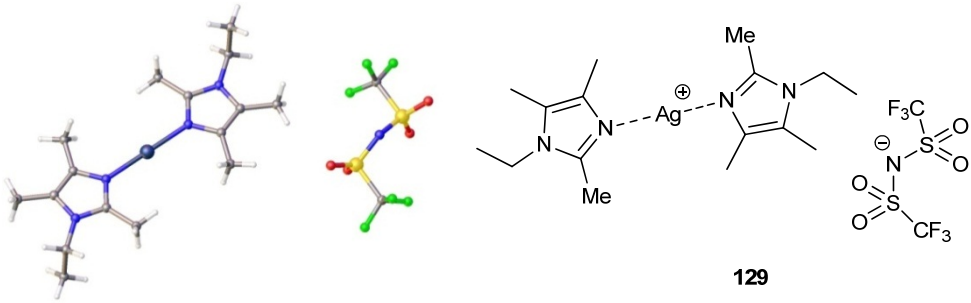

129

Figure 36: Single crystal X-ray diffraction image of $[Ag(C_2C_1m_3im)_2][NTf_2]$.

IV) PERSPECTIVES

The application of the microwave reactor in the quaternisation reaction of peralkylated imidazoles with methyl methanesulfonate was successful due to the pressurisation and precisely controlled temperature. This suggests to investigate this reaction in continuous flow. In this way, temperature and pressure can also be precisely regulated. The application of continuous flow would further allow to synthesise these ionic liquids on an industrial scale.

The investigation of continuous flow hydrogenation with the X-Cube™ reactor (section V.1) has just initiated. Extensive research on novel system set-up, e.g. combination of diverse immobilized (bio)catalysts, will definitely lead to very efficient synthesis methods. Moreover, installation of on-line monitoring probes, e.g. based on IR or UV, can give an enormous amount of data. An automation of the data collection and preferably also of the experimental parameter variation allows for the collection of large data sets of reaction properties.

Some of the alkyl-, alkenyl- and alkoxyimidazolium ionic liquids showed excellent stabilities. This property can be exploited, especially in the case of the chiral alkoxyl substituted analogues. Here, the influence on the reaction outcome can be investigated, e.g. the 2-isopropyl derivatives can be evaluated in addition reactions with organozinc or organomagnesium compounds (Scheme 58).

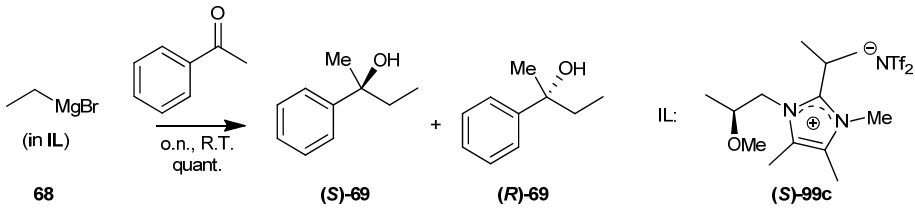

68 **(*S*)-69** **(*R*)-69** **(*S*)-99c**

Scheme 58: Evaluation of asymmetric induction during organomagnesium addition by the chiral ionic liquid.

Because of the weakly acidic C2 proton, complexation with transition metals can be achieved with the 2*H*-imidazolium derivatives (Figure 37). Thus, chiral imidazolylidene ligands can be applied in coordination chemistry. Alternatively, liquid metal salts with different substitution patterns can be designed, leading to different properties. The application of these compounds in electrodeposition can then be investigated.

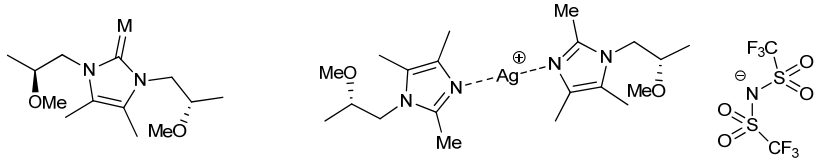

146
M = Au, Cu

147

Figure 37: Chiral coordination complexes based on a *C*-linked imidazolylidene carbene and an *N*-linked imidazole.

V) APPENDIX

1. Continuous flow analysis of catalysts

In the framework of the MAPIL project, the collaborators at the department of Surface Chemistry and Catalysis and the department of Metallurgy and Materials Engineering (KU Leuven) developed a strategy for the electrochemical synthesis of a copper gauze supported Raney Nickel catalyst. The thus designed catalyst was mounted on the continuous flow system (ThalesNano X-Cube™) present at the department of Sustainable Organic Chemistry and Technology (UGent) to analyse catalyst activity over time. Furthermore, the use of the Raney Nickel catalyst in various types of hydrogenation reactions (e.g. hydrogenation, debenzylation, …) was evaluated.

Hydrogenation in continuous flow systems has recently gained interest, thus, (multistep) syntheses involving hydrogenations with H_2 on heterogeneous catalysts have been described by the group of Kappe and others.[194] In the references cited, the ThalesNaNo H-Cube™ system is applied, very similar to the further discussed ThalesNano X-Cube™ system. The general success of continuous flow lies in the use of high temperatures and gas pressures, which are only applied on small volumes in small channels, allowing for fast heat and mass transfer. Second, reactive or hazardous intermediates formed in situ are reacted immediately, hence the need for purification or safety measurements are reduced. Finally, continuous flow processes allow an easy introduction of immobilised catalysts and a straightforward expansion to production scale.[195]

1.1. The X-Cube™ flow reactor

The X-Cube™ flow reactor is demonstrated in Figure 38 andFigure 39. The reagent solutions are pumped in the stainless steel tubing (which represents the system) by means of two high pressure (HPLC) pumps (1, 2). The system pressure (p_{sys}) can be set per 5 bar, up to a maximum of 150 bar. The tubing of the two pumps is connected to a mixer, after which the inlet pressure (p_{in}) is monitored via the inlet pressure sensor (3). The tubing is subsequently connected to the top compartment via the gas mixer (5), which is also connected to the gas check valve (4). The gas/liquid mixture is then pumped through the bubble detector (6), CatCart® (Catalyst Cartridge) holder 1 (7) and cartridge holder 2 (8). The cartridges can be mounted and dismounted easily, changed for inert cartridges and can be heated from 20 to 200 °C in 5 °C intervals, separately. For all experiments with a commercial CatCart, the

bubble detector was connected directly to cartridge 2. Finally, the mixture is pumped to the system pressure sensor (9) and the system valve (10), to which the outlet is connected.

Figure 38: Photograph of the X-Cube™ system. Top: user interface, centre: cartridges with insulation caps, gas valve and bubble detector, bottom: HPLC pumps.

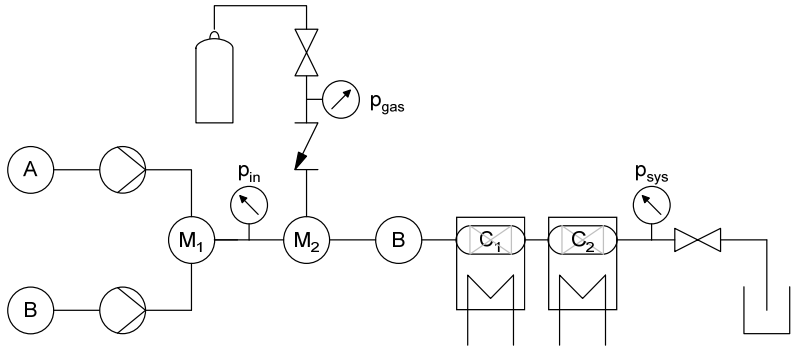

Figure 39: Schematic representation of the X-Cube™ system.

The parameters are set via the user interface, adjustable are: pump (A,B) speeds v_1 and v_2 (min. 5 mL min^{-1} total), system pressure (p_{sys}) and the temperature of the cartridge holders (C1, C2). C1 can be used to preheat the reactant mixture in between 10-15 °C above T_{C2} (see Table 26), the catalyst cartridge is loaded in C2 and the connecting tubing is insulated.

The pressure relation is given by:

$$p_{\mathrm{in}} = p_{\mathrm{sys}} + dp_{\mathrm{sys}} \quad \text{(Equation 4)}$$

$$p_{\mathrm{gas}} = p_{\mathrm{in}} + dp_{\mathrm{gas}} \quad \text{(Equation 5)}$$

$$p_{\mathrm{gas}} = p_{\mathrm{sys}} + dp_{\mathrm{sys}} + dp_{\mathrm{gas}}$$
$$\Rightarrow p_{\mathrm{sys}} \leq p_{\mathrm{gas}} - dp_{\mathrm{sys}} - dp_{\mathrm{gas}} \quad \text{(Equation 6)}$$

The inlet pressure (p_{in}) provided by the pumps is dictated by the set system pressure parameter (p_{sys}) and the pressure drop over the system (dp_{sys}), which is dependent on the solvent, catalyst, system set-up and the pump speed. On the one hand, the minimum gas pressure (p_{gas}) to open the check valve, until the bubble detector (B) detects 1-10% bubbles, needs to be higher (with dp_{gas}: 6-10 bar) than the pressure applied by the pumps (p_{in}). On the other hand, the gas pressure (p_{gas}) is limited by the relief valve of the cylinder ($p_{gas} \leq 50$ bar), hence dictating the maximum system pressure (p_{sys}) (equation 6). Gas evolution is manually measured by recording the time to fill a 8 or 100 mL recipient, i.e. 1.9 mL min^{-1} for p_{sys} = 15 bar and 3.7 to 4.4 mL min^{-1} for p_{sys} = 30 bar, accounting for respectively 17 and 33 to 40 eq. H_2 vs. a 10 mM or 1.4 to 3.3 eq. H_2 vs. a 120 mM concentration of acetophenone.

1.2. Hydrogenation with supported RaNi

During the MAPIL project, a revolutionary method was developed to produce a Raney Nickel (RaNi) catalysts tethered to a copper gauze support.[196] The development of a Raney Nickel catalyst on an inert solid support has several advantages over the conventional catalyst powder. (i) The fine powder is not easily separated from the reaction mixture, decreasing the recyclability and (ii) resulting in an unwanted contamination of the end-product with catalyst metal powder (e.g. in pharmaceutical formulations). (iii) In industrial applications, the leaching of the catalyst powder from a fixed bed reactor results in an activity decrease and (iv) in the clogging of reactor tubing and connections, leading to a backpressure build-up.

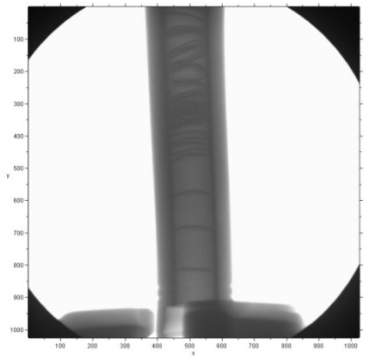

Figure 40: X-Ray image of CatCart filled with Cu gauze supported RaNi (CSRN).

The Copper gauze Supported RaNi (CSRN) catalyst is brought into an empty CatCart (Figure 40) with glass wool as packing material, to mount the catalyst in the continuous flow system. Subsequently, the hydrogenation of a model compound is monitored during long term experiments of at least 300 minutes. In this way, the activity can be studied in function of time which allows to decide whether leeching or activity decrease is apparent.

During the experiments, a 10 mM acetophenone solution (C_{in}) in ethanol is hydrogenated with the parameters given in Table 26. The gas/liquid mixture is preheated by the inert C1 cartridge, to obtain a homogenous temperature in cartridge C2 and to compensate the temperature loss during the C1 to C2 transfer. Effluent samples are collected at time intervals, which are carefully noted for all experiments. The undiluted effluent samples are analysed by the HPLC system, performing three LC-UV measurements of every sample (measurements at 214 nm and 256 nm). After calibration to the concentration of the effluent products (acetophenone (AF) and 1-phenylethanol (PEA)) (see Figure 51), the average values of these three measurements are plotted (Figure 42, Figure 43) with error bars indicating the minimum and maximum of the recorded values. These error bars give an image of the analysis error of the LC-UV system (no standard deviation was calculated for only three measurements). Absorbance results at both 214 and 256 nm obtained from experiment 1-3, show that the trends are proportional. As the signal/noise ratio is greater for the former, the absorbance at 214 nm is preferably monitored.

Table 26: Conditions of continuous flow experiments with the CSRN cartridge.

Exp.	v (ml/s)	C_{in} (mM)	v_{in} (µmol/min)	T_{C1} / T_{C2} (°C)[b]	p_{sys} (bar)	p_{gas} (bar)[c]	length (min)
1-1	0.5	10	5	95/80	15	32-35	300
1-2	0.5	10	5	95/80	15	32-36	300
1-3	0.3[a]	10	3	135/125	15	32-37	400
1-4	0.5	10	5	95/80	30	43-48	130
1-5	0.5	10	5	110/100	30	43-49	600
1-6	0.5	10	5	110/100	30	43-50	320
1-7	0.5	10	5	110/100	30	43-51	470
1-8	0.5	10	5	variable	30	43-51	

[a]Where v_1 < 0.5 mL min^{-1}: v_2 + v_1 = 0.5 mL min^{-1}; [b]C2 is the catalyst cartridge, C1 is an inert preheating cartridge; [c]dp_{sys} = 5-10 bar.

The time to reach steady state conversion (t_{SS}) is calculated by multiplying the residence time (t_{res}) (dead volume/pump speed) with 1.6. Given an estimated dead volume of 8 mL, t_{SS} is

25,6 min for all the experiments given in Table 26. Although t_{SS} is intrinsic to the experiment and should be monitored for every set-up separately, all long-term experiments are found to be stabilised after 30 minutes (see plots of experiments 1-1, 1-2, 1-3 and 1-7 in the experimental section, Figure 54 andFigure 55).

1.2.1) Catalyst activity

Steady conversion is observed in exp. 1-1, 1-2, 1-6 and 1-7 with no trend in time. The variation in concentration, over the course of the experiment, is translated by the standard deviation (σ, see Table 27).

Table 27: Resulting mean (μ) and standard deviation (σ) of AF and PEA effluent concentrations during experiments 1-1 to 1-7.

	$\mu(C_{AF})$ (mM)	$\sigma(C_{AF})$ (mM)	$\mu(C_{PEA})$ (mM)	$\sigma(C_{PEA})$ (mM)	$(C_{PEA}\, C_{tot}^{-1})$ (%)
Exp1-1	7.27	0.38	2.91	0.26	29
Exp1-2	7.97	0.70	3.23	0.40	29
Exp1-3	1.69	0.64	8.65	0.53	84
Exp1-4	6.90	1.06	3.50	0.82	34
Exp1-5a ≤ 300 min	4.83	0.82	5.82	0.63	55
Exp1-5b > 300 min	8.69	0.53	1.90	0.49	18
Exp1-6	8.64	0.68	2.03	0.42	19
Exp1-7	8.40	0.68	1.86	0.33	18

The catalyst activity does not decrease within the time-frame of the experiments, i.e. 300-500 min. Table 27 shows the effluent concentrations of the different experiments. While interexperimental variations in influent concentration C_{in} cannot be excluded, no significant changes in effluent concentrations (translated by the standard deviation σ in Table 27) can be demonstrated. The influence of the gas pressure is only small, as the conversions during experiments 1-1, 1-2 and 1-4 (with different p_{gas}, see Table 26) are about the same. However, the high temperature experiments 1-5b to 1-7 have lower conversion than the experiments 1-1 and 1-2 (see Table 27). As conversion increases with increasing temperature (*vide infra*, Figure 43), the lower conversion observed here indicates a more important contribution of the equilibrium constants at high temperatures. During experiment 1-3, a small amount of a new compound is formed, demonstrated to be ethylbenzene by GC-MS. The formation of the latter compound will be elaborated in the next section.

To illustrate the changes of equilibria in the cartridge, an overview of the mean concentrations in the void volume ($\bar{C}_X$), absorbed numbers on the catalyst (θ_X^*), equilibrium constants (K_X) and rate constants (r_X) is given in Figure 41. Note that the concentrations in the cartridge follow a plug-flow regime, while for simplification, the concentrations in Figure 41 are the overall mean for the void volume.

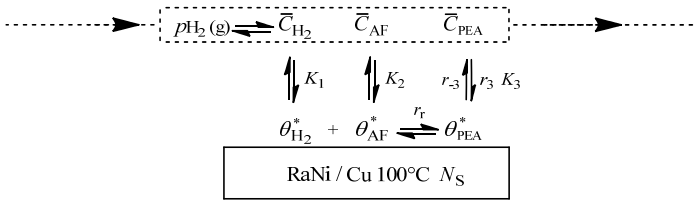

Figure 41: Schematic presentation of the plug flow reactor with mean concentrations ($\bar{C}_X$), equilibrium constants (K_X) and rates (r_X), amount of total adsorption sites (N_S) and fraction of sites occupied by compound x (θ_X^*).

For experiments 1-5b, 1-6 and 1-7, a constant desorption rate of PEA (r_{-3}) is proposed. At steady state, the absorbed amount PEA on the catalyst ($\theta_{PEA}^* N_S$, in moles PEA on the catalyst surface) is constant (= generation + adsorption – desorption):

$$\frac{d\theta_{PEA}^* N_S}{dt} = 0 \Rightarrow r_r + r_3 - r_{-3} = 0 \qquad \text{(Equation 7)}$$

If the contribution of adsorption of PEA is considered negligible vs. the desorption ($r_3 << r_{-3}$) at 100 °C, then the desorption is equal to the generation:

$$r_3 << r_{-3} \Rightarrow r_{-3} = r_r \qquad \text{(Equation 8)}$$

If the difference in the PEA concentration in the liquid phase between the influent and effluent is expressed as ΔC_{PEA}, the mean desorption rate r_{-3} and reaction rate r_r in the cartridge are given as:

$$r_r = r_{-3} = \frac{\Delta C_{PEA}}{t_{res}} = \Delta C_{PEA} \frac{v_{tot}}{V_{void}} \qquad \text{(Equation 9)}$$

Since V_{void} and t_{res} are unknown, the mean reaction rate cannot be determined. Hence, for experiments 1-5b, 1-6 and 1-7, where C_{in} = 10 mM, $\Delta C_{PEA} \cong 1.90\ \mathrm{mM}$ (Table 27) and the production and specific activity are given in equations 10 and 11. The catalyst activity found here (for 110 °C) is comparable to that of the batch experiments performed at 80 °C by the collaborators of the department of Surface Chemistry and Catalysis (0.08 to 0.33 h^{-1}).

$$production = \Delta C_{PEA}\,(v_{tot}) \cong 0.95\ \mu\text{mol}.\,min^{-1} \qquad \text{(Equation 10)}$$

$$activity = \frac{production}{catalyst\ mass} = 20\ \mu mol\ min^{-1}\ g\ RaNi^{-1} = 0.14\ h^{-1} \qquad \text{(Equation 11)}$$

An anomaly is found during experiment 1-5 (Figure 42). A sudden increase of the acetophenone effluent concentration (C_{AF}) is observed after 300 min, while the total concentration (C_{AF} + C_{PEA}) remains constant. A sudden change in parameters is excluded and a reduction of the catalyst activity is expected to give a gradual decrease and therefore not found plausible either. A competition effect of the increased hydrogen pressure from 15 to 30 bar on the desorption kinetics should be visible in experiment 1-4 too, but here conversion is comparable to experiments 1-1 and 1-2. Extensive flushing of the catalyst with an EtOH/H_2 mixture prior to experiment 1-7 does not lead to the same high conversion as seen in 1-5a, showing that the initial high conversion in experiment 1-5 is not caused by a saturation of the catalyst by hydrogen.

Alternatively, the higher conversion to PEA in 1-5a can be attributed to an adsorbed amount of AF on the catalyst, residual from experiment 1-4. Since the sum of the effluent concentrations remains quasi constant, this means that every adsorption site is immediately occupied by an acetophenone molecule. If this were to be the case, an additional 35.3 µmol of PEA is eluted from the CSRN Cartridge during the first 300 minutes. As the cartridge weight is 0.045 grams (ca. 0.7 mmol of supported Ni), the additional desorbed PEA is 5 mol% vs. the catalyst, hence not contradicting the hypothesis of desorption of residual PEA from a previous experiment. The long time to reach steady-state (t_{SS}) might indicate an important temperature dependence of the adsorption/desorption equilibria. Although this is not experimentally verified, this observation is important because this means that during the probing of conversion dependence on temperature (as e.g. performed in experiment 1-8) every temperature should be held longer than 300 min.

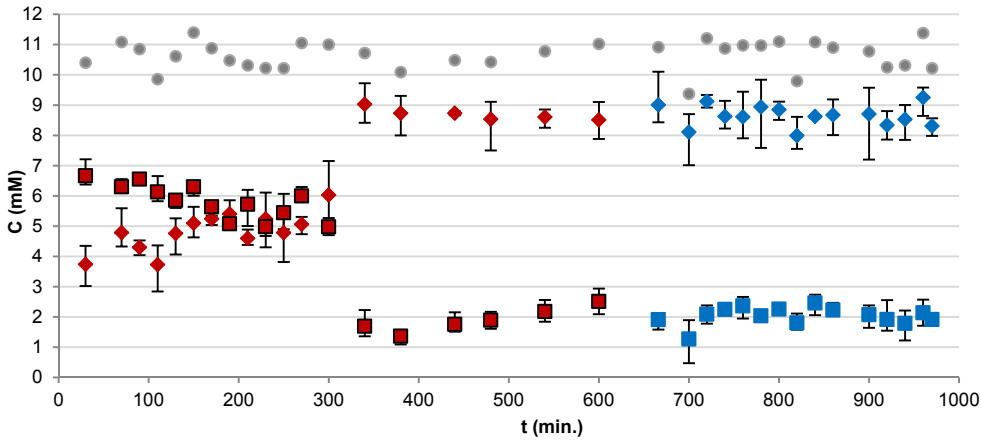

Figure 42: Effluent concentrations during experiment 1-5 (red) and 1-6 (blue) of AF (◆), PEA (■) and the sum of both (●) with conditions as given in Table 26.

In experiment 1-8 (Figure 43), the total effluent concentration significantly changes with varying temperature. Note that the raise in total concentration at 380 min is caused by switching of reagent solutions, while at 690 min, this is not the case. Although the increment of C_{tot} after 690 min seems to be an analysis error, the effluent concentration exceeds the influent concentration over prolonged time. Once again, this significant change in effluent concentration occurs after 300 min The latter might indicate a higher desorption/adsorption ratio for higher temperatures, i.e. increasing temperature induces desorption of products adsorbed at lower temperatures. No side products are observed in the UV spectrum (200-400 nm) of the samples.

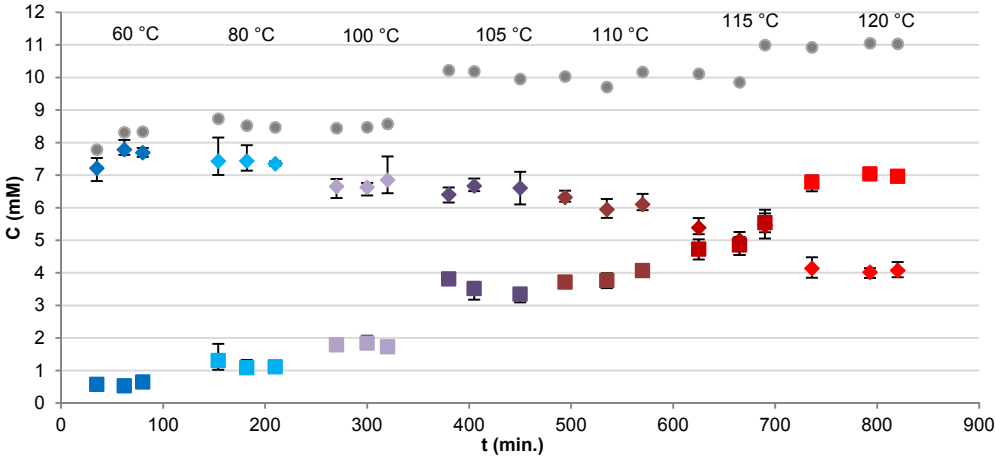

Figure 43: Effluent concentrations of AF (◆), PEA (■) and the sum of both (●) in function of temperature during experiment 1-8 with conditions as given in Table 26 and T_{C2} as given in the graph (T_{C1} = T_{C2} + 15 °C).

1.3. Hydrogenation with commercial RaNi

The activity of the copper supported catalyst (CSRN) is compared to the commercial Raney Nickel CatCart purchased from ThalesNano (batch n°: 02619) (TNRN). The information gathered could also be applied for reduction of other compounds. The influence of different parameters on the reduction of several acetophenone solutions was analysed. For best comparison, the system was evaluated with ethanol solutions (in experiments 2-1 and 2-2). Unfortunately, the pressure drop (dp_{sys}) increased over time, obliging to use less adsorbing solvents such as hexanes during the temperature dependence experiment. The use of hexanes implies analysis of the samples by means of GC-FID; the calibration curves are given in the experimental section, Figure 52. Moreover, cartridge 1 (C1, Figure 39) is by-passed by connecting the bubble detector (B) to cartridge 2 (C2).

From these analyses, it is immediately observed that the conversion is remarkably higher on the TNRN than on the CSRN cartridge, giving more than one compound (see Scheme 59).

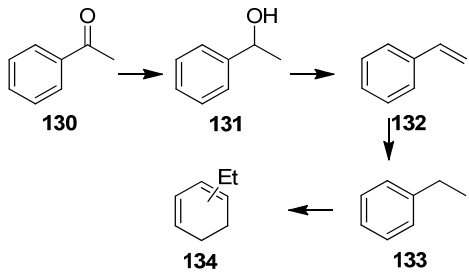

Scheme 59: Reduction and elimination of acetophenone (AF, 130) towards 1-phenylethanol (PEA, 131) and ethylbenzene (EB, 133) with H_2 in a continuous flow setup with TNRN Raney Nickel catalyst.

1.3.1) Reactant concentration and pump speed dependence

The hydrogen concentration in the liquid phase, related to the partial pressure of H_2 (p_{gas}) is altered via the system pressure (p_{sys}) parameter. There is no influence of the partial pressure of hydrogen on the conversion for different pump speeds (the plot of the experiments is given in the experimental part, Figure 56).

In a subsequent experiment, different influent concentrations of acetophenone beneath the desired concentration of 120mM are evaluated, (20 mM (blue) and 60 mM (red) in Figure 44). At these conditions, all starting material (AF, **130**) is consumed. At 80 °C, a small amount of 1-phenylethanol (PEA, **131**) is collected, while most is converted to the alkane, ethylbenzene (EB, **133**). At 100 °C, PEA is completely hydrogenated to form EB and starting from 100 °C,

the EB concentration decreases by reduction of the aromatic ring, rendering the end product undetectable by UV (**134**). Remarkably, for the first experiments (80 and 100 °C at 0.5 mL min^{-1}), the same conversion percentages are observed for both 20 and 60 mM solutions (e.g. 75% EB formed at 100 °C and 0.5 mL min^{-1}), indicating an incomplete occupancy of the catalyst surface. For higher temperatures or pump speeds, the ratios are no longer constant, as for a 60 mM AF solution reacted at 80 °C and 1.5 mL min^{-1}, the EB/PEA ratio is smaller than for a 20 mM AF solution. This indicates a competition for adsorption sites between PEA, and freshly delivered AF. For the 20 mM solution the competition is smaller, allowing more PEA to be absorbed and hence more EB to be formed. The collected results for AF to PEA convertion, indicate that 120 mM concentrations can be applied at this pump speed and at about the same temperatures.

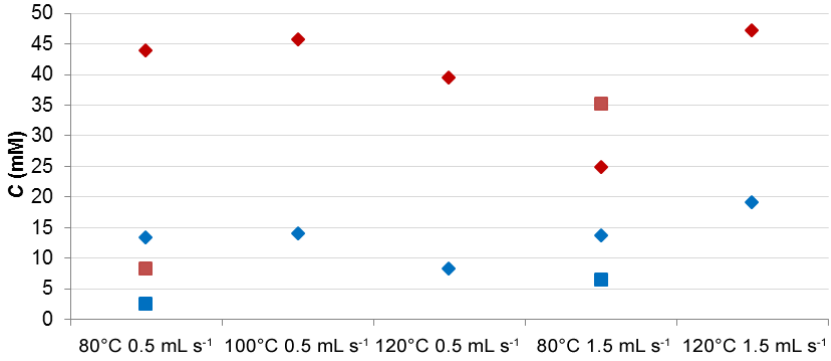

Figure 44: Effluent concentration of PEA (■) and EB (◆) during experiment 2-2 after reduction of acetophenone solutions of 20 mM (blue) and 60 mM (red) in EtOH at different parameters on a commercial RaNi (TNRN) cartridge.

This plot also indicates that, although a 20 mM solution pumped at 1.5 mL min^{-1} and a 60 mM solution at 0.5 mL min^{-1} have the same reagent throughput per time unit, the effluent composition is completely different, *i.e.* conversions at high pump speeds are lower, due to smaller catalyst contact time (t_{res}).

1.3.2) Temperature dependence

In Figure 45 the effluent concentrations of AF, PEA and EB are demonstrated for a reagent solution of 120 mM AF in hexanes. Between 20 and 70 °C, C_{AF} decreases equally with the C_{PEA} increase, they follow a quasi linear regime. Beyond 70 °C, ethylbenzene (EB) is formed at the expense of the formed PEA. The formation of ethylbenzene is found to be complete at 110 °C.

The temperature dependence on the reaction rate and thus on the effluent concentration is related to the ab/adsorption equilibria and reaction constants, which are dependent on the temperature. This complex behaviour is accounted for in the basic Langmuir-Hinshelwood equation (equation 12), which is valid for bimolecular batch reactions on the surface of heterogeneous catalysts.[197]

$$\frac{dC_{PEA}}{dt} = \frac{kK_{H_2}C_{H_2}K_{AF}C_{AF}}{\left(1 + K_{H_2}C_{H_2} + K_{AF}C_{AF}\right)^2} \qquad \text{(Equation 12)}$$

Here k, K_{H_2} and K_{AF} are temperature dependent. In the continuous flow system however, the conversion-temperature relation is more complex, since during steady-state, the equilibrium concentrations are variable in function of the position in the catalyst cartridge and they are also dependent on the flow-rate, which supplies fresh reactants and drains formed products (see Figure 46).

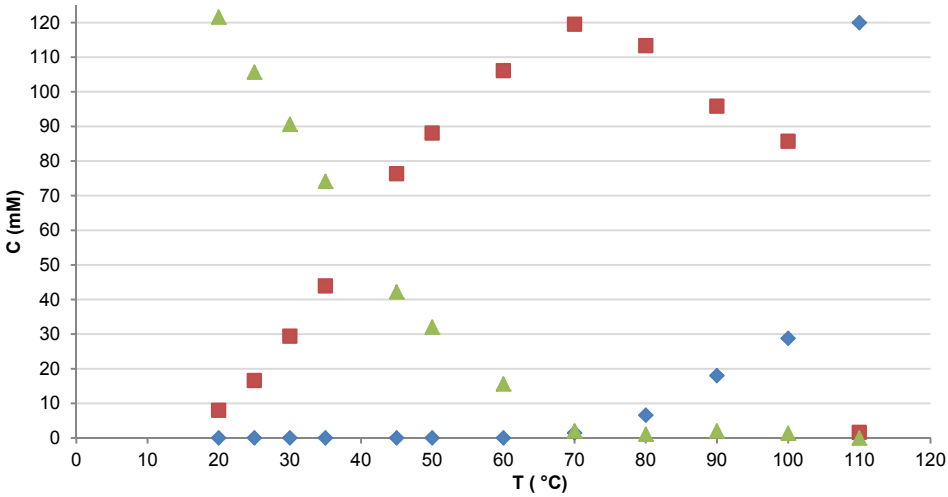

Figure 45: Concentration of AF (▲), PEA (■) and EB (♦) in the effluent of the X-Cube™ flow reactor with the TNRN catalyst. Parameters are p_{sys} = 5 bar, v_1 = 1.5 mL min^{-1} and C_{in} = 120 mM AF in hexanes.

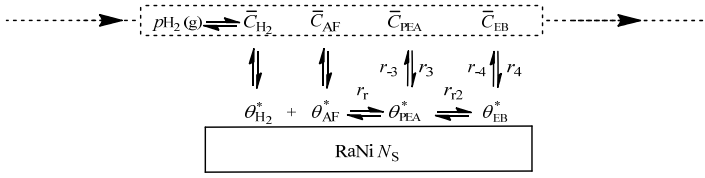

Figure 46: Schematic presentation of the plug flow reactor with mean concentrations ($\bar{C}_X$) and overall rates (r_X), amount of total adsorption sites (N_S) and fraction of sites occupied by compound x (θ^*_X).

While the temperature dependent conversion of AF to PEA is linear, an exponential function can be fitted to the conversion of PEA to EB. The conversion to EB only initiates when AF is no longer present, if AF is more readily absorbed than PEA, then here too, formed PEA is immediately desorbed by AF, competing for adsorption sites (analogous to experiment 1-5). Moreover, the exponential character of the conversion of PEA to EB indicates a negligible contribution of the adsorption/desorption to the kinetics beyond 70 °C. Presumably, the PEA which is still absorbed after the reduction of AF, is used directly in the subsequent reduction, without desorption ($r_{r2} > r_{-3}$; Figure 46). Moreover, styrene (**132**) is never detected by GC-FID in any of the effluent analysis, therefore, if styrene is formed in the reaction, then a very fast alkene reduction is imperative. Although this is not improbable at temperatures > 70 °C, this would mean that all styrene ever present in the liquid phase is hydrogenated. Alternatively, if the formation of ethylbenzene proceeds via a cleavage of the C-O σ-bond, a stabilised ethylbenzyl radical is formed, which reacts on the catalyst surface with an adsorbed hydrogen atom to form ethylbenzene, circumventing the formation of styrene via an elimination reaction in a neutral environment.

1.3.3) Catalyst activity

In the acetophenone hydrogenation, the TNRN is far more active than the CSRN catalyst. At 70 °C, the small CSRN converts approximately 10% of a 10 mM AF in ethanol solution at 0.5 mL min^{-1}, while the TNRN converts 100% of a 120 mM hexane solution at this temperature at 1.5 mL min^{-1}. Unfortunately, the exact weight of the packed catalyst in the latter cartridge is not known.

1.4. Hydrogenation of ethyl pyruvate

As mentioned in the chapter on chiral ionic liquid synthesis, continuous flow hydrogenation of ethyl pyruvate (Etpyr) is applied to obtain the racemic ethyl lactate. In order to achieve the highest possible conversion, the results obtained earlier on the acetophenone conversion are considered. Table 28 shows the necessary parameters for complete acetophenone and ethyl pyruvate conversion, the hereby obtained theoretical maximum production rate (g h^{-1}) and an indication of solvent usage (mL h^{-1}) (see Figure 45 and Figure 47).

Table 28: Ideal parameters with total pumped solution (hexanes, 120 mM) and maximum theoretical production rate (g h^{-1}) for complete conversion with the TNRN cartridge.

	Mm (g/mol)	C_{in} (mM)	v (mL min^{-1})	T (°C)	mL h^{-1}	g h^{-1}
AF	120.15	120	1.5	70	90	1.29
Etpyr	116.12	120	0.5	120	30	0.42

The temperature dependence of the hydrogenation of ethyl pyruvate (120 mM in hexanes) is evaluated in experiment 3-1, analogously to the acetophenone conversion. The resulting GC-FID plot, given in Figure 47, for a pump speed of 0.5 mL min^{-1} indicates that for the ethyl pyruvate hydrogenation lower pump speeds and higher temperatures were required than for acetophenone hydrogenation. At temperatures higher than 110 °C, the total effluent concentration decreases, degradation products might here too be formed (cfr. ethylbenzene formation).

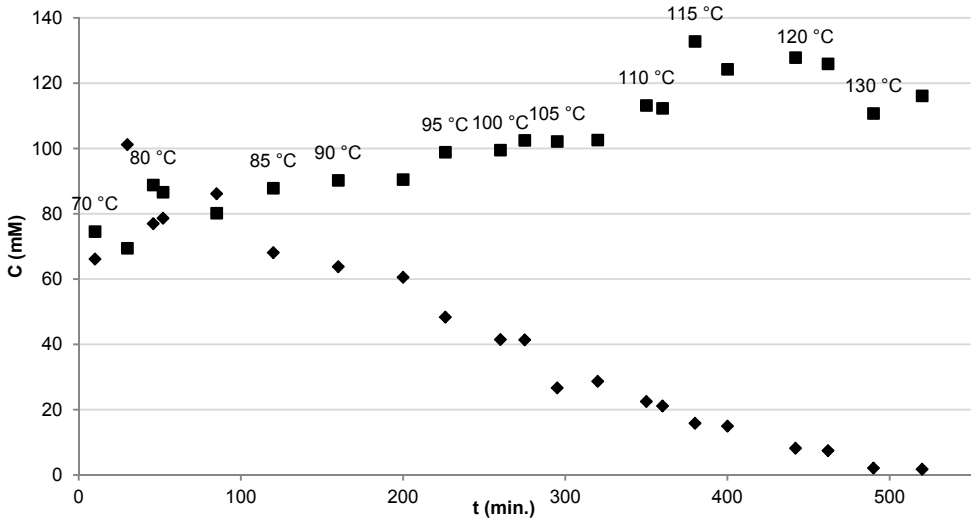

Figure 47: Effluent concentrations of ethyl pyruvate (◆) and ethyl (*rac*)-lactate (■) in function of time and temperature during experiment 3-1 with v_1 = 0.5 mL min^{-1}, C_{in} = 120 mM and T_{c2} (°C) as given in the graph.

In a subsequent production experiment 3-2 (with C_{in} = 120 mM), a temperature of 120 °C was applied, see Scheme 60. The applied conditions are chosen as a compromise between high ethyl (*rac*)-lactate production and low residual ethyl pyruvate. The mean ethyl (*rac*)-lactate and ethyl pyruvate concentrations over experiment 3-2 are 104.9 and 10.5 mM, respectively, i.e. a conversion of 87%.

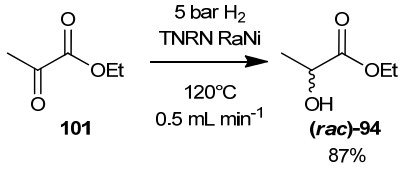

Scheme 60: Hydrogenation of ethyl pyruvate to ethyl (*rac*)-lactate over the TNRN cartridge mounted on the X-Cube™ continuous flow system.

1.5. Deprotection of bicyclic amines

Bicyclic amino compound **135** was synthesised for research towards epibatidine analogues (potent analgesics) by a student researcher at the department of Sustainable Organic Chemistry and Technology of Ghent University. This compound **135** was subjected to hydrogenation, to achieve cleavage of the benzyl moiety towards the free amine **136** (Scheme 61). Given the low conversion in the batch hydrogenation reactions, continuous flow was proposed in order to achieve higher hydrogen pressures and reaction temperatures. This also allowed to investigate the chemoselectivity of the catalyst. As the product solutions were very diluted (4.0 to 5.0 mM in ethanol), the smaller copper gauze supported RaNi (CSRN cartridge) was initially used for the first evaluations.

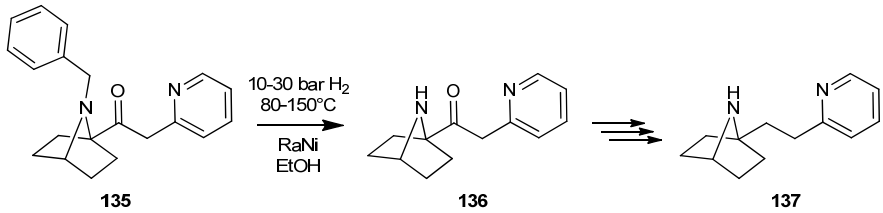

Scheme 61: Envisioned deprotection of picoline-substituted bicyclic amine 135 towards the ketone 136.

1.5.1) Copper gauze supported Raney Nickel

In these first experiments using the CSRN cartridge, the influence of pump speed and temperature was investigated under a p_{sys} of 30 bar (Table 29 and Figure 48). Pump speeds were from 0.2 (mixed with 0.3 mL min^{-1} solvent to achieve the minimum pump speed of 0.5 mL min^{-1}) to 0.7 mL min^{-1}. Temperatures were in the range of 80 to 170 °C

Table 29: Conditions of different X-Cube™ experiments with the CSRN cartridge with p_{sys} = 30 bar and C_{in} = 4-5 mM in EtOH.

Exp.	v_1 (mL min^{-1})[a]	T_1 (°C)
4-1	0.5	80
4-2	0.2	80
4-3	0.2	100
4-4	0.5	120
4-5	0.5	150

[a] **Where v_1 < 0.5 mL min^{-1}: v_1 + v_2 = 0.5 mL min^{-1}.**

Analysis of the LC-MS spectra of samples, taken at times beyond the calculated steady-state time ($t > t_{ss}$), showed the formation of different products, with different molecular masses, eluting at different retention times. Figure 48 shows the response of the mass spectrometer for the different reaction products (represented in the plot by their molecular ion, $[M+H]^+$), for the different conditions given in Table 29.

Experiment 4-1 indicated a low conversion at 80 °C, (demonstrated by the high peak of starting ketone, $[M+H]^+$: 307) and formation of two products, the alcohol **138** ($[M+H]^+$: 309) and an unknown product ($[M+H]^+$: 311), which was later identified as compound **145** (see Scheme 63). In experiments 4-2 and 4-3, the increased residence time allowed a higher conversion and the formation of another product ($[M+H]^+$: 219). The new product could be identified as the debenzylated alcohol **139** (Scheme 62). From 120 °C onwards, an additional product was formed ($[M+H]^+$: 203). It was believed that elimination of the latter alcohol occurred, with formation of the alkane **140**, (analogous to the PEA to EB convertion in Scheme 59 and Figure 45). The formation would have been fruitful, as the debenzylated alkane (**137**) is the actual end-product of the reaction sequence of which the envisioned deprotection step is only a part, as depicted in Scheme 61. Finally, at 150 °C, all starting material was consumed.

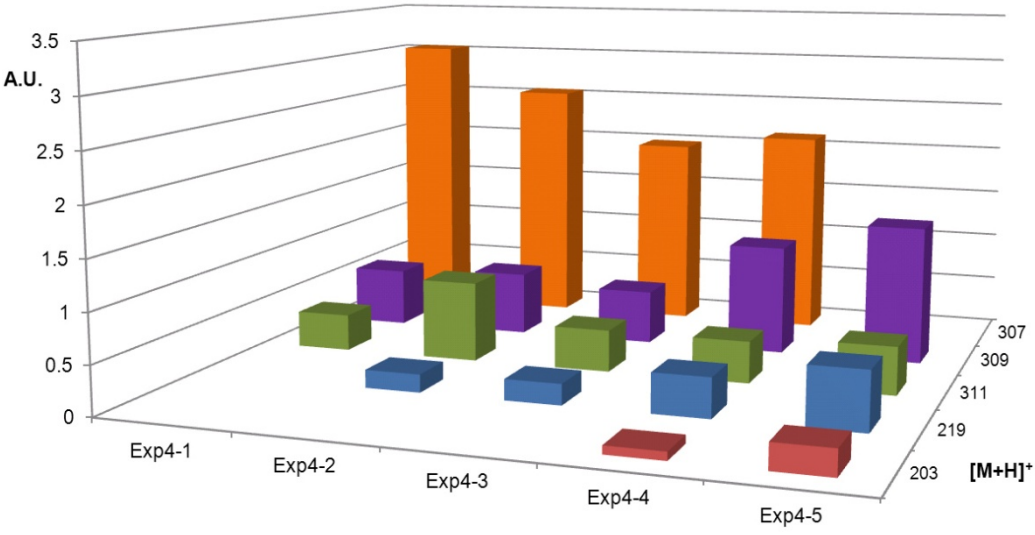

Figure 48: Profile (via LC-MS) of effluent composition of X-Cube™ experiments 4-1 to 4-5 with the CSRN cartridge in a sample (t > 50 min). The conditions of the experiments are given Table 29. The composition of the products with different mass units is represented by the response of the mass spectrometer in arbitrary units (A.U.) calibrated by the influent concentration of the starting material.

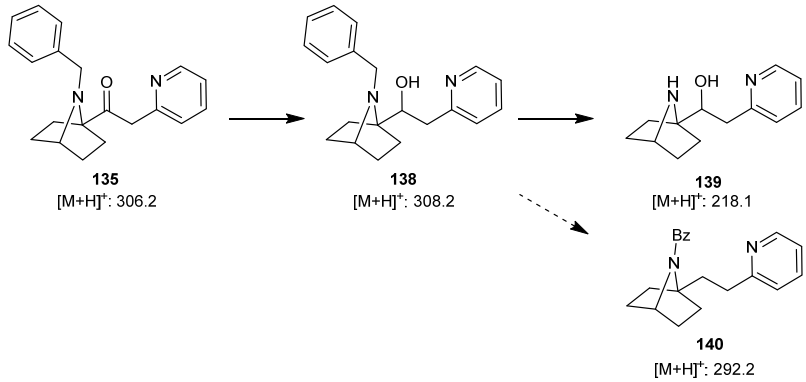

135
$[M+H]^+$: 306.2

138
$[M+H]^+$: 308.2

139
$[M+H]^+$: 218.1

140
$[M+H]^+$: 292.2

Scheme 62: Reduction over Cu gauze supported RaNi (CSRN) of the ketone 135 with formation of the alcohol 138 and debenzylated alcohol 139 and initially proposed dehydrogenation and reduction towards the desired alkane 140 during hydrogenation (with dashed arrow as this reaction was later excluded).

Throughout all the experiments with the CSRN cartridge, mixtures were obtained. Upon increasing the temperature, the amounts of the products with $[M+H]^+$ 203, 219 and 309 increased gradually, while the concentration of the unknown compound ($[M+H]^+$: 311) remained quasi constant (see Figure 48).

In general it was found that the CSRN catalyst was not sufficiently selective for the debenzylation of the ketone **135** towards the product **136** (Scheme 61), but reduces the ketone prior to the debenzylation (Scheme 62). In the following trials, on the one hand, a Pd/C cartridge was evaluated in order to increase the selectivity towards the debenzylation (Scheme 61), and on the other hand the commercial Raney Nickel (TNRN) cartridge to achieve full conversion of all the intermediates towards the desired alkane end-product **137**. However, concurrent batch experiments (performed by the collaborating researcher) revealed the actual structure of the compounds. These were found not to comprise the proposed alkane **140** but the bicycle octane **144**, formed by ring opening and subsequent closure (Scheme 63, pathway A). Upon ring-opening, a ketone is formed, which can be reduced to the unreactive alcohol **145** via pathway B, which was earlier reffered to as the unknown compound with mass 311.

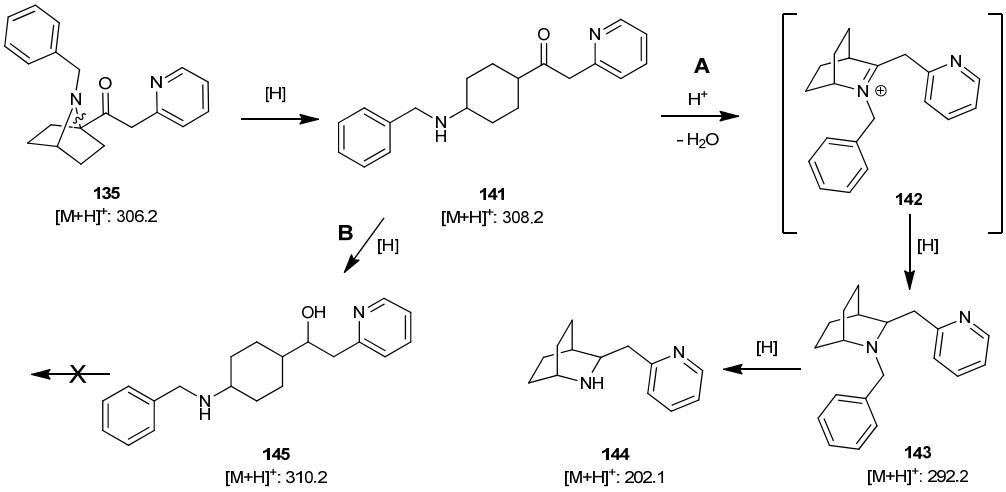

Scheme 63: Formation of 2-azabicyclo[2.2.2]-octane 144 via ring-opening of the 2-azabicyclo[2.2.1]-heptane during hydrogenation over the copper supported RaNi, with the formation of the side-product 145.

1.5.2) Commercial cartridges

Since many product intermediates were formed with the small Mapil copper gauze suported RaNi (CSRN), but no complete conversion was obtained, the more active commercial catalysts were evaluated at high temperatures. Upon application of the ThalesNano Raney Nickel (TNRN) cartridge, also a mixture of compounds was formed, of which the main part was the protected alcohol **138** ([M+H]$^+$: 309).

Table 30: Conditions of different X-Cube™ experiments, using commercial catalysts, C_{in}: 4-5 mM in EtOH.

Exp.	CatCart®, p_{sys}	v (mL min^{-1})	T (°C)	AcOH (eq.)
4-6	TNRN, 30 bar	0.5	50	0
4-7		0.5	50	5
4-8	10% Pd/C, 10 bar"	1.0	20	5.71
4-9		1.0	50	6.31

The conditions applied during the different experiments with the commercial catalysts are given in Table 30. In comparison to the CSRN experiments, mild conditions (i.e. 50 °C, 0.5 mL min^{-1}) already led to significant conversion. As represented in Figure 49, the TNRN cartridge did not allow complete conversion of product **135** ([M+H]$^+$: 307) towards **138**, nor was the starting material completely consumed. The end product **144** ([M+H]$^+$: 203) was only observed

in minute amounts, while also the side product **145** ([M+H]$^+$: 311) was formed. Upon addition of 5 equivalents of acetic acid (experiment 4-7), the reaction was accelerated, i.e. more starting material was consumed, more end product **144** was formed but the profile of the intermediates remained the same.

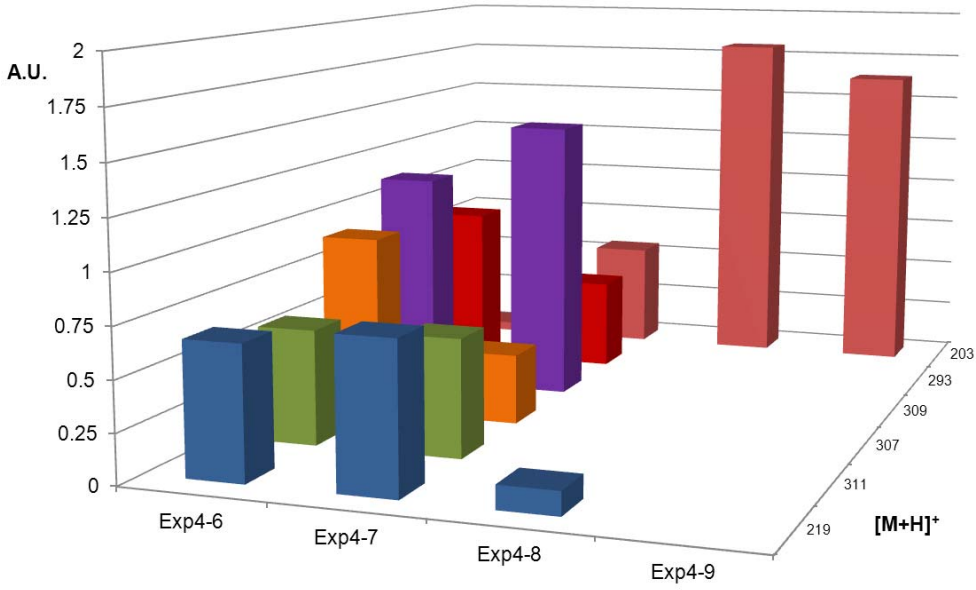

Figure 49: Profile of effluent composition of X-Cube™ experiments 4-6 to 4-9 in a sample (*t* > 50 min). The conditions of the experiments are given Table 30. The composition of the products with different mass units is represented by the response of the mass spectrometer in arbitrary units (A.U.) calibrated by the influent concentration of the starting material.

As still not all starting material was converted and the side product **145** was still formed, using the TNRN cartridge, the 10% Pd/C CatCart® (batch n°: 03729) was mounted in the X-Cube™ system for evaluation. The Pd/C catalyst was expected to selectively deprotect the amine. If this was to be the case, a system set-up would have been considered in which the Pd/C is mounted before the TNRN cartridge, in order to allow a debenzylation of amine **135**, followed by a Raney Nickel catalysed reduction of the deprotected ketone **136**.

Hydrogenation over the Pd/C catalyst, at 1.0 mL min^{-1} and with addition of acetic acid led to the very efficient (at 1.0 mL min^{-1}) formation of compounds **139** (minor) and **144** (major), via different pathways, while the third pathway towards the inert alcohol **145** is no longer present. At low temperatures (experiment 4-8), both pathways occur, while increasing the temperature converts the starting material completely and selectively to the rearranged 2-azabicyclo[2.2.2]octane compound **144**.

In experiment 4-9, only after 30 min a steady-state effluent concentration LC-MS profile was obtained. Assumed was first that the catalyst needed some time to reach the set temperature (50 °C) in its core, therefore the catalyst was preheated before pumping the product solution through the 10% Pd/C CatCart in exp. 4-10. Here too, a steady state time is needed (at 80 min, still a small amount of starting material **135** could be seen, see Figure 50). Interesting to note is that the profile of the effluent at 4 min has a 10-fold lower MS-detection response for the starting material than the influent solution (not plotted). As here products are not yet eluted, this indicates that substantial amounts of the reagents and products are absorbed and retained for a significant amount of time on the catalyst surface. Hence, it is rather this adsorption phenomenon which contributes to the steady-state formation than the internal heating of the catalyst.

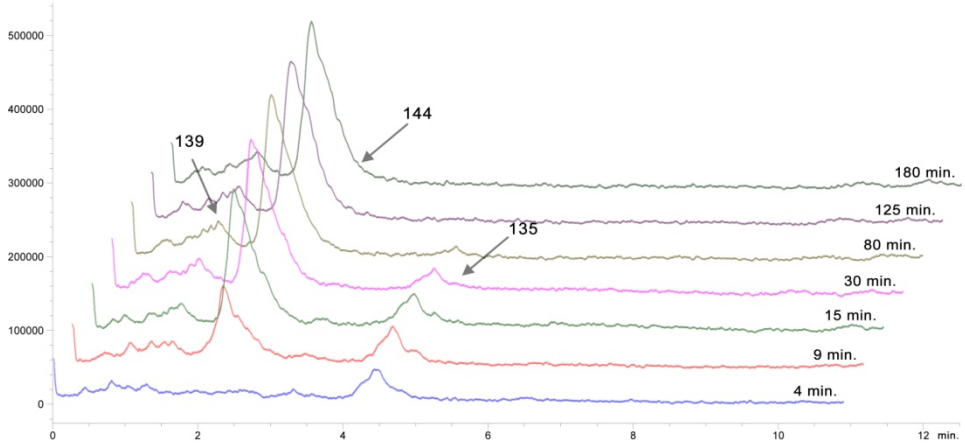

Figure 50: MS absorbance vs. LC retention time for undiluted effluent samples of experiment 4-10 taken after 4 to 180 min. T_{C2}: 50 °C, p_{sys}: 10 bar, v_1: 1.0 mL min^{-1} and C_{in}: 4.47 mM with 6.31 eq. AcOH (EtOH). The figure contains arrows with the compound numbers indicating the peaks.

1.6. Conclusions

The reactor kinetics are complex as they are dependent on internal adsorption/desorption equilibria, and on the reaction rates and pump speeds. A significant contribution of the adsorption equilibria is observed when performing subsequent experiments at different temperatures. Therefore, additional long term production vs. temperature experiments are needed, especially for the TNRN. To better discriminate between adsorption and reaction rates, the activity (production rate) of the catalysts might be evaluated for an array of influent concentrations, thus adsorption site competition might become apparent. The conversion is not related to the gas pressure, hence the hydrogen gas is not the limiting reagent. At low ketone (acetophenone) vs. catalyst loading, alkanes are formed as side products, while the alkene is never observed. Increment of ketone concentration leads to less side product formation, by increased competition of absorption sites. In general, long-term experiments are needed to probe late steady-state formation.

Apart from an autonomous continuous meso-scale reactor, the continuous flow system is a versatile tool for relatively fast analysis of reaction parameters, such as conversion vs. temperature profiles, conversion vs. time and production rate of a catalyst. For example, the large amount of reaction parameters evaluated during the debenzylation of the bicyclic amine led to a substantial amount of data and combined with the batch experiments, they gave an insight in the different pathways involved. However, conditions need to be fine-tuned in order to optimise production and hinder product degradation (e.g. elimination of PEA to EB).

2. List of compounds

a) Peralkylated imidazolium Ionic Liquids

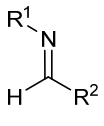

39a-k

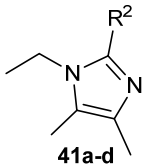

41a-d

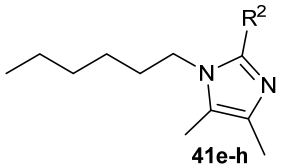

41e-h

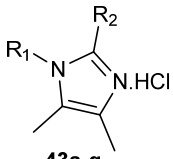

43a-g

more information in Table 4, p38

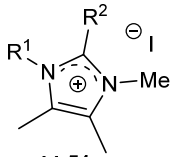

44-51a

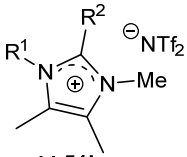

44-51b

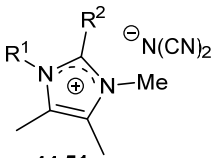

44-51c

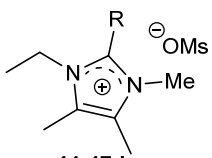

44-47d

more information in Table 5, p42

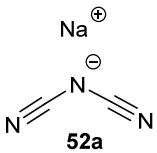

52a

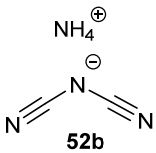

52b

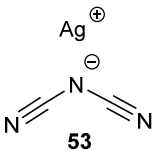

53

b) Alkoxy and alkenylimidazolium Ionic Liquids

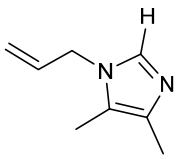

41i

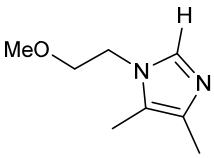

41j

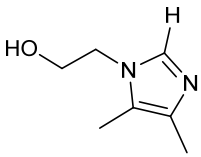

41k

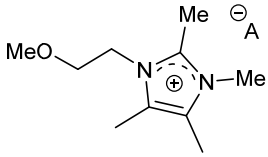

122a: A = I
122b: A = NTf_2

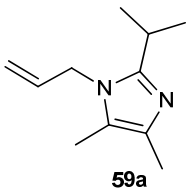

59a

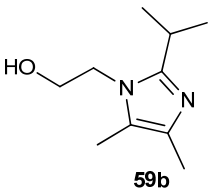

59b

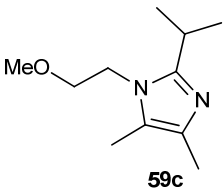

59c

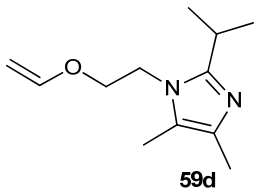

59d

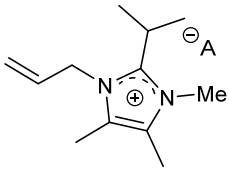

61a-d

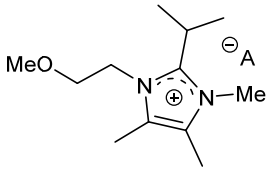

62a-d

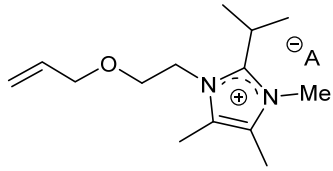

63a-d

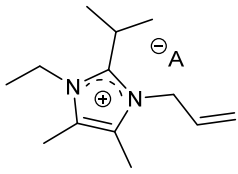

64a-d

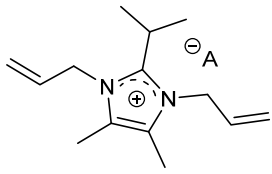

65a-d

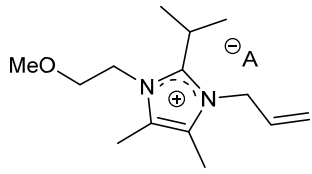

66a-d

more information in Table 11, p53

c) Chiral Ionic Liquids

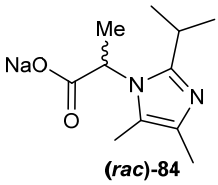

(*rac*)-84

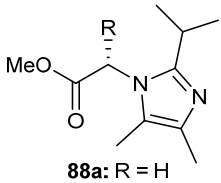

88a: R = H
88b: R = CH_3

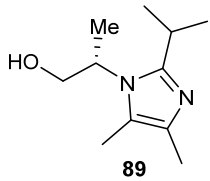

89

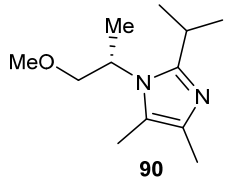

90

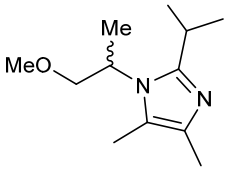

(*rac*)-90

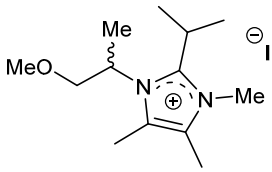

(*rac*)-92a

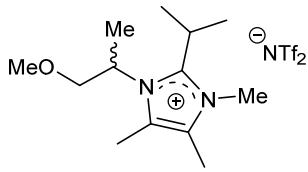

(*rac*)-92b

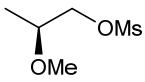

96

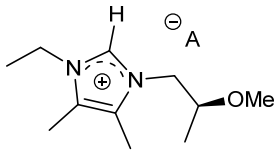

97a: A^- = OMs^-
97b: A^- = NTf_2^-

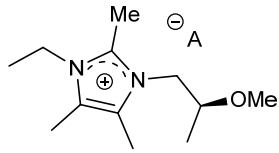

98a: A^- = OMs^-
98b: A^- = NTf_2^-

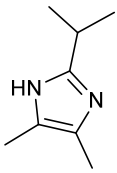

60

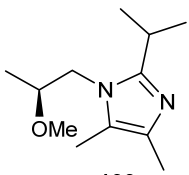

100

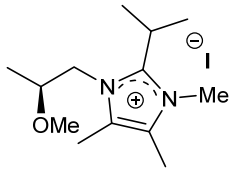

99b

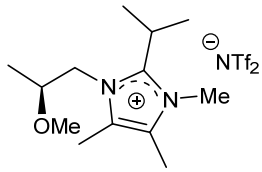

99c

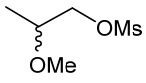

(*rac*)-96

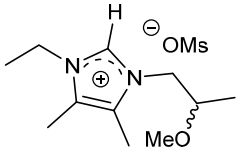

(*rac*)-97a

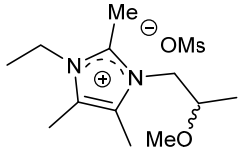

(*rac*)-98a

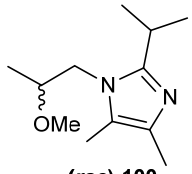

(*rac*)-100

d) Alternative Ionic Liquid preparation

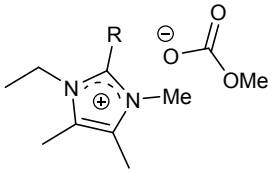

45e: R = Me
47e: R = iPr

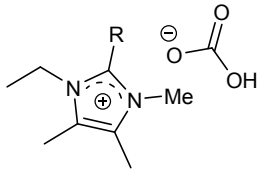

45f: R = Me
47f: R = iPr

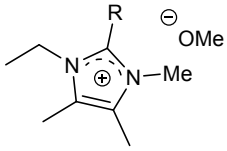

45g: R = Me
47g: R = iPr

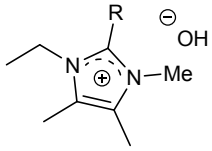

45h: R = Me
47h: R = iPr

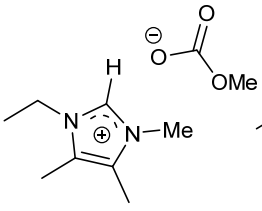

44e

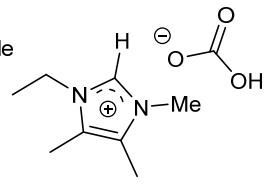

44h

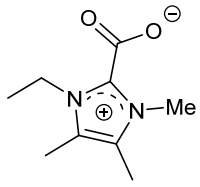

114

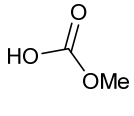

118

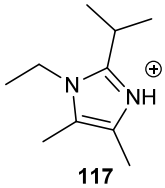

117

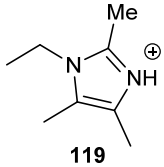

119

VI) EXPERIMENTAL SECTION

1. Used reagents

Allyl bromide (≥97%), allyl alcohol (≥98.5%), methyl methanesulfonate (≥99%), methanesulfonylchloride (≥98%), allylamine (≥98%), 2-aminoethanol (≥98%), 2-methoxyethanamine (≥98%), Δ-Trisphat tetrabutylammonium salt (≥98.5), ammonium chloride (≥99%), (*R*)-(−)-1-(9-Anthryl)-2,2,2-trifluoroethanol, (≥98%), ethyl L-lactate (≥98%), ethyl pyruvate (≥97%), dimethyl sulfate (≥99%), thionyl chloride (≥99%), D/L-alanine (≥99%), L-alanine methyl ester hydrochloride (≥99%), L-glycine methyl ester hydrochloride (≥99%), L-serine methyl ester hydrochloride (≥98%), sulfuric acid (95.0-98.0%), hydrochloric acid (37%), ethylamine (≥99.5%), n-hexylamine (≥99%), 2,3-butanedione (≥97%), propionaldehyde (≥97%), isobutyraldehyde (≥98%), ammonium acetate (≥98%), silver nitrate (≥99.0%), sodium dicyanamide (96%), lithium bis(trifluoromethylsulfonyl)imide (≥99.0%), KOH (90%), NaOH (≥97%), CD_3OD (99.96 atom% D), D_2O (99.99 atom% D), *n*BuLi (2.3 M in hexanes), iodomethane (≥99.0%), bromobenzene (99%), benzaldehyde (≥99%), diphenylmethanol (≥99%), bromoethane (≥98%), acetophenone (≥99%), Amberlite™ IR120, magnesium, tetrahydrofuran, methanol, ethanol, n-pentanol, acetonitrile, dichloromethane and ethyl acetate were purchased from Sigma-Aldrich, paraformaldehyde and acetaldehyde from ACROS Organics, acetone from Fisher Chemicals and acetic acid from Riedel-de Haën. Hydrogen gas (≥99.0%) was purchased from Air Liquide and hydrogen bis(trifluoromethylsulfonyl)imide (98%) from IoLiTec GmbH. Acetone and acetonitrile were dried over 3Å molecular sieves and CH_2Cl_2 was refluxed with CaH and distilled prior to use. Allyl bromide was distilled prior to use. Acetone was dried over 3Å molecular sieves, acetonitrile was dried over anhydrous alumina and stored over 3Å molecular sieves and CH_2Cl_2 was refluxed with CaH_2 and distilled prior to use. THF was refluxed with sodium wire, containing benzophenone ketyl radical as indicator, and distilled before use.

2. Equipment and methodology

Batch pressurised reactions were performed in 15 mL and 150 mL glass pressure vials with PBT cap (Schott) and PTFE seal for reactions up to 20 mmol and 200 mmol respectively. Microwave reactions were performed in a CEM Focused™ Microwave Synthesis System, Model Discover, with adaptable power from 0-300W, equipped with infrared thermosensor and monitored with the Synergy-software v. 1.32. Reagents were held in an 8 mL vial, sealed with snap-on PTFE septum. During the isothermal experiments the maximal power was set to 50W.

The continuous flow reactor used during imidazole synthesis was a Cytos® CPC College System, mixing unit and residence time unit were retained at 120 °C. The internal volume of mixing unit and residence time unit was 48 mL, applied flow rate was 0.5 to 2.0 mL min^{-1}. The continuous flow reactor used during the hydrogenation experiments was a ThalesNano X-Cube™. Experiments were started (0 min) when gas was detected by the system. Cartridges were always insulated by the special cartridge insulation caps, and the connecting SS tubing by means of paper and aluminium foil.

^{1}H NMR, ^{13}C NMR, ^{19}F NMR and HSQC experiments were performed with a JEOL ECP+ 300 spectrometer in $CDCl_3$ with as internal reference TMS, CH_3CN or $CFCl_3$ for ^{19}F NMR experiments. IR spectra were recorded on a Perkin Elmer Spectrum FT-IR apparatus (ZnSe crystal; ATR mode). HPLC-MS spectra were recorded on an Agilent 1100 Series (ES, 4000 V) preceded by a reverse phase LC column (Eclipse plus C18 column). The LC column has dimensions of 50×4.6 mm and has a particle size of 3.5 µm. GC analysis were performed on a Agilent 6890 GC Plus Series, with an EC5 capillary column (30 m×0.25 mm; coating thickness 0.25 µm) (injector temp.: 250 °C; carrier gas: He; flow rate: 1.0 mL min^{-1}, temp. profile: 80-200 °C at 10 °C min^{-1}, 200-280 at 30 °C min^{-1}, 5 min hold at 280 °C; detector: FID). High resolution electron spray atmospheric-pressure chemical ionisation (ES/APCI) mass spectra were obtained with an Agilent Technologies 6210 Series Time-of-Flight. Elemental analysis was performed with a Perkin Elmer Elemental Analyser 2400 Series II, connected to an AD6 Autobalance and controller.

The optical rotations were measured with a Jasco P-2000 Polarimeter, in an optical cell with 3.5 mm ID and length 100 mm at the sodium D line (589 nm). The temperature control was on the cell liquid and samples were recorded between 24.92 and 25.08 °C. Every compound was dissolved in chloroform and concentrations are given (C = 0.3 to 1.0×10^{-2} g mL^{-1}), although the specific optical rotation ($[\alpha]_D^{25}$) is concentration independent. Three times a different sample of the solution was brought in the optical cell and measured three times, the results were analysed with the Jasco Spectra Manager v2. The mean and deviation of the specific rotation between the three different samples were reported (in ° dm^{-1}cm^{3}g^{-1}), while the standard deviation within the three measurements of each sample were always smaller than 0.5 °.

The compounds suitable for single crystal X-ray diffraction were mounted on a nylon loop attached to a copper pin and placed into the cold stream of an Oxford Cryostream 700 at 100(2)K on an Agilent SuperNova diffractometer using Mo Kα radiation (λ = 0.71073 Å). The absorption corrections were applied using CrysAlisPro.[198] All structures were solved using direct methods and refined by the full-matrix least-squares procedure in SHELXL.[199] All hydrogen atoms were placed in calculated positions and refined using a riding model. CCDC 941088-941093 contains the supplementary crystallographic data. These data can be obtained free of charge from The Cambridge Crystallographic Data Centre via www.ccdc.cam.ac.uk/data_request/cif. The program OLEX2 was also used in refinement and making pictures.[200]

Cyclic voltammograms were recorded with a Solartron SI 1287 Electrochemical Interface (scanning rate: 50 mV/s; platinum work and counter electrodes; reference electrode was platinum wire submerged in 1-butyl-3-methylpyrrolidinium bis(trifluoromethylsulfonyl)imide separated from the testing solution by a fritted disk and calibrated with Fc^+/Fc). All CVs were recorded at 90 °C under an argon atmosphere, samples were dried prior to recording. Water contents were measured in Hydranal 34812 (Fluka) with a 719S Titrino coulometric Karl Fischer titrator (Metrohm). DSC measurements were done with a Mettler-Toledo 822 DSC apparatus (heating rate: 10 °C min^{-1}), and all samples were analysed under a dry helium flow. Viscosities were analysed with a Brookfield Viscometer *DV-II* Pro at 23 °C. The thermal stability of the ionic liquids were analysed by thermogravimetric analysis at a heating rate of

10 °C min^{-1} in alumina pans under an argon atmosphere (100 mL min^{-1} flow) using a SDT Q600 V8.3 Build 101 apparatus, the sample weight was between 5 and 15 mg.

ICP analysis was performed on a Thermo Scientific iCAP 6000 Series ICP spectrometer. Calibration was performed with aqueous calibration matrix solutions of 2, 5 and 10 ppm based on the Chem-Lab n.v. Multi Element ICP Standard solution (10E). The elements recorded are Ca (3968, 744.7 nm), Cu (324.6 nm), Fe (259.9 nm), K (766.5 nm), Mg (279.6 nm), Na (589.6 nm), Ni (221.7 nm), S (180.7 nm), Si (212.4 nm) and P (177.5 nm).

3. Procedures and spectra

3.1. Synthesis of tetra- and penta-alkylimidazoles

Procedure for the synthesis of 1-ethyl-2-isopropyl-4,5-dimethylimidazole (41d): A glass 150 mL pressure vial was filled with MeOH (50 mL) and a PTFE stirring bar. The solvent was allowed to cool to 0 °C and isobutyraldehyde (100 mmol, 7.21 g) and ethylamine (120 mmol, 5.41 g) were added. The vial was closed and submerged in a preheated oil bath at 120 °C with temperature controller. After heating for 2h with vigorous stirring, the reaction mixture was carefully cooled to 0 °C, the vial was opened and consecutively 2,3-butanedione (100 mmol, 8.61 g) and NH_4OAc (100 mmol, 7.71 g) were added. The vessel was closed immediately and heated in a preheated oil bath at 120 °C for 2 h under vigorous stirring. After cooling, MeOH and the reaction water were removed *in vacuo*. The reaction mixture was dissolved in CH_2Cl_2 and extracted twice with 100 mL of an aqueous 0.5 M HCl solution. The aqueous phase was alkalinised with 50 mL of 3.0 M NaOH and extracted three times with 40 mL of EtOAc. The resulting organic phase was washed with 100 mL of water and dried over $MgSO_4$. The solvent was removed *in vacuo* and 6.97 g (41%) of a black oil was obtained. The resulting oil was purified by vacuum distillation, yielding a yellow oil, which was further used for the synthesis of ionic liquids.

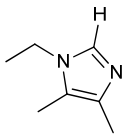

1-Ethyl-4,5-dimethylimidazole (41a): b.p. 52 °C (1.0 mbar); **^{1}H NMR** (300 MHz, $CDCl_3$, 25 °C, TMS): δ = 1.37 (t, ^3J(H,H) = 7.4 Hz, 3H; CH_3CH$_2$), 2.12 (s, 3H; $CH_3C^{4/5}$), 2.15 (s, 3H; $CH_3C^{4/5}$), 3.83 (q, ^3J(H,H) = 7.4 Hz, 2H; CH_2), 7.33 ppm (s, 1H; C^2H); **^{13}C NMR** (75 MHz, $CDCl_3$, 25 °C, TMS): δ = 8.32 ($CH_3C^{4/5}$), 12.75 ($CH_3C^{4/5}$), 16.21 (CH_3CH_2), 39.68 (CH_2), 121.79 ($CH_3C^{4/5}$), 133.79 ($CH_3C^{4/5}$), 134.04 ppm (C^2CH); **IR** (ATR): ν = 1351, 1383, 1415, 2920, 2971 cm^{-1}; **MS** (ES): *m/z* (%): 125.3 (100) [M+H$^+$]; yield: 40%, yellow oil.

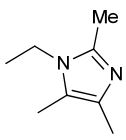

1-Ethyl-4,5-dimethylimidazole (41b): b.p. 58 °C (1.0 mbar); **^{1}H NMR** (300 MHz, $CDCl_3$, 25 °C, TMS): δ = 1.24 (t, ^3J(H,H) = 7.2 Hz, 3H; CH_3CH$_2$), 2.10 (s, 3H; $CH_3C^{4/5}$), 2.15 (s, 3H; $CH_3C^{4/5}$), 2.34 (s, 3H; C^2CH_3), 3.77 ppm (q, ^3J(H,H) = 7.2 Hz, 2H; CH_2); **^{13}C NMR** (75 MHz, $CDCl_3$, 25 °C, TMS): δ = 8.79 ($CH_3C^{4/5}$), 12.49 (CH_3), 13.18 (C^2CH_3), 15.71 (CH_3CH_2), 38.38 (CH_2), 121.15 ($CH_3C^{4/5}$), 131.26 ($CH_3C^{4/5}$), 141.72 ppm (C^2CH); **IR** (ATR): ν = 1311, 1375, 1350, 1413, 2919, 2974 cm^{-1}; **MS** (ES): *m/z* (%): 139.3 (100) [M+H$^+$]; yield: 39%, yellow oil.

1,2-Diethyl-4,5-dimethylimidazole (41c): b.p. 51 °C (1.0 mbar); **^{1}H NMR** (300 MHz, $CDCl_3$, 25 °C, TMS): δ = 1.25 (t, ^3J(H,H) = 7.2 Hz, 3H; CH_3CH$_2$), 1.32 (t, 3H, ^3J(H,H) = 7.7 Hz; $C^2CH_2CH_3$), 2.11 (s, 3H; $CH_3C^{4/5}$), 2.13 (s, 3H; $CH_3C^{4/5}$), 2.65 (q, 2H, ^3J(H,H) = 7.7 Hz;

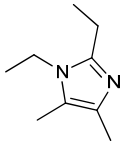

C^2CH_2), 3.78 ppm (q, ^3J(H,H) = 7.4 Hz, 2H; NCH_2); **^{13}C NMR** (75 MHz, $CDCl_3$, 25 °C, TMS): δ = 8.70 ($CH_3C^{4/5}$), 12.46 ($CH_3C^{4/5}$), 12.70 (CH_3CH_2C), 16.02 (NCH_2CH_3), 20.32 (C^2CH_2), 38.08 (NCH_2), 121.06 ($CH_3C^{4/5}$), 131.29 ($CH_3C^{4/5}$), 146.68 ppm (C^2CH_2); **IR** (ATR): ν = 1068, 1311, 1353, 1376, 1429, 2972 cm^{-1}; **MS** (ES): *m/z* (%): 153.3 (100) [M+H$^+$]; yield: 37%, clear liquid.

1-Ethyl-2-isopropyl-4,5-dimethylimidazole (41d): b.p. 60 °C (1.0 mbar); **^{1}H NMR** (300 MHz,

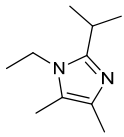

$CDCl_3$, 25 °C, TMS): δ = 1.26 (t, ^3J(H,H) = 7.2 Hz, 3H; CH_3CH_2), 1.32 (d, ^3J(H,H) = 6.6 Hz, 6H; $CH(CH_3)_2$), 2.10 (s, 3H; $CH_3C^{4/5}$), 2.14 (s, 3H; $CH_3C^{4/5}$), 2.94 (m, ^3J(H,H) = 6.6 Hz, 1H; CH), 3.80 ppm (q, ^3J(H,H) = 7.2 Hz, 2H; CH_2); **^{13}C NMR** (75 MHz, $CDCl_3$, 25 °C, TMS): δ = 8.76 ($CH_3C^{4/5}$), 12.66 ($CH_3C^{4/5}$), 16.38 (CH_3CH_2), 22.25 ($CH(CH_3)_2$), 26.02 (CH), 37.80 (CH_2), 120.68 ($CH_3C^{4/5}$), 131.37 ($CH_3C^{4/5}$), 150.48 ppm (C^2CH); **IR** (ATR): ν = 1088, 1311, 1321, 1438, 2924, 2968 cm^{-1}; **MS** (ES): *m/z* (%): 167.3 (100) [M+H$^+$]; yield: 42%, yellow oil.

Optimised continuous flow procedure for the synthesis of 1-hexyl-2-isopropyl-4,5-dimethylimidazole (41h): In an oven dried 500 mL flask containing dry CH_2Cl_2 (200 mL) were added isobutyraldehyde (0.5 mol, 36.05 g), hexylamine (0.5 mol, 50.60 g) and $MgSO_4$ (1 mol, 120.37 g). The mixture was allowed to stir overnight, protected with a drying tube ($CaCl_2$). The reaction mixture was filtered and the solvent was removed *in vacuo*. The product was diluted with n-pentanol in a 1 L volumetric flask to 0.5 M. To a second 1 L volumetric flask containing n-pentanol were added diacetyl (0.5 mol, 43.05 g) and NH_4OAc (0.5 mol, 38.53 g), the solution was diluted to 0.5 M with n-pentanol. Both volumetric flasks were connected to the pumps on the CYTOS® CPC. The flow rate was set to 1.2 mL min^{-1} on each pump (t_{res} = 20 min) after volumetric calibration. Upon obtaining steady state conditions (32 min), a red to black solution was collected, containing 0.087 M (35%) of the product, with a product output of 2.55 g h^{-1}. Vacuum fractional distillation was used to recuperate the solvent (85 °C, 60 mbar), the residual black oil was dissolved in CH_2Cl_2, and extracted twice with 500 mL of 0.5 M HCl, the aqueous phase was alkalinised with 250 mL of 3.0 M NaOH and extracted with 3×100 mL of hexanes. The organic layer was dried with $MgSO_4$ and the solvent was removed *in vacuo*, yielding 31.1 g of a black oil. This oil was fractionally distilled under a high vacuum to afford the product as a yellow oil (83-86 °C, 1.0 mbar).

1-Hexyl-4,5-dimethylimidazole (41e): b.p. 83 °C (1.0 mbar); **^{1}H NMR** (300 MHz, $CDCl_3$,

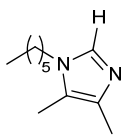

25 °C, TMS): δ = 0.88 (t, ^3J(H,H) = 6.6 Hz, 3H; CH_2CH_3), 1.27-1.34 (m; 6H; $(CH_2)_3CH_3$), 1.63-1.70 (m, 2H; NCH_2CH_2), 2.11 (s, 3H; $CH_3C^{4/5}$), 2.15 (s, 3H; $CH_3C^{4/5}$), 3.76 (t, ^3J(H,H) = 7.4 Hz, 2H; NCH_2), 7.31 ppm (s, 1H; C^2H); **^{13}C NMR** (75 MHz, $CDCl_3$, 25 °C, TMS): δ = 8.44 ($CH_3C^{4/5}$), 12.78 ($CH_3C^{4/5}$), 13.99 ($CH_3(CH_2)_5$), 22.51 (CH_2), 26.29 (CH_2), 30.78 (NCH_2CH_2), 31.33 (CH_2), 44.96 (NCH_2), 121.87 ($CH_3C^{4/5}$), 133.70 ($CH_3C^{4/5}$), 134.76 ppm (C^2H); **IR** (ATR): ν = 647, 1232, 1450, 1500, 2954 cm^{-1}; **MS** (ES): *m/z* (%): 181.3 (100) [M+H$^+$]; yield: 38%, clear liquid.

1-Hexyl-2,4,5-trimethylimidazole (41f): b.p. 84 °C (1.0 mbar); **^{1}H NMR** (300 MHz, $CDCl_3$,

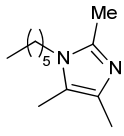

25 °C, TMS): δ = 0.89 (t, ^3J(H,H) = 6.6 Hz, 3H; CH_2CH_3), 1.25-1.34 (m; 6H; $(CH_2)_3CH_3$), 1.53-1.62 (m, 2H; NCH_2CH_2), 2.08 (s, 3H; $CH_3C^{4/5}$), 2.10 (s, 3H; $CH_3C^{4/5}$), 2.32 (3H, C^2CH_3, s), 3.68 ppm (t, ^3J(H,H) = 7.5 Hz, 2H; NCH_2); **^{13}C NMR** (75 MHz, $CDCl_3$, 25 °C, TMS): δ = 8.95 ($CH_3C^{4/5}$), 12.53 ($CH_3C^{4/5}$), 13.36

(C^2CH_3), 13.98 ($CH_3(CH_2)_5$), 22.55 (CH_2), 26.49 (CH_2), 30.60 (NCH_2CH_2), 31.47 (CH_2), 43.83 (NCH_2), 121.40 ($CH_3C^{4/5}$), 131.20 ($CH_3C^{4/5}$), 141.95 ppm (CH); **IR** (ATR): ν = 726, 1128, 1413, 1603, 2925 cm^{-1}; **MS** (ES): *m/z* (%): 195.3 (100) [M+H$^+$]; yield: 36%, yellow oil.

2-Ethyl-1-hexyl-4,5-dimethylimidazole (41g): b.p. 86 °C (1.0 mbar); **^{1}H NMR** (300 MHz, $CDCl_3$, 25 °C, TMS): δ = 0.89 (t, ^3J(H,H) = 6.6 Hz, 3H; CH_2CH_3), 1.26-1.37 (m; 6H; $(CH_2)_3CH_3$), 1.53-1.62 (m, 2H; NCH_2CH_2), 2.09 (s, 3H; $CH_3C^{4/5}$), 2.13 (s, 3H; $CH_3C^{4/5}$), 2.63 (q, ^3J(H,H) = 7.5 Hz, 2H; $C^2CH_2CH_3$), 3.68 ppm (t, ^3J(H,H) = 7.7 Hz, 2H, NCH_2); **^{13}C NMR** (75 MHz, $CDCl_3$, 25 °C, TMS): δ = 8.92 ($CH_3CH_2C^2$), 12.63 (CH_3C^4, CH_3C^5), 13.97 ($CH_3CH_2C^2$), 13.97 ($CH_3(CH_2)_5$), 22.56 (CH_2), 26.55 (CH_2), 30.89 (NCH_2CH_2), 31.48 (CH_2), 43.54 (NCH_2), 121.26 ($CH_3C^{4/5}$), 131.35 ($CH_3C^{4/5}$), 146.91 ppm (C^2CH_2); **IR** (ATR): ν = 1070, 1310, 1372, 1426, 2928, 2957 cm^{-1}; **MS** (ES): *m/z* (%): 209.3 (100) [M+H$^+$]; yield: 32%, yellow oil.

1-Hexyl-2-isopropyl-4,5-dimethylimidazole (41h): b.p. 86 °C (1.0 mbar); **^{1}H NMR** (300 MHz, $CDCl_3$, 25 °C, TMS): δ = 0.90 (t, ^3J(H,H) = 6.6 Hz, 3H; CH_2CH_3), 1.24-1.36 (m; 6H; $(CH_2)_3CH_3$), 1.31 (d, ^3J(H,H) = 6.6 Hz, 6H; $CH(CH_3)_2$), 1.53-1.65 (m, 2H; NCH_2CH_2), 2.09 (s, 3H; $CH_3C^{4/5}$), 2.14 (s, 3H; $CH_3C^{4/5}$), 2.86-2.99 (1H, CH, m), 3.70 ppm (t, ^3J(H,H) = 8.0 Hz, 2H; NCH_2); **^{13}C NMR** (75 MHz, $CDCl_3$, 25 °C, TMS): δ = 8.92 ($CH_3C^{4/5}$), 12.73 ($CH_3C^{4/5}$), 13.99 (CH_3CH_2), 22.28 ($CH(CH_3)_2$), 22.57 (CH_2), 26.05 (CH_2), 26.57 (NCH_2CH_2), 31.27 (CH_2), 31.48 (CH), 43.30 (NCH_2), 120.19 ($CH_3C^{4/5}$), 131.32 ($CH_3C^{4/5}$), 150.71 ppm (C^2CH); **IR** (ATR): ν = 1085, 1312, 1433, 2926, 2960 cm^{-1}; **MS** (ES): *m/z* (%): 223.3 (100) [M+H$^+$]; yield: 40%, yellow oil.

3.2. Synthesis of *N*-alkoxy- and *N*-alkenylimidazoles

1-Allyl-2-isopropyl-4,5-dimethylimidazole (59a): b.p. 52 °C (1.0 mbar); **^{1}H NMR** (300 MHz, $CDCl_3$, 25 °C, TMS): δ = 1.29 (d, ^3J(H,H) = 6.9 Hz, 6H; $CH(CH_3)_2$), 2.05 (s, 3H; $CH_3C^{4/5}$), 2.16 (s, 3H; $CH_3C^{4/5}$), 2.81-2.95 (m, 1H; $CH(CH_3)_2$), 4.38 (dt, ^3J(H,H) = 4.2 Hz, ^4J(H,H) = 2.0 Hz, 2H; CH_2), 4.79 (dtd, ^3J(H,H) = 17.2 Hz, ^4J(H,H) = 2.0 Hz, ^2J(H,H) = 1.1 Hz, 1H; $CH=CH_EH_Z$), 5.15 (dtd, ^3J(H,H) = 10.3 Hz, ^4J(H,H) = 2.0 Hz, ^2J(H,H) = 1.1 Hz, 1H; $CH=CH_EH_Z$), 5.87 ppm (ddt, ^3J(H,H) = 17.2 Hz, ^3J(H,H) = 10.3 Hz, ^3J(H,H) = 4.2 Hz, 1H; $CH=CH_2$); **^{13}C NMR** (75 MHz, $CDCl_3$, 25 °C, TMS): δ = 8.58 ($CH_3C^{4/5}$), 12.70 ($CH_3C^{4/5}$), 22.11 ($CH(CH_3)_2$), 26.03 ($CH(CH_3)_2$), 45.13 (NCH_2), 116.07 ($CH=CH_2$), 121.27 ($C^{4/5}$), 131.26 ($C^{4/5}$), 133.44 ($CH=CH_2$), 150.99 ppm (C^2); **IR** (ATR): ν = 917, 1087, 1304, 1434, 2965 cm^{-1}; **HRMS** (ESI/APCI) calcd for [$C_{11}H_{19}N_2^+$]: 179.1543; found: 179.1540; yield: 63%, colourless liquid.

2-Isopropyl-1-(2-methoxyethyl)-4,5-dimethylimidazole (59c): b.p. 82 °C (1.0 mbar); **^{1}H NMR** (300 MHz, $CDCl_3$, 25 °C, TMS): δ = 1.30 (d, ^3J(H,H) = 7.2 Hz, 6H; $CH(CH_3)_2$), 2.10 (s, 3H; $CH_3C^{4/5}$), 2.14 (s, 3H; $CH_3C^{4/5}$), 2.93-3.06 (m, 1H; CH), 3.31 ppm (t, ^3J(H,H) = 6.1 Hz, 2H; CH_2O), 3.50 (s, 3H, OCH_3), 3.93 (t, ^3J(H,H) = 4.8 Hz, 2H; NCH_2); **^{13}C NMR** (75 MHz, $CDCl_3$, 25 °C, TMS): δ = 8.92 (CH_3C^4), 12.63 ($CH_3C^{4/5}$), 22.18 ($CH(CH_3)_2$), 25.88 (CH), 43.07 (NCH_2), 59.09 (OCH_3), 71.94 (CH_2O), 121.06 ($C^{4/5}$), 131.35 ($C^{4/5}$), 151.44 ppm (C^2); **IR** (ATR): ν = 1086, 1119, 1438, 2925 cm^{-1}; **HRMS** (ESI/APCI) calcd for [$C_{11}H_{21}N_2O^+$]: 197.1648; found: 197.1649; yield: 53%, white waxy solid.

Procedure for the synthesis of 2-(2-isopropyl-4,5-dimethylimidazol-1-yl)ethanol (59b): A glass 150 mL pressure vial was filled with MeOH (50 mL) and a PTFE stirring bar. The solvent was allowed to cool to 0 °C and isobutyraldehyde (100 mmol, 7.21 g) and 2-aminoethanol (100 mmol, 6.11 g) were added. The vial was closed and submerged in a preheated oil bath at 120 °C with a temperature controller. After heating for 2h with vigorous stirring, the reaction mixture was carefully cooled to 0 °C, the vial was opened and consecutively 2,3-butanedione (25 mmol, 2.15 g) and NH_4OAc (25 mmol, 1.93 g) were added. The vessel was closed immediately and heated in a preheated oil bath at 120 °C for 30 min under vigorous stirring. The reaction mixture was again carefully cooled and 2,3-butanedione and NH_4OAc were added and heated for 30 min three times more. After cooling, MeOH and the reaction water were removed *in vacuo*. The reaction mixture was dissolved in EtOAc and extracted twice with 100 mL of an aqueous 0.5 M HCl solution. The aqueous phase was alkalinised with 50 mL of 3.0 M NaOH and extracted three times with 40 mL of EtOAc. The combined organic phase was dried with $MgSO_4$. The solvent was removed *in vacuo* and 7.31 g of a black oil was obtained. The resulting oil was dissolved in an equal volume of boiling CH_3CN and stored at -18 °C until all 1*H*-2-isopropyl-4,5-dimethylimidazole precipitated. If the oil was not sufficiently pure as monitored by GC, an additional precipitation can be applied. The solvent was removed from the resulting mother liquid by rotary evaporation and the resulting product was further used for the synthesis of compound **4d**.

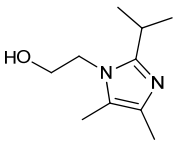

2-(2-Isopropyl-4,5-dimethylimidazol-1-yl)ethanol (59b): R_f = 0.07 (hexanes/EtOAc 4:6); **^{1}H NMR** (300 MHz, $CDCl_3$, 25 °C, TMS): δ = 1.28 (d, ^3J(H,H) = 7.2 Hz, 6H; CH(CH_3)$_2$), 2.11 (s, 6H; $CH_3C^{4/5}$), 2.94-3.09 (m, 1H; CH), 3.79 (t, ^3J(H,H) = 6.1 Hz, 2H; CH_2O), 3.94 ppm (t, ^3J(H,H) = 6.1 Hz, 2H; NCH_2); **^{13}C NMR** (75 MHz, $CDCl_3$, 25 °C, TMS): δ = 8.84 ($CH_3C^{4/5}$), 12.09 ($CH_3C^{4/5}$), 22.02 (CH(CH_3)$_2$), 25.77 (CH(CH_3)$_2$), 45.42 (NCH_2), 60.71 (CH_2O), 121.34 ($C^{4/5}$), 130.71 ($C^{4/5}$), 151.41 ppm (C^2); **IR** (ATR): ν = 729, 1086, 1738, 2966, 3112 cm^{-1}; **HRMS** (ESI/APCI) calcd for [$C_{10}H_{19}N_2O^+$]: 183.1492; found: 183.1495; yield (crude): 38%, black oil.

Procedure for the synthesis of 1-(2-allyloxyethyl)-2-isopropyl-4,5-dimethylimidazole (59d): In a flame dried 250 mL flask containing crude 2-(2-isopropyl-4,5-dimethylimidazol-1-yl)ethanol (70 mmol, 12.81 g), dry THF (80 mL) was added under a nitrogen atmosphere. The mixture was cooled to 0 °C and then slowly pure NaH (77 mmol, 1.85 g) was added. After stirring for 15 min, allyl bromide (73,5 mmol, 8.90 g) was added dropwise. The mixture was allowed to warm to room temperature overnight. After reaction, a fraction of the solvent was evaporated and the resulting slurry was diluted in EtOAc and washed twice with 80 mL of a saturated aqueous $NaHCO_3$ solution and once with 40 mL of water. The organic layer was dried with $MgSO_4$ after which the solvent was removed by rotary evaporation. The resulting oil was distilled via short-path vacuum distillation (108 °C, 1.0 mbar) to obtain a yellow oil.

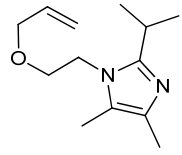

1-(2-Allyloxyethyl)-2-isopropyl-4,5-dimethylimidazole (59d): b.p. 108 °C (1.0 mbar); **^{1}H NMR** (300 MHz, $CDCl_3$, 25 °C, TMS): δ = 1.30 (d, ^3J(H,H) = 6.8 Hz, 6H; CH(CH_3)$_2$), 2.11 (s, 3H; $CH_3C^{4/5}$), 2.14 (s, 3H; $CH_3C^{4/5}$), 2.95-3.09 (m, 1H; CH(CH$_3$)$_2$), 3.56 (t, ^3J(H,H) = 6.3 Hz, 2H; CH_2O), 3.93 (dt, ^3J(H,H) = 5.4 Hz, ^4J(H,H) = 1.4 Hz, 2H; CH_2CH=CH$_2$), 3.96 (t, ^3J(H,H) = 6.3 Hz, 2H; NCH_2), 5.17 (ddt, ^3J(H,H) = 10.1 Hz, ^2J(H,H) = 3.3 Hz, ^4J(H,H) = 1.6 Hz, 1H; CH=CH_EH$_Z$), 5.22 (ddt, ^3J(H,H) = 17.3 Hz, ^2J(H,H) = 3.3 Hz, ^4J(H,H) = 1.6 Hz, 1H;

CH=CH$_E$H$_Z$), 5.83 ppm (ddt, ^3J(H,H) = 17.3 Hz, ^3J(H,H) = 10.1 Hz, ^3J(H,H) = 5.4 Hz, 1H; C*H*=CH$_2$); **^{13}C NMR** (75 MHz, $CDCl_3$, 25 °C, TMS): δ = 8.95 (*C*H$_3$C$^{4/5}$), 12.69 (*C*H$_3$C$^{4/5}$), 22.18 (CH(*C*H$_3$)$_2$), 25.82 (CH), 43.13 (NCH$_2$), 69.33 (CH$_2$*C*H$_2$O), 77.20 (*C*H$_2$CH=CH$_2$), 117.04 (CH$_2$CH=*C*H$_2$), 121.02 (C$^{4/5}$), 131.32 (C$^{4/5}$), 134.22 (*C*H=CH$_2$), 151.37 ppm (C^2); **IR** (ATR): ν = 1052, 1134, 1175, 1378 cm^{-1}; **HRMS** (ESI/APCI) calcd for [$C_{13}H_{23}N_2O^+$]: 223.1805; found: 223.1807; yield: 86%, light yellow oil.

1-Allyl-4,5-dimethylimidazole (41i): ^{1}H NMR (300 MHz, $CDCl_3$, 25 °C, TMS): δ = 2.08 (s, 3H; CH$_3$C$^{4/5}$), 2.16 (s, 3H; CH$_3$C$^{4/5}$), 4.41 (d, ^3J(H,H) = 5.3 Hz, 2H; CH$_2$), 4.98 (d, ^3J(H,H) = 17.1 Hz, 2H; CH=C*H*$_E$H$_Z$), 5.21 (d, ^3J(H,H) = 10.3 Hz, 2H; CH=CH$_E$*H*$_Z$), 5.90 (ddt, ^3J(H,H) = 17.1 Hz, ^3J(H,H) = 10.3 Hz, ^3J(H,H) = 5.3 Hz, 2H; C*H*=CH$_2$), 7.32 ppm (s, 1H; C^{2}H); **^{13}C NMR** (75 MHz, $CDCl_3$, 25 °C, TMS): δ = 8.15 (*C*H$_3$C$^{4/5}$), 12.69 (*C*H$_3$C$^{4/5}$), 47.13 (NCH$_2$), 117.05 (CH=*C*H$_2$), 122.24 (C$^{4/5}$), 133.38 (CH), 133.67 (C$^{4/5}$), 134.92 ppm (C^2); **IR** (ATR): ν = 918, 1239, 1443, 1497, 2981 cm^{-1}; **HRMS** (ESI/APCI) calcd for [$C_8H_{13}N_2^+$]: 137.1073; found: 137.1074; yield: 29%, colourless oil.

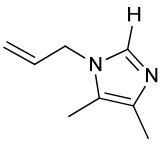

1-(2-Methoxyethyl)-4,5-dimethylimidazole (41j): ^{1}H NMR (300 MHz, $CDCl_3$, 25 °C, TMS): δ = 2.13 (s, 3H; CH$_3$C$^{4/5}$), 2.16 (s, 3H; CH$_3$C$^{4/5}$), 3.33 (s, 3H; OCH$_3$), 3.57 (t, ^3J(H,H) = 5.5 Hz, 2H; CH$_2$O), 3.95 (t, ^3J(H,H) = 5.5 Hz, 2H; NCH$_2$), 7.39 ppm (s, 1H; C^{2}H); **^{13}C NMR** (75 MHz, $CDCl_3$, 25 °C, TMS): δ = 8.44 (*C*H$_3$C$^{4/5}$), 12.78 (*C*H$_3$C$^{4/5}$), 44.72 (NCH$_2$), 58.98 (OCH$_3$), 71.76 (CH$_2$O), 122.04 (C$^{4/5}$), 133.46 (C$^{4/5}$), 135.37 ppm (C^2); **IR** (ATR): ν = 1120, 1190, 1448, 1498, 1920 cm^{-1}; **HRMS** (ESI/APCI) calcd for [$C_8H_{16}N_2O^+$]: 155.1179; found: 155.1181; yield: 42%, pale yellow oil.

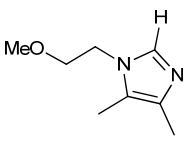

1-(2-Methoxyethyl)-2,4,5-trimethylimidazole (122a): ^{1}H NMR (300 MHz, $CDCl_3$, 25 °C, TMS): δ = 2.10 (s, 6H; CH$_3$C$^{4/5}$), 2.35 (s, 3H; C^{2}CH$_3$), 3.30 (s, 3H; OCH$_3$), 3.51 (t, ^3J(H,H) = 5.8 Hz, 2H; CH$_2$O), 3.89 ppm (t, ^3J(H,H) = 5.8 Hz, 2H; NCH$_2$); **^{13}C NMR** (75 MHz, $CDCl_3$, 25 °C, TMS): δ = 8.93 (*C*H$_3$C$^{4/5}$), 12.54 (C^2*C*H$_3$), 43.73 (NCH$_2$), 59.04 (OCH$_3$), 71.67 (CH$_2$O), 121.75 (C$^{4/5}$), 131.09 (C$^{4/5}$), 142.71 ppm (C^2); **IR** (ATR): ν = 862, 1317, 1545, 1638, 2608, 2680 cm^{-1}; **HRMS** (ESI/APCI) calcd for [$C_9H_{17}N_2O^+$]: 169.1342; found: 168.126924; yield: 42%, yellow oil.

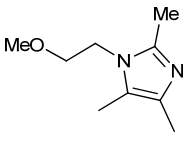

3.3. Synthesis of imidazolium hydrochloride salts

Procedure for the synthesis of 1,2-diethyl-4,5-dimethylimidazolium hydrochloride (43c): Freshly distilled 1,2-diethyl-4,5-dimethylimidazole (73.6 mmol, 11.2 g) is brought in a 250mL flask containing dry CH_2Cl_2 (80 mL). The flask is provided with a septum with exhaust needle. Freshly prepared dry hydrogen chloride gas is added via a submerged pipet under vigorous stirring during 2h. After complete acidification (escape of hydrogen chloride gas via the exhaust), the solvent is removed *in vacuo* until a solid is obtained. This solid is recrystallised from a minimum amount of boiling acetone. A first crop yields 64% of transparent crystals, and a second crop an additional 28% of slightly yellow coloured crystals. Mass spectra of the salts are not recorded, as in the buffered LC eluent solution, the same spectra as for the free imidazole bases would be obtained.

Procedure for the neutralisation of 1,2-diethyl-4,5-dimethylimidazolium hydrochloride (43c): To a separation funnel containing 100 mL of an aqueous 1.0 M NaOH solution and 100 mL of ice water is added 1,2-diethyl-4,5-dimethylimidazolium hydrochloride (50 mmol, 9.44 g). The mixture is shaken vigorously, after which it is extracted three times with EtOAc (50 mL). The organic fractions are combined and dried over $MgSO_4$. The solvent is evaporated, yielding the pure imidazole quantitatively as a clear liquid.

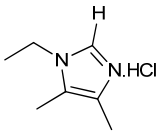

1-Ethyl-4,5-dimethylimidazolium hydrochloride (43a): **^{1}H NMR** (300 MHz, $CDCl_3$, 25 °C, TMS): δ = 1.53 (t, ^3J(H,H) = 7.4 Hz, 3H; CH_2CH_3), 2.23 (s, 3H; $CH_3C^{4/5}$), 2.37 (s, 3H; $CH_3C^{4/5}$), 4.17 (q, ^3J(H,H) = 7.4 Hz, 2H; CH_2CH_3), 8.94 ppm (C^2H); **^{13}C NMR** (75 MHz, $CDCl_3$, 25 °C, TMS): δ = 8.20 ($CH_3C^{4/5}$), 9.65 ($CH_3C^{4/5}$), 15.83 (NCH_2CH_3), 42.37 (NCH_2), 124.88 ($C^{4/5}$), 126.68 ($C^{4/5}$), 132.71 ppm (C^2); **IR** (ATR): ν = 862, 1317, 1545, 1638, 2608, 2680 cm^{-1}; **MW** (g mol^{-1}): 174.67; yield: 95%, colourless crystals.

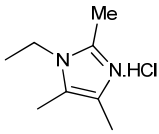

1-Ethyl-2,4,5-trimethylimidazolium hydrochloride (43b): **^{1}H NMR** (300 MHz, $CDCl_3$, 25 °C, TMS): δ = 1.35 (t, ^3J(H,H) = 7.3 Hz, 3H; CH_2CH_3), 2.18 (s, 3H; $CH_3C^{4/5}$), 2.28 (s, 3H; $CH_3C^{4/5}$), 2.65 (s, 3H; C^2CH_3), 3.92 ppm (q, ^3J(H,H) = 7.3 Hz, 2H; CH_2CH_3); **^{13}C NMR** (75 MHz, $CDCl_3$, 25 °C, TMS): δ = 8.23 ($CH_3C^{4/5}$), 9.19 ($CH_3C^{4/5}$), 10.78 (C^2CH_3), 15.04 (NCH_2CH_3), 39.96 (NCH_2), 124.07 ($C^{4/5}$), 124.62 ($C^{4/5}$), 140.96 ppm (C^2); **IR** (ATR): ν = 952, 1162, 1298, 1653, 2966 cm^{-1}; **MW** (g mol^{-1}): 160.64; yield: 93%, colourless crystals.

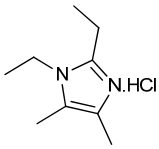

1,2-Diethyl-4,5-dimethylimidazolium hydrochloride (43c): **^{1}H NMR** (300 MHz, $CDCl_3$, 25 °C, TMS): δ = 1.40 (t, ^3J(H,H) = 7.3 Hz, 3H; NCH_2CH_3), 1.48 (t, ^3J(H,H) = 7.7 Hz, 3H; CH_2CH_3), 2.21 (s, 3H; $CH_3C^{4/5}$), 2.35 (s, 3H; $CH_3C^{4/5}$), 3.03 (t, ^3J(H,H) = 7.7 Hz, 3H; CH_2CH_3), 3.98 ppm (t, ^3J(H,H) = 7.3 Hz, 3H; NCH_2CH_3); **^{13}C NMR** (75 MHz, $CDCl_3$, 25 °C, TMS): δ = 8.28 ($CH_3C^{4/5}$), 9.15 ($CH_3C^{4/5}$), 12.49 (CH_2CH_3), 15.54 (NCH_2CH_3), 18.43 (C^2CH_2), 39.91 (NCH_2), 124.05 ($C^{4/5}$), 124.97 ($C^{4/5}$), 145.44 ppm (C^2); **IR** (ATR): ν = 924, 1513, 1650, 1819, 2484 cm^{-1}; **MW** (g mol^{-1}): 188.70; yield: 92%, colourless crystals.

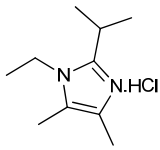

1-Ethyl-2-isopropyl-4,5-dimethylimidazolium hydrochloride (43d): **^{1}H NMR** (300 MHz, $CDCl_3$, 25 °C, TMS): δ = 1.40 (t, ^3J(H,H) = 7.2 Hz, 3H; CH_2CH_3), 1.57 (d, ^3J(H,H) = 7.2 Hz, 6H; $CH(CH_3)_2$), 2.20 (s, 3H; $CH_3C^{4/5}$), 2.38 (s, 3H; $CH_3C^{4/5}$), 3.14-3.28 (m, 1H; $CH(CH_3)_2$), 4.01 ppm (t, ^3J(H,H) = 7.2 Hz, 3H; CH_2CH_3); **^{13}C NMR** (75 MHz, $CDCl_3$, 25 °C, TMS): δ = 8.21 ($CH_3C^{4/5}$), 9.18 ($CH_3C^{4/5}$), 15.85 (CH_2CH_3), 21.31 ($CH(CH_3)_2$), 25.88 (CH), 39.77 (NCH_2), 123.27 ($C^{4/5}$), 125.92 ($C^{4/5}$), 149.09 ppm (C^2); **IR** (ATR): ν = 926, 1331, 1509, 1645, 1822, 2491 cm^{-1}; **MW** (g mol^{-1}): 202.72; yield: 76%, colourless crystals.

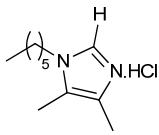

1-Hexyl-2-isopropyl-4,5-dimethylimidazolium hydrochloride (43e): **^{1}H NMR** (300 MHz, $CDCl_3$, 25 °C, TMS): δ = 0.89 (t, ^3J(H,H) = 6.9 Hz, 3H; CH_2CH_3), 1.27-1.38 (m, 6H; $(CH_2)_3CH_3$), 1.76-1.86 (m, 2H; NCH_2CH_2), 2.22 (s, 3H; $CH_3C^{4/5}$), 2.37 (s, 3H; $CH_3C^{4/5}$), 4.09 (t, ^3J(H,H) = 7.4 Hz, 2H; NCH_2), 8.76 ppm (s, 1H; C^2H); **^{13}C NMR** (75 MHz, $CDCl_3$, 25 °C, TMS): δ = 8.05 ($CH_3C^{4/5}$), 9.42 ($CH_3C^{4/5}$), 13.96 (CH_2CH_3), 22.43 (CH_2CH_3), 25.97 ($CH_2CH_2CH_3$), 30.05

(NCH_2CH_2), 31.16 ($NCH_2CH_2CH_2$), 47.01 (NCH_2), 124.67 ($C^{4/5}$), 126.40 ($C^{4/5}$), 123.74 ppm (C^2); **IR** (ATR): ν = 887, 1162, 1320, 1661, 2855 cm^{-1}; **MW** (g mol^{-1}): 216.75; yield: 85%, white powder.

1-Hexyl-2-isopropyl-4,5-dimethylimidazolium hydrochloride (43f): **^{1}H NMR** (300 MHz, $CDCl_3$, 25 °C, TMS): δ = 0.87-0.95 (m, 3H; CH_2CH_3), 1.29-1.41 (m, 6H; $(CH_2)_3CH_3$), 1.53-1.72 (2H, NCH_2CH_2, m), 1.57 (d, ^3J(H,H) = 6.6 Hz, 6H; $CHCH_3$), 2.18 (s, 3H; $CH_3C^{4/5}$), 2.39 (s, 3H; $CH_3C^{4/5}$), 3.09-3.22 (m, 1H; CH), 3.88 ppm (t, ^3J(H,H) = 7.7 Hz, 2H; NCH_2,); **^{13}C NMR** (75 MHz, $CDCl_3$, 25 °C, TMS): δ = 8.43 ($CH_3C^{4/5}$), 9.16 ($CH_3C^{4/5}$), 13.92 (CH_2CH_3), 21.36 ($CH(CH_3)_2$), 22.47 (CH_2CH_3), 26.00 ($CH_2CH_2CH_3$), 26.28 (NCH_2CH_2), 30.57 ($NCH_2CH_2CH_2$), 31.27 (CH), 44.95 (NCH_2), 123.61 ($C^{4/5}$), 125.81 ($C^{4/5}$), 149.37 ppm (C^2); **IR** (ATR): ν = 920, 1298, 1332, 1509, 2483, 2928 cm^{-1}; **MW** (g mol^{-1}): 258.83; yield: 96%, white powder.

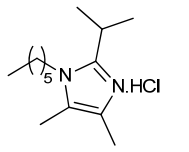

1-Allyl-4,5-dimethylimidazolium hydrochloride (43g): **^{1}H NMR** (300 MHz, $CDCl_3$, 25 °C, TMS): δ = 2.19 (s, 3H; $CH_3C^{4/5}$), 2.37 (s, 3H; $CH_3C^{4/5}$), 4.82 (d, ^3J(H,H) = 5.4 Hz, 2H; CH_2), 5.17 (d, ^3J(H,H) = 17.1 Hz, 1H; $CH{=}CH_EH_Z$), 5.39 (d, ^3J(H,H) = 10.5 Hz, 1H; $CH{=}CH_EH_Z$), 5.96 (ddt, ^3J(H,H) = 17.1 Hz, ^3J(H,H) = 10.5 Hz, ^3J(H,H) = 5.4 Hz, 1H; $CH{=}CH_2$), 9.05 ppm (s, 1H; C^2H); **^{13}C NMR** (75 MHz, $CDCl_3$, 25 °C, TMS): δ = 7.97 ($CH_3C^{4/5}$), 9.41 ($CH_3C^{4/5}$), 49.16 (NCH_2), 120.01 ($CH{=}CH_2$), 125.21 ($C^{4/5}$), 126.54 ($C^{4/5}$), 130.54 ($CH{=}CH_2$), 133.12 ppm (C^2); **IR** (ATR): ν = 844, 923, 1326, 1640, 2609, 2692 cm^{-1}; **elemental analysis** calcd (%) for $C_8H_{13}ClN_2$: C 55.65, H 7.59, N 16.23; found: C 55.44, H 7.93, N 16.10; **MW** (g mol^{-1}): 172.66; yield: 87%, white powder.

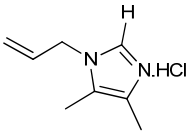

3.4. Synthesis of *N*-alkylimidazolium ionic liquids

3.4.1) N-alkylimidazolium methanesulfonate ionic liquids

Procedure for the synthesis of 1-ethyl-3,4,5-trimethylimidazolium methanesulfonate [C_2m_3im][OMs] (44d): To a flame dried 6 mL vial, containing 4 mL of dry acetonitrile, 1-ethyl-4,5-dimethylimidazole (8.2 mmol, 1.02 g) was added via a syringe under a nitrogen atmosphere. To the mixture, 1.1 eq. of methyl methanesulfonate (9.0 mmol, 1.00 g) was added. The headspace was filled with nitrogen and the vial was sealed with a PTFE cap. The mixture was irradiated for 30 minutes in a microwave reactor to a temperature of 80 °C. After reaction, the solvent was removed *in vacuo* and the mixture was diluted in distilled water (25 mL) and washed twice with EtOAc (20 mL). The aqueous layer was evaporated and dried for 6h at 100 °C and 1.0 mbar.

1-Ethyl-3,4,5-trimethylimidazolium methanesulfonate [C_2m_3im][OMs] (44d): **^{1}H NMR** (300 MHz, $CDCl_3$, 25 °C, TMS): δ = 1.54 (t, ^3J(H,H) = 7.3 Hz, 3H; CH_2CH_3), 2.23 (s, 3H; $CH_3C^{4/5}$), 2.25 (s, 3H; $CH_3C^{4/5}$), 2.81 (s, 3H; CH_3SO_3), 3.88 (s, 3H; NCH_3), 4.19 (t, ^3J(H,H) = 7.3 Hz, 2H; CH_2CH_3), 9.91 ppm (s, 1H; C_2H); **^{13}C NMR** (75 MHz, $CDCl_3$, 25 °C, TMS): δ = 8.53 ($CH_3C^{4/5}$), 8.78 ($CH_3C^{4/5}$), 14.95 (CH_2CH_3), 32.34 (NCH_3), 39.38 (CH_3SO_3), 40.72 (CH_2), 124.56 ($C^{4/5}$), 126.04 ($C^{4/5}$), 142.19 ppm (C^2); **IR** (ATR): ν = 768, 1038, 1178, 3444 cm^{-1}; **MW** (g mol^{-1}): 234.32; yield: 97%, white powder.

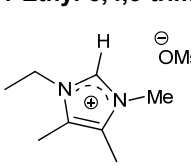

1-Ethyl-2,3,4,5-tetramethylimidazolium methanesulfonate [$C_2C_1m_3im$][OMs] (45d): ^{1}H NMR (300 MHz, $CDCl_3$, 25 °C, TMS): δ = 1.39 (t, ^3J(H,H) = 7.5 Hz, 3H; CH_2CH_3), 2.23 (s, 6H; $CH_3C^{4/5}$), 2.69 (s, 3H; C^2CH_3), 2.79 (s, 3H; CH_3SO_3), 3.75 (s, 3H; NCH_3), 4.14 ppm (t, ^3J(H,H) = 7.5 Hz, 2H; CH_2CH_3); **^{13}C NMR** (75 MHz, $CDCl_3$, 25 °C, TMS): δ = 8.50 ($CH_3C^{4/5}$), 8.75 ($CH_3C^{4/5}$), 10.37 (C^2CH_3), 14.93 (CH_2CH_3), 32.32 (NCH_3), 39.35 (CH_3SO_3), 40.70 (CH_2), 124.50 ($C^{4/5}$), 126.02 ($C^{4/5}$), 142.38 ppm (C^2); **IR** (ATR): ν = 767, 1038, 1180, 1449, 1537, 3444 cm^{-1}; **MW** (g mol^{-1}): 248.34; yield: 98%, pale yellow oil.

1,2-Diethyl-3,4,5-trimethylimidazolium methanesulfonate [$C_2C_2m_3im$][OMs] (46d): ^{1}H NMR (300 MHz, $CDCl_3$, 25 °C, TMS): δ = 1.31 (t, ^3J(H,H) = 7.6 Hz, 3H; $C^2CH_2CH_3$), 1.43 (t, ^3J(H,H) = 7.3 Hz, 3H; NCH_2CH_3), 2.27 (s, 6H; $CH_3C^{4/5}$), 2.69 (s, 3H; CH_3SO_3), 3.20 (q, ^3J(H,H) = 7.6 Hz, 2H; $C^2CH_2CH_3$), 3.78 (s, 3H; NCH_3), 4.15 ppm (q, ^3J(H,H) = 7.3 Hz, 2H; NCH_2CH_3); **^{13}C NMR** (75 MHz, $CDCl_3$, 25 °C, TMS): δ = 8.57 ($CH_3C^{4/5}$), 8.76 ($CH_3C^{4/5}$), 11.91 (CH_2CH_3), 15.62 (NCH_2CH_3) 17.36 (CH_2) 32.15 (NCH_3) 39.36 (CH_3SO_3) 40.67 (NCH_2) 124.76 ($C^{4/5}$), 126.44 ($C^{4/5}$), 146.15 ppm (C^2); **IR** (ATR): ν = 766, 1037, 1178, 3444 cm^{-1}; **MW** (g mol^{-1}): 262.37; yield: 96%, reddish oil.

1-Ethyl-2-isopropyl-3,4,5-trimethylimidazolium methanesulfonate [$C_2C_{i3}m_3im$][OMs] (47d): ^{1}H NMR (300 MHz, $CDCl_3$, 25 °C, TMS): δ = 1.40 (t, ^3J(H,H) = 7.4 Hz, 3H; CH_2CH_3), 1.54 (d, ^3J(H,H) = 7.3 Hz, 6H; $CH(CH_3)_2$), 2.28 (s, 6H; $CH_3C^{4/5}$), 2.70 (s, 3H; CH_3SO_3), 3.60-3.75 (m, 1H; $CH(CH_3)_2$), 3.83 (s, 3H; NCH_3), 4.23 ppm (t, ^3J(H,H) = 7.4 Hz, 2H; CH_2CH_3); **^{13}C NMR** (75 MHz, $CDCl_3$, 25 °C, TMS): δ = 8.73 ($CH_3C^{4/5}$), 8.90 ($CH_3C^{4/5}$), 15.79 (CH_2CH_3), 19.31 ($CH(CH_3)_2$), 25.07 (CH), 33.09 (NCH_3), 39.42 (CH_3SO_3), 40.95 (CH_2), 125.11 ($C^{4/5}$), 127.09 ($C^{4/5}$), 147.70 ppm (C^2); **IR** (ATR): ν = 770, 1039, 1180, 3434 cm^{-1}; **MW** (g mol^{-1}): 276.40; yield: 99%, pale yellow oil.

3.4.2) N-alkylimidazolium iodide ionic liquids

Procedure for the synthesis of 1-ethyl-2-isopropyl-3,4,5-trimethylimidazolium iodide [$C_2C_{i3}m_3im$][I] (47a): In an oven dried flask of 100 mL, 1-ethyl-2-isopropyl-4,5-dimethylimidazole (20 mmol, 3.32 g) was dissolved in dry CH_3CN (40 mL). The solution was cooled to 0 °C and MeI (52 mmol, 7.34 g) was added dropwise at 0 °C. The reaction mixture was allowed to stir at room temperature for 8h. When the reaction was completed, the solvent and residual MeI were removed *in vacuo*. The resulting yellow solid was recrystallised in dry acetone to furnish colourless to white crystals (1st crop: 75%, 2nd crop: 11%). Residual solvent was removed in a high vacuum.

1-Ethyl-3,4,5-trimethylimidazolium iodide [C_2m_3im][I] (44a): ^{1}H NMR (300 MHz, $CDCl_3$, 25 °C, TMS): δ = 1.59 (t, ^3J(H,H) = 7.4 Hz, 3H; NCH_2CH_3), 2.26 (s, 3H; $CH_3C^{4/5}$), 2.27 (s, 3H; $CH_3C^{4/5}$), 3.94 (s, 3H; NCH_3), 4.21 (q, ^3J(H,H) = 7.4 Hz, 2H; NCH_2CH_3), 10.13 ppm (s, 1H; CH); **^{13}C NMR**

(75 MHz, $CDCl_3$, 25 °C, TMS): δ = 8.76 ($CH_3C^{4/5}$), 8.79 ($CH_3C^{4/5}$), 15.34 (CH_3CH_2), 34.41 (NCH_3), 42.70 (CH_2), 126.30 ($CH_3C^{4/5}$), 127.34 ($CH_3C^{4/5}$), 134.92 ppm (*C*H); **IR** (ATR): ν = 1199, 1241, 1572, 1634, 3032 cm^{-1}; **MS** (ES): *m/z* (%): 139.3 (100) $[M+H^+]$; yield: 87%, colourless crystals.

1-Ethyl-2,3,4,5-tetramethylimidazolium iodide [$C_2C_1m_3im$][I] (45a): ^{1}**H NMR** (300 MHz, $CDCl_3$, 25 °C, TMS): δ = 1.42 (t, ^3J(H,H) = 7.4 Hz, 3H; NCH_2CH_3), 2.27 (s, 6H; $CH_3C^{4/5}$), 2.86 (s, 3H; C^2CH_3), 3.79 (s, 3H; NCH_3), 4.17 ppm (q, ^3J(H,H) = 7.4 Hz, 2H; NCH_2CH_3); ^{13}**C NMR** (75 MHz, $CDCl_3$, 25 °C, TMS): δ = 9.04 ($CH_3C^{4/5}$), 9.39 ($CH_3C^{4/5}$), 12.44 (C^2CH_3) , 15.33 (CH_3CH_2), 33.71 (NCH_3), 41.52 (CH_2), 124.80 ($C^{4/5}$), 126.25 ($C^{4/5}$), 142.10 ppm (C^2); **IR** (ATR): ν = 1198, 1456, 1572, 1634, 2358, 3032 cm^{-1}; **MS** (ES): *m/z* (%): 153.3 (100) $[M+H^+]$; yield: 89%, colourless crystals.

1,2-Diethyl-3,4,5-trimethylimidazolium iodide [$C_2C_2m_3im$][I] (46a): ^{1}**H NMR** (300 MHz, $CDCl_3$, 25 °C, TMS): δ = 1.34 (t, ^3J(H,H) = 7.7 Hz, 3H; $C^2CH_2CH_3$), 1.46 (t, ^3J(H,H) = 7.4 Hz, 3H; NCH_2CH_3), 2.28 (s, 6H; $CH_3C^{4/5}$), 3.22 (q, ^3J(H,H) = 7.7 Hz, 2H; $C^2CH_2CH_3$), 3.81 (s, 3H; NCH_3), 4.16 ppm (q, ^3J(H,H) = 7.4 Hz, 2H; NCH_2CH_3); ^{13}**C NMR** (75 MHz, $CDCl_3$, 25 °C, TMS): δ = 6.99 ($CH_3C^{4/5}$), 7.33 ($CH_3C^{4/5}$), 10.32 (CH_3CH_2C), 13.80 (NCH_2CH_3), 16.47 (C^2CH_2), 31.33 (NCH_3), 39.30 (NCH_2), 122.86 ($CH_3C^{4/5}$), 124.47 ($CH_3C^{4/5}$), 143.89 ppm (C^2CH_2); **IR** (ATR): ν = 1090, 1259, 1448, 1529, 1648, 2975 cm^{-1}; **MS** (ES): *m/z* (%): 167.3 (100) $[M+H^+]$; yield: 99%, reddish oil.

1-Ethyl-2-isopropyl-3,4,5-trimethylimidazolium iodide [$C_2C_{i3}m_3im$][I] (47a): ^{1}**H NMR** (300 MHz, $CDCl_3$, 25 °C, TMS): δ = 1.43 (t, ^3J(H,H) = 7.2 Hz, 3H; NCH_2CH_3), 1.55 (d, ^3J(H,H) = 7.2 Hz, 6H; $CH(CH_3)_2$), 2.30 (s, 6H; $CH_3C^{4/5}$), 3.66-3.81 (m, 1H; CH), 3.87 (s, 3H; NCH_3), 4.26 ppm (q, ^3J(H,H) = 7.2 Hz, 2H; NCH_2CH_3); ^{13}**C NMR** (75 MHz, $CDCl_3$, 25 °C, TMS): δ = 9.26 ($CH_3C^{4/5}$), 9.63 ($CH_3C^{4/5}$), 15.94 (CH_3CH_2), 19.91 ($CH(CH_3)_2$), 25.35 (CH), 34.06 (NCH_3), 41.65 (CH_2), 125.18 ($CH_3C^{4/5}$), 127.17 ($CH_3C^{4/5}$), 147.72 ppm (C^2CH); **IR** (ATR): ν = 1088, 1331, 1448, 1521, 1651, 2971 cm^{-1}; **MS** (ES): *m/z* (%): 181.3 (100) $[M+H^+]$; yield: 86%, colourless crystals.

Procedure for the synthesis of 1-hexyl-2-isopropyl-3,4,5-trimethylimidazolium iodide [C6$C_{i3}m_3$im][I] (51a): In an oven dried flask of 100 mL, 1-hexyl-2-isopropyl-4,5-dimethylimidazole (20 mmol, 4.44 g) was dissolved in dry CH_3CN (40 mL). The solution was cooled to 0 °C and MeI (52 mmol, 7.34 g) was added dropwise at 0 °C. The reaction mixture was allowed to stir at room temperature for 20h. When the reaction was completed, the solvent and residual MeI were removed *in vacuo*. The resulting yellow oil was dissolved in 20 mL CH_3CN and washed 3 times with 20 mL hexanes. The solvent was removed *in vacuo*, yielding 6.99 g (96%) of a yellow oil.

1-Hexyl-3,4,5-trimethylimidazolium iodide [C_6m_3im][I] (48a): ^{1}**H NMR** (300 MHz, $CDCl_3$, 25 °C, TMS): δ = 0.89 (t, ^3J(H,H) = 6.6 Hz, 3H; CH_2CH_3), 1.32-1.34 (m; 6H; $(CH_2)_3CH_3$), 1.82-1.92 (m, 2H; NCH_2CH_2; m), 2.27 (s, 3H; $CH_3C^{4/5}$), 2.29 (s, 3H; $CH_3C^{4/5}$), 3.95 (s, 3H; NCH_3), 4.15 (2H, t, ^3J(H,H) =

7.4 Hz, 2H; NCH_2), 9.96 ppm (s, 1H; C^2H); **^{13}C NMR** (75 MHz, $CDCl_3$, 25 °C, TMS): δ = 8.90 (CH_3C^4, CH_3C^5), 14.00 ($CH_3(CH_2)_5$), 22.46 (CH_2), 26.05 (CH_2), 29.93 (NCH_2CH_2), 31.16 (CH_2), 34.54 (NCH_3), 47.47 (NCH_2), 126.36 ($CH_3C^{4/5}$), 127.38 ($CH_3C^{4/5}$), 135.21 ppm (CH); **IR** (ATR): ν = 1202, 1452, 1570, 1633, 2928 cm^{-1}; **MS** (ES): *m/z* (%): 195.3 (100) [M+H$^+$]; yield: 99%, yellow oil.

1-Hexyl-2,3,4,5-tetramethylimidazolium iodide [$C_6C_1m_3im$][I] (49a): ^{1}H NMR (300 MHz, $CDCl_3$, 25 °C, TMS): δ = 0.89 (t, ^3J(H,H) = 6.6 Hz, 3H; CH_2CH_3), 1.27-1.44 (m; 6H; $(CH_2)_3CH_3$), 1.67-1.77 (m, 2H; NCH_2CH_2; m), 2.27 (s, 3H; $CH_3C^{4/5}$), 2.28 (s, 3H; $CH_3C^{4/5}$), 2.82 (s, 3H; C^2CH_3), 3.81 (s, 3H; NCH_3), 4.06 ppm (2H, t, ^3J(H,H) = 7.4 Hz, 2H; NCH_2); **^{13}C NMR** (75 MHz, $CDCl_3$, 25 °C, TMS): δ = 9.22 ($CH_3C^{4/5}$), 9.47 ($CH_3C^{4/5}$), 12.43 (C^2CH_3), 14.00 ($CH_3(CH_2)_5$), 22.41 (CH_2), 26.26 (CH_2), 29.79 (NCH_2CH_2), 31.18 (CH_2), 33.77 (NCH_3), 46.29 (NCH_2), 125.03 ($CH_3C^{4/5}$), 126.25 ($CH_3C^{4/5}$), 142.02 ppm (C^2); **IR** (ATR): ν = 727, 920 1373, 1444, 1533, 1648, 2929 cm^{-1}; **MS** (ES): *m/z* (%): 209.3 (100) [M+H$^+$]; yield: 99%, yellow oil.

2-Ethyl-1-hexyl-3,4,5-trimethylimidazolium iodide [$C_6C_2m_3im$][I] (50a): ^{1}H NMR (300 MHz, $CDCl_3$, 25 °C, TMS): δ = 0.90 (t, ^3J(H,H) = 6.9 Hz, 3H; CH_2CH_3), 1.26-1.44 (m; 6H; $(CH_2)_3CH_3$), 1.34 (t, ^3J(H,H) = 7.7 Hz, 3H; $C^2CH_2CH_3$), 1.69-1.80 (m, 2H; NCH_2CH_2; m), 2.27 (s, 3H; $CH_3C^{4/5}$), 2.29 (s, 3H; $CH_3C^{4/5}$), 3.19 (q, ^3J(H,H) = 7.7 Hz, 2H; $C^2CH_2CH_3$), 3.83 (s, 3H; NCH_3), 4.04 ppm (2H, t, ^3J(H,H) = 8.0 Hz, 2H; NCH_2); **^{13}C NMR** (75 MHz, $CDCl_3$, 25 °C, TMS): δ = 9.36 ($CH_3C^{4/5}$), 9.56 ($CH_3C^{4/5}$), 12.35 ($CH_3CH_2C^2$), 13.94 ($CH_3(CH_2)_5$), 18.49 ($CH_3CH_2C^2$), 22.35 (CH_2), 26.23 (CH_2), 30.38 (NCH_2CH_2), 31.15 (CH_2), 33.64 (NCH_3), 46.19 (NCH_2), 125.14 ($CH_3C^{4/5}$), 126.57 ($CH_3C^{4/5}$), 145.90 ppm (C^2CH_2); **IR** (ATR): ν = 726, 1081, 1452, 1528, 2929 cm^{-1}; **MS** (ES): *m/z* (%): 223.3 (100) [M+H$^+$]; yield: 99%, yellow oil.

1-Hexyl-2-isopropyl-3,4,5-trimethylimidazolium iodide [$C_6C_{i3}m_3im$][I] (51a): ^{1}H NMR (300 MHz, $CDCl_3$, 25 °C, TMS): δ = 0.87-0.89 (m, 3H; CH_2CH_3), 1.28-1.48 (m; 6H; $(CH_2)_3CH_3$), 1.52-1.77 (m, 2H; NCH_2CH_2), 1.55 (d, ^3J(H,H) = 7.2 Hz, 6H; $CH(CH_3)_2$), 2.28 (s, 3H; $CH_3C^{4/5}$), 2.31 (s, 3H; $CH_3C^{4/5}$), 3.60-3.72 (m, 1H; $CH(CH_3)_2$), 3.87 (s, 3H; NCH_3), 4.10 ppm (2H, t, ^3J(H,H) = 7.4 Hz, 2H; NCH_2); **^{13}C NMR** (75 MHz, $CDCl_3$, 25 °C, TMS): δ = 9.50 ($CH_3C^{4/5}$), 9.73 ($CH_3C^{4/5}$), 13.96 ($CH_3(CH_2)_5$), 19.88 ($CH(CH_3)_2$), 22.44 (CH_2), 25.36 (CH_2), 26.28 (NCH_2CH_2), 30.61 (CH_2), 31.24 (NCH_3), 34.29 (CH), 46.18 (CH_2), 125.34 ($CH_3C^{4/5}$), 127.24 ($CH_3C^{4/5}$), 147.72 ppm (C^2CH); **IR** (ATR): ν = 746, 1239, 1334, 1454, 1520, 2928 cm^{-1}; **MS** (ES): *m/z* (%): 237.3 (100) [M+H$^+$]; yield: 99%, yellow oil.

3.4.3) N-alkylimidazolium bis(trifluoromethylsulfonyl)imide ionic liquids

Procedure for the synthesis of 1-ethyl-2-isopropyl-3,4,5-trimethylimidazolium bis(trifluoromethylsulfonyl)imide [$C_2C_{i3}m_3im$][NTf_2] (47b): To a 50 mL flask charged with ionic liquid [$C_2C_{i3}m_3im$][I] (20 mmol, 6.18 g) was added demineralised water (20 mL). Then lithium bis(trifluoromethylsulfonyl)imide (20.6 mmol, 5.79 g) was added to the solution. The

flask was provided with a cooler with cotton plug and the mixture was heated to 50 °C for 8h. After reaction, the mixture was allowed to cool to 0 °C and 10 mL of CH_2Cl_2 was added. The aqueous layer was decanted, and the organic layer was washed 3 times with demineralised water (40 mL), the dichloromethane was removed *in vacuo*. The ionic liquid was dried for 8h at 120 °C under reduced pressure (0.5 mbar). A white solid was obtained in 93% yield.

1-Ethyl-3,4,5-trimethylimidazolium bis(trifluoromethylsulfonyl)imide [C_2m_3im]NTf_2] (44b):

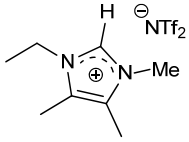

^{1}H NMR (300 MHz, $CDCl_3$, 25 °C, TMS): δ = 1.46 (t, ^3J(H,H) = 7.2 Hz, 3H; NCH_2CH_3), 2.23 (s, 3H; $CH_3C^{4/5}$), 2.24 (s, 3H; $CH_3C^{4/5}$), 3.72 (s, 3H; NCH_3), 4.07 (q, ^3J(H,H) = 7.2 Hz, 2H; NCH_2CH_3), 8.47 ppm (s, 1H; CH); **^{13}C NMR** (75 MHz, $CDCl_3$, 25 °C, TMS): δ = 8.05 ($CH_3C^{4/5}$), 8.14 ($CH_3C^{4/5}$), 14.60 (CH_3CH_2), 33.47 (NCH_3), 42.35 (CH_2), 119.87 (q, ^1J(C,F) = 320.8 Hz; CF_3), 126.85 ($CH_3C^{4/5}$), 127.82 ($CH_3C^{4/5}$), 133.44 ppm (CH); **^{19}F NMR** (282 MHz, $CDCl_3$, 25 °C): δ = -78.95 ppm; **IR** (ATR): ν = 1052, 1134, 1176, 1348, 1575 cm^{-1}; **MS** (ES): *m/z* (%): 139.3 (100) [M+H$^+$]; yield: 93%, white solid.

1-Ethyl-2,3,4,5-tetramethylimidazolium bis(trifluoromethylsulfonyl)imide [$C_2C_1m_3$im]NTf_2] (45b):

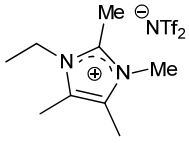

^{1}H NMR (300 MHz, $CDCl_3$, 25 °C, TMS): δ = 1.35 (t, ^3J(H,H) = 7.4 Hz, 3H; NCH_2CH_3), 2.20 (s, 3H; $CH_3C^{4/5}$), 2.22 (s, 3H; $CH_3C^{4/5}$), 2.56 (s, 3H; C^2CH_3), 3.60 (s, 3H; NCH_3), 4.03 ppm (q, ^3J(H,H) = 7.4 Hz, 2H; NCH_2CH_3); **^{13}C NMR** (75 MHz, $CDCl_3$, 25 °C, TMS): δ = 8.18 ($CH_3C^{4/5}$), 8.38 ($CH_3C^{4/5}$), 9.76 (C^2CH_3), 14.54 (CH_3CH_2), 31.80 (NCH_3), 40.63 (CH_2), 119.92 (q, ^1J(C,F) = 320.8 Hz; CF_3), 124.82 ($CH_3C^{4/5}$), 126.27 ($CH_3C^{4/5}$), 141.69 ppm (C^2CH_3); **^{19}F NMR** (282 MHz, $CDCl_3$, 25 °C): δ = -79.25 ppm; **IR** (ATR): ν = 613, 1049, 1136, 1184, 1347 cm^{-1}; **MS** (ES): *m/z* (%): 153.3 (100) [M+H$^+$]; yield: 95%, yellow oil.

1,2-Diethyl-3,4,5-trimethylimidazolium bis(trifluoromethylsulfonyl)imide [$C_2C_2m_3$im][NTf_2] (46b):

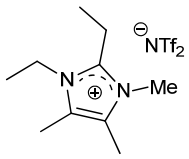

^{1}H NMR (300 MHz, $CDCl_3$, 25 °C, TMS): δ = 1.29 (t, ^3J(H,H) = 7.7 Hz, 3H; $C^2CH_2CH_3$), 1.40 (t, ^3J(H,H) = 7.4 Hz, 3H; NCH_2CH_3), 2.23 (s, 3H; $CH_3C^{4/5}$), 2.25 (s, 3H; $CH_3C^{4/5}$), 3.00 (q, ^3J(H,H) = 7.7 Hz, 2H; $C^2CH_2CH_3$), 3.66 (s, 3H; NCH_3), 4.06 ppm (q, ^3J(H,H) = 7.4 Hz, 2H; NCH_2CH_3); **^{13}C NMR** (75 MHz, $CDCl_3$, 25 °C, TMS): δ = 8.30 ($CH_3C^{4/5}$), 8.46 ($CH_3C^{4/5}$), 11.48 (CH_3CH_2C), 15.25 (NCH_2CH_3), 17.24 (CH_2C), 31.67 (NCH_3), 40.55 (NCH_2), 119.82 (q, ^1J(C,F) = 321.1 Hz; CF_3) 124.95 ($CH_3C^{4/5}$), 126.54 ($CH_3C^{4/5}$), 145.54 ppm (C^2CH_2); **^{19}F NMR** (282 MHz, $CDCl_3$, 25 °C): δ = -78.92 ppm; **IR** (ATR): ν = 314, 788, 1053, 1135, 1176, 1348 cm^{-1}; **MS** (ES): *m/z* (%): 167.3 (100) [M+H$^+$]; yield: 97%, white solid.

1-Ethyl-2-isopropyl-3,4,5-trimethylimidazolium bis(trifluoromethylsulfonyl)imide [$C_2C_{i3}m_3$im][NTf_2] (47b):

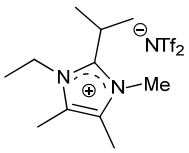

^{1}H NMR (300 MHz, $CDCl_3$, 25 °C, TMS): δ = 1.37 (t, ^3J(H,H) = 7.4 Hz, 3H; NCH_2CH_3), 1.47 (d, ^3J(H,H) = 7.2 Hz, 6H; $CH(CH_3)_2$), 2.21 (s, 3H; $CH_3C^{4/5}$), 2.23 (s, 3H; $CH_3C^{4/5}$), 3.44-3.59 (m, 1H; CH), 3.70 (s, 3H; NCH_3), 4.09 ppm (q, ^3J(H,H) = 7.4 Hz, 2H; NCH_2CH_3); **^{13}C NMR** (75 MHz, $CDCl_3$, 25 °C, TMS): δ = 8.47 ($CH_3C^{4/5}$), 8.58 ($CH_3C^{4/5}$), 15.44 (CH_3CH_2), 19.01 ($CH(CH_3)_2$), 25.19 (CH), 32.55 (NCH_3),

40.74 (CH_2), 119.88 (q, ^1J(C,F) = 321.5 Hz; CF_3), 125.18 ($CH_3C^{4/5}$), 127.11 ($CH_3C^{4/5}$), 147.40 ppm (C^2CH); **^{19}F NMR** (282 MHz, $CDCl_3$, 25 °C): δ = -78.73 ppm; **IR** (ATR): ν = 612, 1053, 1137, 1180, 1347 cm^{-1}; **MS** (ES): *m/z* (%): 181.3 (100) [M+H$^+$]; yield:94%, yellow solid.

1-Hexyl-3,4,5-trimethylimidazolium bis(trifluoromethylsulfonyl)imide [C_6m_3im][NTf_2] (48b):

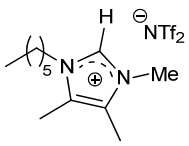

^{1}H NMR (300 MHz, $CDCl_3$, 25 °C, TMS): δ = 0.89 (t, ^3J(H,H) = 6.6 Hz, 3H; CH_2CH_3), 1.27-1.37 (m; 6H; $(CH_2)_3CH_3$), 1.73-1.84 (m, 2H; NCH_2CH_2), 2.24 (s, 6H; $CH_3C^{4/5}$), 3.75 (s, 3H; NCH_3), 4.01 (2H, t, ^3J(H,H) = 7.7 Hz, 2H; NCH_2), 8.55 ppm (s, 1H; C^2H); **^{13}C NMR** (75 MHz, $CDCl_3$, 25 °C, TMS): δ = 8.15 ($CH_3C^{4/5}$), 8.34 ($CH_3C^{4/5}$), 13.85 ($CH_3(CH_2)_5$), 22.32 (CH_2), 25.87 (CH_2), 29.68 (NCH_2CH_2), 31.04 (CH_2), 33.51 (NCH_3), 47.29 (NCH_2), 119.86 (q, ^1J(C,F) = 321.8 Hz; CF_3) 126.86 ($CH_3C^{4/5}$), 127.78 ($CH_3C^{4/5}$), 134.01 ppm (CH); **^{19}F NMR** (282 MHz, $CDCl_3$, 25 °C): δ = -74.89 ppm; **IR** (ATR): ν = 614, 1053, 1177, 1348, 1574, 2934 cm^{-1}; **MS** (ES): *m/z* (%): 195.3 (100) [M+H$^+$]; yield: 95%, colourless oil.

1-Hexyl-2,3,4,5-tetramethylimidazolium bis(trifluoromethylsulfonyl)imide [$C_6C_1m_3$im][NTf_2] (49b):

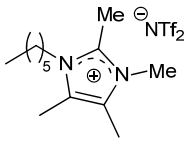

^{1}H NMR (300 MHz, $CDCl_3$, 25 °C, TMS): δ = 0.89 (t, ^3J(H,H) = 6.6 Hz, 3H; CH_2CH_3), 1.26-1.40 (m; 6H; $(CH_2)_3CH_3$), 1.60-1.71 (m, 2H; NCH_2CH_2; m), 2.20 (s, 6H; $CH_3C^{4/5}$), 2.55 (s, 3H; C^2CH_3), 3.59 (s, 3H; NCH_3), 3.92 ppm (2H, t, ^3J(H,H) = 7.7 Hz, 2H; NCH_2); **^{13}C NMR** (75 MHz, $CDCl_3$, 25 °C, TMS): δ = 8.47 ($CH_3C^{4/5}$), 10.08 (C^2CH_3), 13.92 ($CH_3(CH_2)_5$), 22.41 (CH_2), 26.18 (CH_2), 29.65 (NCH_2CH_2), 31.16 (CH_2), 31.90 (NCH_3), 45.64 (NCH_2), 119.89 (q, ^1J(C,F) = 320.8 Hz; CF_3); 125.05 ($CH_3C^{4/5}$), 126.25 ($CH_3C^{4/5}$), 141.81 ppm (C^2); **^{19}F NMR** (282 MHz, $CDCl_3$, 25 °C): δ = -78.95 ppm; **IR** (ATR): ν = 1053, 1135, 1176, 1331, 1348 cm^{-1}; **MS** (ES): *m/z* (%): 209.3 (100) [M+H$^+$]; yield: 98%, yellow oil.

2-Ethyl-1-hexyl-4,5-dimethylimidazolium bis(trifluoromethylsulfonyl)imide [$C_6C_2m_3$im][NTf_2] (50b):

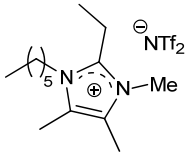

^{1}H NMR (300 MHz, $CDCl_3$, 25 °C, TMS): δ = 0.91 (t, ^3J(H,H) = 6.3 Hz, 3H; CH_2CH_3), 1.25-1.42 (m; 6H; $(CH_2)_3CH_3$), 1.30 (t, ^3J(H,H) = 7.7 Hz, 3H; $C^2CH_2CH_3$), 1.65-1.73 (m, 2H; NCH_2CH_2; m), 2.23 (s, 6H; $CH_3C^{4/5}$), 2.99 (q, ^3J(H,H) = 7.7 Hz, 2H; $C^2CH_2CH_3$), 3.66 (s, 3H; NCH_3), 3.94 ppm (2H, t, ^3J(H,H) = 8.3 Hz, 2H; NCH_2); **^{13}C NMR** (75 MHz, $CDCl_3$, 25 °C, TMS): δ = 8.43 ($CH_3C^{4/5}$), 8.47 ($CH_3C^{4/5}$), 11.36 ($CH_3CH_2C^2$), 13.91 ($CH_3(CH_2)_5$), 17.38 ($CH_3CH_2C^2$), 22.46 (CH_2), 26.23 (CH_2), 30.24 (NCH_2CH_2), 31.25 (CH_2), 31.74 (NCH_3), 45.59 (NCH_2), 120.02 (q, ^1J(C,F) = 321.8 Hz; CF_3), 125.29 ($CH_3C^{4/5}$), 126.69 ($CH_3C^{4/5}$), 145.72 ppm (C^2CH_2); **^{19}F NMR** (282 MHz, $CDCl_3$, 25 °C): δ = -79.21 ppm; **IR** (ATR): ν = 615, 1053, 1134, 1176 cm^{-1}; **MS** (ES): *m/z* (%): 223.3 (100) [M+H$^+$]; yield: 98%, yellow oil.

1-Hexyl-2-isopropyl-3,4,5-trimethylimidazolium bis(trifluoromethylsulfonyl)imide [$C_6C_{i3}m_3$im][NTf_2] (51b):

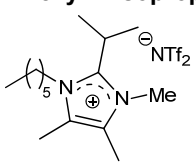

^{1}H NMR (300 MHz, $CDCl_3$, 25 °C, TMS): δ = 0.90 (m, ^3J(H,H) = 6.6 Hz, 3H; CH_2CH_3), 1.24-1.40 (m; 6H; $(CH_2)_3CH_3$), 1.47 (d, ^3J(H,H) = 7.2 Hz, 6H; $CH(CH_3)_2$),1.61-1.69 (m, 2H; NCH_2CH_2; m), 2.21 (s, 6H; $CH_3C^{4/5}$), 3.41-3.65 (m, 1H; CH), 3.70 (s, 3H; NCH_3), 3.97 ppm (2H, t, ^3J(H,H) = 8.2 Hz, 2H; NCH_2); **^{13}C NMR** (75 MHz, $CDCl_3$, 25 °C, TMS): δ = 8.53 ($CH_3C^{4/5}$), 8.67 ($CH_3C^{4/5}$), 13.88 (CH_3CH_2), 18.93 ($CH(CH_3)_2$), 22.40

(CH_2), 25.25 (CH_2), 26.12 (CH_2) 30.40 (CH_2) 31.16 (NCH_3), 32.63 (CH), 45.68 (NCH_2), 119.94 (q, ^1J(C,F) = 321.1 Hz; CF_3), 125.37 ($CH_3C^{4/5}$), 127.18 ($CH_3C^{4/5}$), 147.49 ppm (C^2CH); **^{19}F NMR** (282 MHz, $CDCl_3$, 25 °C): δ = -78.96 ppm; **IR** (ATR): ν = 1054, 1135, 1177, 1349, 2360 cm^{-1}; **MS** (ES): *m/z* (%): 237.3 (100) [M+H$^+$]; yield: 97%, yellow oil.

3.4.4) N-alkylimidazolium dicyanamide ionic liquids

Procedure for the sodium mediated metathesis towards 1-ethyl-2-isopropyl-3,4,5-trimethylimidazolium dicyanamide [$C_2C_{i3}m_3$im][N(CN)$_2$] (47c): To a 50 mL flask charged with the ionic liquid [$C_2C_{i3}m_3$im][OMs] (20 mmol, 5.53 g) was added demineralised water (20 mL) and $Na(CN)_2$ (24 mmol, 2.14 g). The mixture was heated to 50 °C and stirred overnight to ensure complete exchange of the ions. After reaction, the water was removed by rotary evaporation, and acetone was added. After storage at -18 °C, the precipitate was filtered off. The solvent and residual water were removed from the filtrate by rotary evaporation and the resulting ionic liquid was dissolved in 30 mL of chloroform and stored at -18 °C for at least 4h. Again, the precipitate was filtered off and the filtrate evaporated. This last step was repeated until no further precipitation was observed after storage at -18 °C. The solvent was removed *in vacuo* to lead to a yellow oil in quantitative yield.

Procedure for the silver mediated metathesis towards 1-ethyl-2-isopropyl-3,4,5-trimethylimidazolium dicyanamide [$C_2C_{i3}m_3$im][N(CN)$_2$] (47c): To a 50 mL flask charged with the ionic liquid [$C_2C_{i3}m_3$im][I] (20 mmol, 6.18 g) was added demineralised water (20 mL) and CH_3CN (10 mL). Then silver dicyanamide (24 mmol, 4.15g) was added to the solution. The flask was equipped with a cooler with cotton plug and the mixture was heated to 50 °C for 8h. After reaction, the mixture was allowed to cool to 0 °C. The precipitate was filtered off and the water was removed *in vacuo*. The resulting yellow oil was dissolved in dry CH_2Cl_2 and cooled to -18 °C, after filtration of a white precipitate, this step was repeated until no further precipitation was visible, and dichloromethane was removed *in vacuo*. The ionic liquid was dried for 8 h at 80 °C under reduced pressure (0.5 mbar). An opaque white solid was obtained in quantitative yield.

1-Ethyl-3,4,5-trimethylimidazolium dicyanamide [C_2m_3im][N(CN)$_2$] (44c): ^{1}H NMR (300 MHz, $CDCl_3$, 25 °C, TMS): δ = 1.58 (t, ^3J(H,H) = 7.3 Hz, 3H; NCH_2CH_3), 2.30 (s, 3H; $CH_3C^{4/5}$), 2.31 (s, 3H; $CH_3C^{4/5}$), 3.87 (s, 3H; NCH_3), 4.18 (q, ^3J(H,H) = 7.4 Hz, 2H; NCH_2CH_3), 9.05 ppm (s, 1H; CH); **^{13}C NMR** (75 MHz, $CDCl_3$, 25 °C, TMS): δ = 8.20 ($CH_3C^{4/5}$), 8.31 ($CH_3C^{4/5}$), 14.67 (CH_3CH_2), 33.61 (NCH_2), 42.29 (NCH_3), 119.50 ($N(CN)_2$), 126.86 ($CH_3C^{4/5}$), 127.70 ($CH_3C^{4/5}$), 133.60 ppm (CH); **IR** (ATR): ν = 1313, 1571, 2131, 2230, 2362, 2980 cm^{-1}; **MS** (ES): *m/z* (%): 139.3 (100) [M+H$^+$]; yield: 86%, white powder.

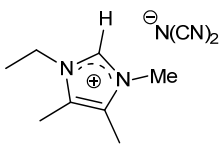

1-Ethyl-2,3,4,5-tetramethylimidazolium dicyanamide [$C_2C_1m_3$im][N(CN)$_2$] (45c): ^{1}H NMR (300 MHz, $CDCl_3$, 25 °C, TMS): δ = 1.42 (t, ^3J(H,H) = 7.4 Hz, 3H; NCH_2CH_3), 2.29 (s, 3H; $CH_3C^{4/5}$), 2.31 (s, 3H; $CH_3C^{4/5}$), 2.71 (s, 3H; C^2CH_3), 3.72 (s, 3H; NCH_3), 4.14 ppm (q, ^3J(H,H) = 7.4 Hz, 2H; NCH_2CH_3); **^{13}C NMR** (75 MHz, $CDCl_3$, 25 °C, TMS): δ = 8.55 ($CH_3C^{4/5}$), 8.76 ($CH_3C^{4/5}$), 10.18 (C^2CH_3), 14.86 (CH_3CH_2), 32.12 (CH_2), 40.83 (NCH_3), 119.56 ($N(CN)_2$), 125.03 ($CH_3C^{4/5}$), 126.34 ($CH_3C^{4/5}$), 141.67 ppm (C^2); **IR** (ATR): ν =

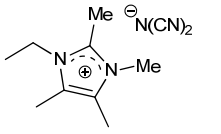

1302, 1447, 1537, 2125, 2223 cm^{-1}; **MS** (ES): *m/z* (%): 153.3 (100) [M+H$^+$]; yield: 83%, yellow oil.

1,2-Diethyl-3,4,5-trimethylimidazolium dicyanamide [$C_2C_2m_3$im][N(CN)$_2$] (46c): ^{1}H NMR

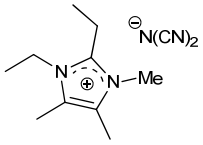

(300 MHz, $CDCl_3$, 25 °C, TMS): δ = 1.36 (t, ^3J(H,H) = 7.7 Hz, 3H; $C^2CH_2CH_3$), 1.45 (t, ^3J(H,H) = 7.4 Hz, 3H; NCH_2CH_3), 2.30 (s, 3H; $CH_3C^{4/5}$), 2.32 (s, 3H; $CH_3C^{4/5}$), 3.09 (q, ^3J(H,H) = 7.7 Hz, 2H; $C^2CH_2CH_3$), 3.75 (s, 3H; NCH_3), 4.14 ppm (q, ^3J(H,H) = 7.4 Hz, 2H; NCH_2CH_3); **^{13}C NMR** (75 MHz, $CDCl_3$, 25 °C, TMS): δ = 8.52 ($CH_3C^{4/5}$), 8.69 ($CH_3C^{4/5}$), 11.73 (CH_3CH_2C), 15.47 (NCH_2CH_3), 17,36 (CH_2C), 31.88 (NCH_2), 40.67 (NCH_3), 119.63 ($N(CN)_2$), 125.09 ($CH_3C^{4/5}$), 126.59 ($CH_3C^{4/5}$), 145.55 ppm (C^2CH_2); **IR** (ATR): ν = 736, 919, 1307, 1530, 2128, 2227 cm^{-1}; **MS** (ES): *m/z* (%): 167.3 (100) [M+H$^+$]; yield: 89%, yellow oil.

1-Ethyl-2-isopropyl-3,4,5-trimethylimidazolium dicyanamide [$C_2C_{i3}m_3$im][N(CN)$_2$] (47c):

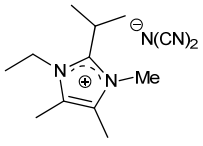

^{1}H NMR (300 MHz, $CDCl_3$, 25 °C, TMS): δ = 1.43 (t, ^3J(H,H) = 7.4 Hz, 3H; NCH_2CH_3), 1.54 (d, ^3J(H,H) = 7.2 Hz, 6H; $CH(CH_3)_2$), 2.30 (s, 3H; $CH_3C^{4/5}$), 2.31 (s, 3H; $CH_3C^{4/5}$), 3.53-3.68 (m, 1H; CH), 3.76 (s, 3H; NCH_3), 4.18 ppm (q, ^3J(H,H) = 7.4 Hz, 2H; NCH_2CH_3); **^{13}C NMR** (75 MHz, $CDCl_3$, 25 °C, TMS): δ = 8.64 ($CH_3C^{4/5}$), 8.76 ($CH_3C^{4/5}$), 15.59 (CH_3CH_2), 19.12 (CH_3CH), 25.13 (CH), 32.70 (NCH_3), 40.81 (CH_2), 119.56 ($N(CN)_2$), 125.21 ($CH_3C^{4/5}$), 127.05 ($CH_3C^{4/5}$), 147.43 ppm (C^2CH); **IR** (ATR): ν = 1089, 1303, 1523, 2126, 2225 cm^{-1}; **MS** (ES): *m/z* (%): 181.3 (100) [M+H$^+$]; yield:82%, yellow oil.

1-Hexyl-3,4,5-trimethylimidazolium dicyanamide [C_6m_3im][N(CN)$_2$] (48c): ^{1}H NMR (300

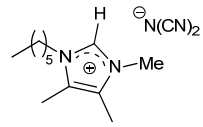

MHz, $CDCl_3$, 25 °C, TMS): δ = 0.90 (t, ^3J(H,H) = 6.9 Hz, 3H; CH_2CH_3), 1.25-1.41 (m; 6H; $(CH_2)_3CH_3$), 1.80-1.90 (m, 2H; NCH_2CH_2), 2.30 (s, 6H; $CH_3C^{4/5}$), 3.86 (s, 3H; NCH_3), 4.08 (2H, t, ^3J(H,H) = 7.7 Hz, 2H; NCH_2), 8.94 ppm (s, 1H; C^2H); **^{13}C NMR** (75 MHz, $CDCl_3$, 25 °C, TMS): δ = 8.44 ($CH_3C^{4/5}$), 8.61 ($CH_3C^{4/5}$), 13.97 ($CH_3(CH_2)_5$), 22.41 (CH_2), 25.99 (CH_2), 29.70 (NCH_2CH_2), 31.12 (CH_2), 33.91 (NCH_3), 47.41 (NCH_2), 119.79 ($N(CN)_2$), 126.89 ($CH_3C^{4/5}$), 127.79 ($CH_3C^{4/5}$), 134.57 ppm (CH); **IR** (ATR): ν = 1303, 1452, 1572, 2126, 2224 cm^{-1}; **MS** (ES): *m/z* (%): 195.3 (100) [M+H$^+$]; yield: 91%, yellow oil.

1-Hexyl-2,3,4,5-tetramethylimidazolium dicyanamide [$C_6C_1m_3$im][N(CN)$_2$] (49c): ^{1}H NMR

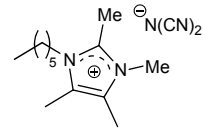

(300 MHz, $CDCl_3$, 25 °C, TMS): δ = 0.90 (t, ^3J(H,H) = 6.6 Hz, 3H; CH_2CH_3), 1.29-1.41 (m; 6H; $(CH_2)_3CH_3$), 1.66-1.76 (m, 2H; NCH_2CH_2; m), 2.29 (s, 6H; $CH_3C^{4/5}$), 2.69 (s, 3H; C^2CH_3), 3.73 (s, 3H; NCH_3), 4.03 ppm (2H, t, ^3J(H,H) = 7.7 Hz, 2H; NCH_2); **^{13}C NMR** (75 MHz, $CDCl_3$, 25 °C, TMS): δ = 8.75 ($CH_3C^{4/5}$), 8.81 ($CH_3C^{4/5}$), 10.44 (C^2CH_3), 13.94 ($CH_3(CH_2)_5$), 22.40 (CH_2), 26.17 (CH_2), 29.64 (NCH_2CH_2), 31.12 (CH_2), 32.19 (NCH_3), 45.77 (NCH_2), 119.60 ($N(CN)_2$), 125.26 ($CH_3C^{4/5}$), 126.36 ($CH_3C^{4/5}$), 141.73 ppm (C^2); **IR** (ATR): ν = 1310, 1538, 1650, 2132, 2238 cm^{-1}; **MS** (ES): *m/z* (%): 209.3 (100) [M+H$^+$]; yield: 99%, yellow oil.

2-Ethyl-1-hexyl-3,4,5-trimethylimidazolium dicyanamide [$C_6C_2m_3$im][N(CN)$_2$] (50c): ^{1}H NMR (300 MHz, $CDCl_3$, 25 °C, TMS): δ = 0.91 (t, ^3J(H,H) = 6.9 Hz, 3H; CH_2CH_3), 1.25-1.44

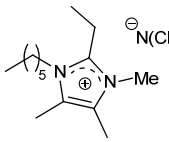

(m; 6H; $(CH_2)_3CH_3$), 1.36 (t, ^3J(H,H) = 7.7 Hz, 3H; $C^2CH_2CH_3$), 1.69-1.85 (m, 2H; NCH_2CH_2; m), 2.30 (s, 6H; $CH_3C^{4/5}$), 3.07 (q, ^3J(H,H) = 7.7 Hz, 2H; $C^2CH_2CH_3$), 3.75 (s, 3H; NCH_3), 4.02 ppm (2H, t, ^3J(H,H) = 8.3 Hz, 2H; NCH_2); **^{13}C NMR** (75 MHz, $CDCl_3$, 25 °C, TMS): δ = 8.81 ($CH_3C^{4/5}$), 11.71 ($CH_3CH_2C^2$), 13.94 ($CH_3(CH_2)_5$), 17.59 ($CH_3CH_2C^2$), 22.41 (CH_2), 26.26 (CH_2), 30.31 (NCH_2CH_2), 31.16 (CH_2), 32.03 (NCH_3), 45.71 (NCH_2), 119.73 ($N(CN)_2$), 125.35 ($CH_3C^{4/5}$), 126.68 ($CH_3C^{4/5}$), 145.72 ppm (C^2CH_2); **IR** (ATR): ν = 1301, 1453, 1531, 2125, 2222 cm^{-1}; **MS** (ES): *m/z* (%): 223.3 (100) [M+H$^+$]; yield: 89%, yellow oil.

1-Hexyl-2-isopropyl-3,4,5-trimethylimidazolium dicyanamide [$C_6C_{i3}m_3$im][N(CN)$_2$] (51c):

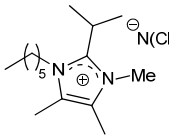

^{1}H NMR (300 MHz, $CDCl_3$, 25 °C, TMS): δ = 0.91 (m, ^3J(H,H) = 6.9 Hz, 3H; CH_2CH_3), 1.30-1.44 (m; 6H; $(CH_2)_3CH_3$), 1.53 (d, ^3J(H,H) = 7.2 Hz, 6H; $CH(CH_3)_2$),1.66-1.76 (m, 2H; NCH_2CH_2; m), 2.29 (s, 6H; $CH_3C^{4/5}$), 3.49-3.63 (m, 1H; C*H*), 3.80 (s, 3H; NCH_3), 4.06 ppm (2H, t, ^3J(H,H) = 8.0 Hz, 2H; NCH_2); **^{13}C NMR** (75 MHz, $CDCl_3$, 25 °C, TMS): δ = 8.84 ($CH_3C^{4/5}$), 8.92 ($CH_3C^{4/5}$), 13.91 ($CH_3(CH_2)_5$), 19.16 ($CH(CH_3)_2$), 22.40 (CH_2), 25.31 (CH_2), 26.15 (NCH_2CH_2), 30.44 (CH_2), 31.16 (NCH_3), 32.85 (CH), 45.80 (CH_2), 119.41 ($N(CN)_2$), 125.46 ($CH_3C^{4/5}$), 127.18 ($CH_3C^{4/5}$), 147.53 ppm (C^2CH); **IR** (ATR): ν = 1300, 1456, 1522, 2124, 2221 cm^{-1}; **MS** (ES): *m/z* (%): 237.3 (100) [M+H$^+$]; yield: 93%, yellow oil.

3.5. Synthesis of *N*-alkoxy and *N*-alkenylimidazolium ionic liquids

3.5.1) N-alkoxy- and N-alkenylimidazolium methanesulfonate ionic liquids

Compounds **61**-**62a** were synthesised using the procedure for compound **44d** described at page 142.

1-Allyl-2-isopropyl-3,4,5-trimethylimidazolium methanesulfonate [$C_AC_1C_{i3}m_2$im][OMs] (61a):

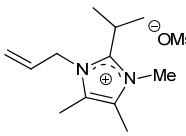

^{1}H NMR (300 MHz, $CDCl_3$, 25 °C, TMS): δ = 1.50 (d, ^3J(H,H) = 7.2 Hz, 6H; $CH(CH_3)_2$), 2.23 (s, 3H; $CH_3C^{4/5}$), 2.29 (s, 3H; $CH_3C^{4/5}$), 2.70 (s, 3H; CH_3SO_3), 3.53-3.67 (m, 1H; $CH(CH_3)_2$), 3.84 (s, 3H; CH_3SO_3), 4.84-4.89 (m, 2H; NCH_2), 4.89 (d, ^3J(H,H) = 17.1 Hz, 1H; $CH=CH_EH_Z$), 5.32 (d, ^3J(H,H) = 10.5 Hz, 1H; $CH=CH_EH_Z$), 5.90-6.04 ppm (ddt, ^3J(H,H) = 17.1 Hz, ^3J(H,H) = 10.5 Hz, ^3J(H,H) = 4.4 Hz, 1H; $CH=CH_2$); **^{13}C NMR** (75 MHz, $CDCl_3$, 25 °C, TMS): δ = 8.66 ($CH_3C^{4/5}$), 8.98 ($CH_3C^{4/5}$), 19.27 ($CH(CH_3)_2$), 25.31 ($CH(CH_3)_2$), 33.09 (NCH_3), 39.39 (CH_3SO_3), 47.65 (NCH_2), 117.76 ($CH=CH_2$), 125.90 ($C^{4/5}$), 126.97 ($C^{4/5}$), 131.02 ($CH=CH_2$), 148.39 ppm (C^2); **IR** (ATR): ν = 726, 1036, 1192, 1452, 1523, 1651 cm^{-1}; **MS** (ES): m/z [%]: 193.3 (100) [M+H$^+$]; yield: 98%, light yellow oil.

2-Isopropyl-1-(2-methoxyethyl)-3,4,5-trimethylimidazolium methanesulfonate [$C_{2O1}C_1C_{i3}m_2$im][OMs] (62a):

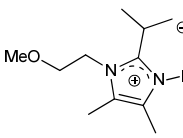

^{1}H NMR (300 MHz, $CDCl_3$, 25 °C, TMS): δ = 1.48 (d, ^3J(H,H) = 7.7 Hz, 6H; $CH(CH_3)_2$), 2.28 (s, 3H; $CH_3C^{4/5}$), 2.30 (s, 3H; $CH_3C^{4/5}$), 2.71 (s, 3H; CH_3SO_3), 3.31 (s, 3H; OCH_3), 3.65 (t, ^3J(H,H) = 5.0 Hz, 2H; CH_2O), 3.67-3.81 (m, 1H; CH), 3.83 (s, 3H, NCH_3), 4.47 ppm (t, ^3J(H,H) = 5.0 Hz, 2H; NCH_2); **^{13}C NMR** (75 MHz, $CDCl_3$, 25 °C, TMS): δ = 8.89 ($CH_3C^{4/5}$), 9.21 ($CH_3C^{4/5}$), 18.93 ($CH(CH_3)_2$),

25.18 (CH), 33.19 (NCH_3), 39.42 (CH_3SO_3), 46.00 (NCH_2), 59.09 (OCH_3), 70.36 (CH_2O), 125.76 ($C^{4/5}$), 126.76 ($C^{4/5}$), 148.96 ppm (C^2); **IR** (ATR): ν = 1039, 1119, 1184, 1458, 1523 cm^{-1}; **HRMS** (ESI/APCI) calcd for $[C_{12}H_{23}N_2O^+]$: 211.1805; found: 211.1803; **elemental analysis** calcd (%) for $C_{13}H_{26}N_2O_4S$: C 50.96, H 8.55, N 9.14; found C 50.51, H 9.11, N 9.00; yield: 96%, white crystals.

Procedure for the synthesis of 1-(2-allyloxyethyl)-2-isopropyl-3,4,5-trimethylimidazolium methanesulfonate [$C_{2OA}C_1C_{i3}m_2$im][OMs] (63a): The synthesis procedure is analogous to the procedure applied for **61a**, although longer irradiation times are to be applied for better conversion. The mixture was irradiated for 40 minutes in a microwave reactor to a temperature of 80 °C, longer reaction times lead to significant colouration. After reaction, the solvent was removed *in vacuo* and the mixture was diluted in distilled water (25 mL) and washed twice with Et_2O (20 mL), due to the better solubility of **63a** in EtOAc compared to **61a**. The aqueous layer was evaporated and dried for 6h at 100 °C and 1.0 mbar.

1-(2-Allyloxyethyl)-2-isopropyl-3,4,5-trimethylimidazolium methanesulfonate [$C_{2OA}C_1C_{i3}m_2$im][OMs] (63a): 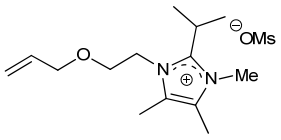 **^{1}H NMR** (300 MHz, $CDCl_3$, 25 °C, TMS): δ = 1.48 (d, ^3J(H,H) = 7.7 Hz, 6H; $CH(CH_3)_2$), 2.28 (s, 3H; $CH_3C^{4/5}$), 2.31 (s, 3H; $CH_3C^{4/5}$), 2.71 (s, 3H; CH_3SO_3), 3.65-3.85 (m, 1H; $CH(CH_3)_2$), 3.71 (t, ^3J(H,H) = 5.0 Hz, 2H; CH_2O), 3.82 (m, 3H; NCH_3), 3.95 (d, ^3J(H,H) = 5.5 Hz; OCH_2CH), 4.49 (t, ^3J(H,H) = 5.0 Hz, 2H; NCH_2), 5.18 (d, ^3J(H,H) = 10.8 Hz, 1H; $CH=CH_ZH_E$), 5.19 (d, ^3J(H,H) = 16.8 Hz, 1H; $CH=CH_ZH_E$), 5.79 ppm (ddt, ^3J(H,H) = 16.8 Hz, ^3J(H,H) = 10.8 Hz, ^3J(H,H) = 5.5 Hz, 1H; $CH=CH_2$); **^{13}C NMR** (75 MHz, $CDCl_3$, 25 °C, TMS): δ = 8.89 ($CH_3C^{4/5}$), 9.24 ($CH_3C^{4/5}$), 18.99 ($CH(CH_3)_2$), 25.13 ($CH(CH_3)_2$), 32.21 (NCH_3), 39.45 (CH_3SO_3), 46.06 (NCH_2), 68.05 (OCH_2CH), 72.36 (CH_2O), 118.05 ($CH=CH_2$), 125.84 ($C^{4/5}$), 126.80 ($C^{4/5}$), 133.69 ($CH=CH_2$), 148.96 ppm (C^2); **IR** (ATR): ν = 763, 1036, 1107, 1190 cm^{-1}; **MS** (ES): m/z [%]: 237.3 (100) $[M+H^+]$; yield: 92%, yellow liquid.

Procedure for the synthesis of allyl methanesulfonate: To a flame dried 250 mL flask, containing 80 mL of dry CH_2Cl_2 and equipped with a $CaCl_2$ tube, ally alcohol (189 mmol, 11.05 g,) and 1.1 eq. triethylamine (207 mmol, 29.2 mL) were added. The mixture was vigorously stirred and allowed to cool in an ice bath, after which dropwise 1.1 eq. methanesulfonate chloride (207 mmol, 12.89 mL) was added via a syringe. The reaction mixture was then allowed to warm to room temperature and stirred for 1 hour. After reaction, the mixture was washed once with a saturated $NaHCO_3$ mixture and once with water. The organic layer was dried with $MgSO_4$ and filtered. The filtrate was evaporated *in vacuo* and the product was distilled via short-path vacuum distillation (53 °C, 1.0 mbar).

Procedure for the synthesis of 1-allyl-3-ethyl-2-isopropyl-4,5-dimethylimidazolium methanesulfonate [$C_AC_2C_{i3}m_2$im][OMs] (64a): To a flame dried 8 mL vial, containing 4 mL of dry acetonitrile, 1-ethyl-2-isopropyl-4,5-dimethylimidazole (10 mmol, 1.66 g) was added via a syringe under a nitrogen atmosphere. To the mixture, freshly distilled allyl methanesulfonate (10.5 mmol, 1.43 g) was added. The headspace was filled with nitrogen and the vial was sealed with a PTFE cap. The mixture was irradiated for 45 minutes in a microwave reactor to a temperature of 100 °C. After reaction, the solvent was removed *in vacuo* and the mixture was diluted in distilled water (25 mL) containing 0.05 mol equivalents NaOH (dependent on

the fraction of **12** observed by ^{1}H NMR in $CDCl_3$). The aqueous layer was washed twice with 20 mL of EtOAc. The water was removed by evaporation or lyophilisation and the product was diluted in an excess of boiling acetone and stored at -18 °C for several hours. The formed crystals were filtered off. The filtrate was evaporated and again diluted in boiling acetone, until no more crystals could be filtered off after storage at -18 °C. The resulting clear solution was evaporated and the obtained oil was dried for 6h at 100 °C and 1.0 mbar.

1-Allyl-3-ethyl-2-isopropyl-4,5-dimethylimidazolium methanesulfonate [$C_AC_2C_{i3}m_2$im][OMs] (64a): 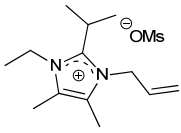
^{1}H NMR (300 MHz, $CDCl_3$, 25 °C, TMS): δ = 1.44 (d, ^3J(H,H) = 7.3 Hz, 3H; CH_2CH_3), 1.51 (d, ^3J(H,H) = 7.7 Hz, 6H; $CH(CH_3)_2$), 2.23 (s, 3H; $CH_3C^{4/5}$), 2.31 (s, 3H; $CH_3C^{4/5}$), 2.71 (s, 3H; CH_3SO_3), 3.59-3.68 (m, 1H; $CH(CH_3)_2$), 4.29 (t, ^3J(H,H) = 7.3 Hz, 3H; CH_2CH_3), 4.89 (d, ^3J(H,H) = 18.7 Hz, 1H; $CH{=}CH_EH_Z$), 4.89-4.97 (m, 2H; $CH_2CH{=}CH_2$), 5.33 (d, ^3J(H,H) = 11.0 Hz, 1H; $CH{=}CH_EH_Z$), 5.94-6.03 ppm (m, 1H; $CH{=}CH_2$); **^{13}C NMR** (75 MHz, $CDCl_3$, 25 °C, TMS): δ = 8.49 ($CH_3C^{4/5}$), 8.64 ($CH_3C^{4/5}$), 15.60 (CH_2CH_3), 19.91 ($CH(CH_3)_2$), 25.18 ($CH(CH_3)_2$), 39.35 (CH_3SO_3), 41.15 (CH_2CH_3), 47.71 ($CH_2CH{=}CH_2$), 117.53 ($CH{=}CH_2$), 125.86 ($C^{4/5}$), 126.77 ($C^{4/5}$), 131.17 ($CH{=}CH_2$), 148.09 ppm (C^2); **IR** (ATR): ν = 1039, 1181, 1513, 1648, 3432 cm^{-1}; **MS** (ES): m/z [%]: 207.3 (100) [M+H$^+$]; yield: 78%, yellow oil.

1,3-Diallyl-2-isopropyl-4,5-dimethylimidazolium methanesulfonate [$C_AC_AC_{i3}m_2$im][OMs] (65a): 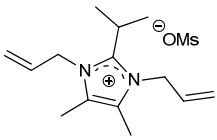
^{1}H NMR (300 MHz, $CDCl_3$, 25 °C, TMS): δ = 1.45 (d, ^3J(H,H) = 7.2 Hz, 6H; $CH(CH_3)_2$), 2.28 (s, 6H; $CH_3C^{4/5}$), 2.83 (s, 3H; CH_3SO_3), 3.57-3.71 (m, 1H; $CH(CH_3)_2$), 4.86 (dt, ^3J(H,H) = 17.5 Hz, ^4J(H,H) = 2.0 Hz, 2H; $CH{=}CH_EH_Z$), 5.02 (dt, ^3J(H,H) = 4.2 Hz, ^4J(H,H) = 2.0 Hz, 4H; NCH_2), 5.35 (dt, ^3J(H,H) = 10.6 Hz, ^4J(H,H) = 1.9 Hz, 2H; $CH{=}CH_EH_Z$), 5.95 ppm (ddt, ^3J(H,H) = 17.5 Hz, ^3J(H,H) = 10.6 Hz, ^3J(H,H) = 4.2 Hz, 2H, $CH{=}CH_2$); **^{13}C NMR** (75 MHz, $CDCl_3$, 25 °C, TMS): δ = 8.58 ($CH_3C^{4/5}$), 19.88 ($CH(CH_3)_2$), 25.30 ($CH(CH_3)_2$), 39.45 (CH_3SO_3), 47.82 ($CH_2CH{=}CH_2$), 117.48 ($CH{=}CH_2$), 126.58 (C^4, C^5), 131.08 (CH), 148.86 ppm (C^2); **IR** (ATR): ν = 920, 1511, 1646; 2358, 3424 cm^{-1}; **MS** (ES): m/z [%]: 219.3 (100) [M+H$^+$]; yield: 76%, colourless oil.

1-Allyl-2-isopropyl-3-(2-methoxyethyl)-4,5-dimethylimidazolium methanesulfonate [$C_{2O1}C_AC_{i3}m_2$im][OMs] (66a): 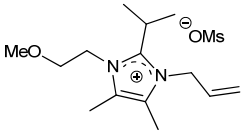
^{1}H NMR (300 MHz, $CDCl_3$, 25 °C, TMS): δ = 1.46 (d, ^3J(H,H) = 7.2 Hz, 6H; $CH(CH_3)_2$), 2.20 (s, 3H; $CH_3C^{4/5}$), 2.33 (s, 3H; $CH_3C^{4/5}$), 2.72 (s, 3H; CH_3SO_3), 3.32 (s, 3H; OCH_3), 3.69 (t, ^3J(H,H) = 5.0 Hz, 2H; CH_2O), 3.69-3.85 (m, 1H; $CH(CH_3)_2$), 4.58 (t, ^3J(H,H) = 5.0 Hz, 2H; CH_2CH_2O), 4.82-4.83 (m, 2H; $CH_2CH{=}CH_2$), 4.95 (d, ^3J(H,H) = 17.1 Hz, 1H; $CH{=}CH_ZH_E$), 5.38 (d, ^3J(H,H) = 10.5 Hz, 1H; $CH{=}CH_ZH_E$), 5.90-6.02 ppm (m, 1H; $CH{=}CH_2$); **^{13}C NMR** (75 MHz, $CDCl_3$, 25 °C, TMS): δ = 8.52 ($CH_3C^{4/5}$), 9.25 ($CH_3C^{4/5}$), 19.86 ($CH(CH_3)_2$), 25.39 ($CH(CH_3)_2$), 39.45 (CH_3SO_3), 46.23 (CH_2CH_2O), 47.94 ($CH_2CH{=}CH_2$), 59.12 (OCH_3), 70.32 (CH_2O), 118.07 ($CH{=}CH_2$), 126.49 ($C^{4/5}$), 126.57 ($C^{4/5}$), 130.82 ($CH{=}CH_2$), 149.51 ppm (C^2); **IR** (ATR): ν = 1038, 1117, 1181, 1513 cm^{-1}; **MS** (ES): m/z [%]: 237.3 (100) [M+H$^+$]; yield: 75%, white glass.

3.5.2) N-alkoxy- and N-alkenylimidazolium iodide ionic liquids

Compounds **61**-**63b** and **122b** were synthesised using the procedure for compound **47a** described at page 143.

1-Allyl-2-isopropyl-3,4,5-trimethylimidazolium iodide [$C_AC_1C_{i3}m_2$im][I] (61b): 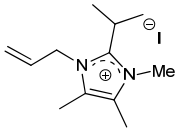
^{1}H NMR (300 MHz, $CDCl_3$, 25 °C, TMS): δ = 1.52 (d, ^3J(H,H) = 7.2 Hz, 6H; $CH(CH_3)_2$), 2.25 (s, 3H; $CH_3C^{4/5}$), 2.33 (s, 3H; $CH_3C^{4/5}$), 3.56-3.68 (m, 1H; $CH(CH_3)_2$), 3.88 (s, 3H; NCH_3), 4.87-4.91 (m, 2H; NCH_2), 4.98 (d, ^3J(H,H) = 17.1 Hz, 1H; $CH=CH_EH_Z$), 5.35 (d, ^3J(H,H) = 10.5 Hz, 1H; $CH=CH_EH_Z$), 5.93-6.02 ppm (m, 1H; $CH=CH_2$); **^{13}C NMR** (75 MHz, $CDCl_3$, 25 °C, TMS): δ = 9.24 ($CH_3C^{4/5}$), 9.82 ($CH_3C^{4/5}$), 19.73 ($CH(CH_3)_2$), 25.24 ($CH(CH_3)_2$), 34.43 (NCH_3), 48.32 (NCH_2), 118.07 ($CH=CH_2$), 125.78 ($C^{4/5}$), 127.02 ($C^{4/5}$), 130.63 ($CH=CH_2$), 148.25 ppm (C^2); **IR** (ATR): ν = 1222, 1362, 1444, 1521, 1707 cm^{-1}; **MS** (ES): m/z [%]: 193.3 (100) [M+H$^+$]; yield: 98%, light yellow oil.

2-Isopropyl-1-(2-methoxyethyl)-3,4,5-trimethylimidazolium iodide [$C_{2O1}C_1C_{i3}m_2$im][I] (62b): 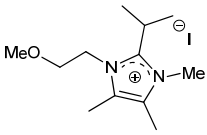
^{1}H NMR (300 MHz, $CDCl_3$, 25 °C, TMS): δ = 1.50 (d, ^3J(H,H) = 7.2 Hz, 6H; $CH(CH_3)_2$), 2.30 (s, 6H; $CH_3C^{4/5}$), 3.32 (s, 3H; OCH_3), 3.67 (t, ^3J(H,H) = 4.8 Hz, 2H; CH_2O), 3.70-3.84 (m, 1H; CH), 3.84 (s, 3H, NCH_3), 4.46 ppm (t, ^3J(H,H) = 4.8 Hz, 2H; NCH_2);**^{13}C NMR** (75 MHz, $CDCl_3$, 25 °C, TMS): δ = 9.65 ($CH_3C^{4/5}$), 9.88 ($CH_3C^{4/5}$), 19.36 ($CH(CH_3)_2$), 25.25 (CH), 34.31 (NCH_3), 46.71 (NCH_2), 59.26 (OCH_3), 70.39 (CH_2O), 125.73 ($C^{4/5}$), 126.89 ($C^{4/5}$), 148.86 ppm (C^2); **IR** (ATR): ν = 1108, 1446, 1523, 2971 cm^{-1}; **HRMS** (ESI/APCI) calcd for [$C_{12}H_{23}N_2O^+$]: 211.1805; found: 211.1810; **elemental analysis** calcd (%) for $C_{12}H_{23}IN_2O$: C 42.61, H 6.85, N 8.28; found: C 42.09, H 6.77, N 8.09; yield: 99%, white crystals.

1-(2-Allyloxyethyl)-2-isopropyl-3,4,5-trimethylimidazolium iodide [$C_{2OA}C_1C_{i3}m_2$im][I] (63b): 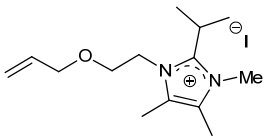
^{1}H NMR (300 MHz, $CDCl_3$, 25 °C, TMS): δ = 1.51 (d, ^3J(H,H) = 7.2 Hz, 6H; $CH(CH_3)_2$), 2.29 (s, 3H; $CH_3C^{4/5}$), 2.32 (s, 3H; $CH_3C^{4/5}$), 3.72-3.90 (m, 1H; $CH(CH_3)_2$) 3.73 (t, ^3J(H,H) = 5.1 Hz, 2H; CH_2O), 3.83 (s, 3H; NCH_3), 3.96 (dt, ^3J(H,H) = 6.1 Hz, ^4J(H,H) = 1.5 Hz; OCH_2CH), 4.49 (t, ^3J(H,H) = 5.1 Hz, 2H; NCH_2), 5.19 (dt, ^3J(H,H) = 10.6 Hz, ^4J(H,H) = 1.5 Hz, 1H; $CH=CH_ZH_E$), 5.20 (dt, ^3J(H,H) = 16.7 Hz, ^4J(H,H) = 1.5 Hz, 1H; $CH=CH_ZH_E$), 5.80 ppm (ddt, ^3J(H,H) = 16.7 Hz, ^3J(H,H) = 10.6 Hz, ^3J(H,H) = 6.1 Hz, 1H; $CH=CH_2$); **^{13}C NMR** (75 MHz, $CDCl_3$, 25 °C, TMS): δ = 9.63 ($CH_3C^{4/5}$), 9.86 ($CH_3C^{4/5}$), 19.39 ($CH(CH_3)_2$), 25.18 ($CH(CH_3)_2$), 34.28 (NCH_2), 46.75 (NCH_3), 68.02 (OCH_2CH), 72.36 (CH_2O), 118.08 ($CH=CH_2$), 125.76 ($C^{4/5}$), 126.89 ($C^{4/5}$), 133.63 ($CH=CH_2$), 148.82 ppm (C^2); **IR** (ATR): ν = 746, 920, 1110, 1447, 1522 cm^{-1}; **HRMS** (ESI/APCI) calcd for [$C_{14}H_{25}N_2O^+$]: 237.1961; found: 237.1963; yield: 99%, yellow liquid.

1-(2-Methoxyethyl)-2,3,4,5-tetramethylimidazolium iodide (122b): 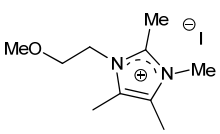
^{1}H NMR (300 MHz, $CDCl_3$, 25 °C, TMS): δ = 2.27 (s, 6H; $CH_3C^{4/5}$), 2.82 (s, 3H; C^2CH_3), 3.33 (s, 3H; OCH_3), 3.67 (t, ^3J(H,H) = 5.0 Hz, 2H; CH_2O), 3.75 (s, 3H; NCH_3), 4.34 ppm (t, ^3J(H,H) = 5.0 Hz, 2H; NCH_2); **^{13}C NMR** (75 MHz, $CDCl_3$, 25 °C, TMS): δ = 9.42 ($CH_3C^{4/5}$), 12.52 (C^2CH_3), 33.63 (NCH_3),

46.71 (NCH_2), 59.29 (OCH_3), 70.40 (CH_2O), 125.81 ($C^{4/5}$), 125.87 ($C^{4/5}$), 143.31 ppm (C^2); **IR** (ATR): ν = 1037, 1094, 1117, 1444, 2900 cm^{-1}; **elemental analysis** calcd (%) for $C_{10}H_{20}IN_2O$: C 38.60, H 6.48, N 9.00; found: C 38.73, H 6.26, N 8.94; yield: 97%, white powder.

3.5.3) N-alkoxy- and N-alkenylimidazolium bromide ionic liquids

Procedure for the synthesis of 1-allyl-3-ethyl-2-isopropyl-4,5-dimethylimidazolium bromide [$C_AC_2C_{i3}m_2$im][Br] (64b): To a flame dried 8 mL vial, containing 4 mL of dry acetonitrile, 1-ethyl-2-isopropyl-4,5-dimethylimidazole (10 mmol, 1.66 g) was added via a syringe under a nitrogen atmosphere. To the mixture distilled allyl bromide (10.5 mmol, 1.27 g) was added. The headspace was filled with nitrogen and the vial was sealed with a PTFE cap. The mixture was irradiated for 45 minutes in a microwave reactor to a temperature of 100 °C. After reaction, the solvent was removed *in vacuo* and the mixture was diluted in 25 mL distilled water containing 0.09 mol eq. NaOH (dependent on the fraction of protonated imidazole observed by ^{1}H NMR in $CDCl_3$). The aqueous layer was washed twice with 20 mL of EtOAc. The water was removed by evaporation or lyophilisation and the product was diluted in an excess of boiling dichloromethane and stored at -18 °C for several hours. The formed suspension was filtered off over filter paper. The filtrate was evaporated and again diluted in boiling dichloromethane, until no more suspension was visible after storage at -18 °C. The resulting clear solution was evaporated and the obtained oil was dried for 6h at 80 °C and 1.0 mbar.

1-Allyl-3-ethyl-2-isopropyl-4,5-dimethylimidazolium bromide [$C_AC_2C_{i3}m_2$im][Br] (64b): ^{1}H NMR (300 MHz, $CDCl_3$, 25 °C, TMS): δ = 1.45 (d, ^3J(H,H) = 7.3 Hz, 3H; CH_2CH_3), 1.52 (d, ^3J(H,H) = 7.2 Hz, 6H; $CH(CH_3)_2$), 2.26 (s, 3H; $CH_3C^{4/5}$), 2.34 (s, 3H; $CH_3C^{4/5}$), 3.67-3.82 (m, 1H; $CH(CH_3)_2$), 4.36 (t, ^3J(H,H) = 7.3 Hz, 3H; CH_2CH_3), 4.91 (d, ^3J(H,H) = 17.2 Hz, 1H; $CH=CH_EH_Z$), 4.98-5.04 (m, 2H; $CH_2CH=CH_2$), 5.35 (d, ^3J(H,H) = 10.5 Hz, 1H; $CH=CH_EH_Z$), 6.00 ppm (ddt, ^3J(H,H) = 17.2 Hz, ^3J(H,H) = 10.5 Hz, ^3J(H,H) = 4.8 Hz, 1H; $CH=CH_2$); **^{13}C NMR** (75 MHz, $CDCl_3$, 25 °C, TMS): δ = 8.99 ($CH_3C^{4/5}$), 9.13 ($CH_3C^{4/5}$), 15.80 (CH_2CH_3), 20.35 ($CH(CH_3)_2$), 25.42 ($CH(CH_3)_2$), 41.77 (CH_2CH_3), 48.43 ($CH_2CH=CH_2$), 118.04 ($CH=CH_2$), 125.95 ($C^{4/5}$), 126.94 ($C^{4/5}$), 130.85 ($CH=CH_2$), 148.30 ppm (C^2); **IR** (ATR): ν = 1091, 1331, 1451, 1511, 1646, 2973, 3455 cm^{-1}; **MS** (ES): m/z [%]: 207.3 (100) [$M+H^+$]; **elemental analysis** calcd (%) for $C_{13}H_{23}BrN_2$: C 54.36, H 8.07, N 9.75; found: C 54.11, H 8.67, N 9.61; yield: 81%, white flakes.

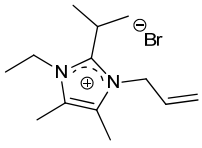

1,3-Diallyl-2-isopropyl-4,5-dimethylimidazolium bromide [$C_AC_AC_{i3}m_2$im][Br] (65b): ^{1}H NMR (300 MHz, $CDCl_3$, 25 °C, TMS): δ = 1.46 (d, ^3J(H,H) = 7.2 Hz, 6H; $CH(CH_3)_2$), 2.30 (s, 6H; $CH_3C^{4/5}$), 3.60-3.75 (m, 1H; $CH(CH_3)_2$), 4.87 (dt, ^3J(H,H) = 17.1 Hz, ^4J(H,H) = 1.8 Hz, 2H; $CH=CH_EH_Z$), 5.05-5.08 (m, 4H; NCH_2), 5.35 (dt, ^3J(H,H) = 10.5 Hz, ^4J(H,H) = 1.8 Hz, 2H; $CH=CH_EH_Z$), 6.06 ppm (ddt, ^3J(H,H) = 17.1 Hz, ^3J(H,H) = 10.5 Hz, ^3J(H,H) = 4.3 Hz, 2H; $CH=CH_2$); **^{13}C NMR** (75 MHz, $CDCl_3$, 25 °C, TMS): δ = 8.81 ($CH_3C^{4/5}$), 20.05 ($CH(CH_3)_2$), 25.36 ($CH(CH_3)_2$), 48.09 ($CH_2CH=CH_2$), 117.55 ($CH=CH_2$), 126.69 (C^4, C^5), 131.00 ($CH=CH_2$), 148.88 ppm (C^2); **IR** (ATR): ν = 724, 921, 1510, 2175, 2977, 3416 cm^{-1}; **HRMS** (ESI/APCI) calcd for [$C_{14}H_{23}N_2^+$]: 219.1856; found: 219.1856; yield: 79%, reddish oil.

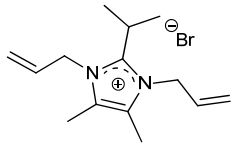

1-Allyl-2-isopropyl-3-(2-methoxyethyl)-4,5-dimethylimidazolium bromide [$C_{2O1}C_AC_{i3}m_2im$][Br] (66b): 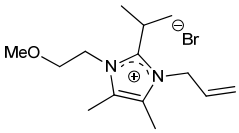

^{1}H NMR (300 MHz, $CDCl_3$, 25 °C, TMS): δ = 1.46 (d, ^3J(H,H) = 7.2 Hz, 6H; CH(CH_3)$_2$), 2.23 (s, 3H; $CH_3C^{4/5}$), 2.35 (s, 3H; $CH_3C^{4/5}$), 3.32 (s, 3H; OCH_3), 3.70 (t, ^3J(H,H) = 5.1 Hz, 2H; CH_2O), 3.78-3.91 (m, 1H; CH(CH$_3$)$_2$), 4.65 (t, ^3J(H,H) = 5.1 Hz, 2H; CH_2CH$_2$O), 4.86-4.91 (m, 2H; CH_2CH=CH$_2$), 4.97 (dt, ^3J(H,H) = 17.3 Hz, ^4J(H,H) = 1.9 Hz, 1H; CH=CH$_Z$H$_E$), 5.39 (dt, ^3J(H,H) = 11.0 Hz, ^4J(H,H) = 1.9 Hz, 1H; CH=CH$_Z$H$_E$), 5.96 ppm (ddt, ^3J(H,H) = 17.3 Hz, ^3J(H,H) = 11.0 Hz, ^3J(H,H) = 4.4 Hz, 1H; CH=CH$_2$); **^{13}C NMR** (75 MHz, $CDCl_3$, 25 °C, TMS): δ = 8.87 ($CH_3C^{4/5}$), 9.65 ($CH_3C^{4/5}$), 19.97 (CH(CH_3)$_2$), 25.30 (CH(CH$_3$)$_2$), 46.60 (CH_2CH_2O), 48.32 (CH_2CH=CH$_2$), 59.10 (OCH_3), 70.31 (CH_2O), 117.75 (CH=CH_2), 126.33 ($C^{4/5}$), 126.69 ($C^{4/5}$), 130.91 (CH=CH$_2$), 149.32 ppm (C^2); **IR** (ATR): ν = 1116, 1451, 1509, 1648, 2978, 3430 cm^{-1}; **MS** (ES): m/z [%]: 237.3 (100) [M+H$^+$]; yield: 74%, yellow oil.

3.5.4) N-alkoxy- and N-alkenylimidazolium bis(trifluoromethylsulfonyl)imide ionic liquids

Compounds **61**-**66c** and **122c** were synthesised using the procedure for compound **47b** described at page 145.

1-Allyl-2-isopropyl-3,4,5-trimethylimidazolium bis(trifluoromethylsulfonyl)imide [$C_AC_1C_{i3}m_2im$][NTf_2] (61c): 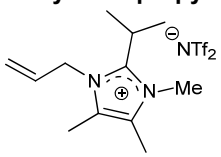

^{1}H NMR (300 MHz, $CDCl_3$, 25 °C, TMS): δ = 1.45 (d, ^3J(H,H) = 7.2 Hz, 6H; CH(CH_3)$_2$), 2.19 (s, 3H; $CH_3C^{4/5}$), 2.25 (s, 3H; $CH_3C^{4/5}$), 3.38-3.50 (m, 1H; CH(CH$_3$)$_2$), 3.74 (s, 3H; NCH_3), 4.69-4.72 (m, 2H; NCH_2), 4.90 (d, ^3J(H,H) = 17.1 Hz, 1H; CH=CH$_E$H$_Z$), 5.34 (d, ^3J(H,H) = 10.5 Hz, 1H; CH=CH$_E$H$_Z$), 5.86-5.98 ppm (ddt, ^3J(H,H) = 17.1 Hz, ^3J(H,H) = 10.5 Hz, ^3J(H,H) = 4.4 Hz, 1H; CH=CH$_2$); **^{13}C NMR** (75 MHz, $CDCl_3$, 25 °C, TMS): δ = 8.34 ($CH_3C^{4/5}$), 8.57 ($CH_3C^{4/5}$), 18.89 (CH(CH_3)$_2$), 25.36 (CH(CH$_3$)$_2$), 32.66 (NCH_3), 47.39 (NCH_2), 118.02 (CH=CH_2), 119.94 (q, ^1J(C,F) = 321.1 Hz; CF_3), 125.92 ($C^{4/5}$), 127.17 ($C^{4/5}$), 130.56 (CH=CH$_2$), 148.21 ppm (C^2); **^{19}F NMR** (282 MHz, $CDCl_3$, 25 °C, $CFCl_3$): -79.32 ppm; **IR** (ATR): ν = 1053, 1134, 1176, 1348 cm^{-1}; **HRMS** (ESI/APCI) calcd for [$C_{12}H_{21}N_2^+$]: 193.1699; found: 193.1697; yield: 95%, light yellow oil.

2-Isopropyl-1-(2-methoxyethyl)-3,4,5-trimethylimidazolium bis(trifluoromethylsulfonyl)imide [$C_{2O1}C_1C_{i3}m_2im$][NTf_2] (62c): 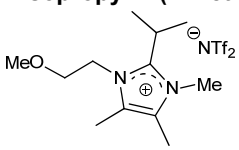

^{1}H NMR (300 MHz, $CDCl_3$, 25 °C, TMS): δ = 1.45 (d, ^3J(H,H) = 7.7 Hz, 6H; CH(CH_3)$_2$), 2.23 (s, 3H; $CH_3C^{4/5}$), 2.24 (s, 3H; $CH_3C^{4/5}$), 3.31 (s, 3H; OCH_3), 3.53-3.66 (m, 1H; CH), 3.59 (t, ^3J(H,H) = 5.1 Hz, 2H; CH_2O), 3.73 (s, 3H, NCH_3), 4.25 ppm (t, ^3J(H,H) = 5.1 Hz, 2H; NCH_2); **^{13}C NMR** (75 MHz, $CDCl_3$, 25 °C, TMS): δ = 8.50 ($CH_3C^{4/5}$), 8.86 ($CH_3C^{4/5}$), 18.60 (CH(CH_3)$_2$), 25.31 (CH), 32.81 (NCH_3), 45.70 (NCH_2), 59.04 (OCH_3), 70.13 (CH_2O), 119.98 (q, ^1J(C,F) = 321.5 Hz; CF_3), 125.70 ($C^{4/5}$), 127.02 ($C^{4/5}$), 148.88 ppm (C^2); **^{19}F NMR** (282 MHz, $CDCl_3$, 25 °C, $CFCl_3$): -79.37 ppm; **IR** (ATR): ν = 1052, 1134, 1175, 1348 cm^{-1}; **HRMS** (ESI/APCI) calcd for [$C_{12}H_{23}N_2O^+$]: 211.1805; found: 211.1806; yield: 99%, white crystals.

1-(2-Allyloxyethyl)-2-isopropyl-3,4,5-trimethylimidazolium bis(trifluoromethylsulfonyl)-imide [$C_{2OA}C_1C_{i3}m_2im$][NTf_2] (63c): 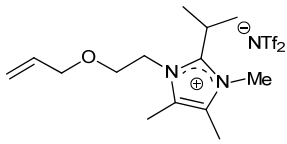 **^{1}H NMR** (300 MHz, $CDCl_3$, 25 °C, TMS): δ = 1.43 (d, ^3J(H,H) = 7.2 Hz, 6H; $CH(CH_3)_2$), 2.22 ($CH_3C^{4/5}$), 2.23 ($CH_3C^{4/5}$), 3.58-3.70 (m, 1H; $CH(CH_3)_2$), 3.65 (t, ^3J(H,H) = 5.0 Hz, 2H; CH_2O), 3.73 (m, 3H; NCH_3), 3.93 (d, ^3J(H,H) = 5.4 Hz; OCH_2CH), 4.25 (t, ^3J(H,H) = 5.0 Hz, 2H; NCH_2), 5.18 (d, ^3J(H,H) = 10.6 Hz, 1H; $CH=CH_ZH_E$), 5.19 (d, ^3J(H,H) = 17.3 Hz, 1H; $CH=CH_ZH_E$), 5.79 ppm (ddt, ^3J(H,H) = 17.3 Hz, ^3J(H,H) = 10.6 Hz, ^3J(H,H) = 5.4 Hz, 1H; $CH=CH_2$); **^{13}C NMR** (75 MHz, $CDCl_3$, 25 °C, TMS): δ = 8.47 ($CH_3C^{4/5}$), 8.87 ($CH_3C^{4/5}$), 18.64 ($CH(CH_3)_2$), 25.24 ($CH(CH_3)_2$), 32.81 (NCH_2), 45.73 (NCH_3), 67.81 (OCH_2CH), 72.40 (CH_2O), 118.02 ($CH=CH_2$), 120.00 (q, ^1J(C,F) = 321.5 Hz; CF_3), 125.75 ($C^{4/5}$), 127.02 ($C^{4/5}$), 133.79 ($CH=CH_2$), 148.83 ppm (C^2); **^{19}F NMR** (282 MHz, $CDCl_3$, 25 °C, $CFCl_3$): -79.35 ppm; **IR** (ATR): ν = 1054, 1135, 1179, 1348 cm^{-1}; **MS** (ES): m/z [%]: 237.3 (100) [M+H$^+$]; yield: 99%, yellow liquid.

1-Allyl-3-ethyl-2-isopropyl-4,5-dimethylimidazolium bis(trifluoromethylsulfonyl)imide [$C_AC_2C_{i3}m_2im$][NTf_2] (64c): 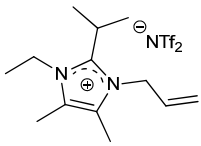 **^{1}H NMR** (300 MHz, $CDCl_3$, 25 °C, TMS): δ = 1.42 (d, ^3J(H,H) = 7.3 Hz, 3H; CH_2CH_3), 1.45 (d, ^3J(H,H) = 7.2 Hz, 6H; $CH(CH_3)_2$), 2.19 (s, 3H; $CH_3C^{4/5}$), 2.27 (s, 3H; $CH_3C^{4/5}$), 3.41-3.55 (m, 1H; $CH(CH_3)_2$), 4.16 (t, ^3J(H,H) = 7.3 Hz, 3H; CH_2CH_3), 4.73-4.74 (m, 2H; $CH_2CH=CH_2$), 4.89 (d, ^3J(H,H) = 17.1 Hz, 1H; $CH=CH_EH_Z$), 5.35 (d, ^3J(H,H) = 10.5 Hz, 1H; $CH=CH_EH_Z$), 5.99 ppm (ddt, ^3J(H,H) = 17.1 Hz, ^3J(H,H) = 10.5 Hz, ^3J(H,H) = 4.4 Hz, 1H; $CH=CH_2$); **^{13}C NMR** (75 MHz, $CDCl_3$, 25 °C, TMS): δ = 8.29 ($CH_3C^{4/5}$), 8.43 ($CH_3C^{4/5}$), 15.33 (CH_2CH_3), 19.70 ($CH(CH_3)_2$), 25.38 ($CH(CH_3)_2$), 41.06 (CH_2CH_3), 47.62 ($CH_2CH=CH_2$), 118.14 ($CH=CH_2$), 119.96 (q, ^1J(C,F) = 321.5 Hz; CF_3), 126.04 ($C^{4/5}$), 126.88 ($C^{4/5}$), 130.53 ($CH=CH_2$), 147.95 ppm (C^2); **^{19}F NMR** (282 MHz, $CDCl_3$, 25 °C, $CFCl_3$): -79.36 ppm; **IR** (ATR): ν = 1054, 1137, 1180, 1334, 1349 cm^{-1}; **HRMS** (ESI/APCI) calcd for [$C_{13}H_{23}N_2^+$]: 207.1856; found: 207.1850; yield: 98%, white crystals.

1,3-Diallyl-2-isopropyl-4,5-dimethylimidazolium bis(trifluoromethylsulfonyl)imide [$C_AC_AC_{i3}m_2im$][NTf_2] (65c): 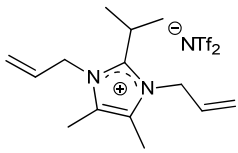 **^{1}H NMR** (300 MHz, $CDCl_3$, 25 °C, TMS): δ = 1.40 (d, ^3J(H,H) = 7.2 Hz, 6H; $CH(CH_3)_2$), 2.20 (s, 6H; $CH_3C^{4/5}$), 3.36-3.51 (m, 1H; $CH(CH_3)_2$), 4.75-4.77 (m, 4H; NCH_2), 4.86 (dt, ^3J(H,H) = 17.1 Hz, ^4J(H,H) = 1.9 Hz, 2H; $CH=CH_EH_Z$), 5.35 (dt, ^3J(H,H) = 10.8 Hz, ^4J(H,H) = 1.9 Hz, 2H; $CH=CH_EH_Z$), 5.95 ppm (ddt, ^3J(H,H) = 17.1 Hz, ^3J(H,H) = 10.8 Hz, ^3J(H,H) = 4.1 Hz, 2H; $CH=CH_2$); **^{13}C NMR** (75 MHz, $CDCl_3$, 25 °C, TMS): δ = 8.37 ($CH_3C^{4/5}$), 19.65 ($CH(CH_3)_2$), 25.47 ($CH(CH_3)_2$), 47.64 ($CH_2CH=CH_2$), 118.07 ($CH=CH_2$), 119.83 (q, ^1J(C,F) = 321.9 Hz; CF_3), 126.74 (C^4, C^5), 130.45 (CH), 148.60 ppm (C^2); **^{19}F NMR** (282 MHz, $CDCl_3$, 25 °C, $CFCl_3$): -79.31 ppm; **IR** (ATR): ν = 1053, 1138, 1177, 1347 cm^{-1}; **HRMS** (ESI/APCI) calcd for [$C_{14}H_{23}N_2^+$]: 219.1856; found: 219.1848**; elemental analysis** calcd (%) for $C_{16}H_{23}F_6N_3O_4S_2$: C 38.47, H 4.64, N 8.41; found: C 38.29, H 4.26, N 8.28; yield: 98%, white crystals.

1-Allyl-2-isopropyl-3-(2-methoxyethyl)-4,5-dimethylimidazolium bis(trifluoromethyl-sulfonyl)imide [$C_{2O1}C_AC_{i3}m_2im$][NTf_2] (66c): **^{1}H NMR** (300 MHz, $CDCl_3$, 25 °C, TMS): δ = 1.43 (d, ^3J(H,H) = 7.2 Hz, 6H; $CH(CH_3)_2$), 2.19 (s, 3H; $CH_3C^{4/5}$), 2.27 (s, 3H; $CH_3C^{4/5}$), 3.33 (s, 3H; OCH_3), 3.55-3.66 (m, 1H; $CH(CH_3)_2$), 3.63 (t, ^3J(H,H) = 5.0 Hz, 2H; CH_2O), 4.32 (t,

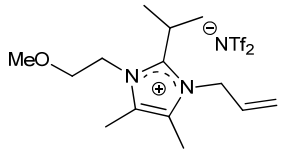

^3J(H,H) = 5.0 Hz, 2H; CH_2CH$_2$O), 4.74-4.78 (m, 2H; CH_2CH=CH$_2$), 4.95 (dd, ^3J(H,H) = 18.2 Hz, ^2J(H,H) = 1.1 Hz, 1H; CH=CH$_E$$H_Z$), 5.39 (dd, ^3J(H,H) = 10.5 Hz, ^2J(H,H) = 1.1 Hz, 1H; CH=CH_EH$_Z$), 5.87-5.98 ppm (m, 1H; CH=CH$_2$); **^{13}C NMR** (75 MHz, CDCl$_3$, 25 °C, TMS): δ = 8.28 (*C*H$_3$C$^{4/5}$), 8.93 (*C*H$_3$C$^{4/5}$), 19.56 (CH(*C*H$_3$)$_2$), 25.48 (*C*H(CH$_3$)$_2$), 45.88 (*C*H$_2$CH$_2$O), 47.79 (*C*H$_2$CH=CH$_2$), 59.07 (OCH$_3$), 69.97 (CH$_2$O), 118.31 (CH=*C*H$_2$), 119.91 (q, ^1J(C,F) = 321.5 Hz; CF$_3$), 126.41 (C$^{4/5}$), 126.77 (C$^{4/5}$), 130.39 (*C*H=CH$_2$), 149.34 ppm (C^2); **^{19}F NMR** (282 MHz, CDCl$_3$, 25 °C, CFCl$_3$): -79.36 ppm; **IR** (ATR): ν = 1054, 1135, 1178, 1348 cm^{-1}; **HRMS** (ESI/APCI) calcd for [C$_{14}$H$_{25}$N$_2$O$^+$]: 237.1961; found: 237.1960; yield: 99%, yellow oil.

1-(2-Methoxyethyl)-2,3,4,5-tetramethylimidazolium bis(trifluoromethylsulfonyl)imide (122c): ^{1}H NMR (300 MHz, CDCl$_3$, 25 °C, TMS): δ = 2.23 (s, 6H; CH$_3$C$^{4/5}$), 2.60 (s, 3H; C^{2}CH$_3$), 3.31 (s, 3H; OCH$_3$), 3.61 (t, ^3J(H,H) = 4.8 Hz, 2H; CH$_2$O), 3.64 (s, 3H; NCH$_3$), 4.20 ppm (t, ^3J(H,H) = 4.8 Hz, 2H; NCH$_2$); **^{13}C NMR** (75 MHz, CDCl$_3$, 25 °C, TMS): δ = 8.57 (*C*H$_3$C$^{4/5}$), 10.41 (C^2*C*H$_3$), 31.94 (NCH$_3$), 45.77 (NCH$_2$), 59.03 (OCH$_3$), 70.17 (CH$_2$O), 119.89 (q, ^1J(C,F) = 321.13 Hz; CF$_3$), 125.31 (C$^{4/5}$), 125.89 (C$^{4/5}$), 143.14 ppm (C^2); **^{19}F NMR** (282 MHz, CDCl$_3$, 25 °C, CFCl$_3$): -79.41 ppm; **IR** (ATR): ν = 1052, 1134, 1176, 1331, 1348 cm^{-1}; **MW** (g mol^{-1}): 449.40; yield: 97%, white powder.

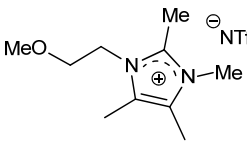

3.5.5) N-alkoxy- and N-alkenylimidazolium dicyanamide ionic liquids

Compounds **61**-**66d** were synthesised using the silver mediated metathesis procedure for compound **47c** described at page 148.

1-Allyl-2-isopropyl-3,4,5-trimethylimidazolium dicyanamide [C$_A$C$_1$C$_{i3}$m$_2$im][N(CN)$_2$] (61d): ^{1}H NMR (300 MHz, CDCl$_3$, 25 °C, TMS): δ = 1.52 (d, ^3J(H,H) = 7.2 Hz, 6H; CH(C*H*$_3$)$_2$), 2.27 (s, 3H; CH$_3$C$^{4/5}$), 2.33 (s, 3H; CH$_3$C$^{4/5}$), 3.45-3.58 (m, 1H; C*H*(CH$_3$)$_2$), 3.83 (s, 3H; NCH$_3$), 4.79-4.83 (m, 2H; NCH$_2$), 4.94 (d, ^3J(H,H) = 17.1 Hz, 1H; CH=CH$_E$$H_Z$), 5.38 (d, ^3J(H,H) = 10.5 Hz, 1H; CH=CH_EH$_Z$), 5.89-6.02 ppm (m, 1H; C*H*=CH$_2$); **^{13}C NMR** (75 MHz, CDCl$_3$, 25 °C, TMS): δ = 8.69 (*C*H$_3$C$^{4/5}$), 8.96 (*C*H$_3$C$^{4/5}$), 19.18 (CH(*C*H$_3$)$_2$), 25.42 (*C*H(CH$_3$)$_2$), 32.93 (NCH$_3$), 47.58 (NCH$_2$), 118.36 (CH=*C*H$_2$), 119.69 (N(CN)$_2$), 126.02 (C$^{4/5}$), 127.15 (C$^{4/5}$), 130.42 (*C*H=CH$_2$), 148.24 ppm (C^2); **IR** (ATR): ν = 749, 1301, 1522, 2124, 2222 cm^{-1}; **MS** (ES): m/z [%]: 193.3 (100) [M+H$^+$]; yield: 97%, light yellow oil.

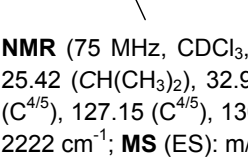

2-Isopropyl-1-(2-methoxyethyl)-3,4,5-trimethylimidazolium dicyanamide [C$_{2O1}$C$_1$C$_{i3}$m$_2$im][N(CN)$_2$] (62d): ^{1}H NMR (300 MHz, CDCl$_3$, 25 °C, TMS): δ = 1.51 (d, ^3J(H,H) = 7.7 Hz, 6H; CH(C*H*$_3$)$_2$), 2.30 (s, 3H; CH$_3$C$^{4/5}$), 2.32 (s, 3H; CH$_3$C$^{4/5}$), 3.34 (s, 3H; OCH$_3$), 3.57-3.66 (m, 1H; CH), 3.64 (t, ^3J(H,H) = 5.0 Hz, 2H; CH$_2$O), 3.81 (s, 3H, NCH$_3$), 4.35 ppm (t, ^3J(H,H) = 5.0 Hz, 2H; NCH$_2$); **^{13}C NMR** (75 MHz, CDCl$_3$, 25 °C, TMS): δ = 8.84 (*C*H$_3$C$^{4/5}$), 9.16 (*C*H$_3$C$^{4/5}$), 18.87 (CH(*C*H$_3$)$_2$), 25.36 (CH), 32.99 (NCH$_3$), 45.85 (NCH$_2$), 59.19 (OCH$_3$), 70.02 (CH$_2$O), 119.78 (N(CN)$_2$), 125.69

($C^{4/5}$), 126.98 ($C^{4/5}$), 148.94 ppm (C^2); **IR** (ATR): ν = 1052, 1134, 1175, 1348 cm^{-1}; **HRMS** (ESI/APCI) calcd for $[C_{12}H_{23}N_2O^+]$: 211.1805; found: 211.1806; yield: 99%, white crystals.

1-(2-Allyloxyethyl)-2-isopropyl-3,4,5-trimethylimidazolium dicyanamide

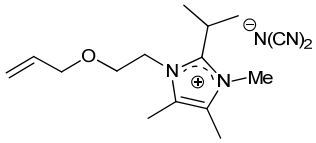

$[C_{2OA}C_1C_{i3}m_2im][N(CN)_2]$ (63d): ^{1}H NMR (300 MHz, $CDCl_3$, 25 °C, TMS): δ = 1.50 (d, ^3J(H,H) = 7.2 Hz, 6H; $CH(CH_3)_2$), 2.30 ($CH_3C^{4/5}$), 2.31 ($CH_3C^{4/5}$), 3.62-3.77 (m, 1H; $CH(CH_3)_2$), 3.70 (t, ^3J(H,H) = 5.0 Hz, 2H; CH_2O), 3.81 (m, 3H; NCH_3), 3.97 (d, ^3J(H,H) = 5.5 Hz; OCH_2CH), 4.35 (t, ^3J(H,H) = 5.0 Hz, 2H; NCH_2), 5.20 (d, ^3J(H,H) = 10.8 Hz, 1H; $CH=CH_ZH_E$), 5.21 (d, ^3J(H,H) = 16.9 Hz, 1H; $CH=CH_ZH_E$), 5.81 ppm (ddt, ^3J(H,H) = 16.9 Hz, ^3J(H,H) = 10.8 Hz, ^3J(H,H) = 5.5 Hz, 1H; $CH=CH_2$); **^{13}C NMR** (75 MHz, $CDCl_3$, 25 °C, TMS): δ = 8.78 ($CH_3C^{4/5}$), 9.11 ($CH_3C^{4/5}$), 18.86 ($CH(CH_3)_2$), 25.21 ($CH(CH_3)_2$), 32.98 (NCH_3), 45.82 (NCH_2), 67.67 (OCH_2CH), 72.36 (CH_2O), 118.14 ($CH=CH_2$), 119.69 ($N(CN)_2$), 125.69 ($C^{4/5}$), 126.95 ($C^{4/5}$), 133.60 ($CH=CH_2$), 148.82 ppm (C^2); **IR** (ATR): ν = 1111, 1311, 1523, 2130, 2232 cm^{-1}; **HRMS** (ESI/APCI) calcd for $[C_{14}H_{25}N_2O^+]$: 237.1961; found: 237.1965; yield: 96%, yellow liquid.

1-Allyl-3-ethyl-2-isopropyl-4,5-dimethylimidazolium dicyanamide $[C_AC_2C_{i3}m_2im][N(CN)_2]$ (64d): ^{1}H NMR (300 MHz, $CDCl_3$, 25 °C, TMS): δ = 1.47 (d, ^3J(H,H) = 7.2 Hz, 3H; CH_2CH_3), 1.53 (d, ^3J(H,H) = 7.7 Hz, 6H; $CH(CH_3)_2$), 2.27 (s, 3H; $CH_3C^{4/5}$), 2.35 (s, 3H; $CH_3C^{4/5}$), 3.49-3.56 (m, 1H; $CH(CH_3)_2$), 4.25 (t, ^3J(H,H) = 7.2 Hz, 3H; CH_2CH_3), 4.81-4.85 (m, 2H; $CH_2CH=CH_2$), 4.95 (d, ^3J(H,H) = 17.1 Hz, 1H; $CH=CH_EH_Z$), 5.39 (d, ^3J(H,H) = 10.5 Hz, 1H; $CH=CH_EH_Z$), 5.96 ppm (ddt, ^3J(H,H) = 17.1 Hz, ^3J(H,H) = 10.5 Hz, ^3J(H,H) = 4.6 Hz, 1H; $CH=CH_2$); **^{13}C NMR** (75 MHz, $CDCl_3$, 25 °C, TMS): δ = 8.66 ($CH_3C^{4/5}$), 8.79 ($CH_3C^{4/5}$), 15.57 (CH_2CH_3), 20.00 ($CH(CH_3)_2$), 25.53 ($CH(CH_3)_2$), 41.25 (CH_2CH_3), 47.82 ($CH_2CH=CH_2$), 118.53 ($CH=CH_2$), 119.78 ($N(CN)_2$), 126.11 ($C^{4/5}$), 126.97 ($C^{4/5}$), 130.37 ($CH=CH_2$), 147.95 ppm (C^2); **IR** (ATR): ν = 1054, 1137, 1180, 1334, 1349 cm^{-1}; **MS** (ES): m/z [%]: 207.3 (100) $[M+H^+]$; yield: 97%, yellow oil.

1,3-Diallyl-2-isopropyl-4,5-dimethylimidazolium dicyanamide $[C_AC_AC_{i3}m_2im][N(CN)_2]$ (65d): ^{1}H NMR (300 MHz, $CDCl_3$, 25 °C, TMS): δ = 1.48 (d, ^3J(H,H) = 7.2 Hz, 6H; $CH(CH_3)_2$), 2.28 (s, 6H; $CH_3C^{4/5}$), 3.47-3.52 (m, 1H; $CH(CH_3)_2$), 4.85-4.87 (m, 4H; NCH_2), 4.92 (dt, ^3J(H,H) = 17.4 Hz, ^4J(H,H) = 1.9 Hz, 2H; $CH=CH_EH_Z$), 5.40 (dt, ^3J(H,H) = 10.6 Hz, ^4J(H,H) = 1.9 Hz, 2H; $CH=CH_EH_Z$), 5.99 ppm (ddt, ^3J(H,H) = 17.4 Hz, ^3J(H,H) = 10.6 Hz, ^3J(H,H) = 4.4 Hz, 2H, $CH=CH_2$); **^{13}C NMR** (75 MHz, $CDCl_3$, 25 °C, TMS): δ = 8.72 ($CH_3C^{4/5}$), 19.91 ($CH(CH_3)_2$), 25.65 ($CH(CH_3)_2$), 47.90 ($CH_2CH=CH_2$), 118.30 ($CH=CH_2$), 119.73 ($N(CN)_2$), 126.91 (C^4, C^5), 130.47 (CH), 148.60 ppm (C^2); **IR** (ATR): ν = 1302, 1514, 1648, 2131, 2224, 3463 cm^{-1}; **MS** (ES): m/z [%]: 219.3 (100) $[M+H^+]$; yield: 98%, white crystals.

1-Allyl-2-isopropyl-3-(2-methoxyethyl)-4,5-dimethylimidazolium dicyanamide

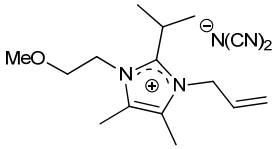

$[C_{2O1}C_AC_{i3}m_2im][N(CN)_2]$ (66d): ^{1}H NMR (300 MHz, $CDCl_3$, 25 °C, TMS): δ = 1.47 (d, ^3J(H,H) = 7.2 Hz, 6H; $CH(CH_3)_2$), 2.25 (s, 3H; $CH_3C^{4/5}$) , 2.34 (s, 3H; $CH_3C^{4/5}$), 3.35 (s, 3H; OCH_3), 3.59-3.73 (m, 1H; $CH(CH_3)_2$), 3.67 (t, ^3J(H,H) = 5.0 Hz, 2H; CH_2O),

4.40 (t, ^3J(H,H) = 5.0 Hz, 2H; CH_2CH$_2$O), 4.81-4.86 (m, 2H;CH_2CH=CH$_2$), 4.97 (d, ^3J(H,H) = 17.1 Hz, 1H; CH=CH$_E$$H_Z$), 5.41 (d, ^3J(H,H) = 10.5 Hz, 1H; CH=CH_EH$_Z$), 5.90-6.00 ppm (m, 1H; CH=CH$_2$); **^{13}C NMR** (75 MHz, CDCl$_3$, 25 °C, TMS): δ = 8.47 (*C*H$_3$C$^{4/5}$), 8.86 (*C*H$_3$C$^{4/5}$), 19.70 (CH(*C*H$_3$)$_2$), 25.48 (*C*H(CH$_3$)$_2$), 45.94 (*C*H$_2$CH$_2$O), 47.85 (*C*H$_2$CH=CH$_2$), 59.15 (OCH$_3$), 69.93 (CH$_2$O), 118.42 (CH=*C*H$_2$), 119.73 (N(CN)$_2$), 126.34 (C$^{4/5}$), 126.79 (C$^{4/5}$), 130.36 (*C*H=CH$_2$), 149.35 ppm (C^2); **IR** (ATR): ν = 1304, 1513, 2126, 2224 cm^{-1}; **MS** (ES): m/z [%]: 237.3 (100) [M+H$^+$]; yield: 86%, yellow oil.

3.6. Synthesis of chiral imidazoles and imidazolium ionic liquids

3.6.1) Synthesis of amino acid based imidazoles and ionic liquids

Procedure for the synthesis of (*rac*)-methyl-2-(2-isopropyl-4,5-dimethylimidazol-1-yl)-propionate ((*rac*)-88b): A 150 mL glass pressure vial was filled with 50 mL of MeOH and a PTFE stirring bar. The solvent was allowed to cool to 0 °C and isobutyraldehyde (4.56 mL, 50 mmol), L-alanine methyl ester hydrochloride (6.98g, 50 mmol) and NaOH (2.00 g, 50 mmol) were added. The vial was closed and submerged in a preheated oil bath at 120 °C with temperature controller. After heating for 2h with vigorous stirring, the reaction mixture was carefully cooled to 0 °C, the vial was opened and consecutively 2,3-butandione (1.08 g, 12,5 mmol) and NH$_4$OAc (0.96 g, 12.5 mmol) were added. The vessel was closed immediately and heated in a preheated oil bath at 120 °C for 30 min under vigorous stirring. The cooling to 0 °C and consecutive addition of diacetyl and NH$_4$OAc were repeated three more times, until 50 mmol of each reagent was added. After final cooling, MeOH and the reaction water were evaporated. The resulting mixture was dissolved in EtOAc and extracted twice with 50 mL of an aqueous 0.5 M HCl solution. The combined aqueous phases were alkalinised with a 3.0 M NaOH (40 mL) solution and extracted three times with EtOAc (40 mL). The organic phases were combined and dried with MgSO$_4$. The solvent was removed *in vacuo* and boiling acetonitrile was added until all solid particles dissolved. After storage at -18 °C, the precipitate was removed and the solvent of the filtrate was evaporated. The resulting oil was brought on a column with neutral alumina packing and eluted with a 1:9 EtOAc:hexanes mixture. The eluted fractions were combined as long as no presence of 1*H*-2-isopropyl-4,5-dimethylimidazole could be detected by GC-FID.

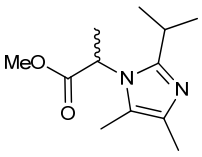

(*rac*)-*O*-methyl-2-(2-isopropyl-4,5-dimethylimidazol-1-yl)propionate ((*rac*)-88b): b.p. 90 °C (1.0 mbar); $[\alpha]_D^{25}$ = -0.3 ± 0.1 (C = 1.1 in CHCl$_3$); **^{1}H NMR** (300 MHz, CDCl$_3$, 25 °C, TMS): δ = 1.30 (d, ^3J(H,H) = 6.6 Hz, 3H; CH(CH_3)$_2$,), 1.31 (d, ^3J(H,H) = 6.6 Hz, 3H; CH(CH_3)$_2$), 1.64 (d, ^3J(H,H) = 7.3 Hz 3H; NCHCH_3,), 2.05 (s, 3H; CH$_3$C$^{4/5}$), 2.13 (s, 3H; CH$_3$C$^{4/5}$), 2.78-2.91 (m, 1H; CH(CH$_3$)$_2$), 3.75 (s, 3H; OCH$_3$), 4.87 ppm (q, ^3J(H,H) = 7.3 Hz, 1H; NCH); **^{13}C NMR** (75 MHz, CDCl$_3$, 25 °C, TMS): δ = 9.48 (*C*H$_3$C$^{4/5}$), 12.63 (*C*H$_3$C$^{4/5}$), 17.73 (NCH*C*H$_3$), 21.88 (CH(*C*H$_3$)$_A$(CH$_3$)$_B$), 22.29 (CH(CH$_3$)$_A$(*C*H$_3$)$_B$) 26.51 (*C*H(CH$_3$)$_2$), 51.94 (N*C*H), 52.81 (OCH$_3$), 120.72 (C$^{4/5}$), 132.28 (C$^{4/5}$), 150.99 (C^2), 171.06 ppm (C=O); **IR** (ATR): ν = 1092, 1316, 1434, 1742, 2965 cm^{-1}; **HRMS** (ESI/APCI) calcd for [C$_{12}$H$_{21}$N$_2$O$_2^+$]: 225.1603; found: 225.1595; yield: 26%, brown oil.

Procedure for the synthesis of (*rac*)-2-(2-isopropyl-4,5-dimethylimidazol-1-yl)-propanol ((*rac*)-89b): To a 100 mL flask containing 50 mL of THF was added (*rac*)-methyl-2-(2-isopropyl-4,5-dimethylimidazol-1-yl)-propanoate (11.2 g, 50 mmol) and methanol (12.15 mL, 9.6 g, 300 mmol). The mixture was cooled to 0 °C and slowly 3 equivalents of $NaBH_4$ were added (5.67 g, 150 mmol). After refluxing for 1 hour, the mixture was allowed to cool and 200 mL of an aqueous 1.5 M NaOH solution was added. After stirring for 20 min, the mixture was extracted 4 times with EtOAc (40 mL). The combined organic phases were washed with a saturated NaCl solution. The organic fraction was dried with $MgSO_4$ and the solvent was removed *in vacuo*. If the thus obtained product was not sufficiently pure, an extraction was applied from EtOAc with an aqueous 0.5 M HCl solution (150 mL), followed by neutralisation with an aqueous 3 M NaOH (40 mL) solution and extraction with EtOAc (3 × 40 mL).

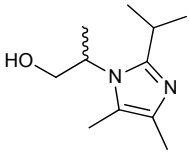

(*rac*)-2-(2-Isopropyl-4,5-dimethylimidazol-1-yl)-propanol ((*rac*)-89b): ^{1}H NMR (300 MHz, $CDCl_3$, 25 °C, TMS): δ = 1.28 (d, ^3J(H,H) = 7.2 Hz, 3H; CH(CH_3)$_2$), 1.33 (d, J^3(H,H) = 6.6 Hz, 3H; CH(CH_3)$_2$), 1.46 (d, J^3(H,H) = 7.2 Hz, 3H; NCHCH_3), 2.12 (s, 3H; $CH_3C^{4/5}$), 2.18 (s, 3H; $CH_3C^{4/5}$), 2.96-3.09 (m, 1H; CH(CH$_3$)$_2$), 3.80 (dd, ^2J(H,H) = 11.4 Hz, ^3J(H,H) = 6.1 Hz, 1H; CH_aH$_b$OH), 3.92 (dd, ^2J(H,H) = 11.4 Hz, ^3J(H,H) = 8.5 Hz, 1H; CH$_a$$H_b$OH), 4.36-4.47 ppm (m, 1H; NCH); **^{13}C NMR** (75 MHz, $CDCl_3$, 25 °C, TMS): δ = 10.64 (C$H_3C^{4/5}$)12.28 (C$H_3C^{4/5}$)17.22 (NCHCH_3) 21.93 (CH(CH_3)$_2$)22.38 (CH(CH_3)$_2$)26.49 (CH(CH$_3$)$_2$)53.24 (NCHCH$_3$) 64.54 (CH_2) 120.95 ($C^{4/5}$) 132.02 ($C^{4/5}$) 151.72 ppm (C^2); **IR** (ATR): ν = 720, 1030, 1069, 1382, 1432, 2970 cm^{-1}; **MW** (g mol^{-1}) 196.29; yield: 73%, pale yellow oil.

Procedure for the synthesis of (*rac*)-1-(1-methoxyprop-2-yl)-2-isopropyl-4,5-dimethylimidazole ((*rac*)-90): In a flame dried flask of 100 mL containing 40 mL of dry THF under nitrogen atmosphere, (*rac*)-2-(2-isopropyl-4,5-dimethylimidazol-1-yl)-propanol (3.93 g, 20 mmol) was added. The mixture was cooled to -78 °C and then slowly pure NaH (0.50 g, 21 mmol) was added. The reaction was stirred for 15 min and dimethylsulfate (1.99 mL, 21 mmol) was added dropwise *via* a syringe. The reaction was allowed to warm to room temperature overnight. After reaction, distilled water (20 mL) and a saturated aqueous $NaHCO_3$ solution (20 mL) were added and the mixture was extracted 3 times with 20 mL of EtOAc. The combined organic fractions were extracted with an aqueous 0.5 M HCl solution (2 × 25 mL). The combined aqueous phases were neutralised with an aqueous 3 M NaOH (15 mL) solution and the product was extracted with EtOAc (3 × 25 mL). The combined organic layers were dried with $MgSO_4$ and the solvent was removed under reduced pressure. A light yellow oil was obtained.

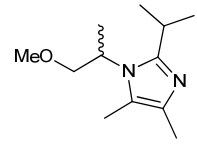

(*rac*)-2-Isopropyl-1-(3-methoxyxyprop-2-yl)-4,5-dimethylimidazole ((*rac*)-90): b.p. 87 °C (1.0 mbar); $[\alpha]_D^{25}$ = -0.3 ± 0.1 (C = 1.0 in $CHCl_3$); **^{1}H NMR** (300 MHz, $CDCl_3$, 25 °C, TMS): δ = 1.29 (d, ^3J(H,H) = 6.6 Hz, 3H; CH(CH_3)$_A$(CH$_3$)$_B$), 1.33 (d, ^3J(H,H) = 6.6 Hz, 3H; CH(CH$_3$)$_A$(CH_3),1.46 (d, ^3J(H,H) = 7.2 Hz, 3H; NCHCH_3), 2.12 (s, 3H; $CH_3C^{4/5}$), 2.16 (s, 3H; $CH_3C^{4/5}$), 2.94-3.06 (m, 1H; CH(CH$_3$)$_2$), 3.32 (s, 3H; CH_2OCH_3), 3.61 (d, ^3J(H,H) = 6.6 Hz, 2H; CH_2OCH$_3$), 4.37-4.48 ppm (m, 1H; NCHCH$_3$); **^{13}C NMR** (75 MHz, $CDCl_3$, 25 °C, TMS): δ = 10.66 (C$H_3C^{4/5}$), 12.63 (C$H_3C^{4/5}$), 17.65 (NCHCH_3), 22.12(CH(CH_3)$_2$), 22.44(CH(CH_3)$_2$), 26.57(CH(CH$_3$)$_2$), 50.78 (NCHCH$_3$), 59.09 (OCH$_3$), 75.29 (CH_2), 120.80 ($C^{4/5}$), 132.31 ($C^{4/5}$),

151.47 ppm (C^2); **IR** (ATR): ν = 1106, 1307, 1432, 2926 cm^{-1}; **HRMS** (ESI/APCI) calcd for $[C_{12}H_{23}N_2O^+]$: 211.1805; found: 211.1807; yield: 58%, pale yellow liquid.

(*rac*)-2-Isopropyl-1-(3-methoxyprop-2-yl)-4,5-dimethylimidazolium bis(trifluoromethylsulfonyl)imide ((*rac*)-92b): 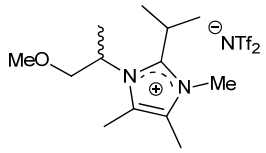

^{1}H NMR (300 MHz, $CDCl_3$, 25 °C, TMS): δ =1.50 (d, ^3J(H,H) = 7.7 Hz, 3H; NCH(CH_3)$_A$(CH_3)$_B$), 1.51 (d, ^3J(H,H) = 7.2 Hz, 3H; NCH(CH_3)$_A$(CH_3)$_B$), 1.64 (d, ^3J(H,H) = 7.2 Hz, 3H; NCHCH_3),2.30 (s, 3H; $CH_3C^{4/5}$), 2.33 (s, 3H; $CH_3C^{4/5}$), 3.34 (m, 3H; OCH_3), 3.68-3.84 (m, 1H; NCHCH_2), 3.76-3.88 (m, 1H; CH(CH_3)$_2$), 3.86 (s, 3H; NCH_3), 4.84-4-95 ppm (m, 1H; NC$H$$CH_2$); **^{13}C NMR** (75 MHz, $CDCl_3$, 25 °C, TMS): δ = 9.13 ($CH_3C^{4/5}$), 10.98 ($CH_3C^{4/5}$), 16.99 (CHCH_3), 19.41 (CH(CH_3)$_2$), 25.34 (CH(CH_3)$_2$), 34.14 (NCH_3), 54.49 (NCH), 59.21 (OCH_3), 73.07 (CH_2O), 119.84 (q, ^1J(C,F) = 321.5 Hz; CF_3), 125.06 ($C^{4/5}$), 127.92 ($C^{4/5}$), 148.99 ppm (C^2); **^{19}F NMR** (282 MHz, $CDCl_3$, 25 °C): δ = -79.46 ppm; **IR** (ATR): ν = 716, 1058, 1106, 1188, 1351, 1519 cm^{-1}; **MW** (g mol^{-1}) 506.50; yield: 97%, brown oil.

3.6.2) Synthesis of lactate based imidazoles and imidazolium ionic liquids

Procedure for the synthesis of (*S*)-2-methoxypropanol ((*S*)-95): To a flame dried 250 mL flask, containing a solution of ethyl L-lactate (20 mL, 174 mmol) in dry THF (100 mL) at 0 °C, methyl iodide (17.32 mL, 279 mmol) was added under a nitrogen flow. After cooling, pure NaH (5.00 g, 208 mmol) was added in 5 portions (every 15 min) and the reaction was stirred overnight. After reaction, THF was removed via cold rotary evaporation until a precipitate became visible. A minimal amount of H_2O was added until the mixture became clear, then the mixture was extracted Et_2O (3 × 40 mL), the organic fractions were washed with a saturated NaCl solution and after drying over $MgSO_4$, most of the solvent was removed by cold evaporation. The resulting solution was diluted with dry THF (80 mL) and cooled to -78 °C under a nitrogen flow. Crushed $LiAlH_4$ (6.58 g, 174 mmol) was added very slowly (attention, violent reaction), and stirred for 60 min at -78 °C. The reaction was further stirred 30 min at room temperature. The reaction was quenched at 0 °C with 4 equivalents of H_2O (12.5 mL, 0.7 mol) in a 1:1 mixture with THF and stirred for 1 h. The resulting slurry was filtered over celite with THF and the solvent was removed by cold evaporation to obtain a clear to pale yellow liquid in 32% overall yield.

Procedure for the synthesis of (*S*)-2-methoxy-1-propyl methanesulfonate ((*S*)-96): To a solution of (*S*)-2-methoxypropanol (4.50 g, 50 mmol) in dry CH_2Cl_2 at 0 °C provided with a $CaCl_2$-tube was added Et_3N (7.66 mL, 55 mmol). After slowly adding MsCl (4.26 mL, 55 mmol), the reaction was stirred for 6 h, while warming to room temperature. The reaction mixture was washed with a saturated $NaHCO_3$ (2 × 50 mL) solution and once with H_2O. The organic fraction was dried with $MgSO_4$ and the solvent was removed via rotary evaporation. The resulting yellow oil was purified by distillation (151 °C, 1.0 mbar), yielding a clear liquid.

(*S*)-2-Methoxypropyl methanesulfonate ((*S*)-96): b.p. 68 °C (1.0 mbar); $[\alpha]_D^{25}$ = 23.2 ± 0.1 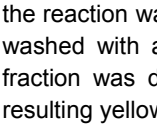

(C = 0.3 in $CHCl_3$); **^{1}H NMR** (300 MHz, $CDCl_3$, 25 °C, TMS): δ = 1.21 (d, ^3J(H,H) = 6.6 Hz, 3H; CHCH_3), 3.06 (s, 3H; CH_3SO_3), 3.40 (s, 3H; OCH_3), 3.58-3.68 (m, 1H; CH), 4.14 (dd, ^2J(H,H) = 10.9 Hz, ^3J(H,H) = 6.1 Hz, 1H;

CH_2), 4.23 ppm (dd, ^2J(H,H) = 10.9 Hz, ^3J(H,H) = 3.6 Hz, 1H; CH_2); **^{13}C NMR** (75 MHz, $CDCl_3$, 25 °C, TMS): δ = 15.60 ($CHCH_3$), 37.28 (CH_3SO_3), 56.58 (OCH_3), 72.52 (CH_2), 74.55 ppm (CH); **IR** (ATR): ν = 958, 1171, 1347 cm^{-1}; **HRMS** (ESI/APCI) calcd for [$C_5H_{13}O_4S^+$]: 169.0529; found: 169.0532; yield: 89%, colourless liquid.

Procedure for the synthesis of (*S*)-1-ethyl-3-(2-methoxyprop-1-yl)-2,4,5-trimethylimidazolium methanesulfonate (98a): To a flame dried 8 mL vial equipped with PTFE stirring bar, containing dry CH_3CN (1 mL), were added (*S*)-2-methoxy-1-propyl methanesulfonate (0.84 g, 5 mmol) and 1-ethyl-2,4,5-trimethylimidazole (0.70 g, 5.05 mmol) under a nitrogen atmosphere. The vial was sealed and locked in the MW apparatus. The sample was isothermally irradiated for 90 min at 100 °C. After reaction, the solvent was removed by rotary evaporation, furnishing a dark oil which was dried for 4h at 80 °C at 0.5 mbar.

(*S*)-1-Ethyl-3-(2-methoxypropyl)-4,5-dimethylimidazolium methanesulfonate (97a): $[\alpha]_D^{25}$ = 20.3 ± 0.5 (C = 0.4 in $CHCl_3$); **^{1}H NMR** (300 MHz, $CDCl_3$, 25 °C, TMS): δ = 1.26 (d, ^3J(H,H) = 6.1 Hz, 3H; $CHCH_3$), 1.55 (t, ^3J(H,H) = 7.3 Hz, 3H; CH_2CH_3), 2.24 (s, 3H; $CH_3C^{4/5}$), 2.25 (s, 3H; $CH_3C^{4/5}$), 2.79 (s, 3H; CH_3SO_3), 3.26 (s, 3H; OCH_3), 3.77-3.87 (m, 1H; CH_2CH), 4.02 (dd, ^2J(H,H) = 14.2 Hz, ^3J(H,H) = 8.3 Hz, 2H; CH_AH_BCH), 4.21 (qd, ^3J(H,H) = 7.3 Hz, ^2J(H,H) = 2.8 Hz, 2H; CH_2CH_3), 4.44 (dd, ^2J(H,H) = 14.2 Hz, ^3J(H,H) = 2.8 Hz, 2H; CH_AH_BCH), 9.91 ppm (s, 1H; C^2H); **^{13}C NMR** (75 MHz, $CDCl_3$, 25 °C, TMS): δ = 8.41 ($CH_3C^{4/5}$), 8.75 ($CH_3C^{4/5}$), 15.21 (CH_2CH_3), 16.14 ($CHCH_3$), 39.48 (CH_3SO_3), 42.40 (CH_2CH_3), 51.55 (CH_2CH), 56.37 (OCH_3), 75.73 (NCH_2CH), 125.56 ($C^{4/5}$), 127.75 ($C^{4/5}$), 135.83 ppm (C^2); **IR** (ATR): ν = 770, 1039, 1176, 1623, 2360, 3447 cm^{-1}; **HRMS** (ESI/APCI) calcd for [$C_{11}H_{22}N_2O^+$]: 197.1648; found: 197.1648; yield: 83%, pale yellow oil.

(*S*)-1-Ethyl-3-(2-methoxypropyl)-4,5-dimethylimidazolium bis(trifluoromethylsulfonyl)-imide (97b): $[\alpha]_D^{25}$ = 14.9 ± 0.7 (C = 0.4 in $CHCl_3$); **^{1}H NMR** (300 MHz, $CDCl_3$, 25 °C, TMS): δ = 1.20 (d, ^3J(H,H) = 6.1 Hz, 3H; $CHCH_3$), 1.50 (t, ^3J(H,H) = 7.4 Hz, 3H; CH_2CH_3), 2.25 (s, 3H; $CH_3C^{4/5}$), 2.27 (s, 3H; $CH_3C^{4/5}$), 3.26 (s, 3H; OCH_3), 3.61-3.70 (m, 1H; CH_2CH), 3.93 (dd, ^2J(H,H) = 13.2 Hz, ^3J(H,H) = 8.3 Hz, 2H; CH_AH_BCH), 4.12 (q, ^3J(H,H) = 7.4 Hz, 2H; CH_2CH_3), 4.17 (dd, ^2J(H,H) = 13.2 Hz, ^3J(H,H) = 2.8 Hz, 2H; CH_AH_BCH), 8.54 ppm (s, 1H; C^2H); **^{13}C NMR** (75 MHz, $CDCl_3$, 25 °C, TMS): δ = 8.21 ($CH_3C^{4/5}$), 8.52 ($CH_3C^{4/5}$), 14.75 (CH_2CH_3), 15.94 ($CHCH_3$), 42.52 (CH_2CH_3), 51.73 (CH_2CH), 56.31 (OCH_3), 75.07 (NCH_2CH), 119.97 (q, ^1J(C,F) = 321.1 Hz; CF_3), 126.48 ($C^{4/5}$), 128.18 ($C^{4/5}$), 133.70 ppm (C^2); **IR** (ATR): ν = 1052, 1134, 1178, 1348 cm^{-1}; **MS** (ES): *m/z* (%): 197.3 (100) [M+H$^+$]; yield: 98%, pale yellow oil.

(*S*)-1-Ethyl-3-(2-methoxypropyl)-2,4,5-trimethylimidazolium methanesulfonate (98a): $[\alpha]_D^{25}$ = 16.1 ± 0.5 (C = 0.4 in $CHCl_3$); **^{1}H NMR** (300 MHz, $CDCl_3$, 25 °C, TMS): δ = 1.28 (d, ^3J(H,H) = 6.1 Hz, 3H; $CHCH_3$), 1.40 (t, ^3J(H,H) = 6.8 Hz, 3H; CH_2CH_3), 2.25 (s, 3H; $CH_3C^{4/5}$), 2.26 (s, 3H; $CH_3C^{4/5}$), 2.68 (CH_3SO_3), 2.76 (C^2CH_3), 3.22 (s, 3H; OCH_3), 3.53-3.64 (m, 1H; CH_2CH), 4.05 (dd, ^2J(H,H) = 15.3 Hz, ^3J(H,H) = 9.3 Hz, 2H; CH_AH_BCH),

4.15 (q, ^3J(H,H) = 6.8 Hz, 2H; CH_2CH$_3$), 4.25 ppm (dd, ^2J(H,H) = 15.3 Hz, ^3J(H,H) = 2.8 Hz, 2H; CH$_A$H$_B$CH); **^{13}C NMR** (75 MHz, $CDCl_3$, 25 °C, TMS): δ = 8.66 (*C*H$_3$C$^{4/5}$), 9.04 (*C*H$_3$C$^{4/5}$), 10.99 (C^2*C*H$_3$), 14.87 (CH$_2$*C*H$_3$), 16.52 (CH*C*H$_3$), 39.45 (CH$_3$SO$_3$), 40.87 (*C*H$_2$CH$_3$), 51.00 (*C*H$_2$CH), 56.51 (OCH$_3$), 75.46 (NCH$_2$*C*H), 124.47 (C$^{4/5}$), 126.22 (C$^{4/5}$), 143.34 ppm (C^2); **IR** (ATR): ν= 1053, 1135, 1177 1348, 1452, 1530 cm^{-1}; **MS** (ES): *m/z* (%): 211.3 (100) [M+H$^+$]; yield: 78%, brown oil.

(*S*)-1-Ethyl-3-(2-methoxypropyl)-2,4,5-trimethylimidazolium bis(trifluoromethylsulfonyl)imide (98b): 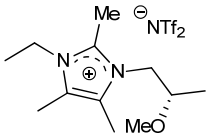

$[\alpha]_D^{25}$ = 12.3 ± 0.2 (C = 0.4 in $CHCl_3$); **^{1}H NMR** (300 MHz, $CDCl_3$, 25 °C, TMS): δ = 1.27 (d, ^3J(H,H) = 6.6 Hz, 3H; CHC*H*$_3$), 1.38 (t, ^3J(H,H) = 7.4 Hz, 3H; CH$_2$C*H*$_3$), 2.23 (s, 3H; CH$_3$C$^{4/5}$), 2.26 (s, 3H; CH$_3$C$^{4/5}$), 2.62 (C^{2}CH$_3$), 3.22 (s, 3H; OCH$_3$), 3.49-3.59 (m, 1H; CH$_2$C*H*), 3.95 (dd, ^2J(H,H) = 14.9 Hz, ^3J(H,H) = 9.4 Hz, 2H; C*H*$_A$H$_B$CH), 4.04 (dd, ^2J(H,H) = 14.9 Hz, ^3J(H,H) = 3.3 Hz, 2H; CH$_A$*H*$_B$CH), 4.07 ppm (q, ^3J(H,H) = 7.4 Hz, 2H; C*H*$_2$CH$_3$); **^{13}C NMR** (75 MHz, $CDCl_3$, 25 °C, TMS): δ = 8.34 (*C*H$_3$C$^{4/5}$), 8.66 (*C*H$_3$C$^{4/5}$), 10.34 (C^2*C*H$_3$), 14.54 (CH$_2$*C*H$_3$), 16.35 (CH*C*H$_3$), 40.72 (*C*H$_2$CH$_3$), 50.86 (*C*H$_2$CH), 56.46 (OCH$_3$), 75.26 (NCH$_2$*C*H), 119.91 (q, ^1J(C,F) = 321.5 Hz; CF$_3$), 124.89 (C$^{4/5}$), 126.18 (C$^{4/5}$), 142.67 ppm (C^2); **IR** (ATR): ν = 1053, 1135, 1177, 1452, 1530 cm^{-1}; **MS** (ES): *m/z* (%): 211.3 (100) [M+H$^+$]; yield: 97%, brown oil.

Procedure for the synthesis of 1*H*-2-isopropyl-4,5-dimethylimidazole (60): A glass 150 mL pressure vial was filled with MeOH (50 mL) and a PTFE stirring bar. The solvent was allowed to cool to 0 °C and isobutyraldehyde (100 mmol, 7.21 g), diacetyl (100 mmol, 8.61 g) and NH_4OAc (200 mmol, 15.62 g) were added. The vessel was closed immediately and submerged in a preheated oil bath at 120 °C for 2 h under vigorous stirring. After cooling, MeOH and the reaction water were removed *in vacuo*. The reaction mixture was dissolved in EtOAc (80 mL) and extracted twice with an aqueous 0.5 M HCl solution (100 mL). The aqueous phase was alkalinised with 50 mL of a 3.0 M NaOH and extracted three times with EtOAc (40 mL). The resulting organic phase was dried over $MgSO_4$. The solvent was removed *in vacuo* and 12.26 g (89%) of a white powder was obtained.

1*H*-2-Isopropyl-4,5-dimethylimidazole (60): 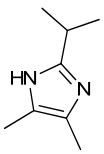

^{1}H NMR (300 MHz, $CDCl_3$, 25 °C, TMS): δ = 2.19 (s, 3H; CH$_3$C$^{4/5}$), 2.37 (s, 3H; CH$_3$C$^{4/5}$), 4.82 (d, ^3J(H,H) = 5.4, 2H; CH$_2$), 5.17 (d, ^3J(H,H) = 17.1 Hz, 1H; CH = CH$_E$*H*$_Z$), 5.39 (d, ^3J(H,H) = 10.5 Hz, 1H; CH = C*H*$_E$H$_Z$), 5.96 (ddt, ^3J(H,H) = 17.1 Hz, ^3J(H,H) = 10.5 Hz, ^3J(H,H) = 5.4 Hz, 1H; C*H* = CH$_2$), 9.05 ppm (s, 1H; C^{2}H); **^{13}C NMR** (75 MHz, $CDCl_3$, 25 °C, TMS): δ = 10.76 (CH$_3$C$^{4/5}$), 21.83 (CH(*C*H$_3$)$_2$), 28.23 (*C*H(CH$_3$)$_2$), 118.69 (C$^{4/5}$), 150.94 ppm (C^2); **IR** (ATR): ν = 1020, 1440, 1462, 1621, 2965 cm^{-1}; **MS** (ES): *m/z* (%): 139.3 (100) [M+H$^+$]; **elemental analysis** calcd (%) for $C_8H_{14}N_2$: C 69.52, H 10.21, N 20.27; found: C 69.36, H 10.89, N 20.28; T_m (°C): 202; yield: 89%, white flakes.

Procedure for the synthesis of (*S*)-1-(2-methoxyprop-1-yl)-2-isopropyl-4,5-dimethylimidazole ((*S*)-100): To a flame dried 100 mL two-necked reaction flask, provided with a water cooler and under nitrogen atmosphere, dry THF (40 mL) and a PTFE stirring bar were added. To the solvent was added 1*H*-2-isopropyl-4,5-dimethylimidazole (20 mmol, 2.76 g). The mixture was stirred (and heated if needed), until all product was dissolved, after which the mixture was cooled to 0 °C. After careful addition of NaH (22 mmol, 0.53 g), the mixture

was allowed to reflux for 15 min The sodium imidazolate solution was again cooled to 0 °C and (*S*)-2-methoxypropyl methanesulfonate (20 mmol, 3.36 g) was added dropwise. The mixture was again refluxed for 4h. After reaction, the mixture was cooled to room temperature and a 1 M NaOH solution (40 mL) was added, and allowed to stir for 15 min while cooling to 0 °C. The mixture was extracted 3 times with a 2:1 EtOAc:Et_2O mixture (40 mL). The combined organic phase was dried over $MgSO_4$. The solvent was removed *in vacuo* and the mixture was dissolved in a minimum amount of boiling acetonitrile. The solution was stored at -18 °C for at least 4h. The precipitate was filtered off and the purity of the filtrate monitored by GC-FID. The side product was consecutively crystallised until the amount of starting 1*H*-2-isopropyl-4,5-dimethylimidazole was sufficiently low. The solvent was removed *in vacuo* and the resulting oil was purified by short-path vacuum distillation. Hereby, the still was kept at 75 °C sufficiently long to remove all (*S*)-2-methoxypropyl methanesulfonate. At 83 °C (1.0 mbar), 2.1 g of the product was collected as a colourless oil, which was further used for the synthesis of ionic liquids.

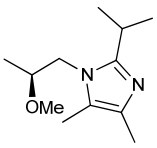

(*S*)-2-Isopropyl-1-(2-methoxypropyl)-4,5-dimethylimidazole ((*S*)-100): b.p. 83 °C (1.0 mbar); $[\alpha]_D^{25}$ = 40.3 ± 0.5 (C = 0.3 in $CHCl_3$); **^{1}H NMR** (300 MHz, $CDCl_3$, 25 °C, TMS): δ = 1.13 (d, ^3J(H,H) = 6.1 Hz, 3H; $CH(OCH_3)C\mathit{H}_3$), 1.26 (d, ^3J(H,H) = 7.2 Hz, 3H; $CH(C\mathit{H}_3)_A(CH_3)_B$), 1.28 (d, ^3J(H,H) = 7.2 Hz, 3H; $CH(CH_3)_A(C\mathit{H}_3)_B$), 2.07 (s, 3H; $CH_3C^{4/5}$), 2.12 (s, 3H; $CH_3C^{4/5}$), 2-93-3.06 (m, 1H; CH) 3.18 (s, 3H; OCH_3), 3.37-3.47 (m, 1H; $CH_2C\mathit{H}$), 3.63 (dd, ^2J(H,H) = 14.7 Hz, ^3J(H,H) = 4.4 Hz, 1H; $NC\mathit{H}_AH_B$), 3.79 ppm (dd, ^2J(H,H) = 14.7, ^3J(H,H) = 8.0 Hz, 1H; $NCH_A\mathit{H}_B$); **^{13}C NMR** (75 MHz, $CDCl_3$, 25 °C, TMS): δ = 9.16 ($C\mathit{H}_3C^{4/5}$), 12.70 $C\mathit{H}_3C^{4/5}$), 17.23 ($CHC\mathit{H}_3$), 22.08 ($CH(C\mathit{H}_3)_A(CH_3)_B$), 22.24 ($CH(CH_3)_A(C\mathit{H}_3)_B$), 25.89 ($C\mathit{H}(CH_3)_2$), 48.81 ($C\mathit{H}_2CH$), 57.24 ($OCH_3$), 76.78 ($NCH_2C\mathit{H}$), 121.14 ($C^{4/5}$), 131.38 ($C^{4/5}$), 151.75 ppm ($C^2$); **IR** (ATR): ν = 1087, 1140, 1308, 1438, 2928, 2970 cm^{-1}; **MS** (ES): *m/z* (%): 211.3 (100) [M+H$^+$]; yield: 61%, colourless oil.

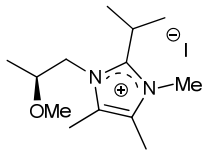

(*S*)-2-Isopropyl-1-(2-methoxypropyl)-3,4,5-trimethylimidazolium iodide ((*S*)-99b): $[\alpha]_D^{25}$ = 18.8 ± 0.3 (C = 0.4 in $CHCl_3$); **^{1}H NMR** (300 MHz, $CDCl_3$, 25 °C, TMS): δ = 1.33 (d, ^3J(H,H) = 6.1 Hz, 3H; $CH(OCH_3)C\mathit{H}_3$), 1.50 (d, ^3J(H,H) = 7.7 Hz, 3H; $CH(C\mathit{H}_3)_A(CH_3)_B$), 1.51 (d, ^3J(H,H) = 7.2 Hz, 3H; $CH(CH_3)_A(C\mathit{H}_3)_B$), 2.30 (s, 6H; $CH_3C^{4/5}$), 3.25 (s, 3H; OCH_3), 3.51-3.61 (m, 1H; CH), 3.66-3.80 (m, 1H; $C\mathit{H}OCH_3$), 3.84 (s, 3H; NCH_3), 4.05 (dd, ^2J(H,H) = 15.4 Hz, ^3J(H,H) = 9.9 Hz, 1H; $NC\mathit{H}_AH_B$), 4.33 ppm (dd, ^2J(H,H) = 15.4, ^3J(H,H) = 2.2 Hz, 1H; $NC\mathit{H}_AH_B$); **^{13}C NMR** (75 MHz, $CDCl_3$, 25 °C, TMS): δ = 9.70 ($C\mathit{H}_3C^{4/5}$), 10.05 ($C\mathit{H}_3C^{4/5}$), 16.72 ($CHC\mathit{H}_3$), 19.30 ($CH(C\mathit{H}_3)_A(CH_3)_B$), 19.47 ($CH(CH_3)_A(C\mathit{H}_3)_B$), 25.35 ($C\mathit{H}(CH_3)_2$), 34.37 ($NCH_3$), 51.55 ($C\mathit{H}_2CH$), 56.75 ($OCH_3$), 75.24 ($NCH_2C\mathit{H}$), 125.81 ($C^{4/5}$), 126.82 ($C^{4/5}$), 148.97 ppm ($C^2$); **IR** (ATR): ν = 1083, 1148, 1450 1521, 1651, 2361, 2976, 3435 cm^{-1}; **MS** (ES): *m/z* (%): 225.3 (100) [M+H$^+$]; yield: 98%, yellow oil.

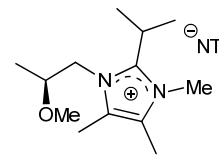

(*S*)-2-Isopropyl-1-(2-methoxypropyl)-3,4,5-trimethylimidazolium bis(trifluoromethylsulfonyl)imide ((*S*)-99c): $[\alpha]_D^{25}$ = 16.0 ± 0.5 (C = 0.4 in $CHCl_3$); **^{1}H NMR** (300 MHz, $CDCl_3$, 25 °C, TMS): δ = 1.27 (d, ^3J(H,H) = 6.1 Hz, 3H; $CH(OCH_3)C\mathit{H}_3$), 1.43 (d, ^3J(H,H) = 7.2 Hz, 3H; $CH(C\mathit{H}_3)_A(CH_3)_B$), 1.46 (d, ^3J(H,H) = 7.7 Hz, 3H; $CH(CH_3)_A(C\mathit{H}_3)_B$), 2.23 (s, 6H; $CH_3C^{4/5}$), 3.23 (s, 3H; OCH_3), 3.45-3.55 (m, 1H; $C\mathit{H}OCH_3$), 3.53-3.66

(m, 1H; CH), 3.74 (s, 3H; NCH_3), 3.96 (dd, ^2J(H,H) = 15.3 Hz, ^3J(H,H) = 9.4 Hz, 1H; NCH_AH_B), 4.05 ppm (dd, ^2J(H,H) = 15.3, ^3J(H,H) = 2.5 Hz, 1H; NCH_AH_B); **^{13}C NMR** (75 MHz, $CDCl_3$, 25 °C, TMS): δ = 8.49 ($CH_3C^{4/5}$), 8.95 ($CH_3C^{4/5}$), 16.17 ($CHCH_3$), 18.57 ($CH(CH_3)_2$), 25.39 ($CH(CH_3)_2$), 32.80 (NCH_3), 50.75 (CH_2CH), 56.54 (OCH_3), 75.13 (NCH_2CH), 119.91 (q, ^1J(C,F) = 321.5 Hz; CF_3), 125.66 ($C^{4/5}$), 126.86 ($C^{4/5}$), 148.96 ppm (C^2); **IR** (ATR): ν = 1053, 1134, 1177, 1348 cm^{-1}; **MS** (ES): *m/z* (%): 225.3 (100) [M+H$^+$]; yield: 97%, yellow oil.

3.7. Synthesis of *N*-alkylimidazolium salts with dimethyl carbonate

3.7.1) Synthesis of N-alkylimidazolium carbonate ionic liquids

Procedure for the synthesis of 1-ethyl-2-isopropyl-3,4,5-trimethylimidazolium hydrogen carbonate [$C_2C_{i3}m_3$im][HCO_3] (47e): A flame-dried glass 15 mL pressure vial was filled with MeOH (5 mmol ,160 mg), dimethyl carbonate (30 mmol, 2.7 g), 1-ethyl-2-isopropyl-4,5-dimethylimidazole (10 mmol, 1.67 g), Montmorillonite K10 (0.83 g) and a PTFE stirring bar. The pressure vial was flushed with nitrogen, closed and submerged in a preheated oil bath at 170 °C. After 24h, the vial was allowed to cool and opened, the mixture was diluted in methanol and filtrated over a filter paper (Euro Scientific, 90 mm) on a sintered glass filter. The solvents were removed by rotary evaporation at room temperature. The resulting oil was brought into 10 mL of demineralised water and stirred at 0 °C. After 3h, the mixture was allowed to cool and the water and methanol were removed via lyophilisation or rotary evaporation. The different spectral data sets of the 1-ethyl-3,4,5-trimethylimidazolium carbonate salts were obtained by dissolving these crystals in different solvents.

1-Ethyl-3,4,5-trimethylimidazolium hydrogen carbonate [C_2m_3im][HCO_3] (44h+114): ^{1}H NMR (300 MHz, $CDCl_3$, 25 °C, TMS): δ = (maj.): δ = 1.49 (t, ^3J(H,H) = 7.2 Hz, 3H; CH_2CH_3), 2.23 (s, 3H; $CH_3C^{4/5}$), 2.24 (s, 3H; $CH_3C^{4/5}$), 3.87 (s, 3H; NCH_3), 4.19 (t, ^3J(H,H) = 7.2 Hz, 2H; CH_2CH_3), 10.07 ppm (s; C^2H), (min.): δ = 1.42 (t, ^3J(H,H) = 7.1 Hz, 3H; CH_2CH_3), 2.24 (s, 3H; $CH_3C^{4/5}$), 2.26 (s, 3H; $CH_3C^{4/5}$), 3.97 (s, 3H; NCH_3), 4.51 ppm (t, ^3J(H,H) = 7.1 Hz, 2H; CH_2CH_3); **^{13}C NMR** (75 MHz, $CDCl_3$, 25 °C, TMS): (maj.): δ = 8.29 ($CH_3C^{4/5}$), 8.38 ($CH_3C^{4/5}$), 15.31 (CH_2CH_3), 33.53 (NCH_3), 42.22 (NCH_2), 125.90 ($C^{4/5}$), 127.03 ($C^{4/5}$), 136.30-136.59 (m, C^2), 160.86 ppm ($[HCO_3]^-$), (min.): δ = 8.52 ($CH_3C^{4/5}$), 8.73 ($CH_3C^{4/5}$), 15.76 (CH_2CH_3), 33.24 (NCH_3), 41.65 (CH_2), 124.44 ($C^{4/5}$), 125.79 ($C^{4/5}$), 141.58 (C^2), 156.04 ppm (CO_2); **IR** (ATR): ν = 625, 985, 1203, 1342, 1377, 1570, 1617, 2341, 2360, 3386 (broad) cm^{-1}; **MW** (g mol^{-1}): 200.24; yield: 52%, colourless crystals.

1-Ethyl-2-deutero-3,4,5-trimethylimidazolium deutero carbonate [C_2m_3im][HCO_3]-d_2 (44i): ^{1}H NMR (300 MHz, D_2O, 25 °C, CH_3CN): δ = 1.43 (t, ^3J(H,H) = 7.3 Hz, 3H; CH_2CH_3) , 2.21 (s, 3H; $CH_3C^{4/5}$), 2.23 (s, 3H; $CH_3C^{4/5}$), 3.71 (s, 3H; NCH_3), 4.08 ppm (q, ^3J(H,H) = 7.3 Hz, 2H; NCH_2); **^{13}C NMR** (75 MHz, $CDCl_3$, 25 °C, TMS): δ = 7.78 ($CH_3C^{4/5}$), 7.92 ($CH_3C^{4/5}$), 14.65 (CH_2CH_3), 33.46 (NCH_3), 42.41 (CH_2CH_3), 127.16 ($C^{4/5}$), 128.06 ($C^{4/5}$), 132.92 (C^2), 161.61 ppm (HCO_3);

1-Ethyl-3,4,5-trimethylimidazolium methyl carbonate [C_2m_3im][CH_3OCO_2] (44e): ^{1}H NMR 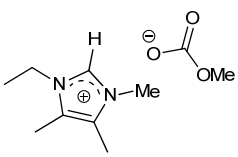 (300 MHz, $CDCl_3$, 25 °C, TMS): δ = 1.52 (t, ^3J(H,H) = 7.4 Hz, 3H; CH_2CH_3), 2.24 (s, 3H; $CH_3C^{4/5}$), 2.26 (s, 3H; $CH_3C^{4/5}$), 3.55 (s, 3H; CH_3OCO_2), 3.88 (s, 3H; NCH_3), 4.20 (t, ^3J(H,H) = 7.4 Hz, 2H; CH_2CH_3), 10.43 ppm (s; C_2H); **^{13}C NMR** (75 MHz, $CDCl_3$, 25 °C, TMS): δ = 8.23 ($CH_3C^{4/5}$), 15.19 (CH_2CH_3), 33.44 (NCH_3), 42.19 (NCH_2), 52.28 (CH_3O), 126.05 ($C^{4/5}$), 127.11 ($C^{4/5}$), 136.28 (C^2), 158.76 ppm (C=O);

1-Ethyl-2,3,4,5-tetramethylimidazolium deutero carbonate [$C_2C_1m_3$im][HCO_3]-*d* (45f): ^{1}H NMR 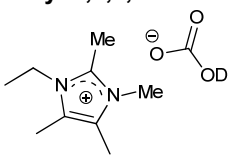 (300 MHz, $CDCl_3$, 25 °C, TMS): δ = 1.31 (t, ^3J(H,H) = 7.3 Hz, 3H; CH_2CH_3) , 2.23 (s, 3H; $CH_3C^{4/5}$), 2.24 (s, 3H; $CH_3C^{4/5}$), 2.70 (s, 3H, C^2CH_3), 3.71 (s, 3H; NCH_3), 4.15 ppm (q, ^3J(H,H) = 7.3 Hz, 2H; NCH_2); **^{13}C NMR** (75 MHz, $CDCl_3$, 25 °C, TMS): δ = 8.50 ($CH_3C^{4/5}$), 8.75 ($CH_3C^{4/5}$), 10.23 (C^2CH_3), 14.93 (CH_2CH_3), 32.15 (NCH_3), 40.55 (NCH_2), 124.69 ($C^{4/5}$), 126.08 ($C^{4/5}$), 142.07 (C^2), 160.27 ppm (HCO_3); **IR** (ATR): ν = 740, 1372, 1626, 2928, 3390 cm^{-1}; **MW** (g mol^{-1}): 214.26; yield: 47%, transparent crystals.

1-Ethyl-2-isopropyl-3,4,5-trimethylimidazolium deutero carbonate [$C_2C_{i3}m_3$im][HCO_3]-*d* (47f): ^{1}H NMR 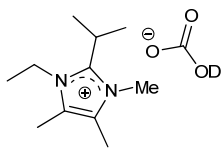 (300 MHz, $CDCl_3$, 25 °C, TMS): δ = 1.36 (t, ^3J(H,H) = 7.4 Hz, 3H; CH_2CH_3), 1.51 (t, ^3J(H,H) = 7.1 Hz, 6H; $CH(CH_3)_2$), 2.27 (s, 6H; $CH_3C^{4/5}$), 3.58-3.72 (m, 1H; $CH(CH_3)_2$), 3.83 (s, 3H; NCH_3), 4.24 ppm (q, ^3J(H,H) = 7.4 Hz, 2H; CH_2CH_3); **^{13}C NMR** (75 MHz, $CDCl_3$, 25 °C, TMS): δ = 8.69 ($CH_3C^{4/5}$), 8.86 ($CH_3C^{4/5}$), 15.73 (CH_2CH_3), 19.30 ($CH(CH_3)_2$), 25.16 ($CH(CH_3)_2$), 32.98 (NCH_3), 40.87 (NCH_2), 125.15 ($C^{4/5}$), 127.15 ($C^{4/5}$), 147.43 (C^2), 160.41 ppm (HCO_3); **IR** (ATR): ν = 1334, 1385, 1522, 1649, 3388 cm^{-1}; **MW** (g mol^{-1}): 242.32; yield: 89%, brown oil.

3.7.2) Carbonate mediated metathesis of N-alkylimidazolium ionic liquids

Procedure for the synthesis of ammonium dicyanamide (121): A glass column was packed with 2.74 g of Amberlite IR120 in distilled water (column height: 3.5 cm). The resin was slowly percolated with a 1 M NH_4Cl solution (200 mL) until the effluent stream pH, monitored by pH indicator paper, had raised to that of the influent. Subsequently, the column was rinsed with aq. dest. (75 mL) until the effluent samples did no longer show precipitation upon addition of $AgNO_3$. Sodium dicyanamide (2 mmol, 178 mg) was dissolved in aq. dest. (40 mL) and MeOH (20 mL), and this solution was percolated very slowly over the column. The percolated solution and the rinsing water (aq. dest., 20 mL) were subjected to lyophilisation to yield the ammonium dicyanamide. Elemental analysis calcd (%) for $C_2H_4N_4$: C 28.57, H 4.80, N 66.64; found: C 27.83, H 4.49, N 64.82; yield: 95%; white powder.

Procedure for the ammonium dicyanamide mediated metathesis towards 1-ethyl-3,4,5-trimethylimidazolium dicyanamide [C_2m_3im][$N(CN)_2$] (44c): To a 50 mL flask charged with the crystalline [C_2m_3im][HCO_3]-d_2 (10 mmol, 2.02 g) were added demineralised water (25 mL) and a PTFE stirring bar. Then ammonium dicyanamide (10.5 mmol, 0.88g) was added to the solution. The flask was equipped with a cooler with cotton plug and the mixture was heated to 50 °C for 16h. After reaction, the water was removed by rotary evaporation. The resulting oil

was dissolved in dry CH_2Cl_2 and cooled to -18 °C, after which a precipitate was filtrated off. Dichloromethane was removed *in vacuo*. The ionic liquid was dried for 8 h at 80 °C under reduced pressure (0.5 mbar). A white solid was obtained in quantitative yield.

Procedure for the synthesis of 1-ethyl-3,4,5-trimethylimidazolium chloride [C_2m_3im][Cl] (44k): To a flame-dried glass 15 mL pressure vial, charged with the 1-ethyl-4,5-dimethylimidazolium hydrochloride (10 mmol, 1.75 g) crystals, were added MeOH (5 mmol ,160 mg), dimethyl carbonate (30 mmol, 2.7 g) and a PTFE stirring bar. The pressure vial was flushed with nitrogen, closed and submerged in a preheated oil bath at 170 °C. After 3h, the vial was allowed to cool to room temperature. The volatiles were removed by rotary evaporation and an opaque powder was obtained

1-Ethyl-3,4,5-trimethylimidazolium chloride [C_2m_3im][Cl] (44k): ^{1}H NMR (300 MHz, $CDCl_3$, 25 °C, TMS): δ = 1.55 (t, J^3(H,H) = 7.3 Hz, 3H; CH_2CH_3) , 2.26 (s, 3H; $CH_3C^{4/5}$), 2.27 (s, 3H; $CH_3C^{4/5}$), 3.95 (s, 3H; NCH_3), 4.24 (q, J^3(H,H) = 7.3 Hz, 2H; NCH_2) 10.74 ppm (s, 1H; C^2H); **^{13}C NMR** (75 MHz, $CDCl_3$, 25 °C, TMS): δ = 8.47 ($CH_3C^{4/5}$), 8.55 ($CH_3C^{4/5}$), 15.42 (CH_2CH_3), 33.85 (NCH_3), 42.45 (NCH_2), 125.98 ($C^{4/5}$), 127.08 ($C^{4/5}$), 136.27 ppm (C^2); IR (ATR): ν = 1200, 1252, 1457, 1572, 1637, 2342, 2362, 2953, 3390 cm^{-1}; **MW** (g mol^{-1}): 174.67; **elemental analysis** calcd (%) for $C_8H_{15}ClN_2$: C 55.01, H 8.66, N 16.04; found: C 54.32, H 8.75, N 15.79; yield: 81%, opaque powder.

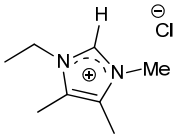

1-Ethyl-2,3,4,5-tetramethylimidazolium chloride [$C_2C_1m_3$im][Cl] (45i): ^{1}H NMR (300 MHz, $CDCl_3$, 25 °C, TMS): δ = 1.40 (t, ^3J(H,H) = 7.4 Hz, 3H; CH_2CH_3), 2.26 (s, 6H; $CH_3C^{4/5}$), 2.94 (s, 3H; C^2CH_3), 3.87 (s, 3H; NCH_3), 4.23 ppm (q, J^3(H,H) = 7.4 Hz, 2H; NCH_2); **^{13}C NMR** (75 MHz, $CDCl_3$, 25 °C, TMS): δ = 8.70 ($CH_3C^{4/5}$), 8.99 ($CH_3C^{4/5}$), 11.18 (C^2CH_3), 15.12 (CH_2CH_3), 32.89 (NCH_2), 41.07 (NCH_3), 124.69 ($C^{4/5}$), 126.16 ($C^{4/5}$), 142.45 ppm (C^2); IR (ATR): ν = 1091, 1346, 1446, 1649, 2978, 3393 cm^{-1}; **MW** (g mol^{-1}): 188.70; yield: 99%, white powder.

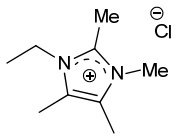

3.8. Base stability testing

Procedure for the synthesis of diphenylmethanol (55) in the IL [$C_6C_{i3}m_3$im][NTf_2]: A flame-dried 10 mL flask, equipped with septum and nitrogen flow, was charged with intensively dried ionic liquid [$C_6C_{i3}m_3$im][NTf_2] (4.8 mmol, 2.50 g). The ionic liquid was cooled to -10 °C in a NaCl/ice bath and bromobenzene (2 mmol, 314 mg) was added with a syringe. After cooling and controlled stirring for 5 min, a homogenous mixture was obtained, to which a 2.3 M *n*Buli solution (2.1 mmol, 0.91 mL) was added dropwise over 15 min, while maintaining a constant temperature of -10 °C. After controlled stirring for 10 min, benzaldehyde (2 mmol, 212 mg) was added dropwise over 5 min with a syringe. The mixture was stirred for 60 min and allowed to obtain room temperature. After reaction, 1 mL of demineralised water was added and the organic fraction was extracted 2 times with 5 mL of dichloromethane. The organic solution was extracted 2 times with 10 mL of diethyl ether, the extracts were combined and GC samples were prepared from the ethereal solution. The presence of diphenylmethanol was demonstrated by comparison of the latter with GC analysis of pure commercial diphenylmethanol.

Procedure for the synthesis of 2-phenylpropan-2-ol (69) in the IL [$C_{201}C_{i3}m_3im$][NTf_2]: A flame-dried 10 mL flask, equipped with a water cooler and nitrogen flow, was charged with intensively dried ionic liquid [$C_{201}C_{i3}m_3im$][NTf_2] (4.9 mmol, 2.40 g) and 2 mL of dry THF. To the mixture was added Mg (2 mmol, 50 mg) and ethyl bromide (2 mmol, 224 mg). The mixture was heated in an oil bath at 100 °C, after 30 minutes when all magnesium was reacted, the mixture was allowed to cool to room temperature. The solvent was evaporated by rotary evaporation, after evaporation, the rotavapor was filled with nitrogen, to remove the flask and provide it with a septum. The flask was cooled to 0 °C, and very slowly acetophenone (2 mmol, 247 mg) was added via a syringe under controlled stirring. The reaction was stirred 2h further at room temperature. After reaction CH_2Cl_2 (20 mL) and distilled water (20 mL) were added. The aqueous phase was extracted twice more with CH_2Cl_2 (10 mL). The combined organic phases were evaporated and extracted twice with cold Et_2O (10 mL). The combined ethereal fractions were, analysed by GC-FID and evaporated. The ionic liquid phase was intensively dried at 100 °C for 4h under reduced pressure, yielding 91% of the pure IL.

4. Mineral composition of dicyanamide ionic liquids

Table 31: Complete mineral composition (in ppm) as analysed by ICP of 4 different 1-ethyl-(2-alkyl)-3,4,5-trimethylimidazolium dicyanamide salts. The alkylgroup/proton on C2 is given under R^2.

Sample	R^2	sample mass (g)	total mass (g)	Ca	Cu	Fe	K
KAS1	Et	0.5188	20.3346	1.37	0.12	0.13	0.26
KAS2	Me	0.449	20.0089	0.041	0.12	0.154	0.0061
KAS3	H	1.0027	20.0124	2.6	0.30	0.115	0.17
KAS4	iPr	0.9992	21.7718	1.47	0.12	0.12	0.1

Sample	Mg	Na	Ni	P	S	Si
KAS1	0.2	41.61	0.079	0.996	3.14	0.974
KAS2	0.064	0.28	0.072	0.282	0.8	0.81
KAS3	0.24	8.16	0.077	1.08	19.3	0.24
KAS4	0.2	0.773	0.074	0.86	1.77	0.118

In Table 31 the content of different minerals is presented in the dicyanamide salts **44-47c**, prepared via the intermediate methanesulfonate salts **44-47d** as well as the used sample mass and the total mass of the aqueous solution (= sample + water).

5. Continuous flow experiments

5.1. Calibration experiments

5.1.1) Ethanol solutions: LC-UV

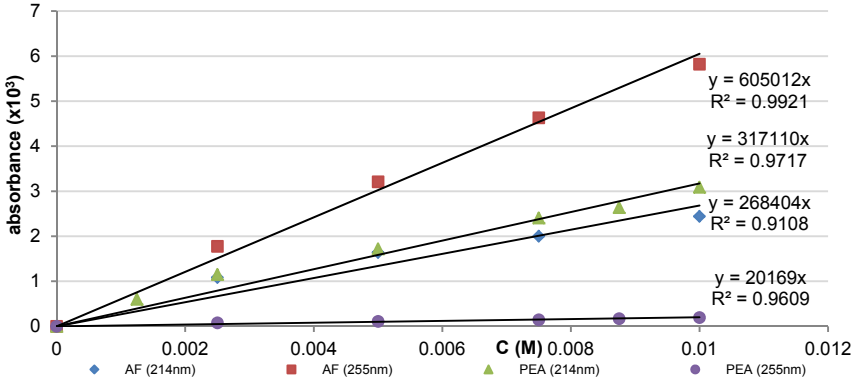

Figure 51: Calibration curve of acetophenone solutions in ethanol on LC-UV at different wavelengths. Calibration of AF is performed by recording three LC-UV measurements of different dilution samples of one stock solution. The mean of these three values is plotted.

In experiment 2-1 the same calibration curves are used and extrapolated to up to 80 mM. This is also applied for the PEA concentration in experiment 2-2. The amount of EtPh (EB) was calculated by assuming only EB and PEA are present when appearing together in the effluent mixture. The experiment at 20 mM is analyzed at 256nm while 60 mM is analyzed at 214nm.

5.1.2) Hexane solutions: GC-FID

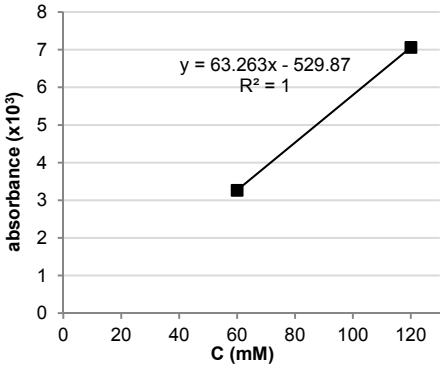

Figure 52: Calibration curve of acetophenone (AF) solutions in hexanes on GC-FID. Calibration of AF is performed by recording three GC-FID measurements of two different samples of one stock solution. The mean of these six values is plotted.

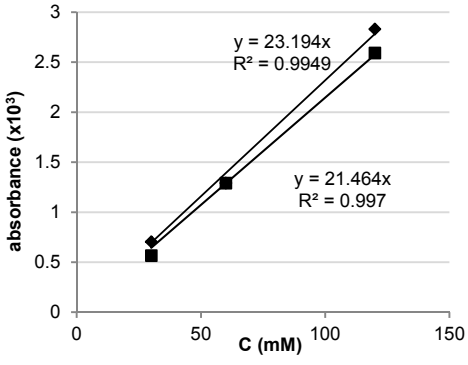

Figure 53: Calibration curve of ethyl lactate (◆) and ethyl pyruvate (■) solutions in hexanes on GC-FID. Calibration is performed by recording one GC-FID measurement of two different samples of one stock solution. The mean of these two values is plotted.

In experiment 1-3, the products (AF, PEA and EB) were calibrated by assuming the highest possible concentration; the side-products formed over 80 °C were not taken into account.

5.2. Long term hydrogenation experiments with the CSRN CatCart

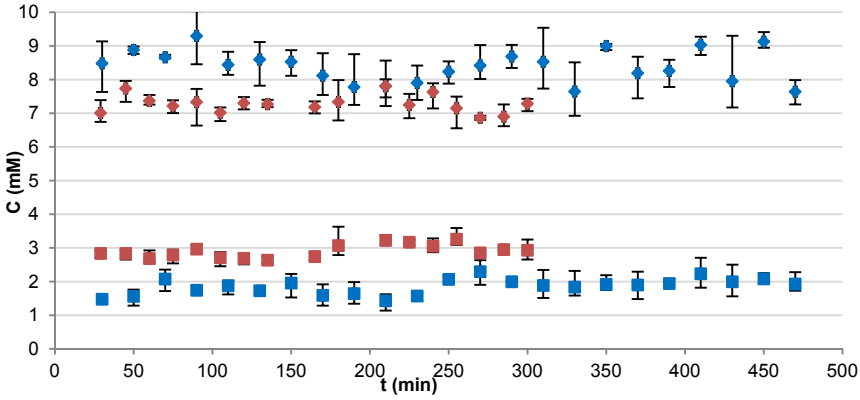

Figure 54: Plot of effluent concentration of PEA (■) and AF (◆) during experiments 1-1 (red) and 1-7 (blue) demonstrating the lower conversion at higher p_{gas} and quasi steady conversion over time.

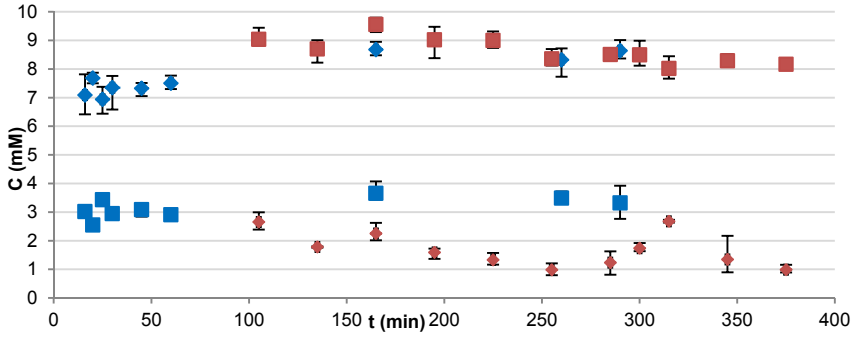

Figure 55: Plot of effluent concentration of PEA (■) and AF (◆) during experiments 1-2 (blue) and 1-3 (red), indicating steady-state formation and anomaly at *t*=30 and *t* =300 min respectively.

5.3. Hydrogenation with the TNRN CatCart

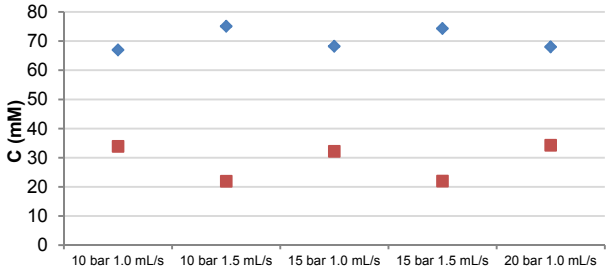

Figure 56: Effluent concentrations of PEA (■) and AF (◆) during experiment 2-1 for different p_{sys} and pump speeds, performed at 50 °C, C_{in}: 120 mM.

VII) SUMMARY

Peralkylated imidazoles were easily obtained via the optimised Debus-Radziszewski reaction procedure. This reaction allows the condensation of a myriad of aldehydes and primary amines with an α,β-diketone and an ammonia source, although the yields were only moderate. The a priori synthesis of the imine (**iii**) allowed an increased selectivity towards the *N*-substituted imidazole (**v**) vs. the 1*H*-imidazole (**vi**). The type of aldehyde only influenced the selectivity and yield to some extent. More sterically hindered amines decreased the selectivity while *N*-ethylimidazoles are produced with a 100% selectivity.

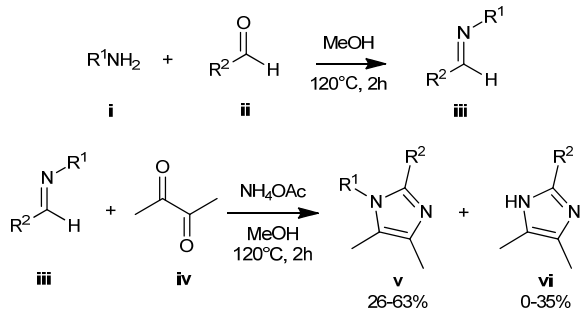

Thus, the lower selectivity was attributed to a higher transimination upon the addition of the ammonia source. For more sterically hindered amines, the selectivity could be further increased by slowly adding the ammonia and diketone source. Alternatively, the diketone and ammonia could be mixed prior to the addition. In this way, the preformed imine could be reacted with this mixture. The success of the reaction with the two mixtures in the formation of imidazoles was shown in a continuous flow setup.

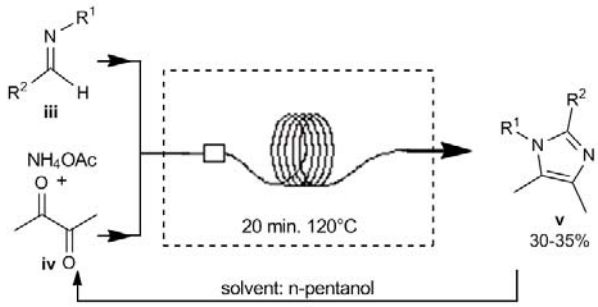

The use of the *Cytos CPC* continuous flow system did not allow pressurised reactions, therefore n-pentanol was used as the solvent. This solvent was found to be recyclable by

distillation without further processing. While the low boiling point of ethyl amine did not allow its application in the micro reactor system, hexyl amine could be used to produce *N*-hexylimidazoles at a production rate of 3.5 to 4 grams h^{-1} with a yield comparable to the maximum yields obtained in batch. Hereby it was important to keep the concentration at 0.5 M, since higher concentrations induced the formation of the 1*H*-imidazole.

The choice of amine allowed different substitution patterns to be easily introduced on the imidazole. Thus, *N*-alkyl, -alkenyl and -alkoxyl functionalisation of the imidazole was efficiently obtained. The different alkyl- and alkenylimidazoles could be obtained as their hydrochloride salts, which allowed to purify the imidazoles extensively via recrystallisation or filtration.

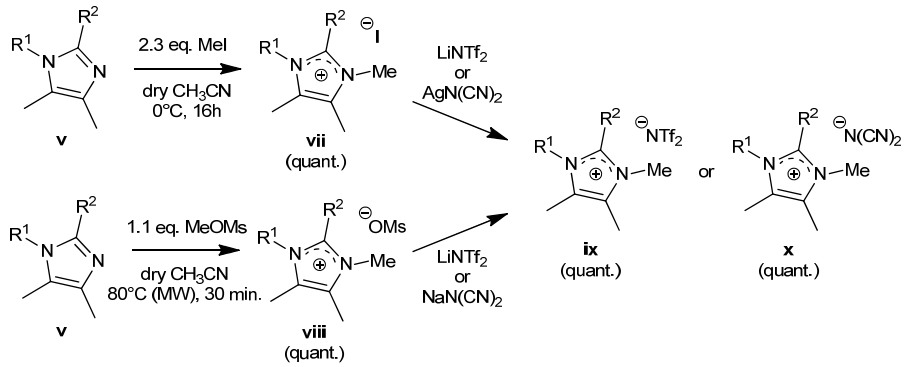

Quaternisation with methyl iodide or methyl methanesulfonate, allowed the imidazoles to be quantitatively transformed into the corresponding *N*-methylimidazolium ionic liquids (**vii**, **viii**) without the formation of side products. The excess of quaternisation agent could be evaporated or extracted. Although higher temperatures were applied when using methyl methanesulfonate, the colouration was more intense during quaternisation with methyl iodide, indicating that an oxidation reaction is responsible for the formation of intensively coloured contaminants. The iodide ionic liquids were often solid, which allowed for recrystallisation prior to metathesis, while most of the methanesulfonate ionic liquids were liquid. Metathesis could be obtained via standard literature procedures, although the methanesulfonate ionic liquids allowed the use of sodium dicyanamide. The purity of the thus resulting ionic liquids was very satisfying, indicating no residual sodium. This method reduced both the cost and environmental impact of the dicyanamide ionic liquid synthesis.

An alternative way to reduce the environmental impact comprises the use of dimethyl carbonate (DMC) as the quaternisation agent. This environmentally benign quaternisation agent allowed the formation of different methyl carbonates (**xi**) in good yields. However, high

temperatures were needed, leading to an intensive colouration. The metathesis towards the $[NTf_2]^-$ ionic liquids (**ix**) was successfully performed. For other Brønsted acids, the strong interaction of acid with the ionic liquids and the unknown stoichiometry of the extracted carbonate ionic liquids, containing a mixture of anions, led to incomplete removal of the excess Brønsted acids.

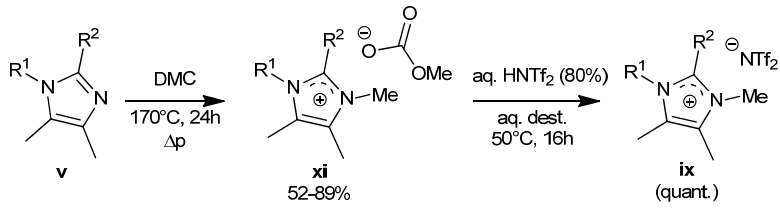

The 1-ethyl-2*H*-imidazole was found to have a crystalline hydrogen carbonate salt, which could be purified by recrystallisation. In deuterated solvents (for ^{1}H NMR analysis), the high basicity of the anion induced a complete deuteration of the anion and the C2 proton (**xii**). This hydrogen carbonate salt showed formation of the carboxylate (**xiii**) upon dissolution in some solvents. In the C2 substituted salts, only the 2-methyl moiety was deuterated (**xiv**, **xv**), albeit slower than the C2 proton. This confirmed the high chemical stability of 2-isopropyl substituted imidazoles and invites for the application of 2-isopropylimidazolium carbonate salts as very alkaline ionic liquids.

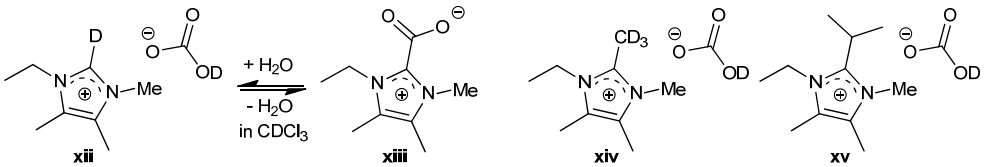

Alternative to the previous quaternisation agents (MeI, MeOMs and DMC), functionalised quaternisation agents could introduce functionalities in the ionic liquids. Thus, an allyl functionalisation could also be established via quaternisation with allyl bromide or allyl methanesulfonate.

Together with the introduction of functionalities in the imidazole, the functionalisation during quaternisation allowed for the variation in viscosities and melting points of 2-isopropylimidazolium ionic liquids. Methoxyethyl substitution decreased the viscosity but the resulting ionic liquids readily formed crystals. Introduction of an *N*-allyl group hindered solidification but increased the viscosity of the ionic liquids. When the symmetry increased, the *N*-allyl functionalised imidazolium salts did solidify. Combination of the *N*,*N'*-diallylimidazolium

analogue with the $[Ntf_2]^-$ anion resulted in a melting point of 63 °C (**xvi**), while the methoxyethyl cation formed a room temperature ionic liquid (T_m: 22 °C) (**xvii**).

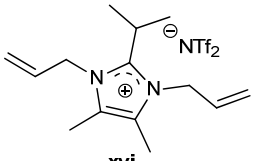

xvi

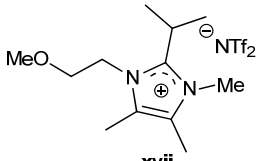

xvii

The incorporation of the amine substitution into the imidazoles also allowed for the incorporation of naturally occurring amines, such as amino acids. Modification of the alanine derived imidazole (**(*rac*)-xviii**) towards the alkoxyl derivative (**(*rac*)-xix**) allowed for (i) the combination of the previously described alkoxyl moieties with an asymmetric centre and (ii) the preparation of ionic liquids with high chemical stability. Unfortunately, the chiral centre was completely racemised and it was found that branching in the α-position significantly decreased the selectivity during the imidazole synthesis.

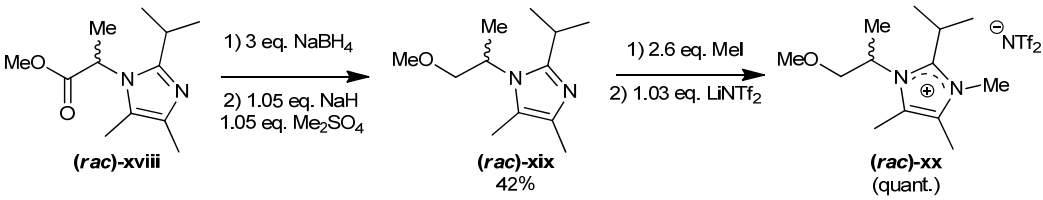

(*rac*)-xviii → **(*rac*)-xix** 42% → **(*rac*)-xx** (quant.)

Alternatively, the methanesulfonate ester of a chiral primary alcohol could be applied for quaternisation. This allows to exploit many naturally occurring or semi-synthetic alcohols as quaternisation agents. These compounds introduce a renewable moiety, and when chiral pool molecules are employed, chiral centres are introduced without the need for asymmetric synthesis. In contrast to the linear synthesis applied in the amino acid derived imidazoles, the convergent synthesis using a lactate derived quaternisation agent (**(*S*)-xxiii**), utilised the imidazole core more efficiently, while the chiral centre was not racemised.

The increased bulk of the C2 substitution on the imidazole decreased the efficiency of quaternisation with the lactate derived agent, hence only 2*H*- and 2-methyl substituted imidazoles could be quaternised, with the formation of **(*S*)-xxiv** and **(*S*)-xxv**, respectively. The formation of the 2-isopropyl substituted imidazolium salt **(*S*)-xxviii** could be established by the synthesis of the chiral imidazole **xxvii**.

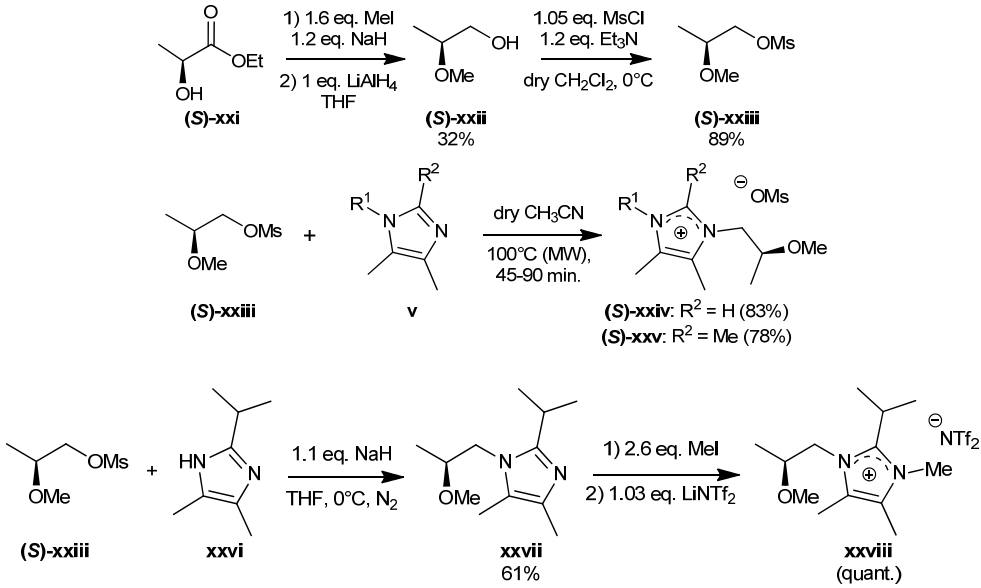

To obtain racemic mixtures of the lactate derived quaternisation agent and the derived ionic liquids, the naturally occurring ethyl pyruvate could be hydrogenated by a continuous flow process over a commercial Raney Nickel catalyst (TNRN). In this green method, metal hydrides were substituted for hydrogen gas and the production rate was about ± 0.4 g h^{-1} of ethyl D/L-lactate.

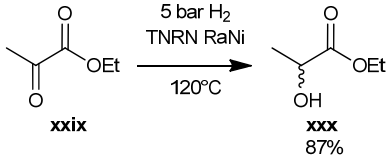

Apart from the rheological properties, the thermal, chemical and electrochemical stabilities of the newly synthesised ionic liquids were assessed. The thermal stability was found to be dependent on the presence of a C2 proton. Alkyl substitution increased the stability, while the nature of the substituent did not further influence the degradation temperatures. On the contrary, the electrochemical stability was found to increase further upon increment of the *2*-alkyl substituent. The chemical stability was evaluated by adding different strong bases or alkaline solutions to the ionic liquids. Thus, it was found that in a 0.1 M KOH solution in D_2O/CD_3OD, the C2 proton of $[C_6m_3im][NTf_2]$ was immediately deuterated, while after 12h, still no deuteration of the $[C_6C_{i3}m_3im][NTf_2]$ salt was observed. The isopropyl substituted ionic liquid was also stable enough to withstand 24 h in a refluxing 1.0 M KOH solution.

The base stability could be successfully exploited by performing lithiation reactions in the $[C_6C_{i3}m_3im][NTf_2]$ ionic liquid. The 1-alkoxyl-2-isopropyl substituted ionic liquids ($[C_{201}C_1C_{i3}m_2im][NTf_2]$ and $[C_{20A}C_1C_{i3}m_2im][NTf_2]$) were successfully applied in the addition of ethylmagnesiumbromide (**xxxii**) to acetophenone. Unfortunately, the Grignard reagent itself could not be synthesised in the ionic liquid.

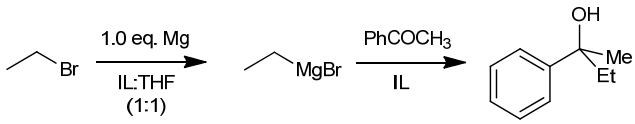

xxxi **xxxii** **xxxiii** 83%

Different analogues were evaluated on their biodegradability. They were all found to be neither readily nor inherently biodegradable. It is to say, the compounds are biodegraded very slowly, but only in the presence of other carbon sources. The 1-hexyl-2*H*-4,5-dimethylimidazolium iodide showed the highest biodegradation and a relatively high adsorption on activated sludge. Overall, the increased lipophilicity was proposed to be the main factor determining the biodegradation of ionic liquids.

VIII) SAMENVATTING

Volledig gesubstitueerde imidazolen werden efficiënt gesynthetiseerd via de geoptimaliseerde Debus-Radziszewski reactie. Tijdens deze condensatiereactie kan een waaier aan aldehyden en primaire aminen gereageerd worden met een α,β-diketon en ammoniak, hoewel de opbrengsten slechts matig waren. Door in een eerste stap het imine (**iii**) te synthetiseren, kon de selectiviteit van het *N*-gesubstitueerde imidazool (**v**) t.o.v. het 1*H*-imidazool (**vi**) verhoogd worden. De keuze van het aldehyde had slechts een geringe invloed op de selectiviteit en het rendement. De selectiviteit daalde echter bij het aanwenden van sterisch gehinderde aminen, terwijl *N*-ethylimidazolen met een selectiviteit van 100% konden worden gesynthetiseerd.

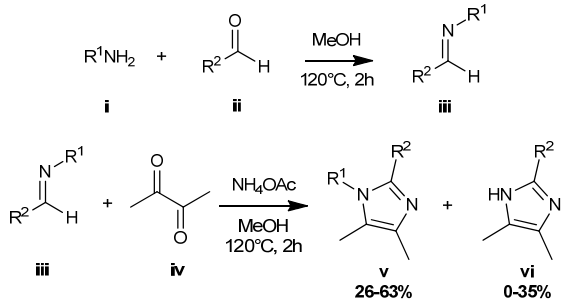

Dit leidde tot de veronderstelling dat de lage selectiviteit te wijten is aan een transiminering die aan belang wint naarmate het amine meer sterisch gehinderd is. De selectiviteit kon voor deze aminen verhoogd worden door ammoniak en het diketon traag toe te voegen. Deze twee reagentia konden ook worden gemengd alvorens toe te voegen. Dit werd succesvol toegepast in de continue imidazoolsynthese in de Cytos CPC flow reactor.

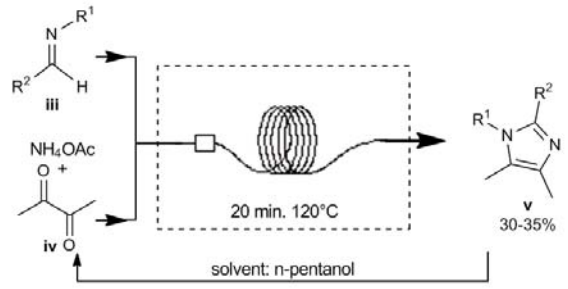

Aangezien het gebruik van de Cytos CPC niet toelaat reacties onder verhoogde druk uit te voeren, werd n-pentanol als solvent gebruikt. Deze keuze liet bovendien toe om het solvent na reactie te recycleren door middel van destillatie. Verdere behandeling van het solvent was

niet nodig voor hergebruik. Wegens het lage kookpunt van ethylamine was de synthese van *N*-ethylimidazolen niet mogelijk, terwijl hexylamine toeliet *N*-hexylimidazolen te synthetiseren met een productiesnelheid van 3.5 tot 4 gram h^{-1}. Hierbij was de opbrengst slechts weinig lager dan in de batchreacties. Het was wel belangrijk de concentratie aan reagentia te beperken tot 0.5 M, aangezien hogere concentraties aanleiding gaven tot de vorming van het 1*H*-imidazool.

De keuze van het amine liet toe verschillende substituenten te introduceren op de imidazolen. Op die manier konden *N*-alkyl, *N*-alkenyl en *N*-alkoxylsubstituenten zeer efficiënt worden ingevoerd. De verschillende alkyl-, en alkenylimidazolen konden worden omgezet in hun hydrochloridezouten. Deze vaste zouten konden worden omgekristalliseerd of gefiltreerd, wat toeliet een extra opzuivering uit te voeren.

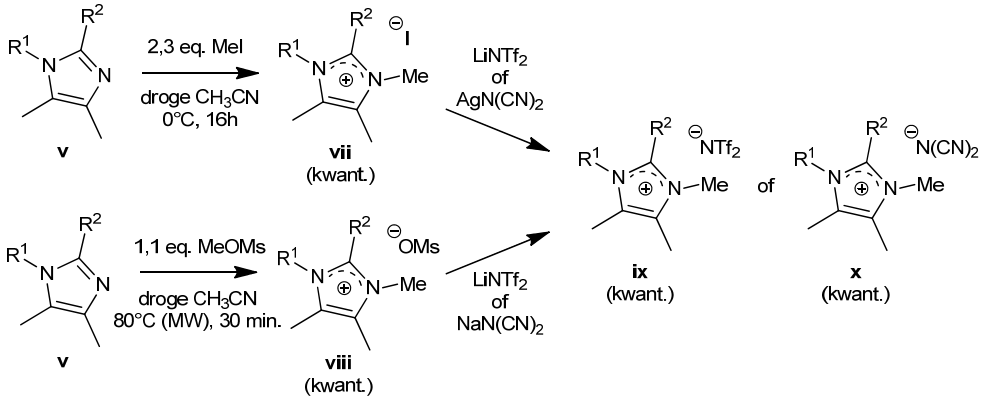

Door te alkyleren met methyljodide of methylmethaansulfonaat, kon een volledige omzetting in de *N*-methylimidazolium ionische vloeistoffen (**vii**, **viii**) bekomen worden, zonder de vorming van nevenproducten. De overmaat aan alkyleringsreagentia kon worden afgedampt of geëxtraheerd. Hoewel tijdens de reactie met methylmethaansulfonaat hogere temperaturen werden aangewend, was de verkleuring van het eindproduct groter na reactie met methyljodide. Dit toonde aan dat een oxidatiereactie aan de basis ligt van de vorming van de intens gekleurde contaminanten. De jodidezouten waren vaak vast of kristallijn, wat een extra omkristallisatie toeliet alvorens de anionuitwisseling uit te voeren. De meeste methaansulfonaatzouten waren vloeibaar. De anionuitwisseling kon worden uitgevoerd via standaard procedures, beschreven in de literatuur. Daarnaast was het mogelijk een anionuitwisseling van de methaansulfonaatzouten uit te voeren met behulp van natriumdicyanamide. De zeer lage natriumconcentratie in het eindproduct toonde aan dat dit

een zeer efficiënte methode is, die toelaat zowel de economische als de ecologische impact van de standaard zilver gemedieerde procedure te omzeilen.

Een alternatieve manier om de ecologische impact van de synthese van ionische vloeistoffen te verlagen is het gebruik van dimethylcarbonaat als alkyleringsreagens. Na toepassen van dit milieuvriendelijke reagens werden imidazoliummethylcarbonaat zouten (**xi**) in goede rendementen bekomen. De reactie vereist echter hoge temperaturen, waardoor de verkleuring van de ionische vloeistoffen intens was. Het carbonaat anion kon succesvol worden omgezet in het $[NTf_2]^-$ anion, waardoor efficiënt en snel de hydrofobe $[NTf_2]^-$ ionische vloeistoffen (**ix**) werden bekomen. Andere Brønstedzuren leidden tot een residuele hoeveelheid zuur in het eindproduct wegens de grote interactie tussen ionische vloeistof en zuur en de moeilijke bepaling van de hoeveelheid geëxtraheerd carbonaatzout.

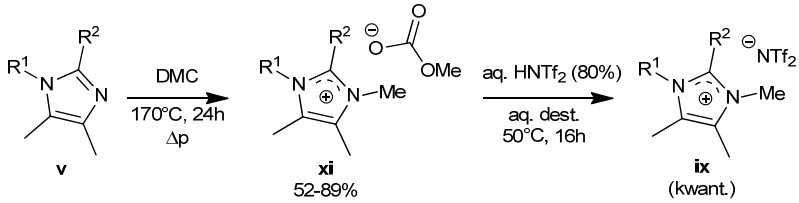

Het 1-ethyl-2*H*-imidazolium waterstofcarbonaatzout werd verkregen als een kristallijn product. Dit liet toe het product op te zuiveren via omkristallisatie. Het erg basische anion leidde in gedeutereerde solventen (voor ^{1}H NMR analyse) tot een complete waterstof/deuterium uitwisseling op het anion en op de C2 positie, maar dit werd niet waargenomen op de andere posities (**xii**). In bepaalde solventen werd dit waterstofcarbonaatzout omgezet in het carboxylaat (**xiii**). Onder de 2-alkylimidazolium kationen werd waterstof/deuterium uitwisseling alleen waargenomen op de 2-methylgroep van het corresponderende analoog (**xiv**, **xv**). Deze uitwisseling verliep trager dan de uitwisseling van het C2 proton. Deze observaties bevestigden de chemische stabiliteit van de 2-isopropyl gesubstitueerde imidazolen en nodigen uit tot het toepassen van deze erg basische ionische vloeistoffen.

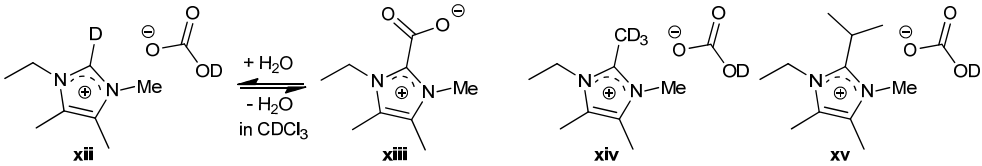

Naast het gebruik van de eerder vermelde alkyleringsreagentia (methyljodide, methyl methaansulfonaat en dimethylcarbonaat), kunnen gefunctionaliseerde alkyleringsreagentia functionele groepen introduceren in de ionische vloeistoffen tijdens de alkyleringsreactie. Op

deze manier kon een allylgroep worden geïntroduceerd door gebruik te maken van allylbromide of allylmethaansulfonaat.

Gecombineerd met het makkelijk te modificeren substitutiepatroon van de neutrale imidazolen, laat het invoeren van functionele groepen tijdens de alkyleringsstap toe om te variëren in de viscositeiten en smeltpunten van de 2-isopropylimidazolium ionische vloeistoffen. Het invoeren van een methoxyethylgroep leidde tot een verlaging van de viscositeit, maar de verkregen zouten waren vaak kristallijn. Het invoeren van een *N*-allyl functionaliteit verhinderde de kristallisatie, maar verhoogde hierbij de viscositeit. De *N*-allyl gesubstitueerde zouten vormden toch kristallen wanneer het kation meer symmetrisch is. Zo resulteerde bijvoorbeeld het *N*,*N'*-diallylderivaat, gecombineerd met het $[NTf_2]^-$ anion in de vorming van een zout met een smeltpunt van 63 °C (**xvi**). Het methoxyethyl analoog vormde op die manier een ionische vloeistof bij omgevingstemperatuur (T_m: 22 °C) (**xvii**).

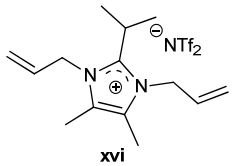

xvi

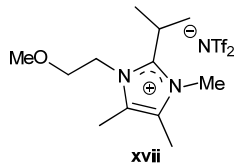

xvii

Het rechtstreekse invoeren van de aminesubstituenten op de imidazooleenheid liet toe natuurlijk voorkomende aminen, zoals bijvoorbeeld aminozuren, te gebruiken. De modificatie van het imidazool gebaseerd op alanine (**(*rac*)-xviii**) tot het alkoxylderivaat (**(*rac*)-xix**) maakte het mogelijk om (i) de hiervoor beschreven alkoxylderivaten te combineren met een asymmetrisch centrum en (ii) ionische vloeistoffen met hoge chemische stabiliteit te synthetiseren. Het chirale centrum werd tijdens de reactie volledig geracemiseerd en de sterische hindering, veroorzaakt door de substitutie in de α-positie, was nadelig voor de selectiviteit van de imidazool synthese.

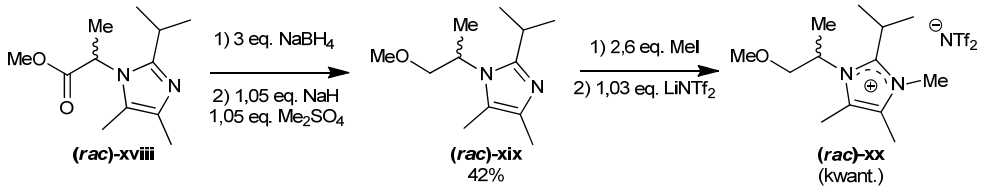

(*rac*)-xviii | **(*rac*)-xix** 42% | **(*rac*)-xx** (kwant.)

Een andere mogelijkheid bestaat erin het methaansulfonaatester van een natuurlijk voorkomend alcohol te gebruiken. Op die manier kan een waaier aan natuurlijk voorkomende of semi-synthetische alcoholen aangewend worden. Hierdoor wordt ook een hernieuwbare fractie in de molecule ingebouwd, maar indien verbindingen uit de *'chiral pool'* worden

aangewend, kan ook een asymmetrisch centrum worden ingevoerd, zonder daarbij gebruik te maken van asymmetrische synthese. In tegenstelling tot de lineaire synthese die toegepast werd om de aminozuur gebaseerde analoga te synthetiseren, werd hierbij een convergente syntheseweg gevolgd, waarbij het imidazool als bouwsteen efficiënter werd benut en bovendien geen racemisatie optrad van het asymmetrisch centrum.

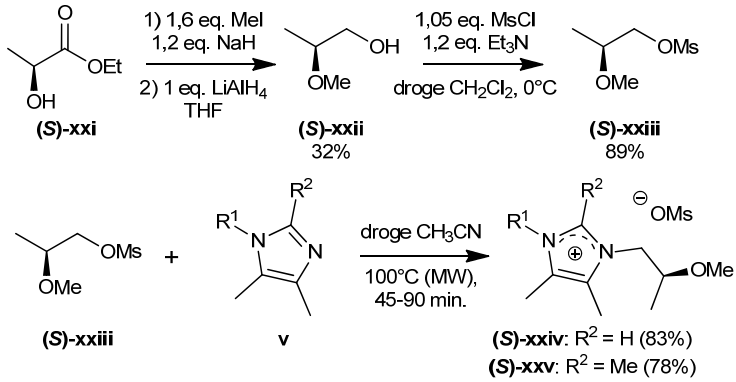

De efficiëntie waarmee dit semi-synthetisch alkyleringsreagens reageerde met imidazolen was sterk afhankelijk van de omvang van de 2-alkylsubstituent. Zo konden alleen de 2*H*- en de 2-methyl derivaten worden gealkyleerd met de respectievelijke vorming van ionische vloeistoffen **(*S*)-xxiv** en **(*S*)-xxv**. De synthese van de 2-isopropyl gesubstitueerde imidazolium ionische vloeistof **(*S*)-xxviii** kon bewerkstelligd worden via de synthese van het chirale imidazool **xxvii**.

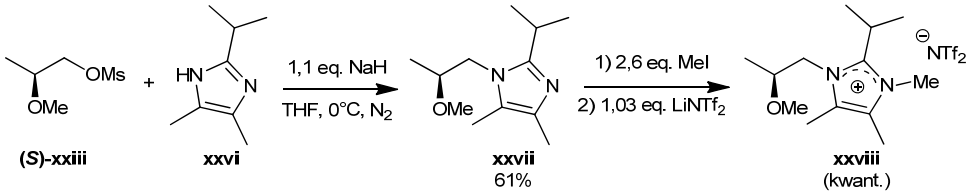

Om een racemisch mengsel te bekomen van het lactaatgebaseerde alkyleringreagens en de daarvan afgeleide ionische vloeistoffen, volstond het om het natuurlijk voorkomend ethylpyruvaat (**xxix**) te reduceren in een continue reactor over een commercieel beschikbare Raney Nickel (TSRN) katalysator. Deze groene alternatieve methode maakte het mogelijk metaal hydrides te vervangen door waterstofgas en D/L-ethyllactaat (**xxx**) te synthetiseren aan een snelheid van ± 0.4 g h^{-1}.

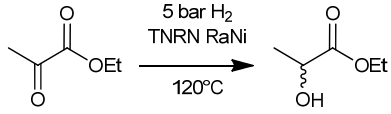

xxix **xxx** 87%

Behalve de invloed op de viscositeit en het smeltpunt werden ook de thermische, chemische en elektrochemische stabiliteit van deze innovatieve ionische vloeistoffen onderzocht. De thermische stabiliteit bleek in sterke mate afhankelijk te zijn van de aanwezigheid van een C2 proton. Na substitutie van dit proton werden hogere decompositietemperaturen bekomen. De aard van de substituent op de C2 positie had weinig of geen invloed op de thermische stabiliteit. Daarentegen leek de elektrochemische stabiliteit wel onderhevig te zijn aan de variatie in de C2 substituent. Zo werd een grotere elektrochemische stabiliteit verkregen naarmate de C2 substituent in grote toenam.

De chemische stabiliteit werd geëvalueerd door verschillende ionische vloeistoffen toe te voegen aan basische oplossingen of toe te passen in reacties met sterke basen. In een 0.1 M KOH oplossing in D_2O/CD_3OD werd het C2 proton van $[C_6m_3im][NTf_2]$ onmiddellijk uitgewisseld met deuterium, terwijl na 12 uur nog steeds geen deuteriumuitwisseling kon worden waargenomen bij de $[C_6C_{i3}m_3im][NTf_2]$ ionische vloeistof. Bij deze 2-isopropyl gesubstitueerde ionische vloeistof kon geen verandering worden waargenomen na 24 uur koken in een 1.0 M KOH oplossing. Deze base stabiliteit kon succesvol toegepast worden door lithieringsreacties te laten plaatsvinden in de $[C_6C_{i3}m_3im][NTf_2]$ ionische vloeistof. De 1-alkoxyl-2-isopropyl gesubstitueerde analogen ($[C_{201}C_1C_{i3}m_2im][NTf_2]$ en $[C_{20A}C_1C_{i3}m_2im][NTf_2]$) werden succesvol gebruikt in de additiereactie van ethylmagnesiumbromide (**xxxii**) met acetofenon. Grignardreagentia konden echter niet worden gesynthetiseerd in de ionische vloeistoffen.

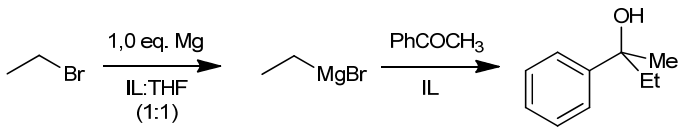

xxxi **xxxii** **xxxiii** 83%

De biodegradeerbaarheid van dit type volledig gesubstitueerde imidazolium ionische vloeistoffen werd geanalyseerd aan de hand van enkele derivaten. De derivaten bleken nauwelijks biodegradeerbaar te zijn, en dan nog enkel in aanwezigheid van een andere koolstofbron. Het 1-hexyl-2*H*-4,5-dimethylimidazolium iodidezout vertoonde de grootste biodegradeerbaarheid en absorptie in actief slib. In het algemeen kon gesteld worden dat de biodegradeerbaarheid beter is voor meer hydrofobe verbindingen.

IX) REFERENCES

[1] P. Walden, *Bull. Acad. Imper. Sci. (St. Petersburg)* **1914**, *6*, 405-422.

[2] a) M. Petkovic, K. R. Seddon, L. P. N. Rebelo, C. Silva Pereira, *Chemical Society Reviews* **2011**, *40*, 1383-1403; b) K. R. Seddon, *Journal of Chemical Technology and Biotechnology* **1997**, *68*, 351-356.

[3] a) M. Gorlov, L. Kloo, *Dalton Trans.* **2008**, 2655-2666; b) H. Matsumoto, H. Sakaebe, K. Tatsumi, M. Kikuta, E. Ishiko, M. Kono, *J. Power Sources* **2006**, *160*, 1308-1313; c) Y. Katayama, in *Electrochemical Aspects of Ionic Liquids*, Wiley-VCH, Hoboken, **2005**, p.111-131.

[4] M. Keating, F. Gao, J. Ramsey, *J. Therm. Anal. Calorim.* **2011**, *106*, 207-212.

[5] a) T. Welton, *Chem. Rev.* **1999**, *99*, 2071-2083; b) F. van Rantwijk, R. A. Sheldon, *Chem. Rev.* **2007**, *107*, 2757-2785.

[6] R. P. Swatloski, S. K. Spear, J. D. Holbrey, R. D. Rogers, *J. Am. Chem. Soc.* **2002**, *124*, 4974-4975.

[7] J. L. Anderson, D. W. Armstrong, *Analytical Chemistry* **2003**, *75*, 4851-4858.

[8] a) H. Debus, *Liebigs Ann. Chem.* **1858**, *107*, 199-208; b) Z. Wang, in *Comprehensive organic name reactions and reagents, Vol. 3,* , Wiley-VCH, Hoboken, **2009**, p.2293-2296; c) B. Radziszewski, *Chem. Ber.* **1882**, *15*, 1493-1496.

[9] S. E. Wolkenberg, D. D. Wisnoski, W. H. Leister, Y. Wang, Z. J. Zhao, C. W. Lindsley, *Org. Lett.* **2004**, *6*, 1453-1456.

[10] D. R. J. Acke, R. V. A. Orru, C. V. Stevens, *QSAR & Comb. Sci.* **2006**, *25*, 474-483.

[11] a) J. Zimmermann, B. Ondruschka, A. Stark, *Org. Process Res. Dev.* **2010**, *14*, 1102-1109; b) A. S. De Miranda, J. C. Gomes, M. T. Rodrigues Jr, I. C. R. Costa, W. P. Almeida, R. d. O. Lopes, L. S. M. Miranda, F. Coelho, R. O. M. A. de Souza, *J. Mol. Catal. B: Enzym* **2013**, *91*, 77-80.

[12] a) H. Iken, F. Guillen, H. Chaumat, M.-R. Mazières, J.-C. Plaquevent, T. Tzedakis, *Tetrahedron Letters* **2012**, *53*, 3474-3477; b) D. Wilms, J. Klos, A. F. M. Kilbinger, H. Löwe, H. Frey, *Org. Process Res. Dev.* **2009**, *13*, 961-964.

[13] a) F. Wendler, L.-N. Todi, F. Meister, *Thermochim. Acta* **2012**, *528*, 76-84; b) K. R. Seddon, A. Stark, M. J. Torres, *Pure Appl. Chem.* **2000**, *72*, 2275-2287.

[14] J. Fisher, W. Siegel, V. Bomm, M. Fisher, K. Mundinger, (BASF). US Patent 6,175,019, **2001**.

[15] a) D. M. Fox, W. H. Awad, J. W. Gilman, P. H. Maupin, H. C. De Long, P. C. Trulove, *Green Chem.* **2003**, *5*, 724-727; b) M. J. Earle, J. Esperanca, M. A. Gilea, J. N. C. Lopes, L. P. N. Rebelo, J. W. Magee, K. R. Seddon, J. A. Widegren, *Nature* **2006**, *439*, 831-834.

[16] T. Belhocine, T. Belhocine, *Green Chemistry* **2011**, *13*, 59.

[17] F. Endres, A. P. Abbott, D. R. MacFarlane, *Electrodeposition from Ionic Liquids*, Wiley-VCH, Weinheim, **2008**.

[18] V. Jurcik, R. Wilhelm, *Green Chem.* **2005**, *7*, 844-848.

[19] P. Wasserscheid, T. Welton, *Ionic Liquids in Synthesis*, 1 ed., Wiley-VCH, Weinheim, **2003**.

[20] Z. J. Zhang, R. G. Reddy, *Thermal stability of ionic liquids*, in *Fundamentals of Advanced Materials for Energy Conversion*, P. R. Taylor, D. Chandra, R. G. Bautista, Editors. **2002**, Minerals, Metals & Materials Soc.: Warrendale. p. 33-39.

[21] a) M. Smiglak, W. M. Reichert, J. D. Holbrey, J. S. Wilkes, L. Sun, J. S. Thrasher, K. Kirichenko, S. Singh, A. R. Katritzky, R. D. Rogers, *Chem. Commun.* **2006**, 2554-2556; b) H.-J. Liaw, C.-C. Chen, Y.-C. Chen, J.-R. Chen, S.-K. Huang, S.-N. Liu, *Green Chem.* **2012**, *14*, 2001-2008.

[22] a) X. X. Han, D. W. Armstrong, *Org. Lett.* **2005**, *7*, 4205-4208; b) R. H. Wang, C. M. Jin, B. Twamley, J. M. Shreeve, *Inorg. Chem.* **2006**, *45*, 6396-6403; c) J. C. Xiao, J. M. Shreeve, *J. Org. Chem.* **2005**, *70*, 3072-3078.

[23] Y. Hao, J. Peng, S. Hu, J. Li, M. Zhai, *Thermochim. Acta* **2010**, *501*, 78-83.

[24] a) R. G. Reddy, *J. Phys.: Conf. Ser.* **2009**, *165*, 12076-12082; b) L. Bai, X. Li, J. Zhu, B. Chen, *Energy Fuels* **2011**, *25*, 1811-1816.

[25] a) M. E. Van Valkenburg, R. L. Vaughn, M. Williams, J. S. Wilkes, *Thermochim. Acta* **2005**, *425*, 181-188; b) H. Liu, E. Maginn, A. E. Visser, N. J. Bridges, E. B. Fox, *Ind. Eng. Chem. Res.* **2012**, *51*, 7242-7254; c) N. J. Bridges, A. E. Visser, E. B. Fox, *Energy Fuels* **2011**, *25*, 4862-4864; d) D. M. Blake, L. Moens, D. Rudnicki, H. Pilath, *J. Sol. Energy Eng.* **2006**, *128*,

54; e) L. Moens, D. M. Blake, D. L. Rudnicki, M. J. Hale, *J. Sol. Energy Eng.* **2003**, *125*, 112-116.

[26] a) Z. Zeng, B. S. Phillips, J.-C. Xiao, J. M. Shreeve, *Chem. Mater.* **2008**, *20*, 2719-2726; b) C.-M. Jin, C. Ye, B. S. Phillips, J. S. Zabinski, X. Liu, W. Liu, J. M. Shreeve, *J. Mater. Chem.* **2006**, *16*, 1529-1535.

[27] a) A. Chowdhury, S. T. Thynell, *Thermochim. Acta* **2006**, *443*, 159-172; b) Y. Zhang, H. Gao, Y.-H. Joo, J. M. Shreeve, *Angew. Chem. Int. Ed.* **2011**, *50*, 9554-9562.

[28] a) J. Le Bideau, L. Viau, A. Vioux, *Chem. Soc. Rev.* **2011**, *40*, 907-925; b) M. P. Singh, R. K. Singh, S. Chandra, *J. Phys. D: Appl. Phys.* **2010**, *43*, 092001.

[29] a) S. Carda-Broch, A. Berthod, D. W. Armstrong, *Rapid Commun. Mass Spectrom.* **2003**, *17*, 553-560; b) D. W. Armstrong, L.-K. Zhang, L. He, M. L. Gross, *Anal. Chem.* **2001**, *73*, 3679-3686; c) K. S. Lovejoy, G. M. Purdy, S. Iyer, T. C. Sanchez, A. Robertson, A. T. Koppisch, S. R. E. Del, *Anal. Chem.* **2011**, *83*, 2921-2930.

[30] a) J. L. Anderson, D. W. Armstrong, *Anal. Chem.* **2003**, *75*, 4851-4858; b) Z. Breitbach, D. Armstrong, *Anal. Bioanal. Chem.* **2008**, *390*, 1605-1617; c) K. Huang, X. Han, X. Zhang, D. W. Armstrong, *Anal. Bioanal. Chem.* **2007**, *389*, 2265-2275; d) J. Álvarez, D. Gomis, P. Abrodo, D. Llorente, E. Busto, N. Lombardía, V. Fernández, M. Álvarez, *Anal. Bioanal. Chem.* **2011**, *400*, 1209-1216.

[31] K. J. Baranyai, G. B. Deacon, D. R. MacFarlane, J. M. Pringle, J. L. Scott, *Aust. J. Chem.* **2004**, *57*, 145-147.

[32] a) A. F. Ferreira, P. N. Simões, A. G. M. Ferreira, *J. Chem. Thermodyn.* **2012**, *45*, 16-27; b) A. Seeberger, A.-K. Andresen, A. Jess, *Phys. Chem. Chem. Phys.* **2009**, *11*, 9375-9381.

[33] a) W. H. Awad, J. W. Gilman, M. Nyden, R. H. Harris, T. E. Sutto, J. Callahan, P. C. Trulove, H. C. DeLong, D. M. Fox, *Thermochim. Acta* **2004**, *409*, 3-11; b) J. G. Huddleston, A. E. Visser, W. M. Reichert, H. D. Willauer, G. A. Broker, R. D. Rogers, *Green Chem.* **2001**, *3*, 156-164.

[34] T. Erdmenger, J. Vitz, F. Wiesbrock, U. S. Schubert, *J. Mater. Chem.* **2008**, *18*, 5267-5273.

[35] H. L. Ngo, K. LeCompte, L. Hargens, A. B. McEwen, *Thermochim. Acta* **2000**, *357*, 97-102.

[36] H. Tokuda, K. Hayamizu, K. Ishii, M. A. B. H. Susan, M. Watanabe, *J. Phys. Chem. B* **2005**, *109*, 6103-6110.

[37] D. R. MacFarlane, J. Golding, S. Forsyth, M. Forsyth, G. B. Deacon, *Chem. Commun.* **2001**, 1430-1431.

[38] P. Bonhôte, A. P. Dias, N. Papageorgiou, K. Kalyanasundaram, M. Grätzel, *Inorg. Chem.* **1996**, *35*, 1168-1178.

[39] G.-H. Min, T.-E. Yim, H.-Y. Lee, D.-H. Huh, E.-J. Lee, J.-Y. Mun, S. M. Oh, Y.-G. Kim, *Bull. Korean Chem. Soc.* **2006**, *27*, 847-852.

[40] J. D. Holbrey, W. M. Reichert, R. P. Swatloski, G. A. Broker, W. R. Pitner, K. R. Seddon, R. D. Rogers, *Green Chem.* **2002**, *4*, 407-413.

[41] D. R. MacFarlane, S. A. Forsyth, J. Golding, G. B. Deacon, *Green Chem.* **2002**, *4*, 444-448.

[42] F. Heym, B. J. M. Etzold, C. Kern, A. Jess, *Green Chem.* **2011**, *13*, 1453-1466.

[43] C. P. Fredlake, J. M. Crosthwaite, D. G. Hert, S. N. V. K. Aki, J. F. Brennecke, *J. Chem. Eng. Data* **2004**, *49*, 954-964.

[44] J. D. Holbrey, K. R. Seddon, *J. Chem. Soc., Dalton Trans.* **1999**, 2133-2139.

[45] J. M. Crosthwaite, M. J. Muldoon, J. K. Dixon, J. L. Anderson, J. F. Brennecke, *J. Chem. Thermodyn.* **2005**, *37*, 559-568.

[46] R. E. Del Sesto, T. M. McCleskey, C. Macomber, K. C. Ott, A. T. Koppisch, G. A. Baker, A. K. Burrell, *Thermochim. Acta* **2009**, *491*, 118-120.

[47] a) K. Tsunashima, S. Kodama, M. Sugiya, Y. Kunugi, *Electrochim. Acta* **2010**, *56*, 762-766; b) H. Shirota, T. Mandai, H. Fukazawa, T. Kato, *J. Chem. Eng. Data* **2011**, *56*, 2453-2459; c) K. Noack, P. S. Schulz, N. Paape, J. Kiefer, P. Wasserscheid, A. Leipertz, *Phys. Chem. Chem. Phys.* **2010**, *12*, 14153-14161; d) T.-Y. Wu, S.-G. Su, S.-T. Gung, M.-W. Lin, Y.-C. Lin, C.-A. Lai, I. W. Sun, *Electrochim. Acta* **2010**, *55*, 4475-4482.

[48] a) J. S. Wilkes, *J. Mol. Catal. A: Chem.* **2004**, *214*, 11-17; b) I. H. J. Arellano, J. G. Guarino, F. U. Paredes, S. D. Arco, *J. Therm. Anal. Calorim.* **2011**, *103*, 725-730; c) T. J. Wooster, K. M. Johanson, K. J. Fraser, D. R. MacFarlane, J. L. Scott, *Green Chem.* **2006**, *8*, 691-696.

[49] M. Kosmulski, J. Gustafsson, J. B. Rosenholm, *Thermochim. Acta* **2004**, *412*, 47-53.

[50] a) Y. Dessiaterik, T. Baer, R. E. Miller, *J. Phys. Chem. A* **2005**, *110*, 1500-1505; b) Y. U. Paulechka, D. H. Zaitsau, G. J. Kabo, A. A. Strechan, *Thermochim. Acta* **2005**, *439*, 158-160.

[51] L. P. N. Rebelo, J. N. Canongia Lopes, J. M. S. S. Esperança, E. Filipe, *J. Phys. Chem. B* **2005**, *109*, 6040-6043.

[52] Y. Chen, Y. Cao, Y. Shi, Z. Xue, T. Mu, *Ind. Eng. Chem. Res.* **2012**, *51*, 7418-7427.

[53] a) S. P. Verevkin, D. H. Zaitsau, V. N. Emel'yanenko, R. V. Ralys, C. Schick, M. Geppert-Rybczyńska, S. Jayaraman, E. J. Maginn, *Aust. J. Chem.* **2012**, *65*, 1487-1490; b) H. Luo, G. A. Baker, S. Dai, *J. Phys. Chem. B* **2008**, *112*, 10077-10081.

[54] U. Domańska, *Thermochim. Acta* **2006**, *448*, 19-30.

[55] S. D. Chambreau, J. A. Boatz, G. L. Vaghjiani, C. Koh, O. Kostko, A. Golan, S. R. Leone, *J. Phys. Chem. A* **2012**, *116*, 5867-5876.

[56] a) D. M. Fox, J. W. Gilman, H. C. De Long, P. C. Trulove, *J. Chem. Thermodyn.* **2005**, *37*, 900-905; b) V. Kamavaram, R. G. Reddy, *Int. J. Therm. Sci.* **2008**, *47*, 773-777.

[57] R. Liang, M. Yang, X. Xuan, *Chin. J. Chem. Eng.* **2010**, *18*, 736-741.

[58] a) J. L. Anderson, J. Ding, T. Welton, D. W. Armstrong, *J. Am. Chem. Soc.* **2002**, *124*, 14247-14254; b) H. Tokuda, K. Ishii, M. A. B. H. Susan, S. Tsuzuki, K. Hayamizu, M. Watanabe, *J. Phys. Chem. B* **2006**, *110*, 2833-2839.

[59] I. W. Sun, Y.-C. Lin, B.-K. Chen, C.-W. Kuo, C.-C. Chen, S.-G. Su, P.-R. Chen, T.-Y. Wu, *Int. J. Electrochem. Sci.* **2012**, *7*, 7206-7224.

[60] M. R. R. Prasad, V. N. Krishnamurthy, *Thermochim. Acta* **1991**, *185*, 1-10.

[61] S. Busi, M. Lahtinen, M. Kärnä, J. Valkonen, E. Kolehmainen, K. Rissanen, *J. Mol. Struct.* **2006**, *787*, 18-30.

[62] M. Montanino, M. Carewska, F. Alessandrini, S. Passerini, G. B. Appetecchi, *Electrochim. Acta* **2011**, *2011*, 153-159.

[63] a) S. Fang, Y. Jin, L. Yang, S.-i. Hirano, K. Tachibana, S. Katayama, *Electrochim. Acta* **2011**, *56*, 4663-4671; b) Z.-B. Zhou, H. Matsumoto, K. Tatsumi, *Chem. Eur. J.* **2006**, *12*, 2196-2212.

[64] Y. Jin, S. Fang, M. Chai, L. Yang, S.-I. Hirano, *Ind. Eng. Chem. Res.* **2012**, *51*, 11011-11020.

[65] a) H.-B. Han, K. Liu, S.-W. Feng, S.-S. Zhou, W.-F. Feng, J. Nie, H. Li, X.-J. Huang, H. Matsumoto, M. Armand, Z.-B. Zhou, *Electrochim. Acta* **2010**, *55*, 7134-7144; b) Y. Jin, S. Fang, M. Chai, L. Yang, S.-I. Hirano, *Ind. Eng. Chem. Res.* **2012**.

[66] S. Fang, Z. Zhang, Y. Jin, L. Yang, S.-i. Hirano, K. Tachibana, S. Katayama, *J. Power Sources* **2011**, *196*, 5637-5644.

[67] J. Pernak, K. Sobaszkiewicz, J. Foksowicz-Flaczyk, *Chem. Eur. J.* **2004**, *10*, 3479-3485.

[68] C. Maton, N. De Vos, B. I. Roman, E. Vanecht, N. R. Brooks, K. Binnemans, S. Schaltin, J. Fransaer, C. V. Stevens, *ChemPhysChem* **2012**, *13*, 3146-3157.

[69] F. G. Bordwell, *Acc. Chem. Res.* **1988**, *21*, 456-463.

[70] J. L. Anderson, R. F. Ding, A. Ellern, D. W. Armstrong, *J. Am. Chem. Soc.* **2005**, *127*, 593-604.

[71] T. Payagala, J. Huang, Z. S. Breitbach, P. S. Sharma, D. W. Armstrong, *Chem. Mater.* **2007**, *19*, 5848-5850.

[72] G. Adamova, R. L. Gardas, L. P. N. Rebelo, A. J. Robertson, K. R. Seddon, *Dalton Trans.* **2011**, *40*, 12750-12764.

[73] K. Tsunashima, Y. Ono, M. Sugiya, *Electrochim. Acta* **2011**, *56*, 4351-4355.

[74] K. Tsunashima, E. Niwa, S. Kodama, M. Sugiya, Y. Ono, *J. Phys. Chem. B* **2009**, *113*, 15870-15874.

[75] Q. Zhang, S. Liu, Z. Li, J. Li, Z. Chen, R. Wang, L. Lu, Y. Deng, *Chem. Eur. J.* **2009**, *15*, 765-778.

[76] D. Gerhard, S. C. Alpaslan, H. J. Gores, M. Uerdingen, P. Wasserscheid, *Chem. Commun.* **2005**, 5080-5082.

[77] a) L. Yang, Z. Zhang, X. Gao, H. Zhang, K. Mashita, *J. Power Sources* **2006**, *162*, 614-619; b) S. Fang, L. Yang, C. Wei, C. Peng, K. Tachibana, K. Kamijima, *Electrochem. Commun.* **2007**, *9*, 2696-2702.

[78] R. B. Myneni, S. Hoffman, Y. Knyazikhin, J. L. Privette, J. Glassy, Y. Tian, Y. Wang, X. Song, Y. Zhang, G. R. Smith, A. Lotsch, M. Friedl, J. T. Morisette, P. Votava, R. R. Nemani, S. W. Running, *Remote Sens. Environ.* **2002**, *83*, 214-231.

[79] N. L. Lancaster, T. Welton, G. B. Young, *J. Chem. Soc., Perkin Trans. 2* **2001**, 2267-2270.

[80] Z.-B. Zhou, H. Matsumoto, K. Tatsumi, *Chem. Eur. J.* **2005**, *11*, 752-766.

[81] J. M. Pringle, J. Golding, K. Baranyai, C. M. Forsyth, G. B. Deacon, J. L. Scott, D. R. MacFarlane, *New J. Chem.* **2003**, *27*, 1504-1510.

[82] K. Liu, Y.-X. Zhou, H.-B. Han, S.-S. Zhou, W.-F. Feng, J. Nie, H. Li, X.-J. Huang, M. Armand, Z.-B. Zhou, *Electrochim. Acta* **2010**, *55*, 7145-7151.

[83] D. M. Fox, J. W. Gilman, H. C. De Long, P. C. Trulove, *Proc. - Electrochem. Soc.* **2006**, *24*, 435-443.

[84] A. A. Strechan, A. G. Kabo, Y. U. Paulechka, A. V. Blokhin, G. J. Kabo, A. S. Shaplov, E. I. Lozinskaya, *Thermochim. Acta* **2008**, *474*, 25-31.
[85] H. Ohtani, S. Ishimura, M. Kumai, *Anal. Sci.* **2008**, *24*, 1335-1340.
[86] N. Meine, F. Benedito, R. Rinaldi, *Green Chem.* **2010**, *12*, 1711-1714.
[87] M. C. Kroon, W. Buijs, C. J. Peters, G.-J. Witkamp, *Thermochim. Acta* **2007**, *465*, 40-47.
[88] B. K. M. Chan, N. H. Chang, M. R. Grimmett, *Aust. J. Chem.* **1977**, *30*, 2005-2013.
[89] M. Sawada, Y. Takai, C. Chong, T. Hanafusa, S. Misumi, Y. Tsuno, *Tetrahedron Lett.* **1985**, *26*, 5065-5068.
[90] C. G. Begg, M. R. Grimmett, P. D. Wethey, *Aust. J. Chem* **1973**, *26*, 2435-2446.
[91] P. A. Hunt, *J. Phys. Chem. B* **2007**, *111*, 4844-4853.
[92] M. R. R. Prasad, K. Krishnan, K. N. Ninan, V. N. Krishnamurthy, *Thermochim. Acta* **1997**, *297*, 207-210.
[93] H. E. Kissinger, *Anal. Chem.* **1957**, *29*, 1702-1706.
[94] ASTM, **2012**. *Standard Test Method for Decomposition Kinetics by Thermogravimetry. E1641-07,* PA, USA
[95] Z. Wang, in *Comprehensive organic name reactions and reagents, Vol. 3*, Wiley-VCH, Hoboken, **2009**, p.3824.
[96] J.-Y. Cheng, Y.-H. Chu, *Tetrahedron Lett.* **2006**, *47*, 1575-1579.
[97] E. Gelens, F. J. J. De Kanter, R. F. Schmitz, L. A. J. M. Sliedregt, B. J. Van Steen, C. G. Kruse, R. Leurs, M. B. Groen', R. A. Orru, *Molecular Diversity* **2006**, *10*, 17-22.
[98] M. Earle, C. Gordon, N. Plechkova, K. Seddon, T. Welton, *Anal. Chem.* **2007**, *79*, 758-764.
[99] P. Nockemann, K. Binnemans, K. Driesen, *Chem. Phys. Lett.* **2005**, *415*, 131-136.
[100] G. Appetecchi, S. Scaccia, C. Tizzani, F. Alessandrini, S. Passerini, *J. Electrochem. Soc.* **2006**, *153*, A1685-A1691.
[101] F. Tang, K. Wu, L. Ding, J. Yuan, Q. Liu, L. Nie, S. Yao, *Sep. Purif. Technol.* **2008**, *60*, 245-250.
[102] D. A. Waterkamp, M. Heiland, M. Schluter, J. C. Sauvageau, T. Beyersdorff, J. Thoming, *Green Chem.* **2007**, *9*, 1084-1090.
[103] A. Renken, V. Hessel, P. Löb, R. Miszczuk, M. Uerdingen, L. Kiwi-Minsker, *Chem. Eng. Process.* **2007**, *46*, 840-845.
[104] H. Löwe, R. D. Axinte, D. Breuch, T. Hang, C. Hofmann, *Chem. Eng. Technol.* **2010**, *33*, 1153-1158.
[105] S. Fang, L. Yang, J. Wang, M. Li, K. Tachibana, K. Kamijima, *Electrochim. Acta* **2009**, *54*, 4269-4273.
[106] K. Fumino, A. Wulf, R. Ludwig, *Angew. Chem. Int. Ed.* **2008**, *47*, 8731-8734.
[107] A. Ahosseini, E. Ortega, B. Sensenich, A. M. Scurto, *Fluid Phase Equilib.* **2009**, *286*, 72-78.
[108] Y. Yoshida, O. Baba, G. Saito, *J. Phys. Chem. B* **2007**, *111*, 4742-4749.
[109] M. J. Deng, P. Y. Chen, T. I. Leong, I. W. Sun, J. K. Chang, W. T. Tsai, *Electrochem. Commun.* **2008**, *10*, 213-216.
[110] M. Begtrup, *Bull. Soc. Chim. Belg.* **1988**, *97*, 573-597.
[111] S. T. Handy, *J. Org. Chem.* **2006**, *71*, 4659-4662.
[112] S. P. Ong, G. Ceder, *Electrochim. Acta* **2010**, *55*, 3804-3811.
[113] a) A. B. McEwen, H. L. Ngo, K. LeCompte, J. L. Goldman, *J. Electrochem. Soc.* **1999**, *146*, 1687-1695; b) B. D. Fitchett, T. N. Knepp, J. C. Conboy, *J. Electrochem. Soc.* **2004**, *151*, E219-E225.
[114] P. C. Howlett, E. I. Izgorodina, M. Forsyth, D. R. MacFarlane, *Z. Phys. Chem.* **2006**, *220*, 1483-1498.
[115] H. Sakaebe, H. Matsumoto, *Electrochem. Commun.* **2003**, *5*, 594-598.
[116] S. Schneider, G. Drake, L. Hall, T. Hawkins, M. Rosander, *Z. Anorg. Allg. Chem.* **2007**, *633*, 1701-1707.
[117] T. Mizumo, E. Marwanta, N. Matsumi, H. Ohno, *Chem. Lett.* **2004**, *33*, 1360-1361.
[118] Z. Fei, W. H. Ang, D. Zhao, R. Scopelliti, E. E. Zvereva, S. A. Katsyuba, P. J. Dyson, *J. Phys. Chem. B* **2007**, *111*, 10095-10108.
[119] a) Z.-B. Zhou, H. Matsumoto, K. Tatsumi, *Chem. Eur. J.* **2004**, *10*, 6581-6591; b) W. A. Henderson, J. V. G. Young, D. M. Fox, H. C. De Long, P. C. Trulove, *Chem. Commun.* **2006**, 3708-3710.
[120] a) K. Fumino, T. Peppel, M. Geppert-Rybczynska, D. H. Zaitsau, J. K. Lehmann, S. P. Verevkin, M. Kockerling, R. Ludwig, *Phys. Chem. Chem. Phys.* **2011**, *13*, 14064-14075; b) E. I. Izgorodina, R. Maganti, V. Armel, P. Dean, J. M. Pringle, K. R. Seddon, D. R. Macfarlane, *J. Phys. Chem. B* **2011**, *115*, 14688–14697.

[121] M. Deetlefs, C. Hardacre, M. Nieuwenhuyzen, A. A. H. Padua, O. Sheppard, A. K. Soper, *J. Phys. Chem. B* **2006**, *110*, 12055-12061.

[122] C. Roth, T. Peppel, K. Fumino, M. Kockerling, R. Ludwig, *Angew. Chem. Int. Ed.* **2010**, *49*, 10221-10224.

[123] M. Wang, Z. Shan, J. Tian, KaiYang, X. Liu, H. Liu, K. Zhu, *Electrochim. Acta* **2013**, *95*, 301-307.

[124] T. Kakibe, N. Yoshimoto, M. Egashira, M. Morita, *Electrochem. Commun.* **2010**, *12*, 1630-1633.

[125] a) S. Ferrari, E. Quartarone, C. Tomasi, D. Ravelli, S. Protti, M. Fagnoni, P. Mustarelli, *J. Power Sources*, DOI: 10.1016/j.jpowsour.2013.1001.1149; b) M. Monteiro, M. J. Monteiro, *J. Phys. Chem. B* **2010**, *114*, 12488.

[126] L. Ford, F. Atefi, R. D. Singer, P. J. Scammells, *Eur. J. Org. Chem.* **2011**, *2011*, 942-950.

[127] T. Ramnial, D. D. Ino, J. A. C. Clyburne, *Chem. Commun.* **2005**, 325-327.

[128] T. Itoh, K. Kude, S. Hayase, M. Kawatsura, *Tetrahedron Lett.* **2007**, *48*, 7774-7777.

[129] M. C. Law, K. Y. Wong, T. H. Chan, *Chem. Commun.* **2006**, 2457-2459.

[130] T. Ramnial, S. A. Taylor, J. A. C. Clyburne, C. J. Walsby, *Chem. Commun.* **2007**, 2066-2068.

[131] a) S. V. Malhotra, Y. Xiao, *Aust. J. Chem.* **2006**, *59*, 468; b) B. Ni, Q. Zhang, A. D. Headley, *Green Chem.* **2007**, *9*, 737-739; c) Z. Wang, Q. Wang, Y. Zhang, W. Bao, *Tetrahedron Lett.* **2005**, *46*, 4657-4660; d) S. Luo, X. Mi, L. Zhang, S. Liu, H. Xu, J.-P. Cheng, *Angew. Chem. Int. Ed.* **2006**, *45*, 3093-3097.

[132] a) P. Wasserscheid, A. Bosmann, C. Bolm, *Chem. Commun.* **2002**, 200-201; b) B. Altava, D. S. Barbosa, M. Isabel Burguete, J. Escorihuela, S. V. Luis, *Tetrahedron: Asymmetry* **2009**, *20*, 999-1003; c) A. Winkel, R. Wilhelm, *Eur. J. Org. Chem.* **2010**, *2010*, 5817-5824; d) H. Clavier, L. Boulanger, N. Audic, L. Toupet, M. Mauduit, J.-C. Guillemin, *Chem. Commun.* **2004**, 1224-1225; e) J. J. Jodry, K. Mikami, *Tetrahedron Lett.* **2004**, *45*, 4429-4431.

[133] a) S. T. Handy, *Chem. Eur. J.* **2003**, *9*, 2938-2944; b) J.-C. Plaquevent, J. Levillain, F. Guillen, C. Malhiac, A.-C. Gaumont, *Chem. Rev.* **2008**, *108*, 5035-5060; c) C. Baudequin, J. Baudoux, J. Levillain, D. Cahard, A. C. Gaumont, J. C. Plaquevent, *Tetrahedron: Asymmetry* **2003**, *14*, 3081-3093; d) C. Baudequin, D. Bregeon, J. Levillain, F. Guillen, J. C. Plaquevent, A. C. Gaumont, *Tetrahedron: Asymmetry* **2005**, *16*, 3921-3945; e) J. Ding, D. W. Armstrong, *Chirality* **2005**, *17*, 281-292; f) T. Payagala, D. W. Armstrong, *Chirality* **2012**, *24*, 17-53; g) S. Z. Luo, L. Zhang, J. P. Cheng, *Chem. Asian J.* **2009**, *4*, 1184-1195.

[134] Y. Matsuoka, Y. Ishida, D. Sasaki, K. Saigo, *Tetrahedron* **2006**, *62*, 8199-8206.

[135] K. Fukumoto, M. Yoshizawa, H. Ohno, *J. Am. Chem. Soc.* **2005**, *127*, 2398.

[136] a) W. Bao, Z. Wang, Y. Li, *J. Org. Chem.* **2002**, *68*, 591-593; b) L. Gonzalez, B. Altava, M. Bolte, M. I. Burguete, E. Garcia-Verdugo, S. V. Luis, *Eur. J. Org. Chem.* **2012**, *2012*, 4996-5009.

[137] A. Winkel, R. Wilhelm, *Tetrahedron: Asymmetry* **2009**, *20*, 2344-2350.

[138] a) G.-N. Ou, M.-X. Zhu, J.-R. She, Y.-Z. Yuan, *Chem. Commun.* **2006**, 4626-4628; b) A. Rouch, T. Castellan, I. Fabing, N. Saffon, J. Rodriguez, T. Constantieux, J.-C. Plaquevent, Y. Genisson, *RSC Adv.* **2013**, *3*, 413-426; c) M. J. Earle, P. B. McCormac, K. R. Seddon, *Green Chem.* **1999**, *1*, 23-25.

[139] K. Nobuoka, S. Kitaoka, K. Kunimitsu, M. Iio, T. Harran, A. Wakisaka, Y. Ishikawa, *J. Org. Chem.* **2005**, *70*, 10106-10108.

[140] J. Pernak, J. Feder-Kubis, A. Cieniecka-Roslonkiewicz, C. Fischmeister, S. T. Griffin, R. D. Rogers, *New J. Chem.* **2007**, *31*, 879-892.

[141] R. A. F. Matos, C. K. Z. Andrade, *Tetrahedron Lett.* **2008**, *49*, 1652-1655.

[142] M. Ikeda, in *Adv. Biochem. Eng. Biotech., Vol. 79*, Springer Berlin / Heidelberg, **2003**, p.1-35.

[143] A. Sutherland, C. L. Willis, *Tetrahedron Lett.* **1997**, *38*, 1837-1840.

[144] D. Parker, *Chem. Rev.* **1991**, *91*, 1441-1457.

[145] a) J. Lacour, C. Ginglinger, C. Grivet, G. Bernardinelli, *Angew. Chem. Int. Ed.* **1997**, *36*, 608-610; b) J. Lacour, C. Ginglinger, F. Favarger, *Tetrahedron Lett.* **1998**, *39*, 4825-4828.

[146] E. Alcalde, I. Dinares, A. Ibanez, N. Mesquida, *Chem. Commun.* **2011**, *47*, 3266-3268.

[147] V. Gallo, P. Mastrorilli, C. F. Nobile, G. Romanazzi, G. P. Suranna, *J. Chem. Soc. Dalton Trans.* **2002**, *0*, 4339-4342.

[148] D. Britton, Y. M. Chow, *Acta Crystallogr., Sect. B* **1977**, *33*, 697-699.

[149] Q. B. Liu, M. H. A. Janssen, F. van Rantwijk, R. A. Sheldon, *Green Chem.* **2005**, *7*, 39-42.

[150] A. S. Larsen, J. D. Holbrey, F. S. Tham, C. A. Reed, *J. Am. Chem. Soc.* **2000**, *122*, 7264-7272.

[151] H. Srour, H. Rouault, C. C. Santini, Y. Chauvin, *Green Chem.* **2013**, *15*, 1341-1347.

[152] K. C. Lethesh, D. Parmentier, W. Dehaen, K. Binnemans, *RSC Advances* **2012**, *2*, 11936-11943.
[153] N. W. Smith, S. P. Gourisankar, J.-L. Montchamp, S. V. Dzyuba, *New J. Chem.* **2011**, *35*, 909-914.
[154] T. M. Alam, D. R. Dreyer, C. W. Bielwaski, R. S. Ruoff, *J. Phys. Chem. A* **2011**, *115*, 4307-4316.
[155] M. J. Earle, K. R. Seddon, WO 2001/077081, **2001**.
[156] R. Seddon K., A. J. Carmichael, M. J. Earle, WO 2001/40146, **2001**.
[157] P. Tundo, M. Selva, *Acc. Chem. Res.* **2002**, *35*, 706-716.
[158] a) J. Golding, S. Forsyth, D. R. MacFarlane, M. Forsyth, G. B. Deacon, *Green Chem.* **2002**, *4*, 223-229; b) Y.-H. Jung, J.-Y. Jung, Y.-R. Jin, B.-C. Lee, I.-H. Baek, S.-H. Kim, *J. Chem. Eng. Data* **2012**, *57*, 3321-3329; c) J. L. Kaar, A. M. Jesionowski, J. A. Berberich, R. Moulton, A. J. Russell, *J. Am. Chem. Soc.* **2003**, *125*, 4125-4131.
[159] C. O. Kappe, B. Pieber, D. Dallinger, *Angew. Chem. Int. Ed.* **2013**, *52*, 1088-1094.
[160] a) B. Albert, M. Jansen, *ZAAC* **1995**, *621*, 1735-1740; b) S. Mori, K. Ida, M. Ue, US Patent 4,892,944, **1990**.
[161] U. Romano, F. Rivetti, N. Di Muzio, (EniChem Anic S.p.A.). US Patent 4,318,862, **1978**.
[162] J. D. Holbrey, R. D. Rogers, S. S. Shukla, C. D. Wilfred, *Green Chem.* **2010**, *12*, 407-413.
[163] a) O. Sieskind, P. Albrecht, *Tetrahedron Lett.* **1993**, *34*, 1197-1200; b) P. Laszlo, *Science* **1987**, *235*, 1473-1477.
[164] J. D. Holbrey, W. M. Reichert, I. Tkatchenko, E. Bouajila, O. Walter, I. Tommasi, R. D. Rogers, *Chem. Commun.* **2003**, 28-29.
[165] a) R. Kalb, (Proionic GmbH). WO 2008/052863, **2008**; b) R. Kalb, W. Wesner, R. Hermann, M. Kotshan, M. Schelch, W. Staber, WO 2005/021484, **2005**; c) N. J. Bridges, C. C. Hines, M. Smiglak, R. D. Rogers, *Chem. - Eur. J.* **2007**, *13*, 5207-5212.
[166] G. Degen, K. Ebel, (BASF). WO 2006/027069, **2006**.
[167] S. Pirketta, *Acta Chem. Scand. Ser. A* **1986**, *A40*, 207-209.
[168] M. Smiglak, J. D. Holbrey, S. T. Griffin, W. M. Reichert, R. P. Swatloski, A. R. Katritzky, H. F. Yang, D. Z. Zhang, K. Kirichenko, R. D. Rogers, *Green Chem.* **2007**, *9*, 90-98.
[169] J.-C. Hsu, Y.-H. Yen, Y.-H. Chu, *Tetrahedron Lett.* **2004**, *45*, 4673-4676.
[170] R. Lo, B. Ganguly, *New J. Chem.* **2012**, *36*, 2549-2554.
[171] a) M. Besnard, M. I. Cabaco, F. V. Chavez, N. Pinaud, P. J. Sebastiao, J. A. P. Coutinho, Y. Danten, *Chem. Commun.* **2012**, *48*, 1245-1247; b) G. Gurau, H. Rodriguez, S. P. Kelley, P. Janiczek, R. S. Kalb, R. D. Rogers, *Angew. Chem. Int. Ed.* **2011**, *50*, 12024-12026; c) Y. Zhang, Z. Wu, S. Chen, P. Yu, Y. Luo, *Ind. Eng. Chem. Res.* **2013**, *52*, 6069-6075; d) H. A. Duong, T. N. Tekavec, A. M. Arif, J. Louie, *Chem. Commun.* **2004**, 112-113.
[172] M. Fèvre, P. Coupillaud, J. Vignolle, D. Taton, *J. Org. Chem.* **2012**, *77*, 10135-10144.
[173] a) I. Tommasi, F. Sorrentino, *Tetrahedron Lett.* **2006**, *47*, 6453-6456; b) P. U. Naik, L. Petitjean, K. Refes, M. Picquet, L. Plasseraud, *Adv. Synth. Catal.* **2009**, *351*, 1753-1756; c) I. Tommasi, F. Sorrentino, *Tetrahedron Lett.* **2005**, *46*, 2141-2145.
[174] A. K. L. Yuen, A. F. Masters, T. Maschmeyer, *Catal. Today* **2013**, *200*, 9-16.
[175] A. M. Magill, K. J. Cavell, B. F. Yates, *J. Am. Chem. Soc.* **2004**, *126*, 8717-8724.
[176] Y. A. Borisov, E. E. Arcia, S. L. Mielke, B. C. Garrett, T. H. Dunning, *J. Phys. Chem. A* **2001**, *105*, 7724-7736.
[177] a) W. J. Xiao, X. X. Wang, Q. Chen, T. H. Wu, Y. Wu, L. Z. Dai, C. S. Song, *Chem. Lett.* **2010**, *39*, 1112-1113; b) Z. Q. Zheng, T. H. Wu, R. W. Zheng, Y. Wu, X. P. Zhou, *Catal. Commun.* **2007**, *8*, 39-42.
[178] P. Tundo, M. Selva, *Green Chem.* **2005**, *7*, 464-467.
[179] B. V. Lotsch, J. Senker, W. Kockelmann, W. Schnick, *J. Solid State Chem.* **2003**, *176*, 180-191.
[180] P. T. Anastas, J. C. Warner, *Green Chemistry: Theory and Practice.* , Oxford University Press: New York, **1998**.
[181] N. Gathergood, P. J. Scammells, *Aust. J. Chem.* **2002**, *55*, 557-560.
[182] a) S. Stolte, J. Arning, U. Bottin-Weber, M. Matzke, F. Stock, K. Thiele, M. Uerdingen, U. Welz-Biermann, B. Jastorff, J. Ranke, *Green Chem.* **2006**, *8*, 621-629; b) S. Stolte, M. Matzke, J. Arning, A. Boschen, W. R. Pitner, U. Welz-Biermann, B. Jastorff, J. Ranke, *Green Chem.* **2007**, *9*, 1170-1179.
[183] a) M. Markiewicz, M. Piszora, N. Caicedo, C. Jungnickel, S. Stolte, *Water Res.* **2013**, *47*, 2921-2928; b) M. T. Garcia, N. Gathergood, P. J. Scammells, *Green Chem.* **2005**, *7*, 9-14.
[184] N. Gathergood, P. J. Scammells, M. T. Garcia, *Green Chem.* **2006**, *8*, 156-160.

[185] A. Romero, A. Santos, J. Tojo, A. Rodriguez, *J. Hazard. Mater.* **2008**, *151*, 268-273.
[186] E. Liwarska-Bizukojc, D. Gendaszewska, *J. Biosci. Bioeng.* **2013**, *115*, 71-75.
[187] OECD Chemical Group, **1992**. *OECD Guidelines for the Testing of Chemicals, Section 3. Method 301 D. Ready Biodegradability,* Paris, France
[188] OECD Chemical Group, **1992**. *OECD Guidelines for the Testing of Chemicals, Section 3. Method 302 B. Inherent Biodegradability: Zahn-Wellens/ EMPA Test* Paris, France
[189] E. Liwarska-Bizukojc, M. Bizukojc, *Enz. Microb. Technol.* **2007**, *41*, 26-34.
[190] E. Liwarska-Bizukojc, R. Scheumann, A. Drews, U. Bracklow, M. Kraume, *Water Res.* **2008**, *42*, 923-930.
[191] Y. Deng, P. Besse-Hoggan, M. Sancelme, A.-M. Delort, P. Husson, M. F. Costa Gomes, *J. Hazard. Mater.* **2011**, *198*, 165-174.
[192] N. R. Brooks, S. Schaltin, K. Van Hecke, L. Van Meervelt, K. Binnemans, J. Fransaer, *Chem. - Eur. J.* **2011**, *17*, 5054-5059.
[193] D. Depuydt, N. R. Brooks, S. Schaltin, L. Van Meervelt, J. Fransaer, K. Binnemans, *ChemPlusChem* **2013**, *78*, 578-588.
[194] a) R. V. Jones, L. Godorhazy, N. Varga, D. Szalay, L. Urge, F. Darvas, *J. Comb. Chem.* **2006**, *8*, 110-116; b) M. Irfan, E. Irfan, T. Petricci, M. Glasnov, C. O. Taddei, M. Kappe, Irfan, *Eur. J. Org. Chem.* **2009**, *2009*, 1327-1334; c) B. Gutmann, J.-P. Roduit, D. Roberge, C. O. Kappe, *Chem. - Eur. J.* **2011**, *17*, 13146-13150.
[195] a) C. Wiles, P. Watts, *Eur. J. Org. Chem.* **2008**, *2008*, 1655-1671; b) C. Wiles, P. Watts, *Chem. Commun.* **2011**, *47*, 6512-6535; c) K. Geyer, J. D. C. Codée, P. H. Seeberger, *Chem. - Eur. J.* **2006**, *12*, 8434-8442; d) J. Wegner, S. Ceylan, A. Kirschning, *Chem. Commun.* **2011**, *47*, 4583-4592.
[196] K. L. Fow, M. Ganapathi, I. Stassen, J. Fransaer, K. Binnemans, D. E. De Vos, *Chemical Communications* **2013**, *49*, 8498-8500.
[197] S. Armenise, E. Garcia-Bordeje, J. L. Valverde, E. Romeo, A. Monzon, *Phys. Chem. Chem. Phys.* **2013**.
[198] CrysAlisPro, Agilent Technologies, Yarnton, UK, **2011**.
[199] G. Sheldrick, *Acta Crystallogr., Sect. A* **2008**, *64*, 112-122.
[200] O. V. Dolomanov, L. J. Bourhis, R. J. Gildea, J. A. K. Howard, H. Puschmann, *J. Appl. Crystallogr.* **2009**, *42*, 339-341.

X) CURRICULUM VITAE

Personal information

Name	Cedric Maton
Address	Ottergemsesteenweg 225, 9000 Gent
Born	November, 12th 1986, Menen
Tel.	0032 (0) 489 98 48 50
E-mail	cedric.maton@pandora.be

Education

2011 Language course German III, UCT Ghent

2004-2009 Master of Science in Applied Biological Sciences: Chemistry and Bioprocessing technology, Ghent University (Distinction)

2008 Erasmus-program at ENSCM, Montpellier, option Chimie Organique Fine

Thesis: "Directed synthesis of functionalised chalcones containing anti-invasive properties."

Promoter: Prof. Dr. ir. Christian V. Stevens

2004 Degree ASO, option Science and Mathematics

Career

2009-2013 Candidate PhD in Applied Biological Sciences: Chemistry, Ghent University

"Design and properties of novel peralkylated imidazolium ionic liquids"

Promoter: Prof. Dr. ir. Christian V. Stevens

2007-2009 Lifeguard at Communal Swimming Pool, Izegem

2003-2006 Collaborator in Toddler Motor Skill Gardens, Moorslede

Publications in international journals with peer-review (A1)

C. Maton, N. De Vos, B. I. Roman, E. Vanecht, N. R. Brooks, K. Binnemans, S. Schaltin, J. Fransaer and C. V. Stevens. 'Continuous Synthesis of Peralkylated Imidazoles and their Transformation into Ionic Liquids with Improved (Electro)Chemical Stabilities', ChemPhysChem, **2012**, *13*, 3146-3157. (I.F.: 3.35)

C. Maton, N. De Vos and C. V. Stevens. 'Ionic liquid thermal stabilities: decomposition mechanisms and analysis tools', Chem. Soc. Rev., **2013**, *42,* 5963-5977 (I.F.: 28.76)

C. Maton, N. R. Brooks, L. Van Meervelt, K. Binnemans, S. Schaltin, J. Fransaer and C. V. Stevens. 'Synthesis and Properties of Alkoxy- and Alkenyl-Substituted Peralkylated Imidazolium Ionic Liquids', ChemPhysChem, **2013,** 14, 3503–3516. (I.F.: 3.35)

E. Liwarska-Bizukojc, C. Maton, C. V. Stevens, and D. Gendaszewska. 'Biodegradability and kinetics of the removal of new peralkylated imidazolium ionic liquids', J. Chem. Technol. Biotechnol., **2013**, doi: 10.1002/jctb.4187. (I.F.: 2.50)

C. Maton, K. Van Hecke and C. V. Stevens. 'Properties and synthesis of peralkylated imidazolium carbonate ionic liquids using dimethylcarbonate', in preparation.

Conferences (active participation)

Ionic Liquid Summer School, August 23-27, 2010, Leuven (Belgium). C. Maton, C. V. Stevens 'Synthesis of Peralkylated Imidazolium Ionic Liquids'. (poster).

14th Sigma-Aldrich Organic Synthesis Meeting, December 2-3, 2010, Spa (Belgium). C. Maton, C. V. Stevens 'Synthesis of Novel Pentasubstituted Imidazolium Ionic Liquids'. Abstract P-38. (poster).

11th International Symposium on Selected Problems of Chemistry of Acyclic and Cyclic Heteroorganic Compounds, November 17th, 2011, Częstochowa (Poland). C. Maton, N. De Vos, B. I. Roman, E. Vanecht, N. R. Brooks, K. Binnemans, S. Schaltin, J. Fransaer and C. V. Stevens 'Peralkylated imidazolium ionic liquids: synthesis and properties'. Abstract leaflet p. 6 (oral presentation).

14th International Symposium 'Advances in the Chemistry of Heteroorganic Compounds', November 18th, 2011, Łódź (Poland). C. Maton, N. De Vos, B. I. Roman, E. Vanecht, N. R. Brooks, K. Binnemans, S. Schaltin, J. Fransaer and C. V. Stevens 'Peralkylated imidazolium ionic liquids: synthesis and properties'. Abstract P-54 (poster).

16th Sigma-Aldrich Organic Synthesis Meeting, December 6-7, 2012, Spa (Belgium). C. Maton, N. De Vos, S. Wellens, N. R. Brooks, K. Binnemans, S. Schaltin, J. Fransaer and C. V. Stevens 'Synthesis and Properties of Alkoxy and Alkenyl Derivatised Imidazolium Ionic Liquids'. Abstract P-42 (poster).

18th National Symposium on Applied Biological Sciences, February 8th, 2012, Ghent (Belgium). C. Maton, N. R. Brooks, K. Binnemans and C. V. Stevens 'Synthesis and Properties of Chiral Imidazolium Ionic Liquids'. Online book of short abstracts P-43 (poster).